Evaluating Tidal Flood Risk on Salt Farming Land

Empirical and Methodological Insights from a Case Study in Northern Java

Institute of Geography
Anang Widhi Nirwansyah

Universität zu Köln

Evaluating Tidal Flood Risk on Salt Farming Land

Empirical and Methodological Insights from a Case Study in Northern Java

Inaugural - Dissertation

zur

Erlangung des Doktorgrades

der Mathematisch-Naturwissenschaftliche Fakultät

der Universität zu Köln

vorgelegt von

Anang Widhi Nirwansyah

aus Semarang, Indonesia

Köln, 2021

Berichterstatter: **Prof. Dr. Boris Braun (Universität zu Köln)**

(Gutachter) **Prof. Dr. Georg Bareth (Universität zu Köln)**

Tag der mündlichen Prüfung: 29 November 2021

Foreword

First and foremost, praise to Allah for the strength, grace, ability, and opportunities during my study. While working on my doctoral project, I was lucky enough to have support from many amazing people. I am indebted to all the people who had a direct or indirect role in the realization of this dissertation. First and foremost, I would like to thank my supervisor, Prof Boris Braun, for his invaluable discussions, challenges, and comments during my research work and throughout this process. Thanks for your trust and for granting me the independence to explore my own ideas and interests. It has been a great chance to be part of this research group. I would also like to thank Prof Georg Bareth and Prof Amelie Bernzen (University of Vechta) as my co-supervisors for their tremendous support and ideas.

I would like to thank Frauke Haensch for her support with great proofreading. I am also indebted to Susanne Weber for helping with the bureaucratic issues. Also thanks to Dr Lisa-Michéle Bott, Konstantin Gisevius, Dr Shantonu Abe, Sule Issaka Ayannor, Dr Jayadi, and Anabel Wandt for their good company. I am grateful to all farmers' representatives as prominent stakeholders in this study and to all Indonesian experts who participated in the analytical hierarchical process via Zoom. Special thanks to Mas Juli's family for hosting me in their home in Rawaurip, Cirebon. I also would like to thank Ibu Yuli from the Department of Ocean and Fisheries, Cirebon for valuable information and guidance during fieldwork. I would like to thank Mahmuda for his assistance during the data collection. My gratitude is expressed to the Indonesia Endowment Fund for Education (LPDP) for sponsoring me for this research: PCIM Jerman Raya, FORMAL Jerman, and Universitas Muhammadiyah Purwokerto, thank you for the support.

I wish to express my gratitude to my family for their presence and continuous support. My heartfelt thanks go to my wife Dwi Rezeki Putri for her love and everything she did for our little family and, of course, our children, Naifa and Maryam. I thank my relatives in Semarang, Kediri and Malang, for their support, especially during difficult times. Finally, thank you to my beloved mother for always supporting me and praying for me during her life. I hope you now find peace in heaven.

For my Mom who has sent me to school and all teachers who taught me about maps

Summary

Coastal regions have been threatened by coastal hazards, including tidal flooding, in recent years. Many studies have focused on evaluating flood risks in urban areas because complete data is available. However, tidal flooding in data-poor rural coastal areas has hardly been discussed. In addition, there is still no consensus among academics concerning the development of methods to evaluate flood risk in rural coastal areas with different local settings, including agriculture, aquaculture, or even salt farming. Filling the research gaps on developing flood risk evaluation on data-sparse regions is crucial to support disaster risk reduction policies integrated with local economic resources.

This dissertation presents an original approach in integrating a hydrodynamic model, geospatial data, and a geographic information system (GIS) in the rural coastal area of Cirebon, West Java, Indonesia, with a salt farming setting. The study focuses on answering the central topic: Developing an initial model to evaluate tidal flood risk in a data-scarce region using geospatial data. Because limited data is available, the model developed must be able to be implemented in rural coastal areas that are subject to regular tidal flooding. The current thesis evaluates the tidal flood hazard through depth and duration factors. The physical vulnerability from natural science and engineering perspectives have been manifested through the so-called damage function. This study also presents detailed economic loss figures for each parcel representing the risk level in different stages of production. Moreover, a comparison method has been implemented by multicriteria analysis (MCA) using an Analytical Hierarchical Process (AHP) to validate the flood risk model. This MCA-AHP process involves experts justifying all selected variables in the hazard, vulnerability, and risk analysis.

The results reveal that tidal floods have affected rural coastal regions, especially in the salt farming area of Cirebon. The established hydrodynamic model has successfully identified the magnitude and distribution of tidal flooding for two events of 2016 and 2018 on salt ponds. This finding extends the utilization of the hydrodynamic model to simulate specific tidal flood events for rural coastal settings with restricted datasets. A synthetic approach using local information from farmers has contributed to the measurement of the expected monetary loss for these two former tidal flood events. This method is employed to construct a damage function that portrays a simple form of physical vulnerability of salt farming based on flood depth and duration factors. The two tidal flood events studied represented the pre-production and harvesting periods had minimal economic impacts. Lastly, the multicriteria approach has also portrayed the risk condition of salt farming by using hazard and vulnerability parameters. With limited data available, this approach has successfully identified the tidal flood risk in salt ponds into the maps. The comparison of this parametric approach with the hydrodynamical approach has shown a strong statistical correlation that marks the relation between risk level and expected loss. However, there are some uncertainties from data input in the numerical hydrodynamic model and the subjectivity of the experts in the analytical process.

The findings in this thesis can be converted to the advancement of crucial policy implications. The thesis has the potential to improve disaster risk reduction, specifically in salt-farming areas. The integration of flood risk maps based on hydrodynamic and multicriteria inputs can support the implementation of a targeted disaster risk reduction policy under data-poor conditions. Finally, the risk evaluation analysis can assist government policies targeting the increase of productivity of salt farming, such as the national Indonesian target of salt self-sufficiency, flood risk reduction via structural measures, mangrove conservation and integrated coastal planning policies.

Zusammenfassung

Küstenregionen sind in den letzten Jahren durch Küstengefahren, einschließlich Überschwemmungen, bedroht worden. Viele Studien haben sich auf die Bewertung von Hochwasserrisiken in städtischen Gebieten konzentriert, da dort vollständige Daten verfügbar sind. Gezeitenüberschwemmungen in datenarmen ländlichen Küstengebieten wurden jedoch kaum erörtert. Darüber hinaus besteht unter den Wissenschaftlerinnen und Wissenschaftlern noch immer kein Konsens über die Entwicklung von Methoden zur Bewertung des Hochwasserrisikos in ländlichen Küstengebieten in unterschiedlichen lokalen Kontexten, wie z.B. Landwirtschaft, Aquakulturen oder Salzgewinnung. Die Schließung der Forschungslücken bei der Entwicklung von Hochwasserrisikobewertungen in datenarmen Regionen ist von entscheidender Bedeutung, um Maßnahmen zur Verringerung des Katastrophenrisikos unter Berücksichtigung der lokalen wirtschaftlichen Ressourcen zu unterstützen.

In dieser Dissertation wird ein neuartiger Ansatz vorgestellt, der ein hydrodynamisches Modell, Geodaten und ein Geographisches Informationssystem (GIS) vereint und für den Salzanbau in der ländlichen Küstenregion von Cirebon, West-Java, Indonesien anwendet. Die Studie konzentriert sich auf die Bearbeitung des zentralen Themas: Entwicklung eines ersten Modells unter Verwendung von Geodaten zur Bewertung des Hochwasserrisikos durch Gezeiten in einer datenarmen Region. Das entwickelte Modell muss in ländlichen Küstengebieten, die regelmäßig von Tidehochwasser betroffen sind, eingesetzt werden können. In der vorliegenden Arbeit wird die Tidehochwassergefährdung durch die Faktoren Tiefe und Dauer bewertet. In dieser Studie werden auch detaillierte Zahlen zu den wirtschaftlichen Verlusten für jede Parzelle vorgelegt, die das Risikoniveau in verschiedenen Produktionsstadien darstellen. Darüber hinaus wurde eine Vergleichsmethode durch eine multikriterielle Analyse (MCA) unter Verwendung eines Analytischen Hierarchischen Prozesses (AHP) eingeführt, um das Hochwasserrisikomodell zu validieren. Dieser MCA-AHP-Prozess beinhaltet, dass Expertinnen und Experten ausgewählte Variablen in der Gefahren-, Anfälligkeits- und Risikoanalyse begründen.

Die Ergebnisse zeigen, dass die ländlichen Küstenregionen, vor allem im Salzanbaugebiet von Cirebon, von Flutkatastrophen betroffen sind. Das erstellte hydrodynamische Modell hat erfolgreich das Ausmaß und die Verteilung von Tidehochwasser auf Salzteichen für zwei Ereignisse in den Jahren 2016 und 2018 ermittelt. Dieses Ergebnis bestätigt die Nutzung des hydrodynamischen Modells für die Simulation spezifischer Tidehochwasserereignisse in ländlichen Küstengebieten mit nur begrenzt vorliegenden Datensätzen. Ein synthetischer Ansatz, der lokale Informationen von Landwirten nutzt, hat dazu beigetragen, den erwarteten monetären Schaden für diese beiden früheren Hochwasserereignisse zu ermitteln. Mit dieser Methode wird eine Schadensfunktion konstruiert, die eine einfache Form der physischen Verwundbarkeit der Salzlandwirtschaft auf der Grundlage der Faktoren Überschwemmungstiefe und -dauer abbildet. Die beiden untersuchten Hochwasserereignisse in der Vorproduktions- und Erntezeit hatten nur geringe wirtschaftliche Auswirkungen. Schließlich hat auch der

multikriterielle Ansatz anhand von Gefahren- und Anfälligkeitsparametern die Risikobedingungen für den Salzanbau dargestellt. Mit diesem Ansatz kann das Hochwasserrisiko in den Salzteichen in den Karten abgebildet werden. Der Vergleich dieses parametrischen Ansatzes mit dem hydrodynamischen Ansatz weist eine starke statistische Korrelation auf, die das Verhältnis zwischen Risikoniveau und erwartetem Schaden kennzeichnet. Allerdings gibt es einige Unsicherheiten durch die Dateneingabe in das numerische hydrodynamische Modell und die Subjektivität der befragten Expertinnen und Experten im analytischen hierarchischen Prozess.

Die in dieser Arbeit gewonnenen Erkenntnisse können zur Entwicklung wichtiger politischer Handlungsempfehlungen genutzt werden. Die Arbeit hat das Potenzial, die Katastrophenvorsorge insbesondere in Salzgewinnungsgebieten zu verbessern. Die Integration von Hochwasserrisikokarten, die auf hydrodynamischen und multikriteriellen Daten basieren, kann die Umsetzung einer gezielten Katastrophenvorsorgepolitik unter datenarmen Bedingungen unterstützen. Schließlich kann die Analyse der Risikobewertung die Politik der Regierung unterstützen, die auf die Steigerung der Produktivität des Salzanbaus abzielt. Dazu zählen z.B. das nationale indonesische Ziel der Selbstversorgung mit Salz, die Verringerung des Hochwasserrisikos durch strukturelle Maßnahmen, der Schutz der Mangroven und eine integrierte Küstenplanung.

Table of Content

List of Figures

List of Tables

List of Equations

List of Abbreviations

AHP - Analytical Hierarchical Process

ASCII - American Standard Code for Information Interchange

B/C – Benefit Cost

BATNAS – Gridded national bathymetry of Indonesia

BIG – *Badan Informasi Geospasial* (National Geospatial Information Agency of Indonesia)

C/R – Cost and Revenue

CONHAZ - Costs of Natural Hazards

CRED - Centre for Research on the Epidemiology of Disasters

CVA – Coastal Vulnerability Assessment

DDF – depth-duration damage function

DEM – Digital Elevation Model

DEMNAS – Indonesian national seamless digital elevation model

DISHIDROS – *Dinas Hidro-Oseanografi* (Indonesian Hydro-Oceanographic Office)

DKP – *Department Kelautan dan Perikanan* (Department of Marine and Fisheries)

ELCIRC – Eulerian-Lagrangian circulation

GDP – Gross Domestic Product

GFDRR - Global Facility for Disaster Reduction and Recovery (GFDRR)

GIS – Geographic Information System

HDM – hydrodynamic model

HDPE – high-density polyethylene

ICCSR - Indonesia Climate Change Sectoral Roadmap

IDR – Indonesian Rupiah

LPDP – *Lembaga Pengelola Dana Pendidikan* (Indonesia Endowment Fund for Education)

MCA – Multicriteria analysis

MCDA – Multiple-criteria Decision Analysis

NWM – Northwest Monsoon

PSSDAL – *Pusat Survei Sumber Daya Alam Laut* (Marine natural resources survey center)

PV – Physical Vulnerability

PVC – polyvinyl chloride

RMSE – Root Mean Square Error

RQ – Research Question

TMD – Tide Model Driver

TPXO – TOPEX/Poseidon Global Inverse Solution of Oregon State University

UTC – Universal Time Coordinated

UTM – Universal Transverse Mercator

WGS – World Geodetic System

Chapter 1
Introduction

CHAPTER 1 - Introduction

1.1. Background

Flood hazards have been causing human fatalities, physical destruction and economic loss worldwide for centuries. Until now, more than 800 million people are living in vulnerable flood areas, with 70 million exposed to floods annually (UNISDR, 2015a). Based on the World Bank's Global Subnational Atlas of Poverty and Global Monitoring Database, it is calculated that around 1.47 billion people worldwide are exposed to the risk of intense flooding. Over a third of them, almost 600 million, are living below the poverty line (Rentschler and Salhab, 2020). In addition, during the 20-year period between 2000-2019, about 44% of disaster events each year were flood disasters (CRED & UNDRR, 2020). In particular regions, such as low-income countries, there are many cases of under-reported losses from these disasters (CRED *et al.*, 2021). Many of these regions are, however, still missing the fundamental data required for flood preparedness, response, and policy-making (Paul *et al.*, 2018).

In a global context, it is recognized that developing countries, such as those in Africa and Asia, are facing the highest flood risk (Winsemius *et al.*, 2016). In recent years, frequent floods have been reported mainly in many coastal cities of these regions, such as Ghana (Addo *et al.*, 2011); Nigeria (Adelekan & Asiyanbi, 2016); Bangladesh (Islam *et al.*, 2013); Myanmar (Win *et al.*, 2018), Vietnam (Toan, 2014); and Indonesia (Bott, 2020). However, many of these countries have a limited capacity to collect flood-related data, especially meteorological, hydrological and geophysical datasets periodically, and to maintain data storage (Kabenge *et al.*, 2017). These conditions have restricted researchers to evaluate the flood risk in these areas, especially with a prominent method that demands vigorous data series and sophisticated calibration process. Until now, there have been many global initiatives providing data that may only be relevant at a global, regional, or national scale. However, high-resolution data provides a better understanding of intervention at a local level (Olbert *et al.*, 2017; Le Roy *et al.*, 2015).

Flood risk is not only an issue for cities but also in rural areas. Despite rural areas having a small population, flood risk still affects dominant economic activities such as agriculture and aquaculture. While there are many approaches that can be applied to urban settings (Kubal *et al.*, 2009), methods for calculating losses to rural settings with simpler procedures are still limited (Forster *et al.*, 2008). This condition is mainly driven by the location of the floodplain areas and the lower expectation of damage (Brémond and Grelot, 2013). With enormous natural resource potential, rural areas have actually begun to focus on flood risk management in recent years to reduce the impact of disasters (Parrott *et al.*, 2009). Attention has also been given to supporting local communities with insurance solutions (Lotsch *et al.*, 2010). However, there are many challenges to establishing appropriate methods to evaluate flood risk under data-scarce conditions in rural areas.

1.2. Research Problem

The urgency of risk analysis, especially in coastal regions, has increased in recent years (GFDRR, 2010). Consequently, flood risk assessments have been carried out for many land-use types, mainly in urban settings (e.g., Adelekan, 2010; Budiyono, 2018; Takagi *et al.*, 2016). There is also a rising awareness of the impact of flooding on rural land use, such as agriculture. In accordance with the relevance of these matters, it is necessary to carry out an appropriate risk evaluation. Under this condition, the hydrodynamic model can provide an acceptable accurate analysis, especially at local and regional levels (Parodi, 2019). However, this approach is challenging for the Global South, especially due to data availability.

This thesis addresses a methodological approach to evaluating the flood risk for rural landscapes with limited data available. This study focuses on tidally driven flooding and farming as the main economic activity in a rural coastal setting in Java, Indonesia. Gaining better knowledge about flood risks is significant to understand the occurring processes and the impact of flood events where data documenting the effects is limited. In this regard, this thesis attempts to address the following research problem: *How can we develop an initial model to evaluate tidal flood risk in data-scarce regions by using geospatial data?* Attaining a better understanding of tidal flooding impact and risk on data-poor regions are urgently needed to support disaster risk reduction in rural areas and integrated coastal management.

1.3. Research Significance

For years, flood management has focused on the most appropriate flood mitigation strategy with deterministic scenarios, in which a single probability of an event has been taken into consideration (Jonkman *et al.*, 2016). Nevertheless, there has been an increasing movement to risk-based approaches in flood management (Apel *et al.*, 2006; Kron, 2005; Nicholls & Cazenave, 2010). However, there is still a knowledge gap regarding the application for non-urban land use in coastal regions with limited data available. On the other hand, most flood studies concern only one part of risk assessment element, such as the hydrodynamic model or damage estimation within locus on developed countries (Parodi, 2019). In addition, flood studies also include the different vulnerability factors such as physical, social, economic, and environmental vulnerabilities (see e.g., Balica *et al.*, 2013; Okazumi *et al.*, 2014; Seenath *et al.*, 2016), as well as the resulting flood risk (Neubert *et al.*, 2016; Rey *et al.*, 2020). These previous studies mainly evaluate the consequences of hazard scenarios, i.e., by using 'what-if?' questions without investigating and simulating the flood occurrence in the past (Böttle, 2016). Extending the flood risk assessment in rural area settings could initiate chances for the community to create a tailored solution to reduce the impact of flood disasters (Gilard, 2016).

1.4. Research Aim and Objectives

This study aims to develop a methodological approach to evaluate flood damage and risk in data-poor environments. Moreover, the approach is structured by the opportunities of geospatial technology improvement, especially in

spatial modeling, where a case study was necessary to be done in order to demonstrate and evaluate tidal flood risk. To fulfill this focus, the study presents the results of the original approach with a combination of a physical-based hydrodynamic model, geospatial technology, and the Geographic Information System (GIS). This study concentrates on a coastal region of northern Java due to its complex environmental ecosystem for both natural and artificial ecosystems (Marfai, 2011). This area also has been identified to be affected by coastal hazards, including flooding and land subsidence (Bott, 2020; Marfai and King, 2008). Cirebon, West Java, has been chosen as a case study location that represents a coastal rural area with limited data available. Cirebon also has its distinctive status as the biggest salt production center in Indonesia. In addition, the selected study site is highly vulnerable to coastal hazards, including frequent tidal floods and sea-level rises (Rositasari *et al.*, 2011). There are three main objectives of this thesis that are expected to progress.

1) Developing a method to assess the impact of tidal flood hazards based on previous events using a hydrodynamic approach and GIS tools.
2) Identify and estimate the economic impact of tidal floods and establish an applicable method.
3) Developing a GIS approach to evaluate tidal flood risk on salt farming land with available geospatial data.

1.5. Research Questions

Based on the objectives mentioned above, the following research questions (RQ) will be answered:

Methodological:

1) RQ 1: How can we assess post-events of tidal floods in coastal regions using a hydrodynamic model and limited geospatial data? What are the minimum requirements?
2) RQ 2: How can we integrate available data for economic damage calculations for data-scarce environments?
3) RQ 3: Can we use local information in damage assessment with no available data comparison?
4) RQ 4: What kind of GIS approach can be applied to evaluate tidal flood risk in data-scarce regions?

Empirical with reference to the study area:

5) RQ 5: What was the impact of tidal floods on salt farming in the study area of Cirebon, Indonesia?
6) RQ 6: What kind of vulnerability aspects can be used in the risk assessment for salt farming?
7) RQ 7: How can we validate the flood risk evaluation with limited data available?

1.6. Research Framework

Before starting to discuss the study location and the methodology, I shall provide definitions on the conceptually relevant terms that will be used in this dissertation. These terms are understood differently by some researchers and from different theoretical perspectives.

1.6.1. Tidal Floods

For the purpose of this thesis, tidal flooding is the focus of the current flood risk evaluation. This is because tidal-induced flood is mainly related to the tidal cycle in coastal zones. In many coastal regions, tides have triggered nuisance flooding (Jacobs *et al.*, 2018; Ray and Foster, 2016; Vandenberg-Rodes *et al.*, 2016), and sometimes are reinforced by an additional factor such as storm surges (Larson *et al.*, 2014; Rey *et al.*, 2018), or even tsunamis (Martínez-Graña *et al.*, 2016). Even without considering the aforementioned factors, the presence of high tide flooding in coastal areas has amplified flood risk, coastal inundation, infrastructure damage, or even population displacement (Moftakhari *et al.*, 2017; Ray and Foster, 2016). Some recent studies have stated that the frequency of the tidal or nuisance flood in many places has been rising in response to sea level rise (Dahl *et al.*, 2017; Moftakhari *et al.*, 2018; Ray and Foster, 2016). In this regard, this thesis focuses on tidal flooding as a generic event without further investigation on the sea level rise factor. The tides themselves have been evaluated through water movements. Seawater movements are periodic and can be foreseeable (Haigh, 2017; Marfai and King, 2008; Wolf, 2009). However, the sun-moon gravitation has affected most coastal areas due to sea level rise and created larger and longer disruptions for growing populations (Spanger-Siegfried *et al.*, 2014).

1.6.2. Hazard

For this thesis' framework, a hazard is described as a dangerous phenomenon of a given magnitude and frequency that happens in a particular area (Thouret *et al.*, 2014). As an example, flood depth resulting from the combined water levels and waves represents a flood hazard (Parodi, 2019). In a broader context, such as river flooding, hazards can also be measured by their depth and velocity (Merz and Thieken, 2009). A flood is noted as a hazard that is conventionally visualized in a maps format to portray the characteristics, including depth, velocity and duration (Kreibich *et al.*, 2009; Ward, De Moel, *et al.*, 2011). Flood hazard is mostly modeled through numerical approaches using hydrologic or hydrodynamic models that allow assessing flood peaks and propagation in time and space (Bates *et al.*, 2017). In farming, hazard parameters, i.e., water depth, duration, velocity, contamination and salinity of the water, can be presented through a damage function (Brémond and Grelot, 2013). Based on the aforementioned explanation, this thesis addresses damage functions using depth and duration factors.

The hazard is not the single driver of risk. As a consequence, there must be people or assets that have to be exposed to hazards to turn them into disasters (Takara, 2013). Exposure means elements located in areas where extreme natural phenomena may occur (UNISDR, 2009), including people, properties, economic activities, infrastructures, and the environment. Exposure can also be distinguished into different spatial and non-spatial components since people might be exposed spatially to a certain degree and or over a specific period of time because of their workplace or place for living (De Brito *et al.*, 2018). For rapid measurement, flood exposure in coastal areas can be assessed using topographic data and GIS (Marfai, King, *et al.*, 2008).

1.6.3. Vulnerability

In risk assessment, the vulnerability aspect has been approached from many different angles, not only in terms of disciplines, but also research paradigms. The definitions are also associated with specific contexts, objectives, and motivations (Balica *et al.*, 2013). Vulnerability has become more comprehensive to be quantified because a full set of socio-economic, cultural, psychological, etc. aspects have to be reflected (Gilard, 2016). Within various interests in examining vulnerability, social scientists tend to extend the radar to the human aspect, where the term 'social vulnerability' is used. Social vulnerability commonly manifests in various characteristics of people or communities such as age, race, health, income, and employment (Cutter *et al.*, 2003). In the social science debate, this term is also commonly considered as the predisposition of communities or individuals who are affected by hazards and are incapable of coping with them (Villagrán de León, 2006). Moreover, vulnerability also relates to the exposure to welfare losses (Vatsa, 2004). On the other hand, physical and engineering sciences focus on physical vulnerability. This term is restricted to the measurement of damaging effects, i.e., fatalities, business interruption, or economic losses (Apel *et al.*, 2009). WHO (2009) has highlighted a strong relationship between physical vulnerability and other vulnerability dimensions, and has also underlined how the disruption of physical aspects directly influences a community's social economic conditions. Physical vulnerability can also be integrated to estimate social economic aspects linked to vulnerability, such as poverty, by using geospatial technology (Birkmann, 2006).

Generally, there are several ways to measure vulnerability, as formerly compiled by Birkmann (2006), including (i) using vulnerability curves (Bhakta Shrestha *et al.*, 2019; Kappes *et al.*, 2012; Ward, De Moel, *et al.*, 2011); (ii) damage matrices (Papathoma-Köhle *et al.*, 2017); and (iii) vulnerability indicators (Roy and Blaschke, 2015). These mentioned methods were implemented in different cases with different data needed and different scales of analysis (Brito, 2018). *The vulnerability curve* is also called the damage function, damage curve, or fragility curve, related to the expected damage of an individual element at risk with hazard intensity in various studies (Brito, 2018). In most common methods, researchers present high damage percentages for a given inundation depth, including in buildings (Apel *et al.*, 2009; Win *et al.*, 2018), agriculture (Bhakta Shrestha *et al.*, 2019; Dutta *et al.*, 2003) or even infrastructure (Setiadi, 2013). Vulnerability curves provide reliable quantitative damage estimations, although they require large amounts of data input and computation hardware (Brito, 2018). The following *damage matrices* are constructed based on the understanding that a given element at risk will respond at the same damage level when submitted by a similar intensity of the hazard (Godfrey *et al.*, 2015). Both vulnerability curves and damage matrices can be established by using observation data, statistical analyses, or expert assessment (Brito, 2018). With the subjectivity that may occur in the justification of damage level among experts, the transferability and comparison possibilities at some point are limited (Papathoma-Köhle *et al.*, 2017). Finally, *vulnerability indicator-based methods* are developed with aggregated variables to evaluate the state of a system (e.g., building resistance) and generate information on the

level to which this system will be affected by certain hazard magnitudes (Birkmann, 2006; Malgwi *et al.*, 2020).

Due to the data availability, the narrow vulnerability perspective from physical science and engineering, as represented in physical vulnerability, has been chosen to build the perspective on this thesis and to address methodological development by using geospatial data within specifically addressed economic aspects. In the rural-agricultural setting, the tangible direct loss may involve crops and livestock destruction (Chau *et al.*, 2015). Intangible costs, however, are difficult to collect and measure, due to poor data availability and minimum knowledge of the overall damage (Dassanayake et al., 2015). As mentioned in Brémond and Grelot (2013), according to the CONHAZ consortium, costs of intangible damage cannot be estimated by market-based approaches.

1.6.4. Risk

In many discussions, the risk is agreed to be a product of a potential hazard and its consequences. In the scientific framework, this current study refers to the straightforward term of risk taken from the fundamental combination of hazard and vulnerability (Gilard, 2016). in areas where there are no humans or values that can be affected by natural processes or phenomena, there is no risk (Kron, 2005). This is because risk is a combination of hazard and vulnerability, so the expected loss can be estimated by a value mixture of the elements-at-risk and the calculated damage curve (Baky *et al.*, 2020). According to a more complex definition by UNISDR (2015), risk can be understood as a combined probability of a hazardous event and its effects, which results from the interaction between natural or man-made hazards, vulnerability, exposure, and capacity. In this thesis, the risk was first evaluated by estimating loss as within derived data input from a hydrodynamic model. However, the combination of hazard and vulnerability parameters has also been compared. Furthermore, this study did not take the coping capacity of the community into account and mainly focused on physical aspects.

1.6.5. Flood risk evaluation in data scarce-region

Given the probability of flood hazard occurrence, the possible consequences cannot be measured or estimated without a model for computing the loss, using the relationship between flood parameters and damage (Brémond and Grelot, 2010; Shokoohi *et al.*, 2018). To respond to the importance of risk analysis for floods, there are many studies focusing on developing scenarios (5-year event; 10-year event; 100-year event), probabilities, and using damage functions to evaluate loss in a certain region (Apel *et al.*, 2006), especially in urban areas. Despite the poor-data environment in many rural agriculture settings in the Global South, risk evaluation remains important in flood risk management. For example, in the European Union and the United Kingdom (UK), an economic appraisal is mandatory, especially in relation to the drainage infrastructure and flood protection projects intended for improving productivity and agriculture yield (Brémond and Grelot, 2010). However, as mentioned earlier, loss estimation is still needed in order to examine the risk, especially in developing countries where farming activities remain economically important (Nguyen *et al.*, 2017).

Based on several previous sources in this thesis, flood analysis is carried out by combining numerical simulations (hydrodynamic models) and loss calculations to determine the level of tidal flood risk on salt land (Shokoohi *et al.*, 2018).

Adding the perspective of flood risk evaluation in this thesis, the evaluation tool available is the flood risk map that visualizes at-risk locations and shows the elements at risk, for example, the location of the population, building and civil engineering works, and economic activities (Apel *et al.*, 2006). For this reason, the incorporation of flood risk evaluation into a Geographic Information System (GIS) framework has been implemented at various levels, from global and regional to domestic scales, in many recent studies (Luu and von Meding, 2018). A comprehensive flood risk assessment has to consider all the constituents of flood risk and combine many related parameters (de Moel *et al.*, 2009). At this point, the geospatial techniques have played a significant role to support the flood risk evaluation in a spatial context (Dewan, 2013).

Multicriteria Decision Analysis (MCDA) or, simply referred to as Multicriteria Analysis (MCA), is often combined with GIS to examine geographical problems such as flood vulnerability, susceptibility and risk assessment (e.g., Fernandez *et al.*, 2016; Souissi *et al.*, 2020). GIS-based MCA combines several criteria in the form of maps and independent preferences into a final decision map (Malczewski, 1999). This approach only demands the spatial layers of the parameters that contribute to flood hazards and vulnerability (Rincón *et al.*, 2018). As a result, flood risk maps can be generated with a relatively low budget and time investment (Sadek and Li, 2019).

There are several methods that can be applied in MCA, including machine learning (e.g., Bui *et al.*, 2019), the technique for order preference by similarity to the ideal solution (TOPSIS) (e.g., Chen *et al.*, 2021), Analytical Network Process (ANP) (e.g., Dano *et al.*, 2019) and reliable Analytical Hierarchal Process (AHP) (e.g., see Ghosh & Kar, 2018; Hadipour *et al.*, 2020; Luu & von Meding, 2018; Rimba *et al.*, 2017). In recent years, AHP has been broadly implemented in flood risk analysis and integrated with GIS technology (de Brito and Evers, 2016; Siddayao *et al.*, 2014). This semi-quantitative method is powerful in sponsoring priority selection and decision-making (Luu *et al.*, 2018). Considering all of these benefits, this thesis extends the application of AHP in flood risk evaluation with limited data available in a rural coastal region.

1.6.6. How to deal with uncertainty

One of the main problems in flood modeling is that validation is rarely implemented (De Brito *et al.*, 2018). However, this stage is crucial to the questions of whether a model can be used in various conditions and also whether it can be applied for forecasting (Merz *et al.*, 2010). In hydrodynamic models, the main source of uncertainty, especially in floodplains, is surface roughness (Vanderkimpen and Peeters, 2008). As alternatives, there are several options to test the reliability of the model through sensitivity analysis (De Brito *et al.*, 2018). Sensitivity analysis can be done by changing the input scores (e.g., more or less than 10% of initial values) to examine the sensitivity of the output value (Parodi, 2019). Another strategy is comparative analysis, which compares different modeling assumptions with data limitations. This method is suitable to explain the

model limitations or trustworthiness of data input. For this purpose, this thesis compares two different models to evaluate the reliability of the established method.

1.7. Outline of the Dissertation

The tools used and the results acquired to answer the research questions are presented in *Figure 1.1*.

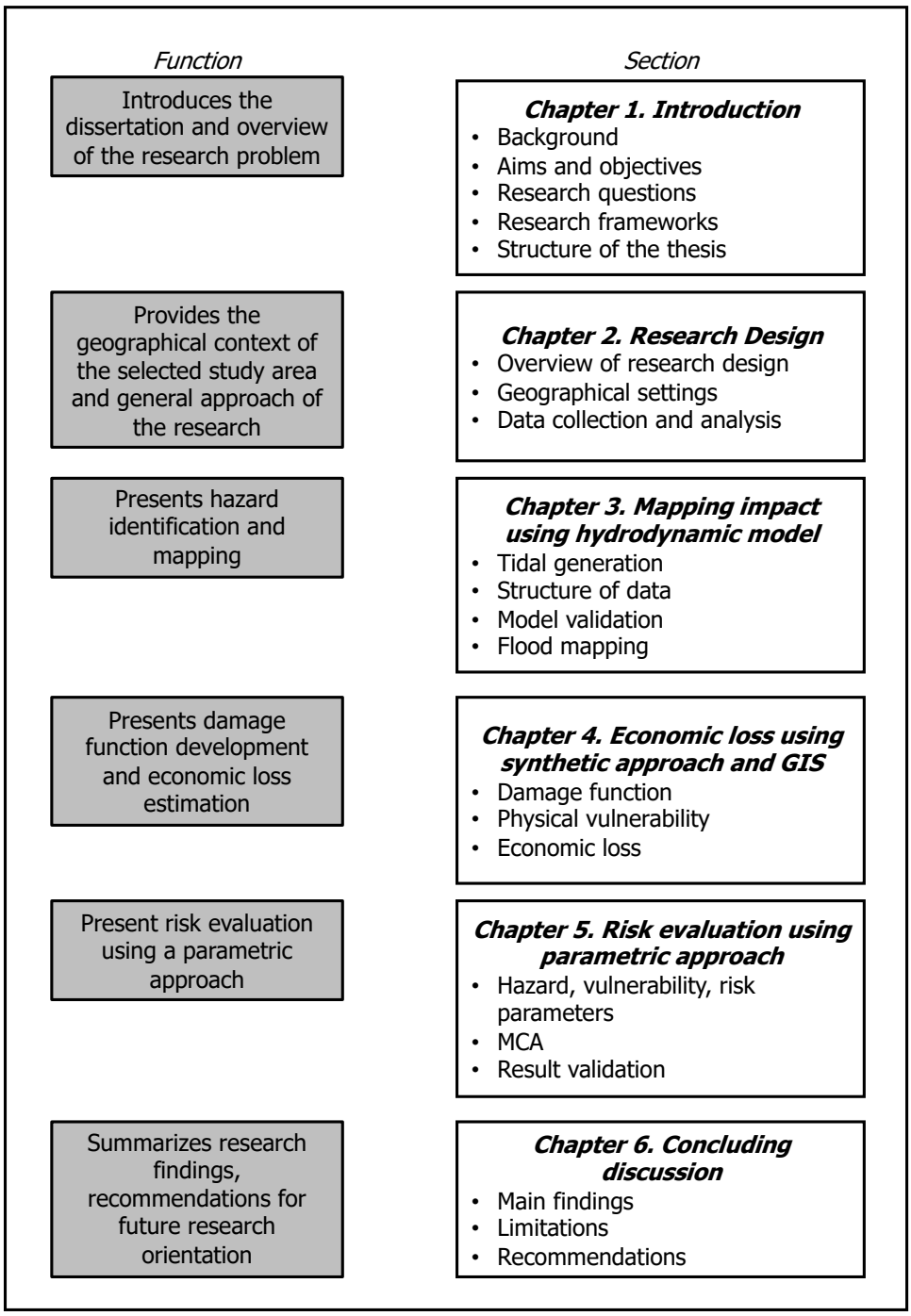

Figure 1.1. Overview of chapters of the dissertation

1) **Chapter 1** delivers the introduction to this research, including the background, the aims and objectives of the research, the theoretical framework, and the structure of the thesis.
2) **Chapter 2** describes the geographical settings of the research area, including the topography, climate condition, and waters condition. In addition, this chapter also describes the salt farming practice on the site study and the general approach used in this thesis.
3) **Chapter 3,** the first research study (paper 1) presents mapping the impacts of the tidal flood on solar salt farming in the northern part of Java. In this chapter, tidal flood occurrences from post events are investigated through a case study in Cirebon, West Java. Geospatial technology supports the measuring of potential coastal flood implications through a numerical model, tidal records from a local station, and GIS.
4) **Chapter 4** examines the degree of damage to the salt farming landscape (paper 2). In the second part, this study develops an initial method to examine economic loss by using a synthetic approach and GIS. Additionally, in this chapter, the local depth-duration damage function (DDF) has been established with salt farmers' representatives.
5) **Chapter 5** portrays risk evaluation in solar salt farming towards tidal flooding. In this chapter, the parametric approach to assessing risk by using hazard, vulnerability indicators, and MCA is performed (paper 3). This chapter also sponsors the usage of GIS applications as the main tools integrated with expert judgment for all selected indicators. Finally, the comparison between parametric and physical-based is also presented to validate the model.
6) **Chapter 6** presents a concluding discussion. In this chapter, the main findings of the study are synthesized and discussed to evaluate tidal flood risk in data-poor environments as implemented in the selected case study.

Chapter 2
Research Design

CHAPTER 2 - Research Design

2.1. Overview of Research Design

The empirical findings presented in this dissertation (Chapter 3, 4, and 5) are scientific papers in peer-reviewed journals. In addition, these chapters contain a section dealing with the methods that explain the data required and the specific methodology applied. For the broader context of the research design, this chapter illustrates a circumstantial explanation of the geographical overview of Cirebon, northern Java, and traditional salt farming practices in the on-site study area. Furthermore, this chapter explains the selected methods and their relevance to answer the research questions set in the previous chapter. This study applies a case study approach (cf. Castree, 2005) to investigate the impact of tidal flooding and to evaluate the risks on salt farming land.

2.2. Geographical Settings of Study Area

The study was carried out in Cirebon, on the northern coast of Java. Administratively, this region belongs to West Java Province. Cirebon covers around 990.36 km^2 and connects the capital city of Jakarta to other provinces in Java, including Central Java and East Java (see *Figure 2.1*). In general, Cirebon consists of two typical topographical features. First, the low-land area, which is heavily affected by erosion and sedimentation processes. This area covers around 64.5 thousand hectares and is located mostly in the northern part of the region, adjacent directly to the Java Sea. The area is mostly structured by mud sediments, silt, and grey clay containing shell sediments. Second, the region also has a mountainous area in the south part with the domination of hills and mountains. Cirebon typically consists of flat zones (lower than 5°), moderate zones (5°-30°), and steep zones (higher than 30°) (Suhendra *et al.*, 2018).

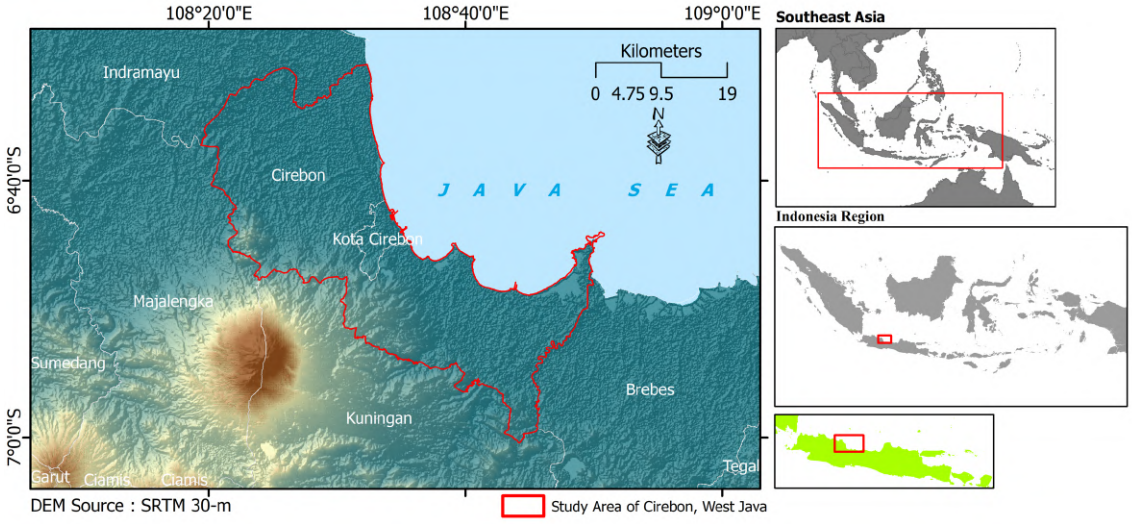

Figure 2.1. The geographical setting of the study location (red polygon) and position in the regional context

Monsoon and topographical conditions affect Cirebon's climate conditions. Referring to the Schmidt and Ferguson classification, the climatic conditions in Cirebon Regency are of types C and D (BPS Cirebon, 2020). The area is characterized by a tropical climate. The dry season usually lasts from March to September, while the rainy season begins in October and ends in February, with 1,300-1,500 mm/per year of rainfall (see *Figure 2.2*) and a mean temperature of 24.2°C (BPS Cirebon, 2020). Cirebon has a tropical climate with the highest average rainfalls of 437.3 mm/month in January. The lowest rainfall occurred in August, with 16 mm/month during the period of 2006 to 2015. The dry season starts from June to October, with an average rainfall of 16.0-167.5 mm/month (PT Cirebon Energi Prasarana, 2016). The monsoon and topographical conditions affect the general climatical condition of this area, with a relative humidity of 65-85%. In the coastal area, the wind blows dominantly from east, northeast, northwest, and north with an average speed of approximately 3.18 m/s.

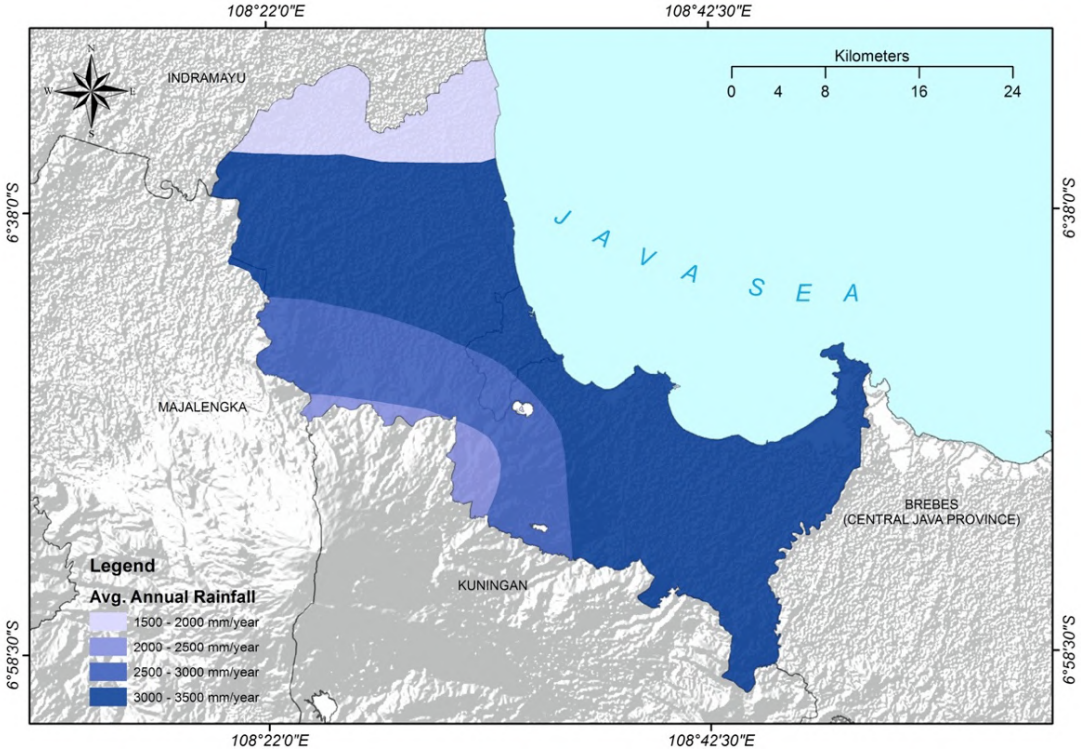

Figure 2.2. Distribution of average annual rainfall in Cirebon (analyzed from Development Planning Board, 2014)

The Java Sea is characterized by relatively shallow water with a mean depth of 50 m, a length of 950 km, and a width of 440 km (Durand and Petit, 1995; Koropitan and Ikeda, 2008). The Java Sea is dominated by the monsoon climate. The northwest monsoon (NWM), with frequent rainfalls and winds, reaches its peak between December and February (DJF), while the Southeast monsoon (SEM) is relatively dry with low rainfalls and commonly occurs from June to August (JJA) (Nagara *et al.*, 2010). The tidal range in the Java Sea is approximately 1.2–2 m, with peak values around Surabaya, Madura, and Bali (ICCSR, 2010; Takagi *et al.*, 2016). In Cirebon Bay, the characteristics of ocean currents and tidal areas are affected by the coastal and geographical positions and its bathymetry (Leksono *et al.*, 2013).

2.3. Illustration of Salt Harvesting in Cirebon, West Java

Currently, salt production dominates the coastal part of Cirebon, involving eight districts along the coastline. Based on KKP (2015), Cirebon has been acknowledged as the most prominent salt production area in Indonesia, with approximately 438 thousand tons per-year of "people's salt," or *'garam rakyat'* in the Indonesian language. It supplied approximately 15% of the domestic salt product in 2015 (KKP, 2015). This sector also absorbs the local domestic job market in West Java. Within a coverage area of around 7,800 ha, salt farming secures jobs for at least 3,700 people, including farmers, workers, and intermediaries (KKP, 2015; PSSDAL, 2010). Until now, traditional salt farming in this region has supported the economic and social welfare of the local population. In addition, salt farming has also been taken forward by the central government into a national program on self-sufficiency (Dharmayanti et al., 2013; Suwarno, 2014). Through the Empowerment of People's Salt Program (PUGAR), the national authority established 40 regencies in 9 provinces in 2011 and covered 33,854.36 hectares (Mun'im, 2015), with around 23% areas located in Cirebon.

Currently, salt farmers in Cirebon mostly apply a traditional technique called the "*Maduranese method*" to produce raw salt. This method can support the domestic market with 60/tons/ha/year (see Munadi *et al.*, 2016). On a daily basis, the current technique relies mostly on solar energy for the evaporating process and the tidal cycle for seawater transport. This traditional method involves (i) purification of the seawater, (ii) evaporation with solar energy, (iii) concentration, (iv) crystallization, and (v) harvesting (Susanto *et al.*, 2015). Here, a farmer installs the windmill to pump the seawater from the channels into the circulated system of ponding. In the worst case, they use a long bamboo scoop to distribute water manually, especially due to low wind force (Apriani *et al.*, 2018).

Conventional salt farming is applied on coastal mudflats as the ground floor for evaporation ponds, with different salinity levels and crystallization ponds (Wang *et al.*, 2015) (*Figure 2.3*). Salt farming applies stages and periodicity where farmers maintain different operations, including construction and production periods (April-May) where farmers prepare the land, such as compacting the salt bed and maintaining the dikes and canals. In the following harvesting period (June-October), farmers start to allow seawater to enter the circular system, where the evaporation process takes place. Guntur *et al.* (2018) stated that seawater evaporation takes around 7-10 days until brine formation. It should be noted that farmers collect salt in this production period and transfer it to the warehouse. At the same time, market transactions are occurring. At a national level, the salt price is regulated through the Rules of the Ministry of Trade No. 125/2015[1]. However, in the local context, it is also formed based on supply-demand and existing stocks. By the end of 2019, Cirebon recorded at least 135.9 thousand tons of salt yields for the whole season (BPS Cirebon, 2020). And lastly, in the off-period, some fields lie barren during the rainy season. Salt is only harvested during the summer period (Davis, 2000). However, during the off period, there is a small number of farmers who go fishing to sustain the household income. *Figure 2.4* portrays the seasonality of salt farming.

[1] The regulation has been renewed through Rules of the Ministry of Law No. 63/2019

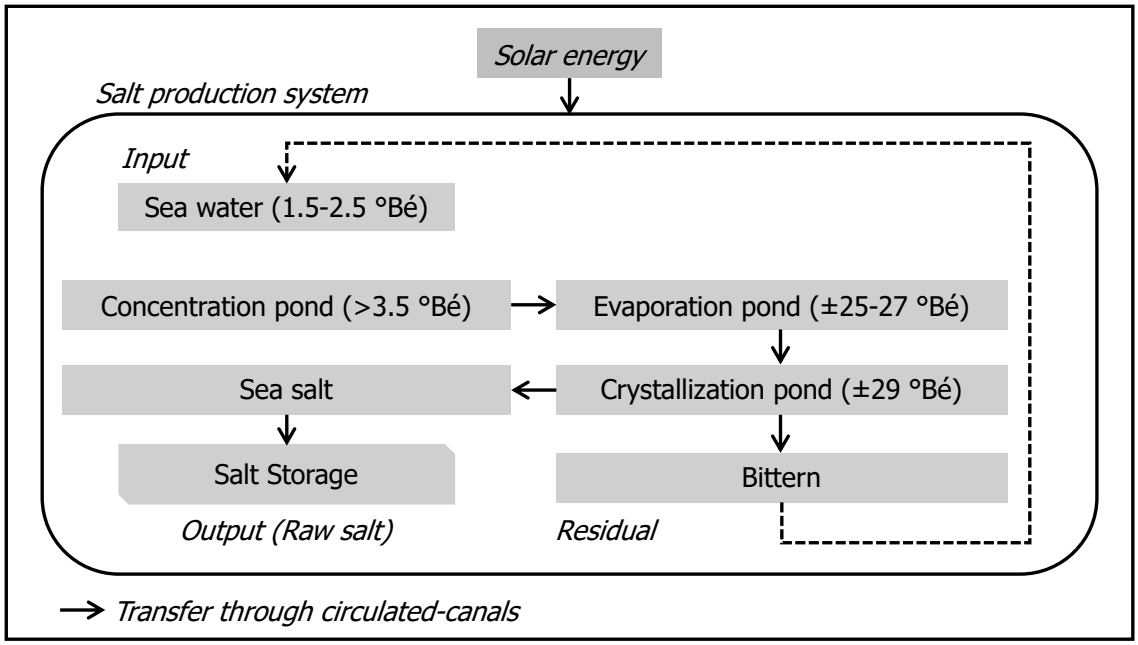

Figure 2.3. General flow process of traditional salt production in the coastal area by mainly using solar energy

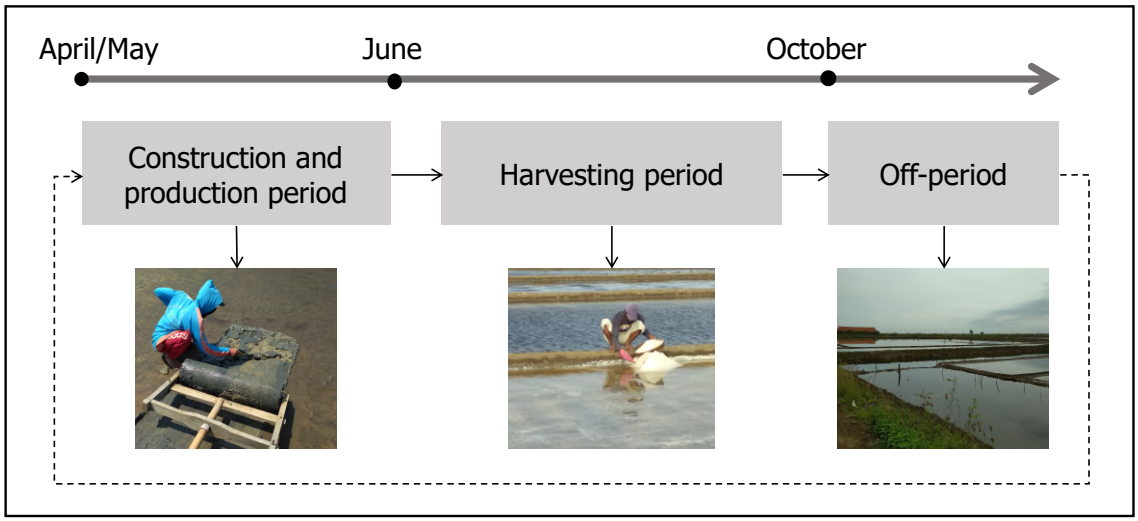

Figure 2.4. Seasonality of traditional salt farming in Cirebon, West Java and main activities of the farmers

2.4. General Approach of the Research: Data Collection and Analysis

A GIS-based approach has been established in this study to obtain a comprehensive understanding of tidal flood occurrence and its implication to salt farming within a poor-data environment and to evaluate the risk. This approach is divided into three phases. Phase 1 includes the literature review, fieldwork I, hydrodynamic simulation using DHI MIKE, and geospatial analysis. Phase 2 consists of fieldwork II, damage function establishment, economic loss estimation and risk evaluation, using a parametric approach. Finally, phase 3 compares a physical-based and parametric model in the risk evaluation. *Figure 2.5* depicts research methods and the research questions' position in this dissertation.

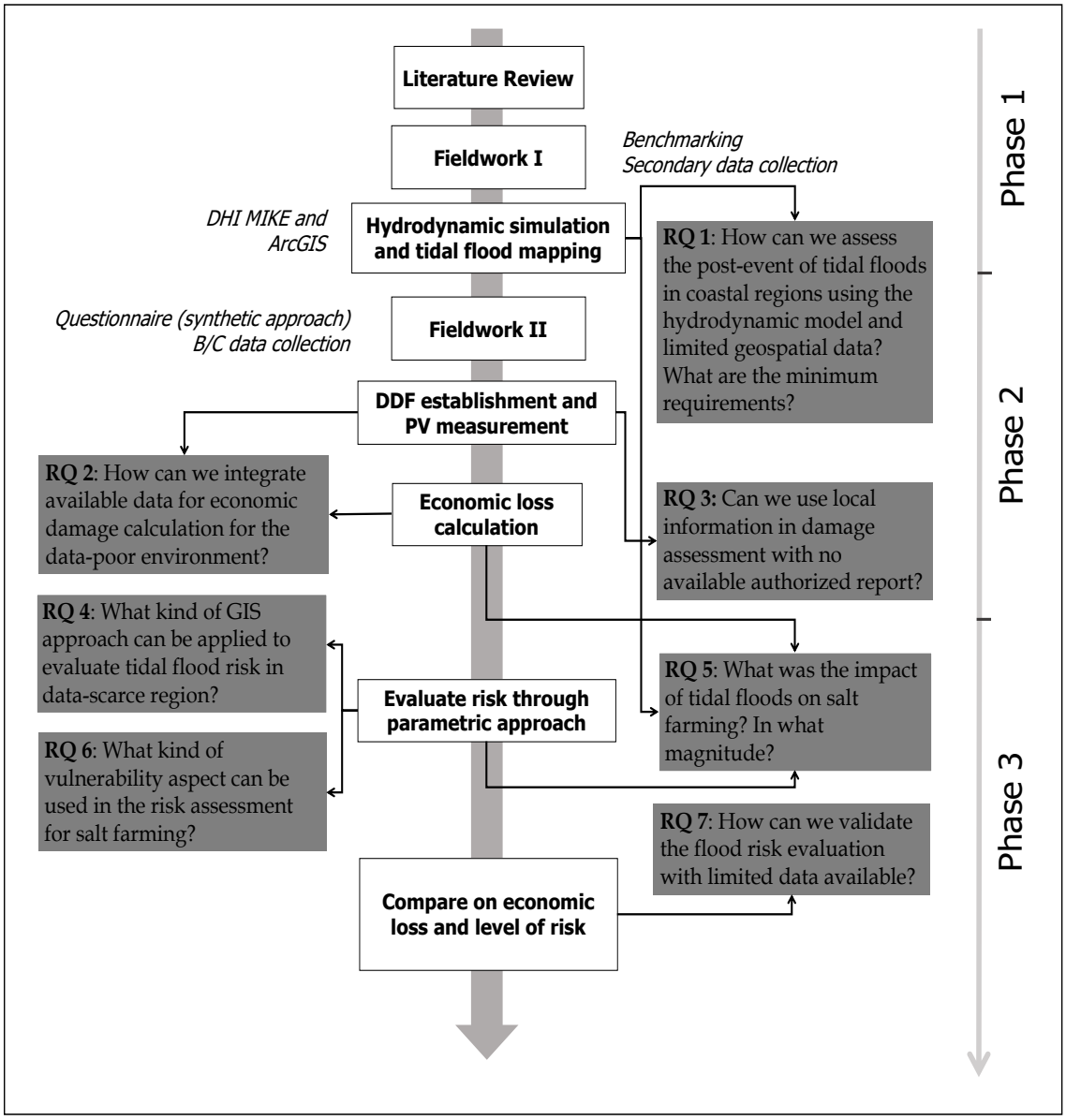

Figure 2.5. Overview of methods used to address the research questions (RQ)

2.4.1. Simulating and mapping of tidal flooding for two-chosen events

The tidal flood simulation of salt farming and mapping with hydrodynamic modeling and GIS is beneficial to identify the magnitude and the spatial distribution of flooding in the study area (as presented in Chapter 3). In this chapter, the simulation was targeted to reconstruct June 2016 (Event A) and May 2018 (Event B), based on the articles from local news (see e.g., Lia, 2016; Metrotv, 2016 for Event A and see also e.g., radarcirebon.com, 2018 for Event B). The objectives of this stage are to (i) validate the tidal flooding occurrence of two events; (ii) identify the maximum water elevation and driving factor through tidal constituent analysis; and (iii) obtain a depth of the inundation and its distribution on salt farming land with GIS.

For the tidal flood simulation and mapping, this research mainly uses a variety of data, including the bathymetry of the Java Sea, the gridded bathymetry of Indonesia (BATNAS) obtained from the Geospatial Information Agency

(referred to as BIG: '*Badan Informasi Geospasial'* in the Indonesian Language) (accessed on http://tides. big.go.id /DEMNAS/) within a 6-second arc resolution. In addition, the data topography for the model was collected from the DEMNAS (0.27 arc-second resolution) and BIG. For the purpose of this research, at least five subsets of DEM were utilized and merged into a one raster layer using GIS. The two types of high-resolution data in the model have been taken to address the need for detailed elevation data (Leitold, 2020; Tehrany *et al.*, 2015; Zalite, 2016). The wind data used in the model was obtained from data provider OGIMET (www.ogimet.com) and salt parcel data on a scale of 1:15,000 from BIG. The hourly water level data from BIG was obtained during Fieldwork 1.

The results of phase 1, as described in Chapter 3, provides valuable information on previous tidal flood events in June 2016 and May 2018. In the model, the expected high-water level (HWL) and low-water level (LWL) has been obtained. In addition, the model also measures the wind parameter and its contribution to tidal generation. It should be noted that the simulation was done using DHI MIKE, as this platform offers beneficial features for the assessment of impacts on the extent, depth, and damage of floods in the present or future (DHI Water and Environment, 2017; Yang *et al.*, 2002). The grid data. resulting from the simulation and combined with salt parcel data in this chapter, delivers the spatial distribution of tidal flooding sequences for both selected events, with crucial detailed information of depth. The validation of the simulated seawater level was held by using TPXO9 as the latest version of the TPXO-series (Green *et al.*, 2018; Seifi *et al.*, 2019). Meanwhile, the water velocity was verified by using the Tidal Model Driver (TMD) in MATLAB (see Padman, 2005). Ultimately, the method gives a fundamental answer for **RQ 1** and **RQ 5**. However, with the characteristics of salt farming features, the model still requires a higher resolution of data (Seenath *et al.*, 2016; Simpson *et al.*, 2015; Webster, 2010), i.e., LiDAR data (Kalligeris *et al.*, 2018; Raji *et al.*, 2011), and more extended tidal gauges data. In contrast to the general bathtub model (e.g., Didier *et al.*, 2018; Marfai *et al.*, 2008), the current approach demands a relatively higher standard of a computing device and takes hours to run the simulation.

2.4.2. Damage function establishment and physical vulnerability assessment

The second fieldwork was conducted from November to December 2019 (Phase 2). The framework of constructing damage function was employed to generate a value of loss towards tidal flood occurrence. As presented in Chapter 4, the research then extracted the water level series data in raster format (ASCII) from the previous numerical model to obtain the flood duration. Due to the limitation, the MIKE simulation was not directly filtered the inundation data. Here, the Mike2Grid tool was used within maximum water level as a benchmark of exporting process. In the final step, depth (f_d) and duration (f_t) layers were reclassified into 25-m cell sizes. In addition to the geospatial data processing, the study specifically distributed a questionnaire to 14 representatives of salt farmer groups from six districts affected by the high-tide flood events. This questionnaire was applied in a synthetic approach, as previously practiced in Vozinaki *et al.* (2015). Specifically, this method was chosen to obtain depth-damage function (DDF). This function was used to address the damage response of ponds to depth

and duration aspects. In addition, the scale of DDF was from 0 to 1 to describe the damage due to tidal flood events.

The integration between DDF and the GIS to evaluate the physical vulnerability (PV) was taken to examine the possible loss due to both events of 2016 and 2018 (**RQ 2**). To formulate the loss, the cost and revenue (C/R) were initiated for two different periods of base pricing (see subchapter 4.1.3). In that section, the basic productivity of 60/tons/hectare (by Munadi *et al.*, 2016) per year was used in the assumption that the majority of salt farmers were traditional farmers (**RQ 3**). The cost for each component, i.e., rent, labor, tools, and devices, etc., was evaluated for each stage of production, while the salt price was also obtained during the second fieldwork. All costs and prices were updated in a short interview with the local authority.

At the end of Chapter 4, this study estimated multiplied vulnerability value based on depth and duration with C/R variables in order to measure the economic impact of tidal events on salt farming. By using salt parcel vector data from BIG, the detailed loss estimation for these two selected events has been presented and mapped to visualize the direct loss. As mentioned in subchapter 4.2.3, the expected loss for the two events was presented, and it answered the previous **RQ 2** and **RQ 5**. At last, this method succeeded in examining the loss on 10,721 parcels individually. However, there were sophisticated procedures that should be noticed in the implementation of this method[2], especially in the extraction of flood duration information in ArcGIS that demands relatively high computing hardware. For this process, the hourly flood depth raster datasets had to be exported individually from a previous hydrodynamic model. Other considerations should be addressed in this model related to the salt parcel data that should represent the recent condition. In addition, the cost and revenue elements probably change from time to time and differ for each location. However, there is still room for further research that includes more components in salt farming, such as warehouse, roads, and existing stocks (Brémond and Grelot, 2013; Molinari *et al.*, 2019).

2.4.3. Risk evaluation and comparison of both approaches

Evaluating the risk of salt farming due to tidal floods was examined, using a parametric approach (**RQ 4**) in Phase 3. The approach, as presented in Chapter 5, employs relevant indicators from the hazard (H) and vulnerability (V) parameters. The method applies a well-known multicriteria approach (MCA) to evaluate the risk based on the R=H*V function. For the purpose of this study, three indicators for hazards, including depth (Luu *et al.*, 2020), duration (Molinari *et al.*, 2014; Serinaldi *et al.*, 2018) and timing of flooding (Glaz and Lingle, 2012), were applied and classified into certain categories. To answer **RQ 6**, the vulnerability parameter was measured by six indicators, i.e., Elevation (Luu *et al.*, 2018; Rincón *et al.*, 2018), coastal slope (Wang *et al.*, 2011), geological feature (Bui *et al.*, 2019), soil type (Cabrera and Lee, 2019), distance to channel and distance to shore (Lyu *et al.*, 2018).

In order to evaluate the risk, the Analytical Hierarchical Process (AHP) was implemented. The reliable method developed by Saaty (1977) has been

[2] In this current model, we used 3-hours separation in order to minimize the processing timespan

widely applied in flood risk assessment (Chakraborty and Mukhopadhyay, 2019; Danumah *et al.*, 2016; Hsu *et al.*, 2017; Tehrany *et al.*, 2015). In this method, as described in subchapter 5.2, the study involved four experts in justifying the all-selected parameters. These experts were from several institutions, including the Ocean and Fisheries Department (DKP) of Cirebon, the Geospatial Agency of Indonesia (BIG), the Spatial Planning Official (BAPPEDA) of West Java, and a researcher from the geomatic department, Brawijaya University, Indonesia. The data collection for the expert judgment itself was held through Zoom, due to the global pandemic, by using a structured sheet taken from the free template available on https://bpmsg.com/ containing the AHP justification variables. This template offers 20 input worksheets for pair-wise comparison in basic Microsoft Excel format (Goepel, 2013).

Following Ghosh and Kar (2018) and Rimba *et al.* (2017), after all the pair-wise comparisons were made, several steps were taken, including determining the Consistency Index (CI), Random Index (RI), and Consistency Ratio (CR). These previous steps were followed to maintain the consistency of the experts' assessment. Within CR < 0.10, the model could be used to generate a weighted score for each indicator in the model. In the formulation presented in subchapter 5.3, the H, V, and R scoring and weighting were expressed in the simple equation. On the same side, the difference of H, V, and R scores in the two chosen periods could be obtained. By using GIS, these scores were used to evaluate each indicator from the H, V maps that were already superimposed with salt parcel data. Finally, the weighted calculation presented in the composite R index was used to portray the risk level of salt farming for each pond (**RQ 5**).

Two distinguished methods can be performed in the flood risk assessment, including the deterministic approach by using a physical-based model and a parametric approach (Balica *et al.*, 2013). With all the pros and cons of both approaches, however, this study tries to evaluate its correlation. To do so, the random sampling (N=270 parcels) was completed to validate this physical-based model with the prior expected economic damage from the numerical model. Again, all sampling and data extraction was done in ArcGIS. For statistical analysis, the study used simple Pearson correlation and compared extracted values from the Risk (R) score and total loss (D_{tot}) scores from all samples. This final step was taken to correspond to **RQ 7**.

Chapter 3

Mapping Impact of Tidal Flooding on Solar Salt Farming in Northern Java using a Hydrodynamic Model

Published as:

Nirwansyah and Braun. (2019), "Mapping Impact of Tidal Flooding on Solar Salt Farming in Northern Java using a Hydrodynamic Model", *ISPRS International Journal of Geo-Information*, Vol. 8 No. 10, p. 451.

CHAPTER 3 - Mapping impact of tidal flooding on solar salt farming in Northern Java using a hydrodynamic model

Abstract

The number of tidal flood events has been increasing in Indonesia in the last decade, especially along the north coast of Java. Hydrodynamic models in combination with Geographic Information System applications are used to assess the impact of high tide events upon the salt production in Cirebon, West Java. Two major flood events in June 2016 and May 2018 were selected for the simulation within inputs of tidal height records, national seamless digital elevation dataset of Indonesia (DEMNAS), Indonesian gridded national bathymetry (BATNAS), and wind data from OGIMET. We used a finite method on MIKE 21 to determine peak water levels, and validation for the velocity component using TPXO9 and Tidal Model Driver (TMD). The benchmark of the inundation is taken from the maximum water level of the simulation. This study utilized ArcGIS for the spatial analysis of tidal flood distribution upon solar salt production area, particularly where the tides are dominated by local factors. The results indicated that during the peak events in June 2016 and May 2018, about 83% to 84% of salt ponds were being inundated, respectively. The accurate identification of flooded areas also provided valuable information for tidal flood assessment of marginal agriculture in data-scarce region.

Keywords: mapping impact; tidal flood; hydrodynamic model; solar salt farming

3.1. Introduction

Globally, coastal flooding have been devastating events causing cost for human environment, increase property damage, and around 20 million people are exposed to present high tide levels and 200 million to storm tide levels (Church *et al.*, 2010; Marfai, King, *et al.*, 2008). Currently, the Intergovernmental Panel for Climate Change (IPCC) report suggests that the global mean sea levels will increase 36–71 cm by 2100 based on Representative Concentration Pathway (RCP) 4.5 mid emissions scenario (Church *et al.*, 2013). This situation may increase the vulnerability of coastal regions, especially of cities, due to demographic trends and economic expansion (Bouwer *et al.*, 2009; Ward, Marfai, *et al.*, 2011). Meanwhile, in developing countries where various types of agricultural activities dominated the local economies, the impact is either ignored or simplified using rough estimates because of low expected losses (Brémond and Grelot, 2013; Forster *et al.*, 2008; Merz *et al.*, 2010). Moreover, local types of agriculture such as solar salt production in tropical countries are also facing the impact of tidal flooding in particular location, which is overlooked in the global discussion. This type of agriculture, however, has the potential to generate revenue from salt in various aspects, not only in terms of salt product quality, but also for tourism, or even partly for coastal research centers (Rodrigues *et al.*, 2011).

Currently, solar salt production is acknowledged to be a marginal economic sector, especially in Indonesia (Rochwulaningsih, 2008). It manually operates through traditional technology by using solar evaporation (Munadi *et al.*, 2016), locally referred to as '*maduranese*' method. The process starts in the saltpan. Seawater is let into the first and largest concentrating pond, or concentrator, through an inlet (Antczak, 2017a). Most of the salt farmers are producing sea salt only during the dry season (April–October). The timing of the process highly depends on weather conditions, as rain reduces salinity and clouds decelerate evaporation (Helmi and Sasaoka, 2018). Tidal flooding upon solar salt farming areas frequently occurs during high tide in the production period and thus threatens the production and distribution processes (see *Figure 3.1*). Between the 5th and 8th of June 2016, high tide flooding inundated hundreds of hectares of salt ponds in Cirebon, West Java, which is one of the major producer sites for salt in Indonesia (Lia, 2016; Metrotv, 2016). Concurrently, the similar astronomic phases during the inundation events, showed the increase of high water level and low water level (Nugraheni *et al.*, 2017). Temporarily, there was another nuisance flood between 23rd and 25th May 2018 along the north coast of Java (locally referred to '*Pantura*') during high tide (radarcirebon.com, 2018). Both events were narrated widely in both electronic and printed media.

Figure 3.1. Setting of traditional solar salt production area including: (**a**) salt evaporation pan and channel; (**b**) nearest pond to the sea; and (**c**) inundated pond due to high tide during fieldwork on 7 January 2018, 11:00 UTC (17:00 local time).

Tidal hydrodynamics in the Java Sea are complicated, due to their rough shallow bottom topography, diverse types of coastlines, and the interference of tidal waves propagating from the Pacific Ocean, Indian Ocean, and South China Sea (Hasan and Rambabu, 2017). Koropitan & Ikeda (2008) previously investigated the implication of the barotropic tides into four tidal harmonic constituents

using a three-dimensional (3D) hydrodynamic model combined with observation data and have suggested that the semi-diurnal M_2 component dominates over Java Sea. Several studies show that wind factor has a minimum contribution to tidal propagation in Java Sea (Hasan and Rambabu, 2017; Koropitan and Ikeda, 2008; Robertson and Ffield, 2005). Tidal flooding in the northern part of Java periodically rises in July and August during the East Monsoon period (Khasanah *et al.*, 2016). In recent years, the tidal inundation comes not only at high tide but even at the regular tide in some areas along *Pantura* (Andreas *et al.*, 2017). Furthermore, the local economy, such as salt production which is dependent on coastal conditions, is eventually disrupted during these events.

Tides caused by the gravitational effects of sun and moon are periodic and very predictable (Haigh, 2017; Marfai and King, 2008; Wolf, 2009). Tidal floods (also defined as "nuisance" flooding) are occurring more often during seasonal high tides or minor wind events, and the frequency is likely to escalate intensely in the forthcoming decades (Jacobs *et al.*, 2018). Currently, the impact of tidal flood is usually modeled using planar approach in geographic information analysis. This approach assumes areas lower than a particular elevation to be inundated utilizing digital elevation model (DEM) and geographic information system (GIS) (Poulter and Halpin, 2008; van de Sande *et al.*, 2012). Geophysical processes including bottom friction or motion transfer are not considered in these particular models (Kumbier *et al.*, 2018). Ultimately, the uncertain behavior of the coastal system during a coastal flooding event is still a challenge in this model (Verwaest *et al.*, 2007). Previous work on GIS modeling presents various resolutions of DEM, which suggest using high resolution of elevation data to increase accuracy (Budiyono *et al.*, 2015; Marfai and King, 2008; Samanta and Koloa, 2014). However, it is the hydrodynamics of the tide that is responsible for the size of the tide range, high and low waters momentum, and tidal characteristic, as well as the speed and timing of the tidal current (Parker, 2007). An integrated approach considering both aspects is recommended, particularly for smaller areas and in cases where details are essential (Kumbier *et al.*, 2018; Seenath *et al.*, 2016; Yang *et al.*, 2002).

In this study, a simulation of the tidal flooding on salt production area is presented. Furthermore, investigations of high tide flooding in the salt production area of Cirebon are not available. The method, implemented in past events using hydrodynamic model with additional inputs on behavior of the coastal system during a tidal flooding event. This approach retrieves the values of the flood impact on the parcel of salt pond from two-dimensional (2D) (floodplain flow) tidal inundation simulation. Against the above background, the objectives of this study are to: (i) validate the tidal flooding that happened in June 2016 and May 2018 using a hydrodynamic model; (ii) analyze the highest tidal elevation and factors associated with flooding using tidal constituent and wind; (iii) plots tidally inundated area upon solar salt production area by considering the spatial distribution and the depths. Finally, this research offers better accuracy of analysis on the distribution of tidal flooding in salt production areas within limitation of tidal flood data.

3.2. Location of the Study Area

Cirebon is located 6°30′—7°00′ S and 108°40′—108°48′ E. It covers an area of 990.36 km². Administratively, Cirebon is a part of the West Java Province and is bordered by the Java Sea, and by Indramayu in the north, Kuningan in the south, Central Java Province in the east, and Majalengka in the west (*Figure 3.2*). It is a typical lowland with an average elevation of 0–25 m and covers 64,500 hectares. Cirebon connects the capital city of Jakarta with major cities in central and east Java. Cirebon has 40 districts, 424 villages, and 12 sub-districts. Based on BPS Cirebon (2016), the port city has an approximate population of 2.1 million, with 2205 inhabitants per km² and a population growth averaging of 1.28% per year.

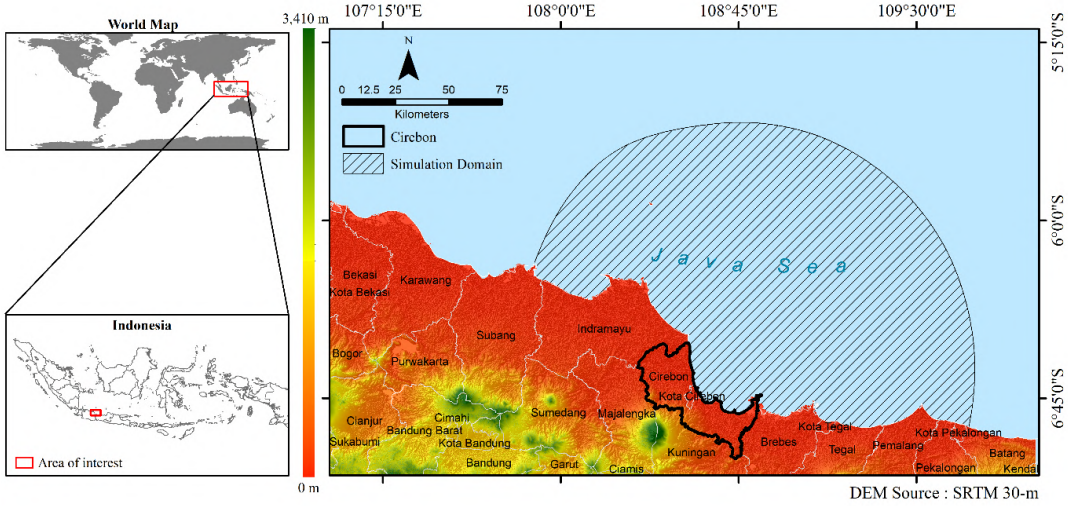

Figure 3.2. Geographical situation in Cirebon within typical coastal lowland adjacent to Java Sea and simulation coverage area.

Along with agriculture, salt production is shaping the local economy in the coastal region of Cirebon. The salt ponds cover 7819.32 hectares and provide jobs for 3707 people, such as pond owners, salt workers, and intermediaries (KKP, 2015; PSSDAL, 2010). Salt production predominantly takes place in low-lying areas dominated by alluvial deposits alongside with mangrove ecosystems. The salt production period in Cirebon begins during southeast monsoon. Most of the farmers start to store seawater in April, May, or June depending on the weather. They start to collect the brine daily and generate yields 0.5-1 ton/hectare/day. The dry season begins in March and ends in September, with a mean temperature of 32.8 °C, while the rainy season usually lasts from October to February, with an average rainfall of 1300-1500 mm/year and an average temperature of 24.2 °C (BPS Cirebon, 2016). The tidal regime is dominated by a mixed semidiurnal type and experiences two high and two low tides of different scales each lunar day. This tidal characteristic dominates the tidal cycle along Java sea (Mustaid and Tetsuo, 2013).

The Java Sea is mainly identified as shallow water within roughly rectangular morphology, a mean depth of 50 m, a length of 950 km, and a width of 440 km (Durand and Petit, 1995; Koropitan and Ikeda, 2008). The tidal range in the Java Sea is approximately 1.2–2 m, with peak values around Surabaya, Madura, and Bali (ICCSR, 2010; Takagi *et al.*, 2016). The Java Sea is strongly

governed by the monsoon climate. The northwest monsoon (NWM) reaches its peak between December and February (DJF) and it is usually characterized by frequent rainfalls and windy periods, while the Southeast monsoon (SEM) extends from June to August (JJA) and is usually characterized by much lower rainfalls (Nagara *et al.*, 2010).

3.3. Materials and Model Description

3.3.1. Data acquisition

This study has used several data to simulate post-events of tidal floods. Firstly, the bathymetry and land topography information for the domain areas were handled as two main inputs for the model. Bathymetry of the Java Sea has been generated using gridded national bathymetry of Indonesia (BATNAS) provided from the Geospatial Information Agency (we referred to BIG: '*Badan Informasi Geospasial*' in Indonesian) (http://tides.big.go.id/DEMNAS/) within a 6 arc-second resolution. This data has been produced through the inversion of gravity anomaly of altimetry by adding sounding data carried with single and multi-beam surveys, which has better resolution in coastal areas than GEBCO (30 arc-second) (BIG, 2018; Heidarzadeh *et al.*, 2018). Land topography data was resolved using the DEMNAS (0.27 arc-second resolution) also from BIG. DEMNAS is national seamless digital elevation data which already constructed within assimilated data of IFSAR (5-m resolution), TerraSAR-X (5-m resolution) and ALOS PALSAR (resolution 11.25 m), by adding stereo-plotting mass-point data (BIG, 2018). This research draws on a previous approach by Tehrany *et al.* (2015) and Zalite (2016) to utilize detailed topographic data for flood models. Here, five subsets (1309-12, 1309-14, 1309-21, 1309-23, and 1309-24) of DEM within the 0.27 arc-second spatial resolution were employed, and merged into a single raster data using GIS.

Secondly, tidal level data for Cirebon waters were captured from local tidal station in Cirebon port operated by BIG. In this case, we used hourly data of both selected period of simulations. As additional input, the simulation included wind data in the form of wind velocity, and wind direction of the Jatiwangi station. This data was extracted from OGIMET online meteorological database (https://www.ogimet.com/). Lastly, this model involved the latest (updated 2015) of the salt parcel dataset taken from the ministry of marine and fisheries affair during the salt inventory mapping project together with the national geospatial agency and PT. Garam (PSSDAL, 2010). At this point, salt parcel can clearly separate each pond by scale of 1: 15,000 in polygon format and was referenced into the World Geodetic System 1984. Details of data needed on this research are mentioned in *Table 3.1.*

Table 3.1 Data requirement for salt farming impact due to tidal flood

Data type	Resolution	Location	Period	Source
Bathymetry	6-arc "	Modeled expanse	2018	BIG
Topography	0.27 arc"	Cirebon area	2018	BIG

Water level (ζ)	1 h	Cirebon port	June 2016, May 2018	BIG
Wind velocity (u, v) and direction	1 h	Jatiwangi	June 2016, May 2018	OGIMET
Tidal calibration (ζ, u, and v)	1 h	T. Sari, Pangenan, Bungko	June 2016, May 2018	TPXO, TMD
Salt parcel	1:15,000	Cirebon area	2015	BIG

3.3.2. Model setup

This research applied a numerical hydrodynamic model (HDM) to forecast run-up and tidal inundation in the salt production area in Cirebon. HDMs originated through resolving Laplace Tidal Equations and using bathymetry data as boundary conditions (Arabelos *et al.*, 2011). The module of MIKE 21 package was used, as one of the most widely used hydrodynamic model in computation by Danish Hydraulic Institute (DHI), including the assessment of hydrographical sequences in non-stratified waters, coastal flooding and storm surge, inland flooding, and overflow (Nguyen, 2017; Qiao *et al.*, 2018; Thambas, 2016). The MIKE package also represents user-friendly GIS interfaces and provides better possibilities to simulate the flooding using elevation data and bathymetry (Faber, 2006).

The model employed MIKE 21 Flexible Mesh (FM) to simulate water levels and tidal flooding in selected events. These tools were utilized using the input of tidal gauge records to indicate the spatial variability of tidal flood characteristics of two events. The model was applied for two separated months, June 2016 (event A) and May 2018 (event B), which covered the occurrence of the selected tide flood events. The unstructured triangular mesh with 87,103 nodes and 170,501 elements was generated in the simulation and covered 11,515.20 km^2 (see *Figure 3.3*). The mesh file in ASCII format included information of the coordinates and bathymetry for each node point in the mesh (Thambas, 2016). The grid dimension differs by 2800 m in the northeast ocean boundary, the smaller grid size around 450 m in the outland, and 120 m in the inland area.

The tidal flood events, which were triggered by high tides, were simulated through forcing tidal elevations at open borders, winds, and temperatures. The tidal height was calculated by hourly local station measurement using a harmonic approach. This classical harmonic analysis represents the tidal forcing as a set of spectral lines, demonstrating the predetermined set of sinusoids at specified frequencies (Consoli *et al.*, 2014; Pawlowicz *et al.*, 2002). This stage resulted in nine tidal components (M_2, S_2, N_2, K_2, K_1, O_1, P_1, M_4, and MS_4) that correspond to specific physical phenomena such as the period of the moon around the earth or friction against the seabed in shallow seas.

Following step of this model was to include the wind energy and set tilt facility to declare water level correction along the boundary of the waters using Navier-Stokes equations. These equations deliver an appropriate model for wave overtopping and overcome sophisticated hydrodynamics, including wave breaking and its theoretical limitation (Fernández *et al.*, 2018; Kalligeris *et al.*, 2018). Furthermore, the flood and drying (FAD) ability of this model assisted the water run-up simulation and executed the inundation process of high tides. This

scheme has been alternated to describe the coastal situation, where it can be flooded at one time but dry at other times. This study use recommended value in Thambas (Thambas, 2016), h_{dry} = 0.005 m, flooding depth h_{flood} = 0.05 m and wetting depth h_{wet} = 0.1 m.

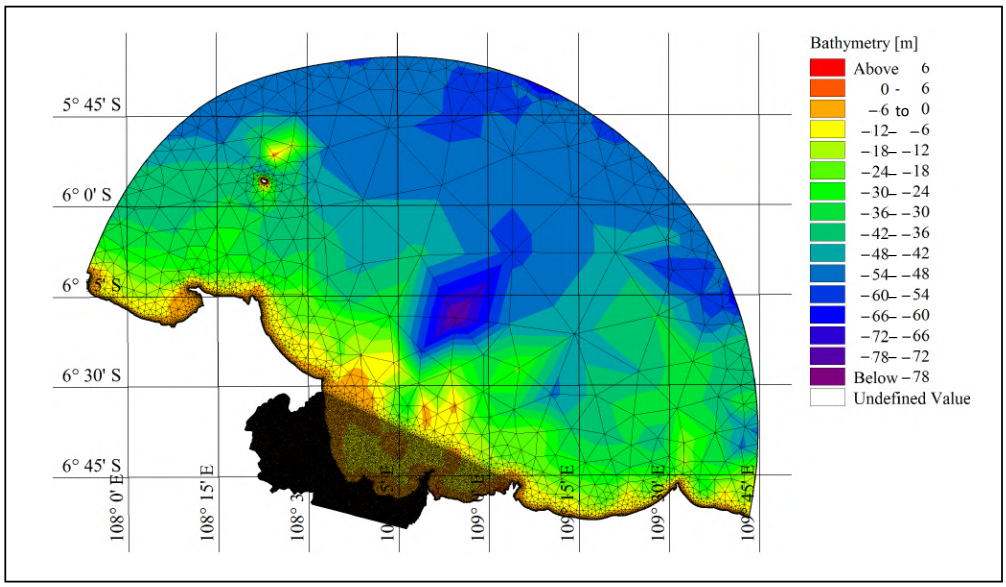

Figure 3.3. Mesh generation of Cirebon waters and part of Java Sea, bathymetry (in meters), comprising of 87,103 nodes and 170,501 triangular elements.

It should be noted that the elevation data is used in this simulation without considering water surface evaporation. Due to the high complexity of the site study and the limitations of the model, the following steps were considered for the tidal flood simulation: bottom friction is based on Manning's approach, with the ranges of friction coefficients from 40 for water to 32 for land (Department of Environmental Protection, 2014). A Manning number in the range 20-40 m $^{1/3}$/s is typically applied with an advised value of 32 m $^{1/3}$/s if other data is unavailable (Elsaesser *et al.*, 2010). The Manning number relates to the flow path and peak time of flooding and does not have a significant effect on flood distribution and depth (Wang *et al.*, 2006). Furthermore, the simulation included horizontal eddy viscosity using the Smagorinsky type within a value of 0.28 (Nguyen, 2017).

After the work with MIKE had been completed, the result was exported using "MIKE2Grid" for further spatial processes. This produced an ASCII file that is readable in ArcGIS. Importing this file and reorganizing the classes produced the inundation map of MIKE 21. Finally, we superimposed the grid data to the salt parcel dataset and used the tidal simulation as a basis in inundation analysis process. This plot dataset has a shapefile format, which is suitable for further handling in ArcGIS. The inundation map was created by using grid data of both simulations in ArcGIS. The two-top water levels of the selected simulations, which were identified with the maximum value in the data series that was used as a benchmark for inundation analysis. In this research, certain assumptions were made, such as that no precipitation data inputs were used during the period of the incident as it may raise the inundation level, no sea-level rise and land subsidence were considered in the simulation, as there is still no strong local

evidence of both factors in the research location. The overall steps of this research are summarized in *Figure 3.4.*

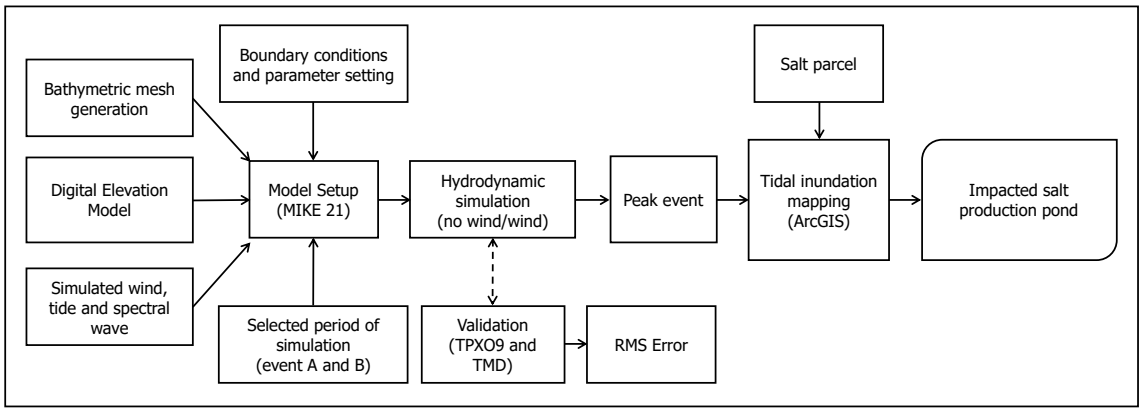

Figure 3.4. Diagram of simulation of tidal flood and impact mapping procedure including validation process.

3.4. Results

3.4.1. Validation of tidal simulation

To get a sound validation of our model for tidal simulation, this study used tidal data of the open boundary model that were obtained from the global tidal model. Following the step from Ningsih *et al.* (2011), the model compared the results of simulated sea level from MIKE 21 with tidal station in Cirebon from BIG and also the global tidal model TPXO9 (this model can be accessed on http://volkov.oce.orst.edu/tides/global.html). TPXO9 is the latest version of TPXO-series (Green *et al.*, 2018; Seifi *et al.*, 2019), which includes global tidal solutions with 1/6° resolution that fit, in least-square, both the Laplace's equation and also the long track averaged data from TOPEX/Poseidon and Jason (on T/P tracks since 2002) (Egbert and Erofeeva, 2002; Green *et al.*, 2018). Tidal constituents of the tide record from BIG tidal station perform comparable values with tidal constituents from the global tide modeling TPXO in Indonesian waters (Taufik and Safitri, 2014). At this point, the wind factor was excluded and focused on gravitational force only. Moreover, the tidal current velocity was verified with Tidal Model Driver (TMD). This free MATLAB package offers harmonic constituents for tide models, making predictions of tide height and also currents (Padman, 2005). Verification points of the selected simulations (event A and B) are located in Tawangsari, Pangenan, and Bungko (as pointed P1-P3 in *Figure 3.5*). The model exposed the statistical correlation using the Pearson value (r) of the three locations with general tidal model of TPXO9, and presented the value of the Root Mean Square (RMS) error. The RMS error was calculated with equation 1:

$$x_{RMS} = \sqrt{(\sum_{i=1}^{n} x_i^2) / n} \qquad \text{Eq. 1}$$

where x_i is the i^{th} point of the chosen area, were calculated in the region 6°S-7°S, 108°E-109°E (the Java Sea). The overall locations verified excellent correlations between simulated outcomes and those of TPXO9 and TMD.

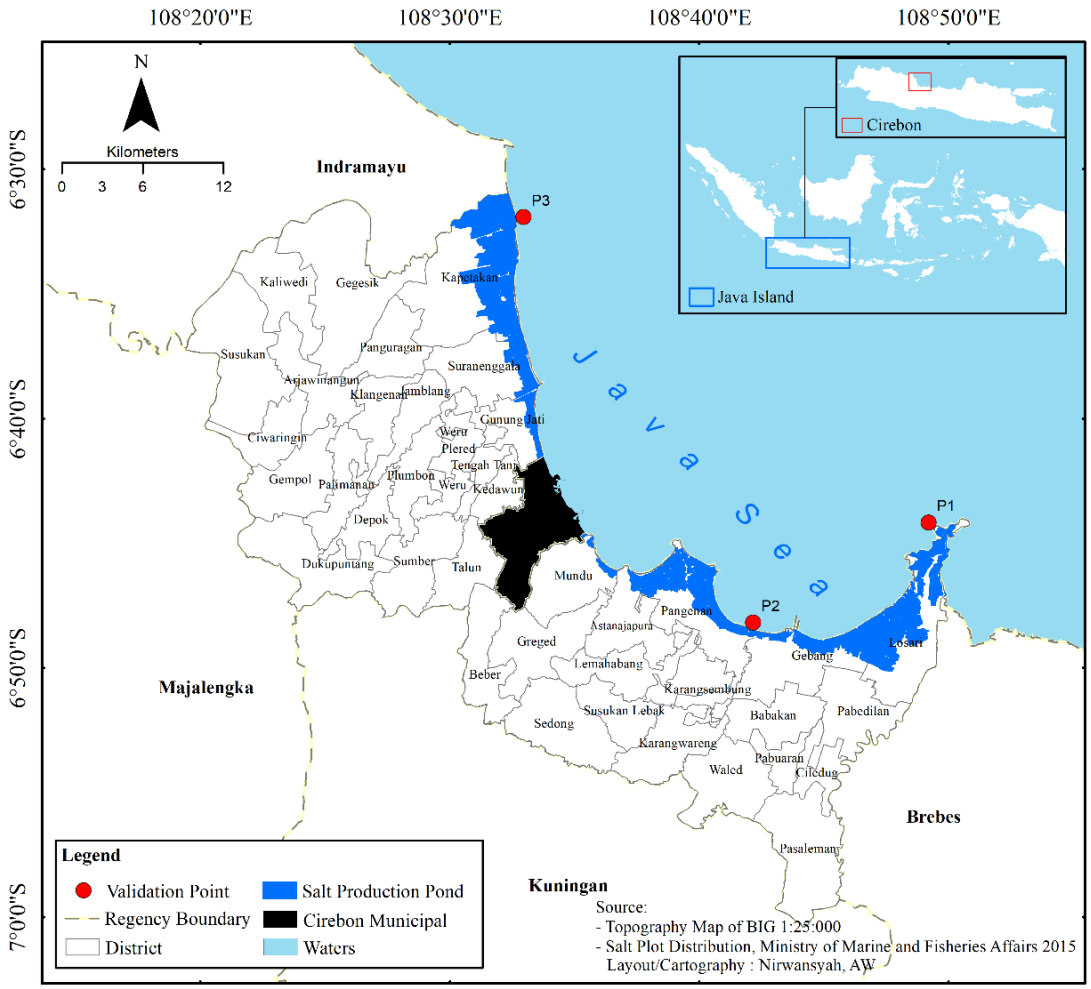

Figure 3.5. Salt production area for tidal simulation and validation points (P1-P3).

The Pearson correlation of the tidal height simulation is in the range of 0.903–0.908 for event A and of 0.848–0.903 for event B with the RMS Error within approximately 0.069–0.100 m. For the *u*-velocity component, the correlation shows a coefficient around 0.833–0.965 with RMS Error of about 0.023–0.0196 m/s for event A. For event B, the correlation coefficients range between 0.570 and 0.877 with RMS Error around 0.019–0.190 m/s. Furthermore, the *v*-velocity component shows a good agreement of the correlation coefficient, whereas the number of the correlation is about 0.683–0.824 with RMS Error about 0.040–0.061 m/s. Although there were some inconsistencies between *u*-velocity components in MIKE 21 simulation on event B, overall, the simulation results managed well with the TMD data. Lower values of RMS Error suggested the appropriate model to the data points; likewise, values of Pearson close to the maximum point of one (value of 1) indicated that the model has a strong correlation to the water level data (Berlianty and Yanagi, 2011; Latief *et al.*, 2018). Detailed values of Pearson Correlation and RMS Error between simulation and global tide model of TPXO9 for water elevation and those TMD for tidal velocity elements are shown in *Table 3.2*. The illustration for tidal height (ζ), *u* and *v*-velocity at verification points can be seen in *Figure 3.6–3.8*.

Table 3.2 Pearson Coefficient (r) and Root Mean Square (RMS) Error between simulation rates in MIKE and TPXO9 for water elevation and velocity components from TMD.

Stations	Tidal height (ζ)		u-velocity component		υ-velocity component	
	r	RMSE (m)	r	RMSE (m/s)	r	RMSE (m/s)
Tawang-sari						
• Event A	0.903	0.071	0.894	0.0196	0.715	0.061
• Event B	0.891	0.075	0.877	0.0190	0.683	0.059
Pangenan						
• Event A	0.904	0.100	0.833	0.029	0.724	0.050
• Event B	0.903	0.075	0.814	0.019	0.755	0.059
Bungko						
• Event A	0.908	0.069	0.965	0.023	0.824	0.048
• Event B	0.848	0.088	0.570	0.073	0.705	0.040

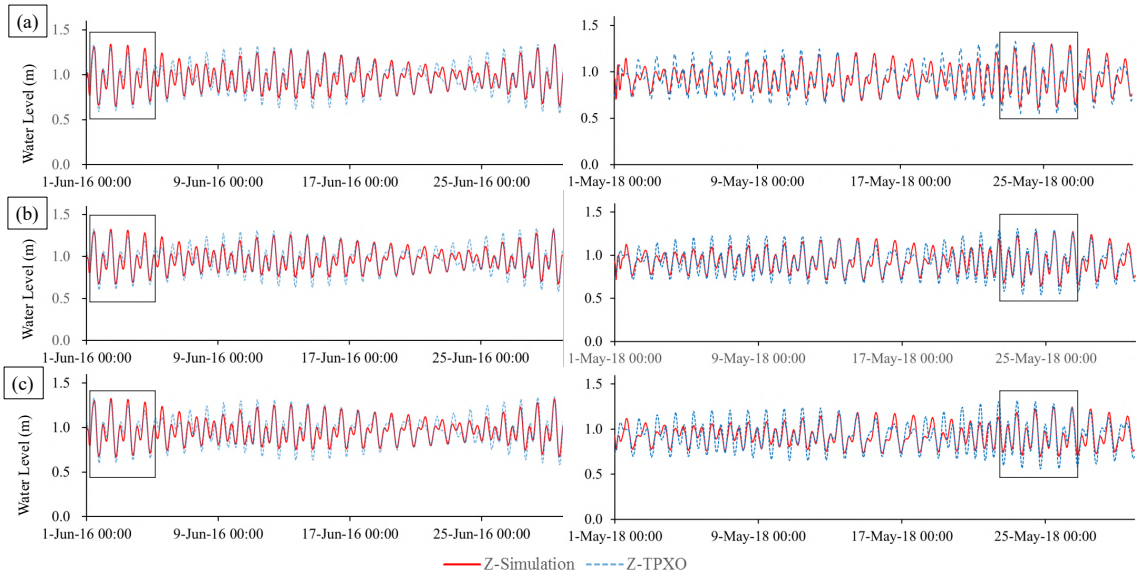

Figure 3.6. Comparison of water level between simulation and TPXO on June 2016 (left) and May 2018 (right) at (**a**) P1—Tawangsari; (**b**) P2—Pangenan; and (**c**) P3—Bungko.

Spring tides (at the new moon phase) appeared in between the flooding events of event A, which was recorded from June 1st–5th, 2016. In event B, the high tides were tracked from the 23rd to the 28th of May during the end of the moon phase. In both of these conditions, the rise of waves is a natural phenomenon due to moon force (M_2) (Robertson and Ffield, 2005). However, on the three tide validation points, the increase of high-water levels (HWL) and low water levels (LWL) during the inundation events can clearly be compared to the same astronomic phases' tides data before and after the events (see black boxes in *Figure 3.6* above). Moreover, the horizontal (u) velocity on three sample locations

show typical performances within range of 0-10 m/s and vertical (v) velocity in range of 0-28 m/s (see *Figure 3.8-3.9*). Here, it can be seen that there are differences velocity level between the simulation and the TPXO model in three sample locations, which are explained in the previous section.

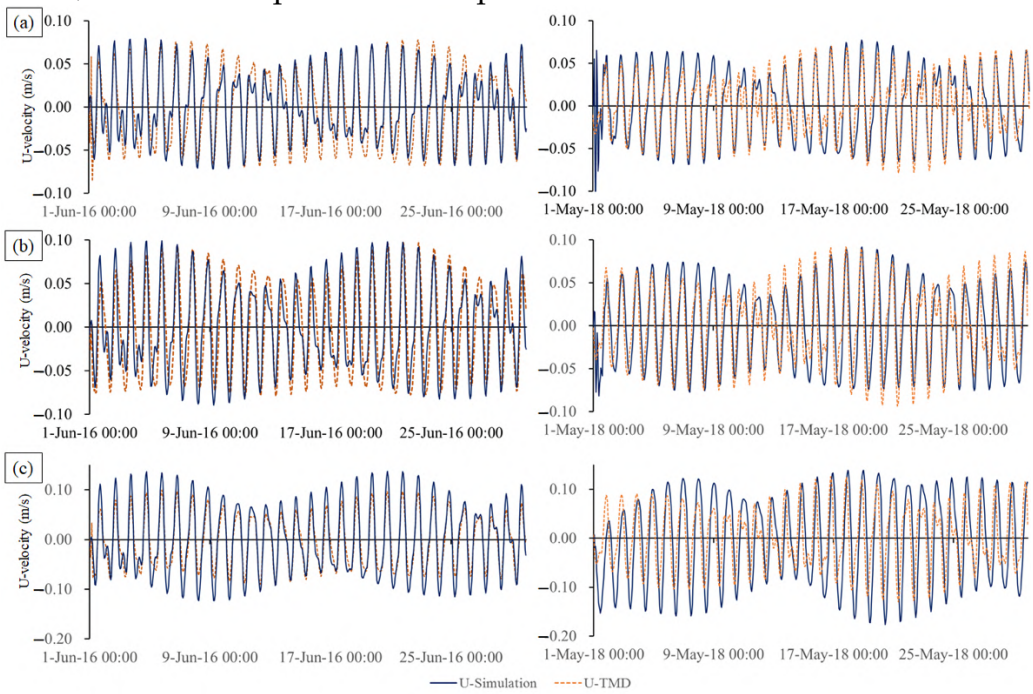

Figure 3.7. Comparison of u-velocity component between MIKE and TMD on June 2016 (left) and May 2018 (right) at (**a**) P1—Tawangsari; (**b**) P2—Pangenan; and (**c**) P3—Bungko.

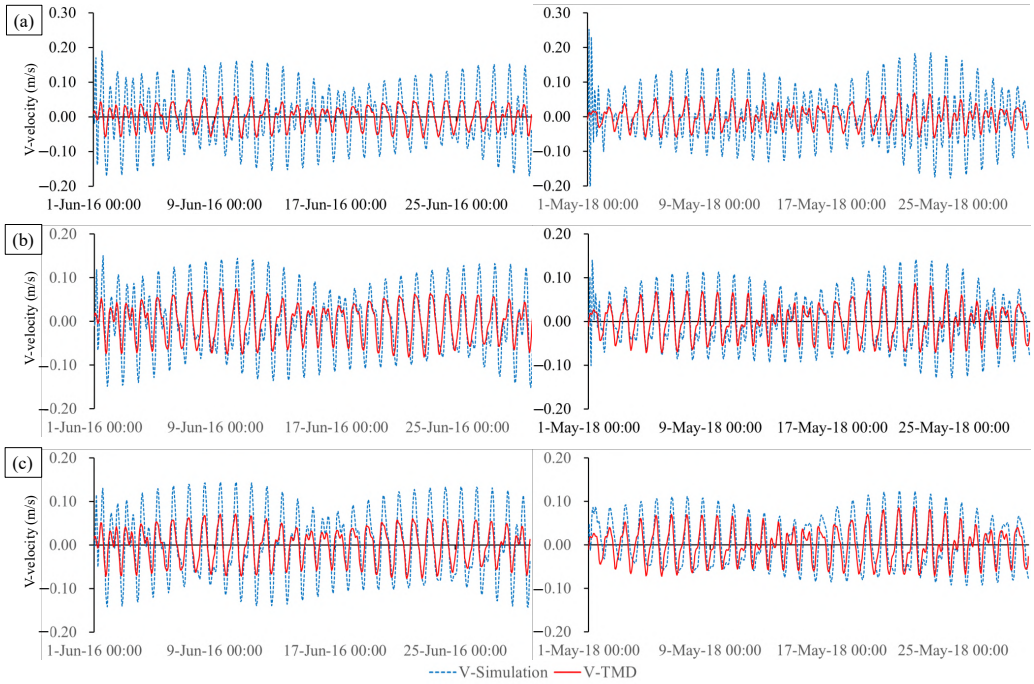

Figure 3.8. Comparison of υ-velocity at verification points and TMD on June 2016 (left) and May 2018 (right) at (**a**) P1—Tawangsari; (**b**) P2—Pangenan; and (**c**) P3—Bungko.

In the next step, the wind air pressure data were engaged in the model as an additional factor in tidal propagation. Wind data from OGIMET has been entered into the simulation for both selected periods. Adding hourly wind data into the model shows minor differences of amplitudes and phases of tidal constituents. The simulations show that there is an insignificant difference in the tidal pattern due to the relatively small effect of wind, as the velocity of wind dominantly emerged from the north with a maximum speed of 6.8 m/s during event A and an average velocity around 0.81 m/s. For event B, an extreme increasing velocity of 60.48 m/s is recorded in the simulation. Ultimately, the average wind speed is approximately 0–1.49 m/s. Here, the assumption has been made that typically calm wind in both selected periods has a minor impact on tidal floods along the coast.

Wind velocity confirmed a minimum correlation to the water level (Pearson correlation 0.1902-0.1905 for event A and –0.021 to –0.031 for event B). The negative correlation probably relates to the minimum velocity of the wind, as OGIMET provides hourly datasets in both periods of simulation. The typically calm wind during these periods provides a better situation for evaporation in the salt production process. Nevertheless, high tide continually increases the potential of inundation in coastal areas where salt production takes place. At the same time, the water elevation of the simulation also shows significant correlation to the observation data from tide gauges (see *Figure 3.9a-b*). *Figure 3.9c-d* present the peak tide levels for both events. Here, the series of surface water (*z*) data from MIKE 21 simulation are also used to determine the nine tidal components. Here, *Table 3.3* presents the variability of tidal constituents in both periods of the model.

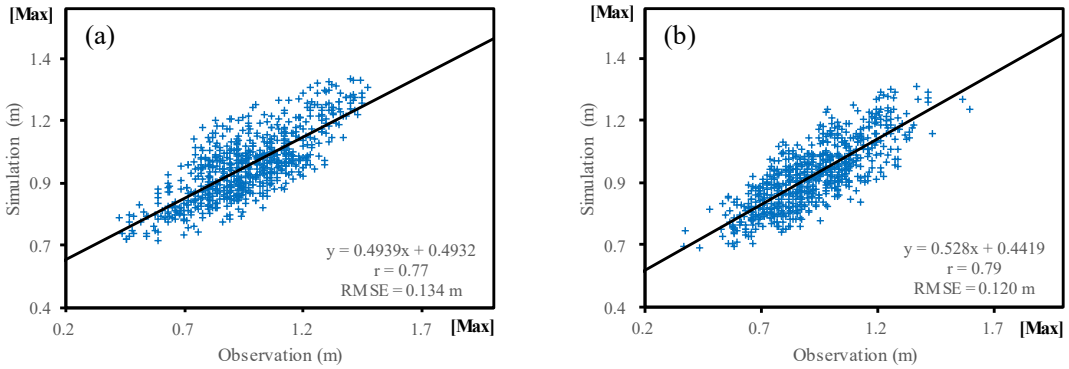

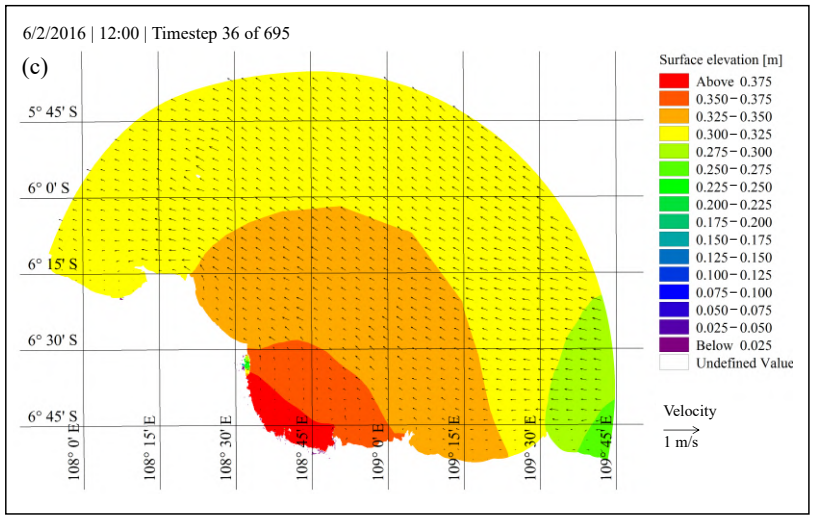

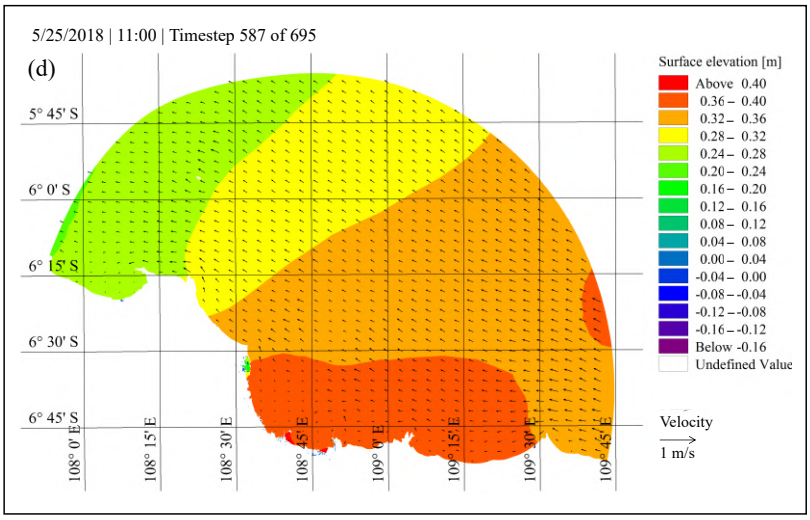

Figure 3.9. Scatterplot and RMS error of simulated surface water elevation with tide gauge observation on: (**a**) event A; (**b**) event B within peak level of water during simulation on; (**c**) 2 June 2016 12:00 UTC (steps 36); and (**d**) 25 May 2018 11:00 UTC (steps 587).

Table 3.3 Tidal amplitudes constituents in Cirebon resulted from simulation

Simulation	Tidal Constituent									
	Z_0	M_2	S_2	N_2	K_2	K_1	O_1	P_1	M_4	MS_4
Event A	0.939	0.143	0.062	0.044	0.051	0.107	0.040	0.042	0.001	0.002
Event B	0.902	0.143	0.059	0.048	0.004	0.088	0.049	0.014	0.004	0.001

Based on the calculation, the wind involved in the simulation showed correlation values to tidal gauge observation 0.761 with RMSE of 0.134 m for event A and 0.79 with RMSE 0.120 m for event B. As a result, surface elevation at the peaks of both tidal events in Cirebon reached 0.38 m (event A) on the 2nd of June 2016 12:00 UTC and 0.40 m (event B) on the 25th of May 2018 11:00 UTC. Gurumoorthi and Venkatachalapathy (2017) and Pugh (1987) mentioned that the relative importance of diurnal and semi-diurnal components differ with geographical position and can be calculated by the formulation factor:

$$F = (O_1 + K_1) / (M_2 + S_2) \quad (2)$$

In Equation (2), the average constituents confirm the typical mixed, predominantly semi-diurnal tide within 0.73 and 0.68 for both events A and B. Considerably, the amplitudes of semidiurnal tidal constituents were higher than the diurnal tides.

3.4.2. Maximum tidal height and exposed salt production area

Understanding the impact of tidal flood dispersal on the coastal area demands a model of inundated area caused by tide water level (Marfai and King, 2008). Equilibrium flood mapping or the "bathtub" approach compare the maximum total water level and ground height. At those places, where the land is lower than the expected maximum water level, it will be flooded (Gallien *et al.*, 2011). The expected water depth for each salt pond can have major implications for tidal management, especially for vulnerability measurements as damage is

often associated with the depth of inundation and its duration. The simulation showed that both tidal floods were forecasted to be generated by meteorological factors. Here, M_2 tidal response provides the dominant influence (which both events record 0.143) in amplitudes of Cirebon waters. As a result, the surface elevation during the maximums of both tidal events have been exported in ArcGIS using Mike2Grid tools and visualized water level and the spatial distribution of the inundation upon salt production area (see *Figure 3.10).*

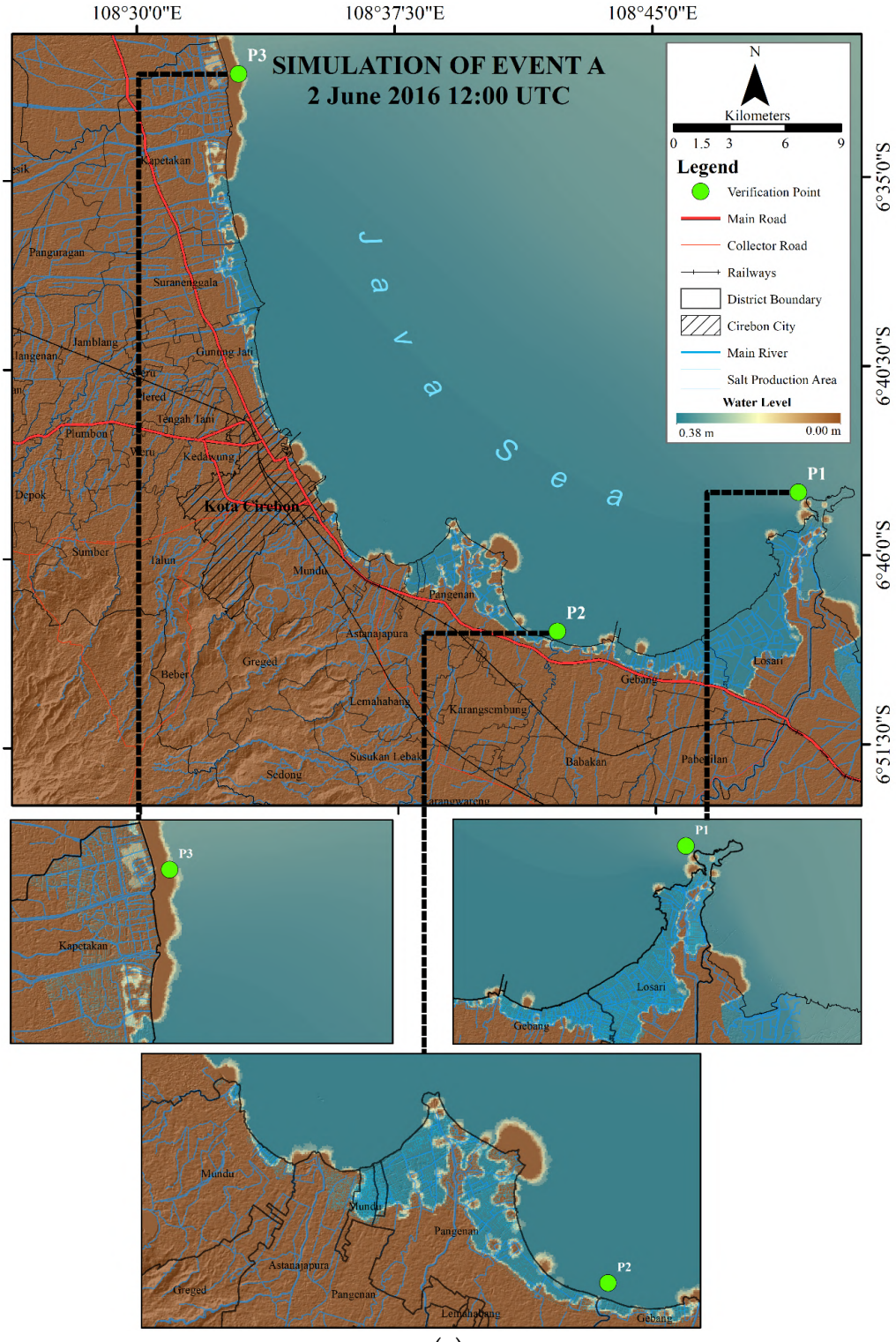

(a)

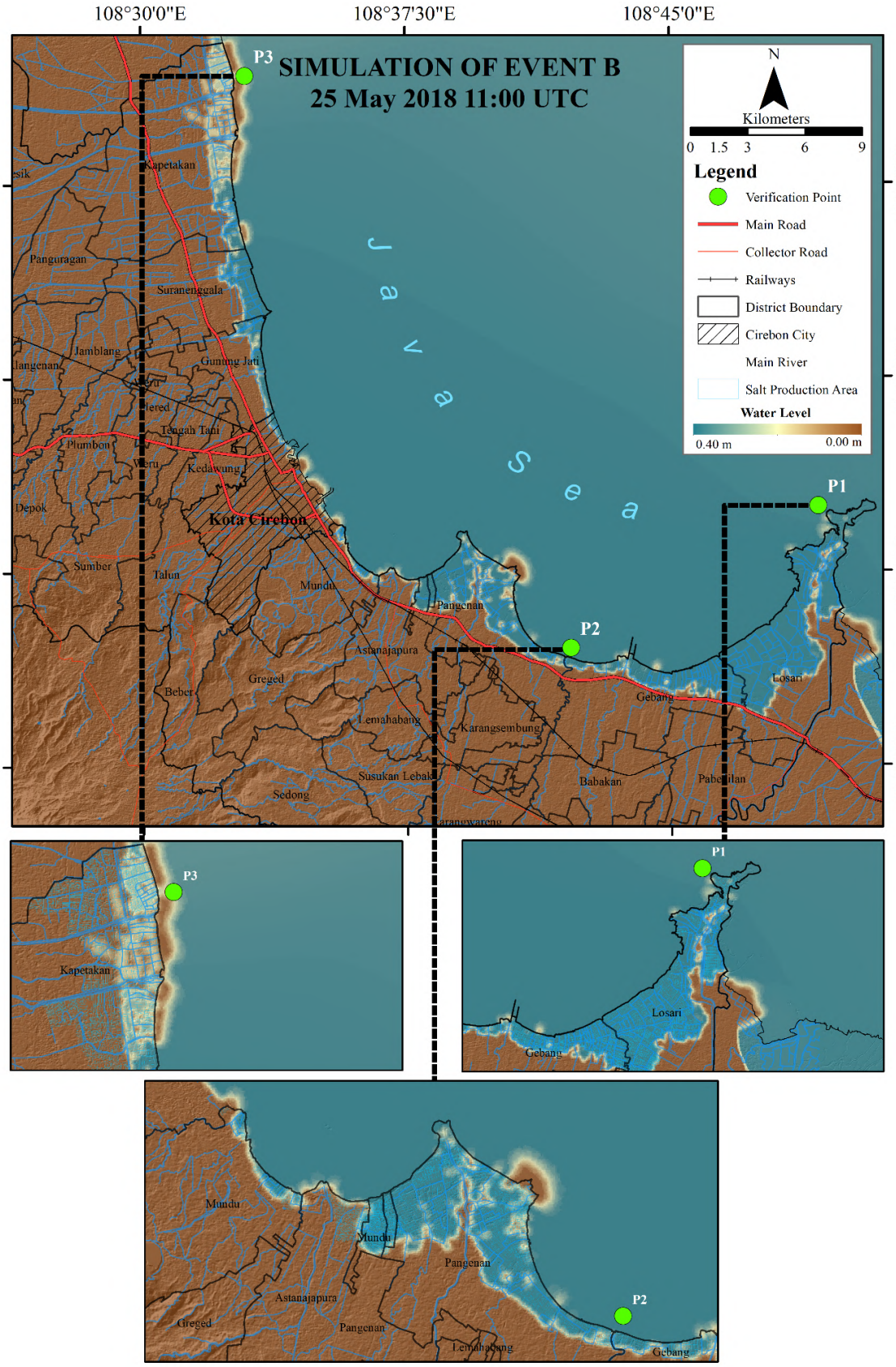

(b)

Figure 3.10. Simulation of water level during peak period of: (**a**) event A and (**b**) event B.

The simulation map shows that tidal inundation occurs along the coastline of Cirebon during peak water levels. The grid data was superimposed with detailed DEMNAS to investigate the impact of tidal flooding upon solar salt production land. A reclassification process in GIS elaborates the tidal dynamics and flood depth upon salt pond in the study area. Here, each salt parcel has a single value of depth level through spatial joint between both vector types of water level and parcel of salt pond datasets (*Figure 3.11).* Thus, this results in the appropriate value for inundation for each pond that has been impacted by the tidal occurrence for both events.

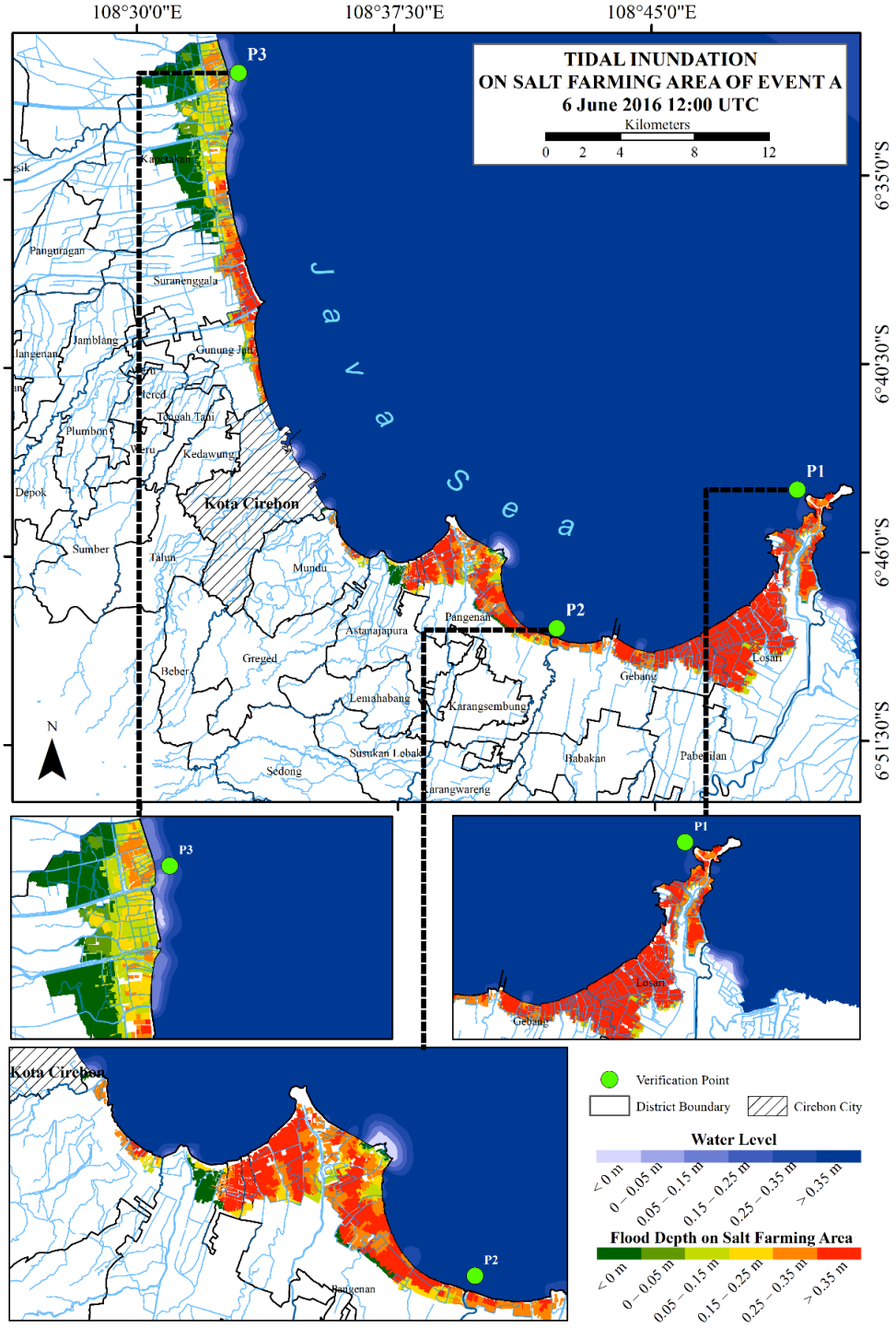

(a)

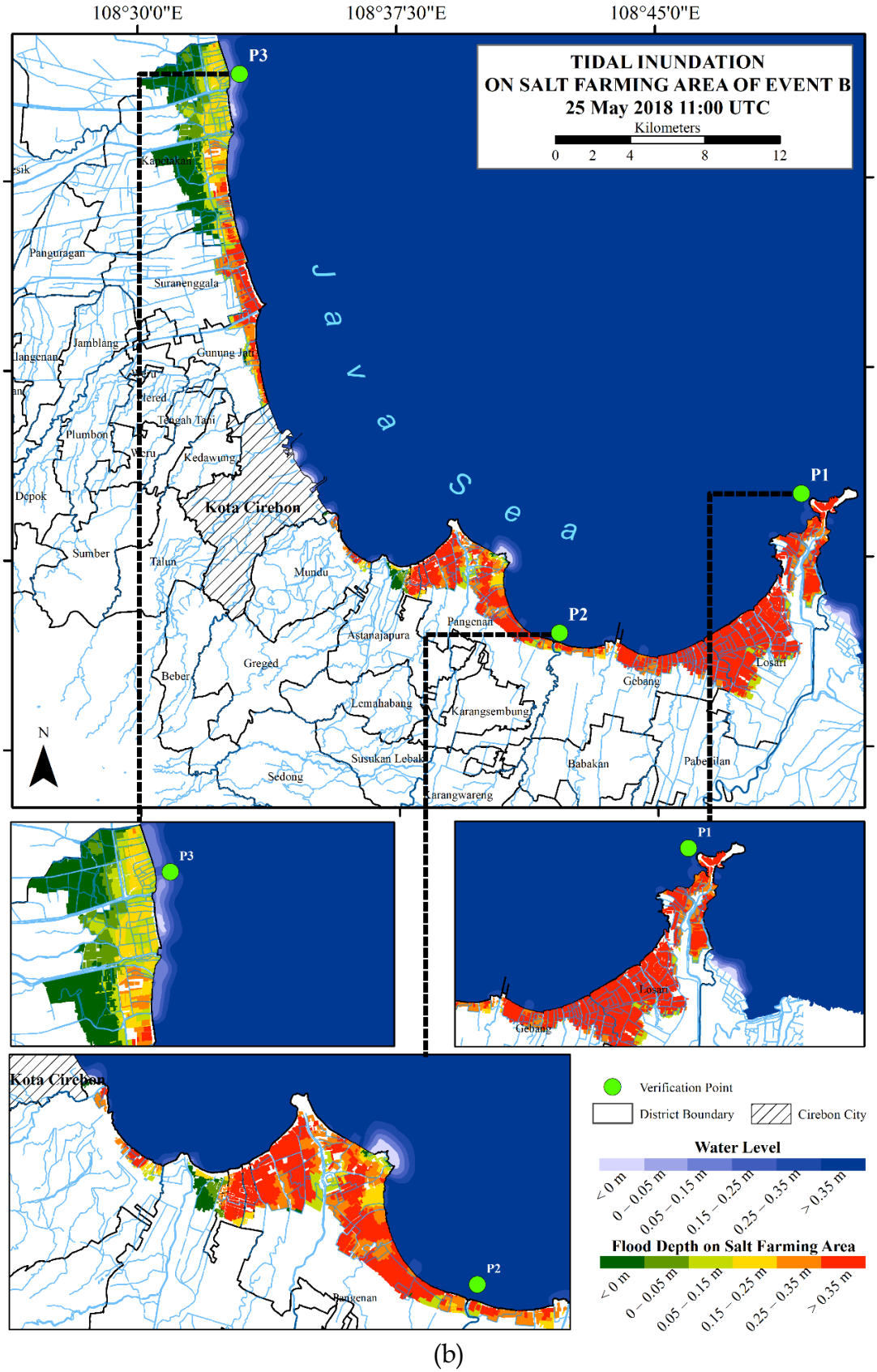

(b)

Figure 3.11. Estimated inundation level for each pond of during the highest tide of (**a**) event A and (**b**) event B (each parcel contains single value of inundation depth).

As mentioned in the previous section, the results regarding the submerged area of around 0–0.38 m for (event A) and 0–0.40 m for (event B), have significantly affected the salt production areas in Cirebon. Based on previous maps (*Figure 3.11*), it can be seen that around 1990.55 ha of salt production pond in Losari were inundated during event A and 1992.07 ha during event B. This district is also recorded as the most impacted area due to both tidal flood events (99.92% and 99.99% of total cultivated area in Losari). The salt production area of Gebang, which is located in the west part of the study area, has also been flooded up to 816.32 ha (100%) during the events A and B. At the same time, a slight increase of flood coverage has occurred in Kapetakan due to both tidal events. During the peak level of event A, almost 56.15% or 1,538.96 ha were exposed to tidal floodings, and 57.22% or 1,568.34 ha suffered inundation according to our simulations. In the middle part, tidal heights of both selected simulations in events A and B have submerged Suranenggala, Gunungjati, Mundu, and Astanajapura to a lesser degree in terms of total area, but with more significant percentages of inundated salt pond (approximately 49–99% in both events). The model presents the areas of inundation on A and B events as it is drawn *Figure 3.12*.

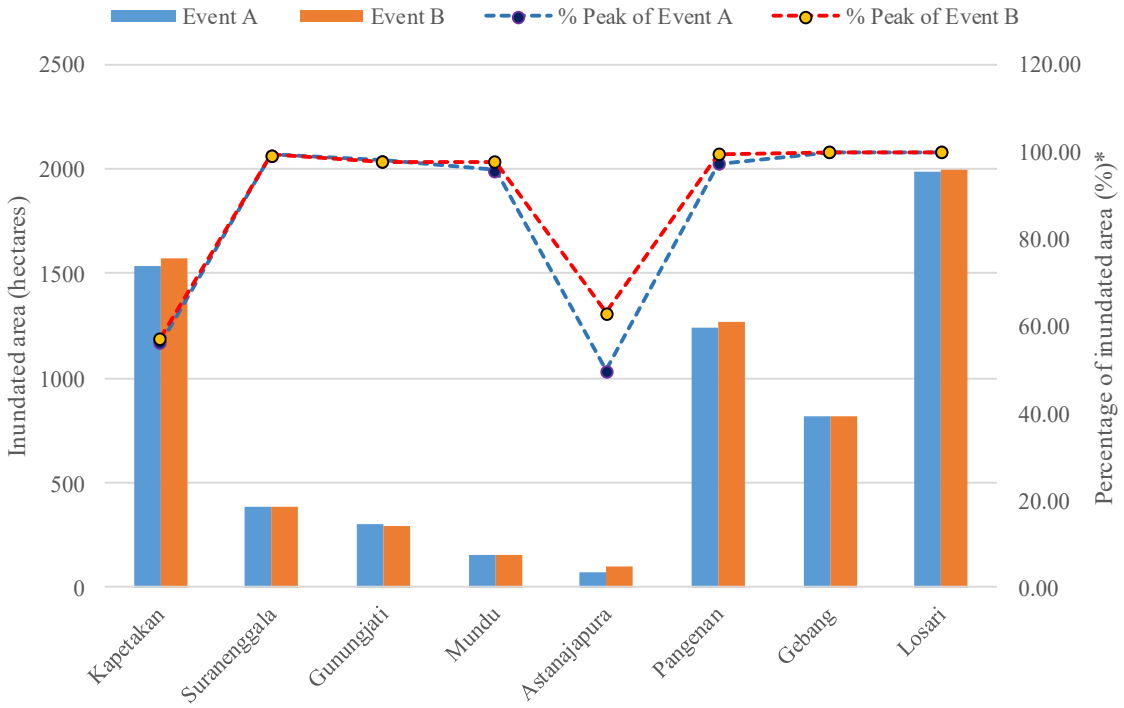

Figure 3.12. Tidal flood accumulative distribution area of inundation in Cirebon due to high tide at event A and event B.

This model shows relatively small differences in terms of the affected area during both simulation periods, as the wind factor has less impact and relatively similar water level. The simulated inundated salt production areas for A and B peak events are estimated to be 6489 ha and 6570 ha, respectively, which equals to 83 % and 84.2 % of the total salt production area in Cirebon. Overall, the peak depth of > 0.35 m dominates the tidal flood sequence, with 41.9% and 45.5% of the area being inundated to such a degree. This depth level has a significantly larger effect in destructing dikes compared to a lower flood level.

Meanwhile, around 16–17 % of ponds are relatively safe from these events, as they are located further inland on higher elevations. The less impacted area is estimated within >0-5 cm depth, which covers 1.7% (event A) and 4.1% (event B) of the total inundated area. During the flood, salt production was postponed and stopped until the water receded. It has to be noticed that higher flood levels also take a longer time to recede, which prolongs the preparation and the pre-production process, thus worsening the impact of the floods upon the salt production. Estimations of the salt production area that have been inundated based on simulation is presented in *Table 3.4.*

Table 3.4 Estimated areas and percentage of salt production in Cirebon affected by tidal flood in selected events (area in hectare).

Water depth	Inundated	Event A	Event B
>0–5 cm	Area	132.4	317.2
	%	1.7	4.1
5–15 cm	Area	894.3	847.4
	%	11.4	10.8
15–25 cm	Area	722.6	687.9
	%	9.2	8.8
25–35 cm	Area	1463.1	1156.1
	%	18.7	14.8
>35 cm	Area	3277.1	3561.4
	%	41.9	45.5
Total Inundated		**6489.4**	**6570.0**

3.5. Discussion

This paper presents simulation of the inundated areas upon salt farming due to tidal flood events. Tidal floods that occurred upon salt production area were triggered by the high tide events in Java Sea. That two events were similarly situated to tidal incidents located along the southern part of Java adjacent with Indian Ocean (Hanifah and Ningsih, 2018; Kurniawan *et al.*, 2016). Both periods studied present similar tidal elevations. Inundation dominantly occurred in the western and eastern parts of the region. The total impacted salt production area in both events were about 6489.4 ha (event A) (83%) and 6570 ha (84%) (event B). As illustrated by Châu (2014), the inundated area may be overrated based on data characteristics and the methods employed. Different resolutions of DEM may result in different total area of inundation. Furthermore, bathymetry, wind velocity, and Manning coefficient also correlate with the hydrodynamic process of tidal forcing.

This method, which relies on tidal characteristics and hydrodynamic parameters, leads to a usefulness tidal flood mapping for salt production areas. This idea improves the marine environment evaluation through cost-effective technique and limited data collection in particular coastal regions (Nayak and Bajaji, 2016), and improved flood forecasting (Kalligeris *et al.*, 2018). Based on performance, the hydrodynamic simulation's high degree of confidence with the global tide model can be placed as input to identify inundated area during tide events. The results express the significance of gaining reliable datasets into calibration

and validation processes (Kregting and Elsäßer, 2014). The availability of spatial data for the study area, including DEM, bathymetry, meteorological data, and salt parcel area, also give beneficial support for the models. Although wind data do not confirm significantly in the simulation performance, there were secure connections between our models with tidal records from local station (see Figure 9).

In this study, DEMNAS (0.27 arc-second) was the highest resolution elevation data available in Cirebon and representative for the simulation and tidal inundation mapping; however, more accurate results would be achievable through higher resolutions (Seenath *et al.*, 2016; Simpson *et al.*, 2015; Webster, 2010) such as LiDAR-derived DTMs (Kalligeris *et al.*, 2018; Raji *et al.*, 2011), and more extended tidal gauges data. Previous work by Seenath *et al.* (2016) acquired 10-m DEM in the flood modeling component and delivered relatively higher RMS error. Additionally, smaller frequencies of simulation, i.e., 5-sec (Chen and Liu, 2014; Rey *et al.*, 2018) and 6-min (Gallien, 2016) will improve the model's stability. While there are advantages to use a hydrodynamic model for tidal flood mapping, the required computation time and the resolution of input data may limit its application in practice, especially for larger areas (compare Seenath *et al.*, 2016). In this case, DEMNAS performs better resolution on water depth visually, but within a more extended handling time. This data was also previously exported into polyline format along with bathymetry in the preparation step. Processing simulations take a much longer time than calculating a general bathtub model. The hourly data during the 30-day period of simulation took almost 48 hours (using a standard PC with Intel I5 and 8GB of RAM).

As Cirebon salt production operates in a very traditional manner, the local salt farmers rely on daily harvests and the tidal cycle. Meanwhile, the ability to recover from disasters is far from sufficient. A comprehensive risk analysis of the salt production area is urgently needed to be better prepared to deal with the more prominent impacts of tidal floods on coastal areas. Tidal flood simulations have the potential ability to lead for better evaluations, including the potential damage loss on case-based analysis. This data will enable farmers and stakeholders to better respond to future hazards and to build capacity to improve the quality of livelihoods in the tidally flooded areas.

3.6. Conclusions and Future Works

This study has developed a method to identify the tidal flood impact in different types of agriculture areas in the coastline where the tide is generally forced by local factors, using hydrodynamic models. The model simulates typical aspects of tidal flood in Cirebon coastal regions, where lunar force dominates the domestic tidal properties during salt production periods. The method allows for critical identification points of flooding in the simulation, rather than using sets of scenarios. This study also underlines the main interest in the possible analysis of marginal agriculture along the coast, where the tidal hazard may continue in the future and would make a more significant impact. Meanwhile, there is still a limited number of studies that emphasizes the exposure of tidal hazard in local traditions economic activities. Tidal flood impact mapping can be beneficial to increase awareness of salt farmers to the flood occurrences. Additionally, the

uncertainty and volatility level of this type of flooding is driving the local government to put more attention, especially for countermeasure planning and efficient mitigation strategies. Using higher-resolution DEM, such as LiDAR, and echo-sounder survey data for detailed bathymetry can lead to an improvement for tidal flood assessments accuracy. Although this particular model is initiated for local-case study, it is believed that this technique can be developed at a regional scale with data limitation. Finally, this research will be more substantial to include the benefit-cost (B/C) analysis of the post tidal flood events.

Author Contributions:

Conceptualization, A.W.N. and B.B.; methodology, software, validation, formal analysis and writing-Original draft preparation, A.W.N.; writing-review & editing, A.W.N. and B.B.; supervision, B.B.

Funding:

The authors would like to acknowledge financial support provided by Indonesia Endowment Fund for Education (LPDP) within code of LPDP: PRJ-115 /LPDP.3/2017 provided to Anang Widhi Nirwansyah, Institute of Geography (University of Cologne) for publication funding and Universitas Muhammadiyah Purwokerto, Indonesia.

Acknowledgments:

This project has been part of doctoral research at the Institute of Geography, University of Cologne, Germany. The authors express their gratefulness to the anonymous reviewers for their valuable advice. Part of the data used for this paper, such as bathymetry, DEM, salt parcel on scale 1: 15,000, administrative boundary was made possible through the support of Indonesian National Geospatial Agency (BIG), and Indonesia Ministry of Marine and Fisheries Affairs (KKP). Finally, we would like to thank Junika A. Fathonah (UNDIP) for helping us during MIKE simulation, and salt farmers in Cirebon for valuable information during fieldwork.

Conflicts of Interest:

The authors declare no conflicts of interest and the founding sponsors had no role in the design of the study; in the collection, analyses, or interpretation of data; in the writing of the manuscript; or in the decision to publish the results.

3.7. References

Andreas, H., Usriyah, Zainal Abidin, H. and Anggreni Sarsito, D. (2017), "Tidal inundation ('Rob') investigation using time series of high-resolution satellite image data and from institu measurements along northern coast of Java (Pantura)", IOP Conference Series: Earth and Environmental Science, Vol. 71 No. 1, p. 012005.

Antczak, K.A. (2017), Entangled By Salt: Historical Archaeology Of Seafarers And Things In The Venezuelan Caribbean, 1624–1880, College of William and Mary, available at: https://doi.org/10.21220/S2RS97.

Arabelos, D.N., Papazachariou, D.Z., Contadakis, M.E. and Spatalas, S.D.

(2011), "A new tide model for the Mediterranean Sea based on altimetry and tide gauge assimilation", Ocean Science, Vol. 7 No. 3, pp. 429–444.
Berlianty, D. and Yanagi, T. (2011), "Tide and tidal current in the Bali strait, Indonesia", Marine Research Indonesia, Vol. 36 No. 2, pp. 25–36.
BIG. (2018), "DEMNAS Seamless Digital Elevation Model (DEM) dan Batimetri Nasional", available at: http://tides.big.go.id/DEMNAS/ (accessed 26 March 2019).
Bouwer, L.M., Bubeck, P., Wagtendonk, A.J. and Aerts, J.C.J.H. (2009), "Inundation scenarios for flood damage evaluation in polder areas", Natural Hazards and Earth System Science, Vol. 9 No. 6, pp. 1995–2007.
BPS Cirebon. (2016), Cirebon Regency in Figure, edited by BPS-Statistics of Cirebon Regency, 32.09.1501., BPS - Statistics of Cirebon Regency, Cirebon.
Brémond, P. and Grelot, F. (2013), "Review Article: Economic evaluation of flood damage to agriculture - Review and analysis of existing methods", Natural Hazards and Earth System Sciences, Vol. 13 No. 10, pp. 2493–2512.
Budiyono, Y., Aerts, J., Brinkman, J.J., Marfai, M.A. and Ward, P. (2015), "Flood risk assessment for delta mega-cities: a case study of Jakarta", Natural Hazards, Vol. 75 No. 1, pp. 389–413.
Châu, V.N. (2014), Assessing the Impacts of Extreme Floods on Agriculture in Vietnam: Quang Nam Case Study, Massey University, New Zealand, available at: https://mro.massey.ac.nz/handle/10179/6250.
Chen, W.B. and Liu, W.C. (2014), "Modeling flood inundation induced by river flow and storm surges over a river basin", Water (Switzerland), Vol. 6 No. 10, pp. 3182–3199.
Church, J.A., Clark, P.U., Cazenave, A., Gregory, J.M., Jevrejeva, S., Levermann, A., Merrifield, M.A., et al. (2013), Sea Level Change, Climate Change 2013: The Physical Science Basis. Contribution of Working Group I to the Fifth Assessment Report of the Intergovernmental Panel on Climate Change, Cambridge and New York.
Church, J.A., Woodworth, P.L., Aarup, T. and Wilson, W.S. (2010), Understanding Sea-Level Rise and Variability, edited by Church, J.A., Woodworth, P.L., Aarup, T. and Wilson, W.S., Wiley-Blackwell, Oxford, UK, available at: https://doi.org/10.1002/9781444323276.
Consoli, S., Recupero, D.R. and Zavarella, V. (2014), "A survey on tidal analysis and forecasting methods for Tsunami detection", Science of Tsunami Hazards, No. 1, pp. 1–58.
Department of Environmental Protection. (2014), Rebuild by Design-Hudson River Project Feasibility Study Report, New Jersey, available at: https://www.state.nj.us/dep/floodresilience/rbd-hudsonriver-fs.htm.
Durand, J.R. and Petit, D. (1995), "The Java Sea Environment", in Nurhakim, S. (Ed.), Biodynex: Biology, Dynamics and Exploitation of the Small Pelagig Fishes in the Java Sea, Agency for Agricultural Research and Development, Jakarta, pp. 15–38.
Egbert, G.G.D. and Erofeeva, S.Y. (2002), "Efficient inverse modeling of barotropic ocean tides", Journal of Atmospheric and Oceanic Technology, Vol. 19 No. 2, pp. 183–204.
Elsaesser, B., Bell, A.K., Shannon, N. and Robinson, C. (2010), "Storm surge hind-and forecasting using Mike21FM-Simulation of surges around the

Irish Coast", Proceedings of the International MIKE by DHI Conference--Modelling in a World of Change, Copenhagen, Denmark. See Http://Www. Dhisoftware. Com/GlobalEvents/PastMajorEvents/MIKEByDHI2010/PresentationsAndPapers. Aspx (Accessed 17/01/2013), No. January 2017.

Faber, R. (2006), Flood Risk Analysis: Residual Risks and Uncertainties in an Austrian Context, University of Natural Resources and Applied Life Sciences, Vienna.

Fernández, V., Silva, R., Mendoza, E. and Riedel, B. (2018), "Coastal flood assessment due to extreme events at Ensenada, Baja California, Mexico", Ocean and Coastal Management, Elsevier, Vol. 165 No. September, pp. 319–333.

Forster, S., Kuhlmann, B., Lindenschmidt, K.E. and Bronstert, A. (2008), "Assessing flood risk for a rural detention area", Natural Hazards and Earth System Science, Vol. 8 No. 2, pp. 311–322.

Gallien, T.W. (2016), "Validated coastal flood modeling at Imperial Beach, California: Comparing total water level, empirical and numerical overtopping methodologies", Coastal Engineering, Elsevier B.V., Vol. 111, pp. 95–104.

Gallien, T.W., Schubert, J.E. and Sanders, B.F. (2011), "Predicting tidal flooding of urbanized embayments: A modeling framework and data requirements", Coastal Engineering, Elsevier B.V., Vol. 58 No. 6, pp. 567–577.

Green, J.A.M., Bowers, D.G. and Byrne, H.A.M. (2018), "A mechanistic classification of double tides", Ocean Science Discussions, Vol. 1 No. June, pp. 1–15.

Gurumoorthi, K. and Venkatachalapathy, R. (2017), "Hydrodynamic modeling along the southern tip of India: A special emphasis on Kanyakumari coast", Journal of Ocean Engineering and Science, Elsevier B.V., Vol. 2 No. 4, pp. 229–244.

Haigh, I.D. (2017), "Tides and Water Levels", Encyclopedia of Maritime and Offshore Engineering, pp. 1–13.

Hanifah, F. and Ningsih, N.S. (2018), "Identifikasi Tinggi dan Jarak Genangan Daerah Rawan Bencana Rob di Wilayah Pantai Utara Jawa yang Disebabkan Gelombang Badai Pasang dan Variasi Antar Tahunan", Jurnal Teknik Sipil, Vol. 25 No. 1, pp. 81–86.

Hasan, S. and Rambabu, C. (2017), "Enhanced Representation of Java Sea Tidal Propagation through Sensitivity Analysis", Journal of Water Resource and Hydraulic Engineering, Vol. 6 No. 1, pp. 9–21.

Heidarzadeh, M., Muhari, A. and Wijanarto, A.B. (2018), "Insights on the Source of the 28 September 2018 Sulawesi Tsunami, Indonesia Based on Spectral Analyses and Numerical Simulations", Pure and Applied Geophysics, available at: https://doi.org/10.1007/s00024-018-2065-9.

Helmi, A. and Sasaoka, M. (2018), "Dealing with socioeconomic and climate-related uncertainty in small-scale salt producers in rural Sampang, Indonesia", Journal of Rural Studies, Vol. 59 No. February, pp. 88–97.

ICCSR. (2010), Scientific Basis: Analysis and Projection of Sea Level Rise and Extreme Weather Event, Jakarta.

Jacobs, J.M., Cattaneo, L.R., Sweet, W. and Mansfield, T. (2018), "Recent and Future Outlooks for Nuisance Flooding Impacts on Roadways on the U.S.

East Coast", Transportation Research Record: Journal of the Transportation Research Board, Vol. 2672 No. 2, pp. 1–10.
Kalligeris, N., Winters, M., Gallien, T., Tang, B.-X., Lucey, J. and Delisle, M.-P. (2018), "Coastal Flood Modeling Challenges in Defended Urban Backshores", Geosciences, Vol. 8 No. 12, p. 450.
Khasanah, I.U., Heliani, L.S. and Basith, A. (2016), "Trends and Seasonal to Annual Sea Level Variations of North Java Sea Derived from Tide Gauges Data", Proceeding of the First International Conference on Technology, Innovation and Society, pp. 308–316.
KKP. (2015), Salt Production of Indonesia (in Bahasa), Jakarta, available at: http://statistik.kkp.go.id/sidatik-dev/Berita/Analisis Produksi Garam Indonesia.pdf.
Koropitan, A.F. and Ikeda, M. (2008), "Three-dimensional modeling of tidal circulation and mixing over the Java Sea", Journal of Oceanography, Vol. 64 No. 1, pp. 61–80.
Kregting, L. and Elsäßer, B. (2014), "A Hydrodynamic Modelling Framework for Strangford Lough Part 1: Tidal Model", Journal of Marine Science and Engineering, Vol. 2 No. 1, pp. 46–65.
Kumbier, K., Carvalho, R. and Woodroffe, C. (2018), "Modelling Hydrodynamic Impacts of Sea-Level Rise on Wave-Dominated Australian Estuaries with Differing Geomorphology", Journal of Marine Science and Engineering, Vol. 6 No. 2, p. 66.
Kurniawan, R., Ramdhani, A., Sakya, A.E. and Pratama, B.E. (2016), "High wave and coastal inundation in south of Java and west of Sumatera (Case studies on 7-10 June 2016)", Jurnal Meteorologi Dan Geofisika, Vol. 17 No. 2, pp. 69–76.
Latief, H., Putri, M.R., Hanifah, F., Afifah, I.N., Fadli, M. and Ismoyo, D.O. (2018), "Coastal Hazard Assessment in Northern part of Jakarta", Procedia Engineering, Elsevier B.V., Vol. 212, pp. 1279–1286.
Lia, E. (2016), "Puluhan Ribu Ton Garam di Cirebon Tersapu Banjir Rob page-2 : Okezone News", Okezone.Com, available at: https://news.okezone.com/read/2016/06/17/525/1418255/puluhan-ribu-ton-garam-di-cirebon-tersapu-banjir-rob?page=2 (accessed 10 June 2019).
Marfai, M.A. and King, L. (2008), "Tidal inundation mapping under enhanced land subsidence in Semarang, Central Java Indonesia", Natural Hazards, Vol. 44 No. 1, pp. 93–109.
Marfai, M.A., King, L., Sartohadi, J., Sudrajat, S., Budiani, S.R. and Yulianto, F. (2008), "The impact of tidal flooding on a coastal community in Semarang, Indonesia", Environmentalist, Vol. 28 No. 3, pp. 237–248.
Merz, B., Kreibich, H., Schwarze, R. and Thieken, A. (2010), "Review article 'Assessment of economic flood damage'", Natural Hazards and Earth System Science, Vol. 10 No. 8, pp. 1697–1724.
Metrotv. (2016), "700 Hectares of Salt Pond in Cirebon Submerged Coastal Flood (in Bahasa)", Metrotvnews.Com, available at: http://m.metrotvnews.com/jabar/peristiwa/JKR4MYQb-700-hektare-tambak-garam-di-cirebon-terendam-banjir-rob (accessed 29 September 2017).
Munadi, E., Ardiyanti, S.T., Ingot, S.R., Lestari, T.K., Subekti, N.A., Salam, A.R., Alhayat, A.P., et al. (2016), Info Komoditi Garam, edited by Salim, Z. and

Munadi, E., Badan Pengkajian dan Pengembangan Perdagangan, Jakarta, available at: http://bppp.kemendag.go.id/media_content/2017/08/Isi_BRIK_Garam.pdf.
Mustaid, Y. and Tetsuo, Y. (2013), "Numerical modeling of tidal dynamics in the Java Sea", Coastal Marine Science, Vol. 36 No. 1, pp. 1–12.
Nagara, G.A., Sasongko, N.A. and Olakunle, O.J. (2010), Introduction to Java Sea, Stavanger, available at: https://doi.org/10.1007/978-1-84882-972-5_26.
Nayak, D. and Bajaji, R. (2016), "Numerical modeling of tides, currents and waves off Maharashtra coast", Indian Journal of Geo-Marine Sciences, Vol. 45 No. October, pp. 1255–1263.
Nguyen, T. (2017), An Evaluation of Coastal Flooding Risk Due to Storm Surge under Future Sea Level Rise Scenarios in Thua Thien Hue Province, Vietnam, Texas Tech University.
Ningsih, N.S., Hadi, S., Utami, M.D. and Rudiawan, A.P. (2011), "Modeling of storm tide flooding along the southern coast of Java, Indonesia", edited by Gan, J. Advances in Geosciences, World Scientific Publishing Co. Pte. Ltd., Vol. 24, pp. 87–103.
Nugraheni, I.R., Wijayanti, D.P., Sugianto, D.N. and Ramdhani, A. (2017), "Study of inundation events along the southern coast of Java and Bali, Indonesia (case studies 4-9 June 2016)", IOP Conference Series: Earth and Environmental Science, Vol. 55 No. 1, p. 012014.
Padman, L. (2005), "Tide Model Driver (TMD) Manual", Earth & Space Research, Oregon.
Parker, B.B. (2007), Tidal Analysis and Prediction, No. 2007925298, NOAA Special Publication, Silver Spring, Maryland, available at: https://tidesandcurrents.noaa.gov.
Pawlowicz, R., Beardsley, B. and Lentz, S. (2002), "Classical tidal harmonic analysis including error estimates in MATLAB using TDE", Computers and Geosciences, Vol. 28 No. 8, pp. 929–937.
Poulter, B. and Halpin, P.N. (2008), "Raster modelling of coastal flooding from sea-level rise", International Journal of Geographical Information Science, Vol. 22 No. 2, pp. 167–182.
PSSDAL. (2010), Peta Lahan Garam Indonesia, edited by Saputro, G.B., Edrus, I.N., Hartini, S. and Poniman, A., PSSDAL BAKOSURTANAL, Cibinong, available at: https://perpustakaan.big.go.id/opacbig/index.php?p=show_detail&id=10283.
Pugh, D.T. (1987), "Tides, Surges and mean sea-level", Marine and Petroleum Geology, Vol. 5 No. 3, p. 301.
Qiao, H., Zhang, M., Jiang, H., Xu, T. and Zhang, H. (2018), "Numerical study of hydrodynamic and salinity transport processes in the Pink Beach wetlands of the Liao River estuary, China", Ocean Science, Vol. 14 No. 3, pp. 437–451.
radarcirebon.com. (2018), "Waspada Rob Susulan, Ini Sebabnya", available at: http://www.radarcirebon.com/waspada-rob-sususlan-ini-sebabnya.html (accessed 26 March 2021).
Raji, O., Del Rio, L., Gracia, F.J. and Benavente, J. (2011), "The use of LIDAR data for mapping coastal flooding hazard related to storms in Cadiz Bay

(SW Spain)", Journal of Coastal Research, No. 64, pp. 1881–1885.
Rey, W., Salles, P., Mendoza, E.T., Torres-Freyermuth, A. and Appendini, C.M. (2018), "Assessment of coastal flooding and associated hydrodynamic processes on the south-eastern coast of Mexico, during Central American cold surge events", Natural Hazards and Earth System Sciences, Vol. 18 No. 6, pp. 1681–1701.
Robertson, R. and Ffield, A. (2005), "M2 Baroclinic Tides in the Indonesian Seas", Oceanography, Vol. 18 No. 4, pp. 62–73.
Rochwulaningsih, Y. (2008), Marginalization of Salt Farmers and Global Economic Expansion: The Case in Rembang Regency of Central Java (in Bahasa), IPB.
Rodrigues, C.M., Bio, A., Amat, F. and Vieira, N. (2011), "Artisanal salt production in Aveiro/Portugal - an ecofriendly process.", Saline Systems, Vol. 7 No. 1, p. 3.
Samanta, S. and Koloa, C. (2014), "Modelling Coastal Flood Hazard Using ArcGIS Spatial Analysis tools and Satellite Image", International Journal of Science and Research, Vol. 3 No. 8, pp. 961–967.
van de Sande, B., Lansen, J. and Hoyng, C. (2012), "Sensitivity of Coastal Flood Risk Assessments to Digital Elevation Models", Water, Vol. 4 No. 4, pp. 568–579.
Seenath, A., Wilson, M. and Miller, K. (2016), "Hydrodynamic versus GIS modelling for coastal flood vulnerability assessment: Which is better for guiding coastal management?", Ocean and Coastal Management, Elsevier Ltd, Vol. 120, pp. 99–109.
Seifi, F., Deng, X. and Baltazar Andersen, O. (2019), "Assessment of the Accuracy of Recent Empirical and Assimilated Tidal Models for the Great Barrier Reef, Australia, Using Satellite and Coastal Data", Remote Sensing, Vol. 11 No. 10, p. 1211.
Simpson, A.L., Balog, S., Moller, D.K., Strauss, B.H. and Saito, K. (2015), "An urgent case for higher resolution digital elevation models in the world's poorest and most vulnerable countries", Frontiers in Earth Science, Vol. 3 No. March 2016, available at: https://doi.org/10.3389/feart.2015.00050.
Takagi, H., Esteban, M., Mikami, T. and Fujii, D. (2016), "Projection of coastal floods in 2050 Jakarta", Urban Climate, Vol. 17, pp. 135–145.
Taufik, M. and Safitri, D.A. (2014), "Determining LAT Using Tide Modeling TPXO IO (A Case Study : Fani Island)", International Conference Data Mining, Civil and Mechanical Engineering (ICDMCME'2014), Feb 4-5, 2014 Bali (Indonesia), Vol. 2002, International Institute of Engineers, pp. 4–7.
Tehrany, M.S., Pradhan, B., Mansor, S. and Ahmad, N. (2015), "Flood susceptibility assessment using GIS-based support vector machine model with different kernel types", Catena, Elsevier B.V., Vol. 125, pp. 91–101.
Thambas, A.H. (2016), Inundation Risk Analysis of the Storm Surge and Flood for the Ariake Sea Coastal Disaster Management, Saga University, available at: http://portal.dl.saga-u.ac.jp/bitstream/123456789/122898/4/zenbun_fulltext_arthur.pdf.
Verwaest, T., Vanneuville, W., Peeters, P., Mertens, T. and De Wolf, P. (2007), "Uncertainty on coastal flood risk calculations, and how to deal with it in coastal management: case of the Belgian coastal zone", Flood Risk

Assessment II: Proceedings of a Conference Held by the Institute of Mathematics and Its Applications, September 2007, pp. 151–157.
Wang, F., Hartnack, J.N. and Road, W.S. (2006), "Simulation of Flood Inundation in Jilin City, Songhua River Project", City, No. 10, available at: http://www.cjk3d.net/DHIPaper/flood/6.pdf.
Ward, P.J., Marfai, M.A., Yulianto, F., Hizbaron, D.R. and Aerts, J.C.J.H. (2011), "Coastal inundation and damage exposure estimation: a case study for Jakarta", Natural Hazards, Vol. 56 No. 3, pp. 899–916.
Webster, T.L. (2010), "Flood risk mapping using LiDAR for annapolis Royal, Nova Scotia, Canada", Remote Sensing, Vol. 2 No. 9, pp. 2060–2082.
Wolf, J. (2009), "Coastal flooding: impacts of coupled wave–surge–tide models", Natural Hazards, Vol. 49 No. 2, pp. 241–260.
Yang, X., Grönlund, A. and Tanzilli, S. (2002), "Predicting Flood Inundation and Risk Using Geographic Information System and Hydrodynamic Model", Geographic Information Sciences, Vol. 8 No. 1, pp. 48–57.
Zalite, K. (2016), Radar Remote Sensing for Monitoring Forest Floods and Agricultural Grasslands, University of Tartu Press, available at: www.tyk.ee.

Chapter 4

Assessing the Degree of Tidal Flood Damage to Salt Harvesting Landscape using a Synthetic Approach and GIS – A Case Study: Cirebon, West Java

Published as:

Nirwansyah, A.W. and Braun, B. (2021), "Assessing the degree of tidal flood damage to salt harvesting landscape using synthetic approach and GIS - Case study: Cirebon, West Java", International Journal of Disaster Risk Reduction, Elsevier Ltd, Vol. 55 No. January, p. 102099.

CHAPTER 4 - Assessing the degree of tidal flood damage to salt harvesting landscape using a synthetic approach and GIS – A case study: Cirebon, West Java

Abstract
Tidal flood implications for agricultural areas have been relatively neglected in research due to their relatively low economic values. Nevertheless, many rural coastal communities are facing these types of floods regularly, especially salt harvesters. Based on a synthetic approach using damage functions and the Geographic Information System, this study applies previous simulations from a hydrodynamic model to quantify vulnerability through flood depth and duration. A depth-duration damage function using a synthetic approach was applied to develop damage curves based on previous events. Data was collected through a questionnaire aimed at salt harvesters' group representatives. This data was used to evaluate the direct monetary loss related to two recorded events in Cirebon, West Java: in June 2016 (Event A) and in May 2018 (Event B). Those events brought losses of about Indonesian Rupiah (IDR) 74.11 x 10^9 (5.37%) and IDR 13.79 x 10^9 (8.1%) for Event A and Event B respectively. This study reveals the different vulnerability levels of the events, which represent different production stages in salt harvesting. This paper presents methods and information to support risk management in salt harvesting, including prioritizing mitigation strategies.

Keywords: physical vulnerability, tidal flood, salt harvesting, damage function, GIS

4.1. Introduction

Salt harvesting is acknowledged as the most efficient system to transform solar energy into an inorganic commodity (Sedivy, 2009). Most of the salt products are generated through seawater, with some manufactured through underground and surface mining of natural salt deposits (Thys, 2003). The salt production is currently dominated by the nations of the Global North, with China, as the biggest producer, the United States, Germany, and Canada among the top six producing countries (USGS, 2020). In addition, Global South countries around the equator, including in south-east Asia, west Africa, and south America, produce this mineral at solar ponds in their coastal low-lands and generate returns for local communities. However, as a consequence of the hydro-meteorological hazards, tsunamis, and flooding, the risk to coastal areas has increased remarkably.

In coastal regions, a flood occurs when the sea level rises to a critical height above the land surface due to tidal sea and sea surges (Marfai, King, *et al.*, 2008). According to Hinton (Hinton, 2000) pp. 180, the tidal hazard itself consists

of three parts: (i) tidal inundation – maximum water levels and tidal range, including the duration of tidal inundation; (ii) salt and freshwater mixture – during tidal flows to rivers and other watercourses; and (iii) tidal currents – current direction and velocity, which play considerable roles in sediment movement and erosion. High-tide flooding seriously impacts local economic activities and adaptation responses (Hino *et al.*, 2019). In the coastal area of the Global South, tidal flooding creates substantial problems for livelihoods, especially in major cities. Additionally, many food production areas located along the coastline in tropical regions are also negatively affected by massive tidal inundation. As a result, potential yields of various products, including rice, are significantly decreasing. The same is true for aquaculture operations or minor types of rural activities such as salt harvesting.

The evaluation of flood damage, especially for salt harvesting, has been rarely discussed for both the global and the regional setting. A study by Mason and Kipp Jr. (1997) has exemplarily implemented a financial loss analysis for salt harvesting. That paper presents the potential loss of salt by extensive flooding during winter and early spring of 1992-1993 on the playa surface in Bonneville, north-western Utah. It showed that the flood events transported millions of tons of salt beyond the salt crust area. That simulation indicated the loss of crystalline salt to be about 975 thousand tons per year. Another study by Picado *et al.* (2009) employs the Eulerian-Lagrangian circulation (ELCIRC) model to assess the hydro-dynamic sequence in the salt pans of the Ria de Aveiro lagoon in Portugal and to emphasize the consequences of the disruptions. That study clearly shows that the number of productive salt areas substantially decreased from 500 ha to 8 ha between 1600 and 2009. Those two cases have enriched the principal understanding of the impact of flood disruptions on salt production. However, further analysis of salt production and tidal flooding relation is still needed, especially in the Global South where the industry supports the local economy. Presently, most southeast Asian countries such as Vietnam, Thailand, Myanmar, and Indonesia are harvesting salt close to shorelines that could be affected by coastal hazards.

Some studies on economic loss in agriculture still use rather simplistic approaches and coarse approximations. Agriculture landscapes mostly show a relatively lower cost of damage compared that of built-up areas (Brémond and Grelot, 2013; Forster *et al.*, 2008; Merz *et al.*, 2010). Recently, some studies have started to develop a more sophisticated approach to the losses on agricultural land (Chau *et al.*, 2015; Huda, 2015). They proposed using a stage function for direct and tangible flood damage evaluations. This procedure assesses the regional setting, determines damage classifications, obtains information and data, establishes the method, and finally estimates the loss. The approach includes uncertainty factors and provides valuable inputs for managing economic estimations in non-urban regions. Flood damage measuring capacity is one of the significant factors for establishing effective flood management strategies, implementing protection plans, and minimizing expected flood loss (Wijayanti *et al.*, 2017).

Today, numerous loss models have emerged with an emphasis on purpose, structure, and local attention (Gerl *et al.*, 2014). Several papers have approached the economic impact on agricultural land (Bhakta Shrestha *et al.*, 2019;

Chau *et al.*, 2015; Huda, 2015). Brémond and Grelot (2013) portrayed 41 studies related to economic evaluations of flood damage in agriculture using both qualitative and quantitative methods. The majority of flood categories referred to in the study are rain flood regimes; a small number of the studies are related to seawater flooding. Their review study describes previous hazard parameters, including the period of occurrences, water depth, duration, velocity, deposits, contaminations, and the water salinity impact on crops. However, all these previous papers have assessed mainly agriculture, including crops, cattle, soil, stocks, and plant material. For salt harvesting, the research design and models used in those studies need to be modified in line with the particular setting and specific process dynamics.

Based on the research work mentioned above, this study investigates, to our knowledge for the first time, the application of loss estimation on salt harvesting in the coastal area. Therefore, the aims of this paper are (i) to provide insight into the characteristics of tidal inundation (depth and duration) of previously recorded events, (ii) to assess physical vulnerability for each stage of production, and (iii) to estimate the damage loss on the salt harvesting area based on previous events. The objectives will be addressed through damage functions based on quantitative data gathered from the local community and using a geographic information system (GIS). As a consequence, this paper is organized as follows. The first section is the introduction. Section 2 presents the state of the art in this research and the context of the study. Section 3 introduces the case study area, the local procedure of salt production, and tidal events. Section 4 provides an overview of the methodology, and Section 5 contains the results and a discussion. Finally, Section 6 concludes this paper.

4.2. State of The Art and Context of The Study

Many studies on flood risk assessment have been set up using flood hazard maps derived from satellite images (Kotera *et al.*, 2016; Sakamoto *et al.*, 2007). Despite limitations to their accuracy, especially for events of relatively short duration, the datasets arising from the satellite images can generate useable damage information. Flood damage is generally influenced by hydrodynamic parameters such as water depth, inundation duration, and flow velocity (Merz *et al.*, 2010; Vozinaki *et al.*, 2015). Those inputs are thus essential for flood simulations (Chung *et al.*, 2019; de Moel *et al.*, 2009). A flood damage function, which is defined as the association between flood factors and the level of potential damage, is commonly used for assessing economic loss during flooding events (Nguyen *et al.*, 2017). Flood damage function offers total asset values (damage ratio) and evaluates benefits (avoided damage) by using flood parameters (Brémond and Grelot, 2010; Nguyen *et al.*, 2017). For agriculture, some established damage functions include parameters such as inundation depth and flood duration (Win *et al.*, 2018). Both parameters play a significant role in damage analysis.

Buildings, structures, facilities, agriculture, or arable land and natural properties (tangible vulnerability) have been investigated in many studies (Fuchs *et al.*, 2012; Molinari, Menoni, *et al.*, 2014; Papathoma-Köhle *et al.*, 2019). A social science-oriented vulnerability concept should, however, also include broader environmental, social, and economic aspects. Without wanting to disregard social

concerns, our study implements the axiom of physical vulnerability (PV), as the flood hazard in salt harvesting areas mainly affects physical structures (Karagiorgos *et al.*, 2016; Thouret *et al.*, 2014). The physical construction of salt ponds as the main asset of salt production is mainly considered as the element at risk, which can be evaluated after the hazard events. From the viewpoint of this study, the vulnerability can be defined as the potential damage caused to a system by tidal flood hazards. A vulnerability index within a range of 0 to 1 indicates the entity's relative weakness, with a value of 1 representing total damage (Thouret *et al.*, 2014).

A GIS is a crucial part of flood damage evaluations because it can deliver various data and parameters, including vulnerability aspects such as exposed assets, damage susceptibility, and potential damage (Penning-Rowsell *et al.*, 2013). Many GIS platforms have embraced the Digital Elevation Model (DEM), including numerical hydrodynamic models, to generate proper flood hazard maps (Eleutério *et al.*, 2010). Additionally, both the hazard and the vulnerability elements have to be merged to provide new information on economic damage and flood management. In the Global North countries The Netherlands (Messner *et al.*, 2007), Germany (Thieken *et al.*, 2008), and Japan (Dutta *et al.*, 2003), the disaster mitigation authorities have employed damage functions in flood risk assessment. Calculations are commonly performed by averaging the damage allocations to homogenous properties classifications that were inundated to a similar depth (Merz *et al.*, 2010; Zhai *et al.*, 2005).

4.3. Study Area, Salt Harvesting, and Tidal Events

4.3.1. Study area

This study has selected Cirebon, West Java, Indonesia, for a pilot case because of its prominent position as the largest Indonesian salt production area for traditional farmers (KKP, 2015). Cirebon lies at 6°30′-7°00′ S and 108°40′-108°48′ E and covers 990.36 km^2. The Cirebon region has more than 2.1 million inhabitants living in 40 districts. Eight districts are located on alluvial flood plains adjacent to the Java Sea in the northern part. The relative flatness of the study area means the area is majorly affected by erosion and sedimentation processes. The other districts are dominated by hills, especially in the east and west. The mountainous landscape characterizes the southern part with 11-130 meter of elevation. According to a multinational energy company, PT Cirebon Energi Prasarana (2016), the dry season lasts from June to October, with an average rainfall of 16 mm/month. In the coastal area, the wind blows dominantly from the east, northeast, northwest, and north with an average speed of approximately 3.18 m/s. The average tidal range in the area is 1.2-2 meters (ICCSR, 2010; Takagi *et al.*, 2016). Tide patterns are semidiurnal, and wind velocity is mainly influenced by the monsoon (Nagara *et al.*, 2010). Tidal flood occurrences have been recorded in this area, including severe tidal flood events in 2016 and 2018 (Lia, 2016; Metrotv, 2016; tirto.id, 2018).

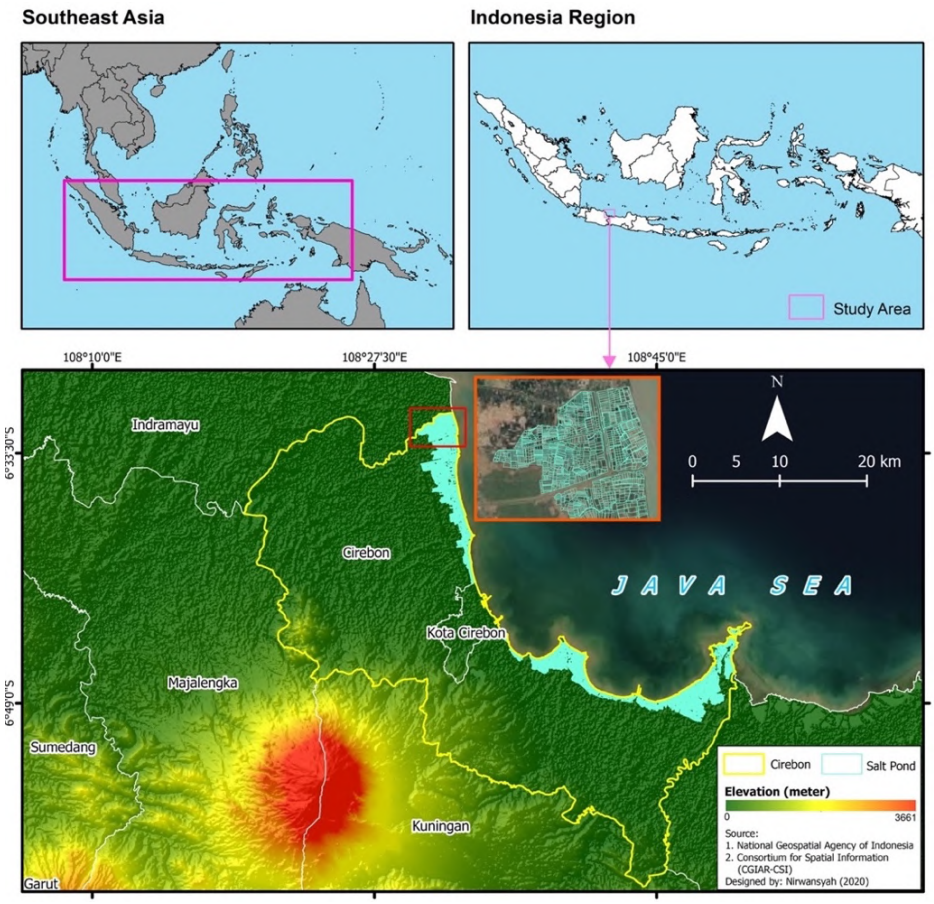

Figure 4.1. The geographical situation of the study location in Cirebon, West Java

The agricultural sector economically dominates the region. The region's gross domestic product (GDP) stood at IDR 33.73 trillion (EUR 200.96 million) in 2019 (BPS Cirebon, 2018), and ranked 12th out of 27 regencies in West Java (BPS Provinsi Jawa Barat, 2020). Currently, salt production in Cirebon takes place in the eight districts along the coastline. It covers around 7,800 ha and provides approximately 3,700 jobs, including for farmers, workers, and intermediaries (KKP, 2015; PSSDAL, 2010). The regency is deemed as the most prominent salt production area in Indonesia, with approximately 437.56 thousand tons of "people's salt", locally named '*garam rakyat*' (15 % of the national yield in 2015 (KKP, 2015)). In general, salt harvesters harvest for four months per year during the dry season, with an additional month for construction and preparation (Trikobery *et al.*, 2017). They practically start the pre-production period in April/May, including draining the ponds, repairing the dikes and channels, and preparing the mechanical tools. Until now, salt harvesting through solar evaporation in coastal areas has been one of the prime activities for sustaining the economic and social welfare of the population on the north coast of Java. Furthermore, salt production has also been included in a national program on self-sufficiency by the state government (Dharmayanti *et al.*, 2013; Suwarno, 2014). However, high tide incidences have been part of potential hazards for the salt producers in the area for many years. Therefore, further analysis, including disaster risk assessment related to coastal hazards in the salt harvesting landscape, is essential for flood mitigation and the positive development of this local economic activity.

4.3.2. Salt harvesting procedure

Salt harvesting can be explained through a simple agricultural analogy (Antczak, 2017b). It follows a seasonal pattern and requires intensive labour (Lai, 2013). In tropical regions where high levels of solar radiation occur, salt production has been established mainly through the evaporation process using salt pan and seawater distribution (Guntur *et al.*, 2018). According to Vieira and Bio, (2011), evaporation ponds, which are connected to supply ponds by sluice gates, receive water from the sea through canals. They provide water to the crystallizer ponds. Ultimately, the deposition of sodium chloride takes place in crystallizer ponds. Their salinity fluctuates during the production period, depending on the salinity of the supply ponds when the flood happens. This dependency means that a coastal flood can be considered anything from a nuisance to a destructive force, depending on the extent of the flooding. Some solar salt farms produce sodium chloride continuously throughout the year. However, some fields lie barren during rainy season and salt is only harvested during the summer period (Davis, 2000).

The local salt harvesting technologies in the study area have not advanced much since the 19th century (Guntur *et al.*, 2018). Salt harvesting practices involve (i) purifying the seawater from contamination and using it as reservoir input, (ii) water evaporation, (iii) concentration, (iv) crystallization, and (v) harvesting (Susanto *et al.*, 2015). A small numbers of farmers have started to optimized the evaporation and crystallization process by placing high-density polyethylene (HDPE) material as a layer in the evaporation and crystallization ponds (Guntur *et al.*, 2018; Sumiati, 2015). Nevertheless, due to the expense of that material, small-scale farmers are still using the soil layer (or without HDPE). Through local salt harvesting, small-scale farmers produce 60 tons/ha/year of salt (Munadi *et al.*, 2016). Daily, they rely on the tidal cycle to distribute seawater to their pond systems through channeling and withdrawing the water using a windmill. In certain conditions, when the wind is not blowing or is insufficient to rotate the windmill, the water is distributed using a long bamboo scoop (Apriani *et al.*, 2018).

Within the salt harvesting process, it usually takes several days for the water to change from seawater into a brine, with several steps. However, the early-production process in salt production is more complex and capital consuming than the harvesting stage, especially for setting up the land. Sea salt making requires a large area of coastal mudflat for the evaporation ponds, with different salinity levels, and the crystallization pond (Wang *et al.*, 2015). The land setting period usually takes 1-2 months before the production season starts. It starts with sterilizing the pond, flattening the salt floor, and constructing dikes out of soil. A production system consists of the reservoir/concentration pond, the evaporation pond (referred to '*kolam peminihan*' in Indonesia), and the crystallization or table salt pond (Achmadi, 2013) (see *Figure 4.2*). After preparation, farmers start to allow seawater to enter the system, where it evaporates, and harvesting is performed during the production period. According to Guntur *et al.* (2018), the seawater evaporation process takes around 7-10 days. By comparison, for the processes investigated in our study, the farmers transported the evaporated seawater into the evaporation pond. This process may take 10-15 days.

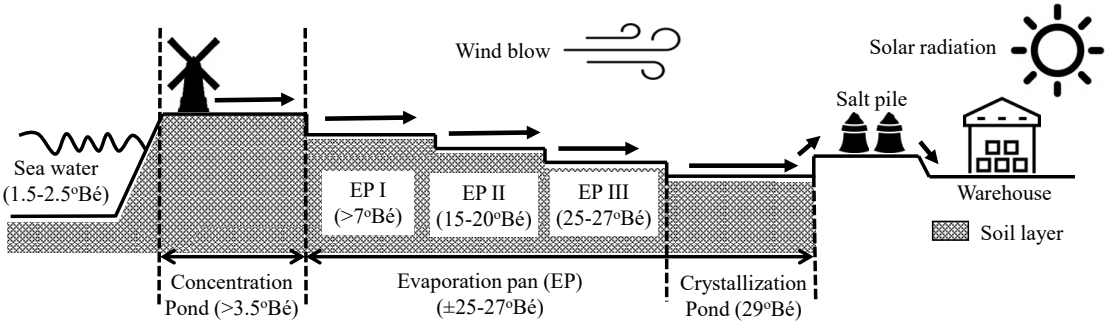

Figure 4.2. Schematic layout of traditional salt producing in Indonesia (modified from Gozan *et al.* (2018); Guntur *et al.* (2018); Jaya *et al.* (2016)

As part of the process, farmers also prepare the evaporation ponds, which commonly cover nearly 0.25 hectares (size 7-8 m x 30-40 m), work that usually starts at the beginning of the dry season (around April) (Gozan *et al.*, 2018) (*Figure 4.3a*). This preparation step includes compressing the soil using a wooden roller (locally called '*slender*') (see *Figure 4.3b*). Moreover, this pond consists of around 15 cm dikes, and the water has an average depth of 5-7 cm (*Figure 4.3c*). During the evaporation process, the salt brine has already layered in the crystallization pond, which covers at least 200 m^2 (Jaya *et al.*, 2016). Brine contains high concentration of salt. Farmers harvest the salt brine using long wooden rakes (called by local farmers '*garok*'), then drag the salt aside, collect it in sacks that are then transferred to the warehouse. Meanwhile the residual compound of brine flows back into concentration pond.

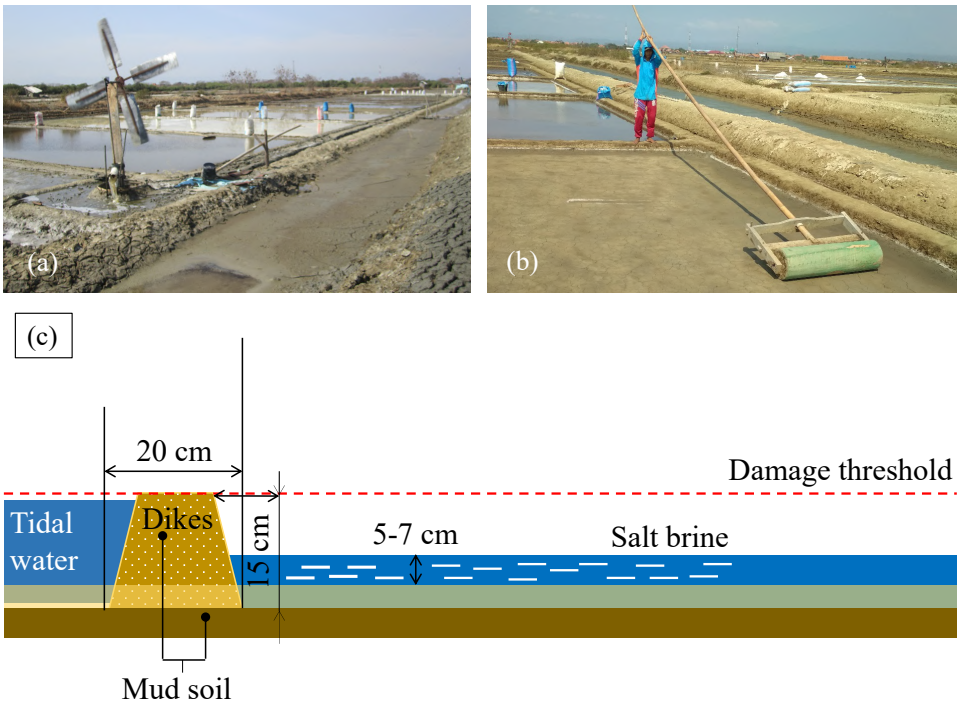

Figure 4.3. The typical preparation process in traditional salt harvesting including (a) the evaporation pond sequence where (b) the farmer usually rolls the evaporation pan surface using a '*slender*' and pushes the highly concentrated salt water (7-27° Be) in the pond; (c) a typical horizontal cross-section and its flood threshold (modified from Gozan *et al.* (2018))

4.3.3. Selected tidal flood events

Severe tidal flooding has occurred in most of the areas along the coastline of Cirebon for years. Some events have disrupted local economic activities, including salt harvesting. Tidal flood events in the salt production area of Cirebon have been simulated by Nirwansyah and Braun (2019) through a numerical model based on the 2016 and 2018 recorded events (see *Table 4.1*). That model includes wind velocity and Manning's coefficient. It was also validated through a water-level record from a local tidal station in Cirebon port and a global tide model. In that simulation, the inundation was mainly in the eight districts along the shore and submerged most of the salt harvesting ponds. Both events were mainly driven by the tidal cycle in the Java Sea and affected respectively 83.0% and 84.2% of the area with a maximum depth of 0.38 m and 0.40 m. The events economically impacted the local farmers in eight coastal districts and were mainly related to tidal phenomena (M_2) as there was no storm recorded in the simulation. Most of the affected districts were categorized into coastal prone areas (Rositasari *et al.*, 2011).

Table 4.1 Tidal flood events recorded and identified based on numerical simulations taken from Nirwansyah and Braun (2019)

Year	Production Period (month)											
	1	**2**	**3**	**4**	**5**	**6**	**7**	**8**	**9**	**10**	**11**	**12**
2016						●						
2018					●							

Off-production ● Tidal event Construction and production period

Harvesting period

4.4. Proposed method: combining damage functions with GIS

This study was designed using various data, as listed in the boxes in *Figure 4.4.* The numerical hydrodynamic model (HDM) from Nirwansyah and Braun (2019) was set up with additional features on the vulnerability aspect. While the GIS is the main instrument in the study, several inputs, e.g., spatial data and local indigenous information, were added (white boxes). In addition, a questionnaire was established to investigate the damage function (or susceptibility function) using a synthetic approach. Meanwhile, geospatial data from the national government and previous studies also support this current research (grey boxes). The following section provides more details about this model.

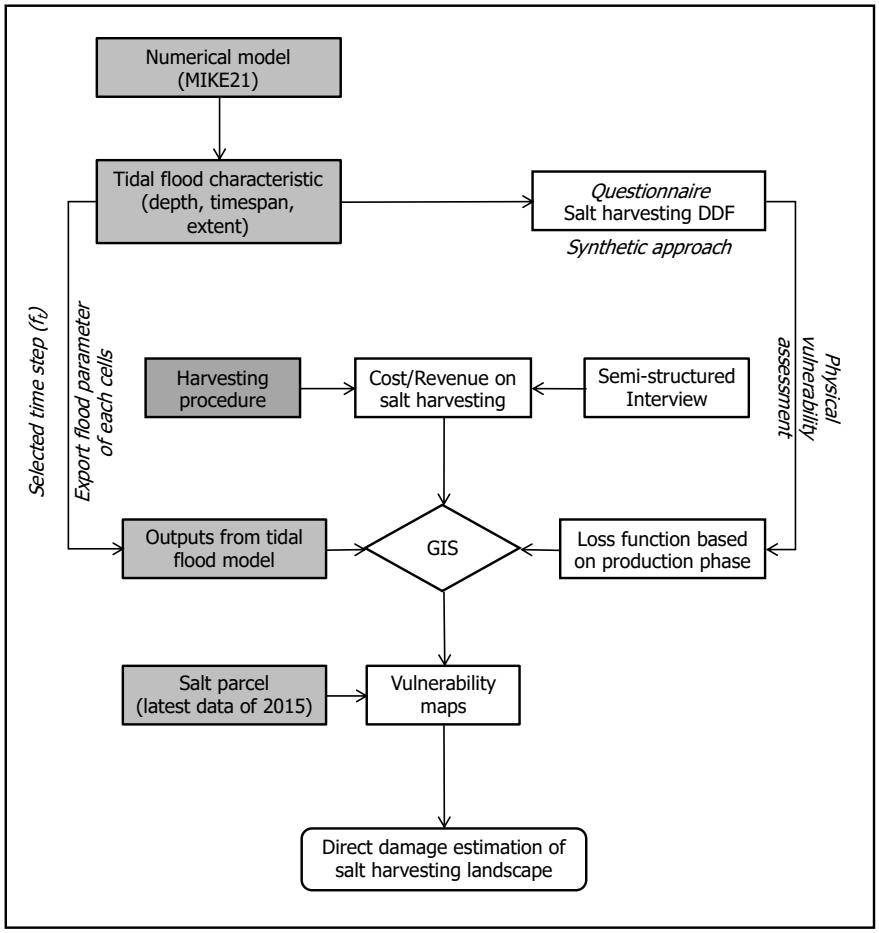

Figure 4.4. Structure of the current study

Since one of the goals of this study was to characterize salt harvesting damage through tidal floods, the authors define the salt harvesting sequence elements that are related to the flood events by modifying the approach from Okazumi *et al.* (2014) as follows: (i) salt farmers usually start working during early dry season (April/May), where the pre-production and early production process begins; (ii) salt farmers harvest from the salt pond during the production period (June to October); (iii) the harvest damage to the salt yield begins when the flood depth in the ponds is higher than the elevation of the dikes; and (iv) higher tides can lead to more severe damage and the seawater retreat takes longer. In this study, this relative depth-duration damage function (DDF) is used to estimate the PV of each salt parcel in the study area.

In order to relate the DDF to the local situation, the study mainly applied a synthetic (*what-if*) approach, as presented in Vozinaki *et al.* (2015). This approach is part of a knowledge-based approach that, basically, poses questions to informants who have a specific experience-based expertise (Schibuola and Byer, 1993). Therefore, the authors distributed a questionnaire to 14 local farmers as group representatives from six of the eight districts affected by tidal floods in both events: Losari, Gebang, Pangenan, Mundu, Gunungjati, Suranenggala. Those farmer representatives were part of a total of 81 groups of the PUGAR (People's Salt Development Program) and chosen through purposive sampling. Although data was not collated from two other districts, the questionnaire responses were deemed to apply to all districts.

As part of the questionnaire, our respondents used their experience to assess the average yield, the investment, the price of salt on the market, and the period of production during both tidal events based in order to determine cost and revenue (C/R) information. The losses were calculated for the stages of production in the salt ponds. As the DDF was originally established to describe PV, the reliable damage function of this study was first used to measure the expected loss based on the events in 2016 (Event A) and 2018 (Event B). Based on data availability and the use of established methods presented in recent research activities by Nirwansyah and Braun (2019), this study attempts to model the direct economic loss under the following premises: (i) the gravitational force of the moon (M_2) mainly triggers the inundation and, (ii) the expected parameters of flood characteristic are the flood depth and the flood duration.

The yields on salt harvesting were adapted from Munadi *et al.* (2016), and additional cost data was collected through semi-structured interviews with the Department of Marine and Fisheries (DKP) and local farmer group representatives (referred to a '*kelompok tani*' in Indonesia) from the research area. Cost items for traditional salt farmers were divided into two periods, namely: (i) construction and production period; and (ii) harvesting period (Munadi *et al.*, 2016). Generally, most of the farmers have to pay costs for rent, labour costs for maintenance (including for channel, pond, and compaction), tools and infrastructures, i.e., windmills, vinyl pipes (PVC), hoses, bamboo, buckets, plastic sheeting, salinity meter, pumps, gasoline, and synthetic ropes at the beginning of the season. Then, during the harvest period, salt farmers need to pay for labour, plastic sacks, and freight costs to transfer the harvested salt into storage or to the market. The price of tools usually changes depending on the market, but these changes are small. Some updates on the standard cost items for 2016 and 2018 were taken during fieldwork in November-December 2019[5]. All costs are presented on a per-hectare basis, as are benefits from harvest yields. *Table 4.2* presents the general costs for salt harvesting per hectare for the study area.

Table 4.2 Expenses of traditional salt producing in Cirebon (price per-hectare)

Components	IDR (in thousand)	%
Rent	10,000	17.71
Construction and production period		
Labour (dikes, channel, and pond maintenance)		4.82
Tools and devices (windmill, bamboo, wooden stick, and etc.)	9,060	16.04
Harvesting period		
Transporting workers (harvest, freight)	31,500	55.77
Tools and devices (Plastic sack, ropes)	3,200	5.67
Total	**56,480**	**100.0**

Source: compiled from Munadi *et al.* (2016) with some update on price during interviews

[5] This study implements a single cost since there was no significant price difference during the selected period

4.4.1. Generating flood hazard using water depth and flood duration

Two-time series of maps were produced by using GIS. The water-level data was taken from the numerical flood simulation by Nirwansyah and Braun (2019). In that simulation, topography data (DEM) was acquired from Indonesian national seamless digital elevation data (DEMNAS) within 0.27 arc-second resolution by Geospatial Information Agency (here referred to as BIG: *Badan Informasi Geospasial*). The affected salt pond area was detected by superimposing the raster data of tidal flood on the salt parcel area of the region at a scale of 1:15,000 polygon data from BIG. The earlier study in Nirwansyah and Braun (2019), which employed numerical and GIS-based modelling constructions, also provides both depth and duration of the inundation. There all geospatial datasets were set into the Universal Transverse Mercator (UTM) zone 48 and the World Geodetic System (WGS) 1984 datum. Most of the spatial calculations and analyses were performed on ArcGIS 10.6.

Water depth and flood duration were taken as critical inputs and processed in a MIKE 21 application. The water-level information was gathered in ASCII datasets transferred using Mike2Grid, which was evaluated using ArcGIS. Each dataset contains single values of every cell of the simulation. Depth information is commonly represented as the maximum value of each cell in the simulation (Susetyo, 2008). Comparable with flood depth, the timespan of the flood events in this case also plays a crucial role as it determines potential damage and loss to each element at risk. However, it requires further computing processes and reduces exportation data in an HDM. A shortcut is to use snapshots of the modelled flood at certain time-steps and to evaluate the dataset when the simulation is accomplished (Chen *et al.*, 2016). Currently, MIKE 21 has a wide-ranging purpose and a minimum specification and relatively user-friendly interface. Additionally, this platform is also capable of being integrated with GIS, thus allowing assessment of the full impacts on flood extent, flood depth, flood damage in the present or future (DHI Water and Environment, 2017; Yang *et al.*, 2002). However, MIKE 21 simulation does not present flood duration directly. Further processing requires 3 hours of 72 hours (3-days flood isolation) to be calculated separately, with the maximum water level (h_{max}) as an entrance. Here, the flood depth (f_d) and flood duration (f_t) were reclassified into the finest class at 25x25 m cell size.

4.4.2. Questionnaire for the depth-duration-damage function (DDF)

As mentioned earlier, data concerning damage to salt harvesting due to tidal flood inundation aspects have not been collected in Cirebon in the past; hence, historical flood damage curves are not available. After completing the depth and duration maps, using the prior method from Bhakta Shrestha *et al.* (2019) on rice crops, this study quantifies relative damage by using the DDF. In the context of this study, the DDF represents general response (damage) of a group of ponds with related properties to tidal flooding in each cell. The minimum value of 0 and the maximum value of 1 represent the extent of the damage caused by both events. This value was extracted from both water depth and duration through fuzzy membership and developed criteria. These relative damage functions state the degree of losses as a percentage of the total value of the

damaged assets (i.e., the declined value or the substitution cost) while absolute functions express the extent of damages in monetary values (Nafari, 2018).

In the structured questionnaire (as listed in *Table 4.3*),[6] selected farmers were requested to identify the tidal flood depth, duration, and any damage or loss to salt harvesting. The damage threshold started from 0.15 m, related to a minimum dike height, and rose until 1.50 m, as a maximum water level. This threshold reflects the inundation values from forecasting simulations and the Indonesian Hydro-Oceanographic Office (DISHIDROS) records until 2019 (Pratama, 2019). In addition, the flood duration begins from ≤ 1 day as minimum duration and continues until ≥ 7-days as the most extended timespan. The damage was converted into percentages and related to the probability of harvest loss. Here, farmers also differentiated potential loss in the different periods of production. Following Win *et al.* (2018), this model simply selects the average value from the wide answers each respondent provided based on their personal experiences and memories. All calculations were processed in Microsoft Excel and converted into a graphical format.

Table 4.3 Damage assessment sheet for salt harvesting based on depth and duration

Production stage	**Month of work**	**Avg Production (ton)**	**% Damage with flood depth (in meter)**						
			0.15	**0.25**	**0.50**	**0.75**	**1.00**	**1.25**	**1.50**
Construction and production period	April-May	…..	…..	…..	…..	…..	…..	…..	…..
Harvesting period	June-September	…..	…..	…..	…..	…..	…..	…..	…..
Off-period	October-March	…..	…..	…..	…..	…..	…..	…..	…..
Production stage	**Month of work**	**Avg Production (ton)**	**% Damage with flood duration (in days)**						
			≤ 1	**2**	**3**	**4**	**5**	**6**	**≥7**
Construction and production period	April-May	…..	…..	…..	…..	…..	…..	…..	…..
Harvesting period	June-September	…..	…..	…..	…..	…..	…..	…..	…..
Off-period	October-March	…..	…..	…..	…..	…..	…..	…..	…..

In this study, the DDF portrays PV based on local information. In the DDFs that were identified through the questionnaire on tidal floods in the salt-making landscape, different responses were found for each period of production. The relative damage increases along with the different levels for each period of production, especially during the harvesting period, which has the highest vulnerability level for both depth and duration. Salt farmers agreed that 1.0 m of flood depth would disrupt all of the salt-making processes, including infrastructure (i.e., dikes, channel, and salt bed), also cultivating and harvesting activities

[6] The questionnaire was designed with a simple format and tested on a few respondents before data collection

due to access difficulties. Further, the farmers believed that five days (or more) of inundation will profoundly disrupt salt production in the harvesting phase, related to the evaporation process, salt brine decaying through inundation water, and the possibility of dike and channel damage. The following *Figure 4.5* portrays the DDF for traditional salt harvesting in the selected study area, for each stage of production.

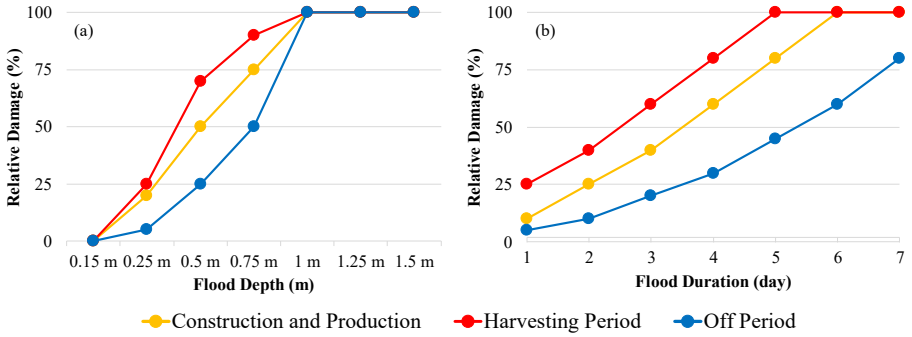

Figure 4.5. Damage function based on the developed questionnaire for each production phase against (a) depth of the inundation, and; (b) duration of the inundation

4.4.3. Quantifying physical vulnerability (PV) and the estimation of direct losses

The local domestic salt prices of IDR 2,000/kg in 2016 and IDR 700/kg in 2018 were employed in the study as average deal prices taken from the interview, though the standardized price was regulated in the Rules of the Ministry of Trade No. 125/2015.[7] Local prices can vary through the season since they are related to the supply-demand and amount of stock. In this research, the higher price during 2016 resulted from the short dry season (Warta Ekonomi, 2016). A productivity of 60 tons/hectare (by Munadi *et al.*, 2016) was used since the traditional farmers using the '*maduranese*' method dominate salt production in the region. Here, the authors assumed that salt harvesters started the pre-production period at relatively the same time, the beginning of May. Local farmers frequently harvest the salt in the pond twice a week with average yields of 3 tons/hectare/week (pers. comm. Department of Ocean and Fisheries facilitator).[8] However, during a tidal flood event, salt production is stopped while the farmers wait until the flood has drained away and the pond has been cleaned.

Table 4.4 Productivity, and revenue for salt harvesting (IDR thousands, in local price)

Tidal events	Productivity (tons/ha/year)	Salt price/tons (in thousand IDR)	Revenue/ha/year (in thousand IDR)
Event A	60	2,000	120,000
Event B	60	700	42,000

[7] The regulation has been renewed through Rules of the Ministry of Law No. 63/2019

[8] The official is appointed by Department of Marine and Fisheries (DKP) with a responsibility to advocate and regularly collect data from local salt harvesters.

As the DDF was gathered in the previous steps, the next step in this study is to evaluate the susceptibility level for the selected events. Flood hazard maps that contain depth and duration parameters are simply multiplied by the relevant DDF to calculate a PV level on each cell. The damage increment relates to the depth level. The same effect is also caused by the flood duration associated with the process of salt formation and the evaporation process. These curves relatively describe the damage percentage of salt and hazard magnitudes depending on the production stage. By using the customized approach on the paddy field, Bhakta Shrestha *et al.* (2019) focused primarily on rice growing stages. This study investigates the typical condition of the respective salt pond for each production stage. When a tidal flood event hits during the initial construction and production period, during which no salt is expected to be produced, farmers only repair the dike or pond and clean the ponds. Under such conditions, the flood damage to the salt harvest can be evaluated as the cost of input. The same approach can also be used during the off-period of production. The damage will rise to the top level during the harvesting period, as salt brine is typically collected. In this situation, salt harvesting is expected to be disrupted; at the same time, farmers need ancillary cash to restore the ponds, including dikes, channel, and salt pond floors.

The direct loss of salt harvesting based on the salt productivity rate was considered as yield loss and the value of yield losses was assessed as related to the local domestic price in a particular period. Due to the timeframe of the event and the salt harvest periodicity, different DDFs were used to estimate the damage consequences and evaluate the direct economic impact on salt harvesting, as listed in *Table 4.5.* The DDF was also illustrated in PV maps. Ultimately, all calculations in both periodicities were superimposed with the salt parcel dataset from BIG to evaluate the potential direct loss of each pond.

Table 4.5 Estimation method for flood damage of each period of salt harvesting

Period of salt harvesting	Expected loss formula
Construction and production period (*c*); and off-period (*o*)	*Direct loss (D)* $_{(c\ or\ o)}$ *= area inundated x physical vulnerability* $_{(c\ or\ o)}$ *x cost input/ha*
Harvesting period (*h*)	*Direct loss (D)* $_{(h)}$ *= area inundated x physical vulnerability*$_{(h)\ x}$ *((cost input/ha) + (productivity rate x local salt price))*

4.5. Results

4.5.1. Depth and duration of tidal inundation in the 2016 and 2018 events

The combination of both maps on flood depth (f_d) and duration (f_t) reveals the magnitude of the tidal flood events along Cirebon waters and its coastal area. As previously simulated in Nirwansyah and Braun (2019), the maximum tidal

flood levels of both events were obtained for the present paper. Here, in June 2016, Event A had a 0.38 m maximum flood depth, and Event B had a maximum 0.40 m in May 2018. Furthermore, the inundation for both incidents lasted for several days (2.23 days for Event A and 2.32 days for Event B). This length of time reflects the low topographical condition of the area and different wind velocities (u,v) in both events. The tidal hazard in both simulated events submerged most of the salt ponds along the coast to various depths and for different durations. For both events, it seems that the eastern part of the region was more affected than the western part. Both periods show relatively similar sequences, as related to their slightly different h_{max} (2 cm). Further details of the tidal hazard for both events can be seen in *Figure 4.6.*

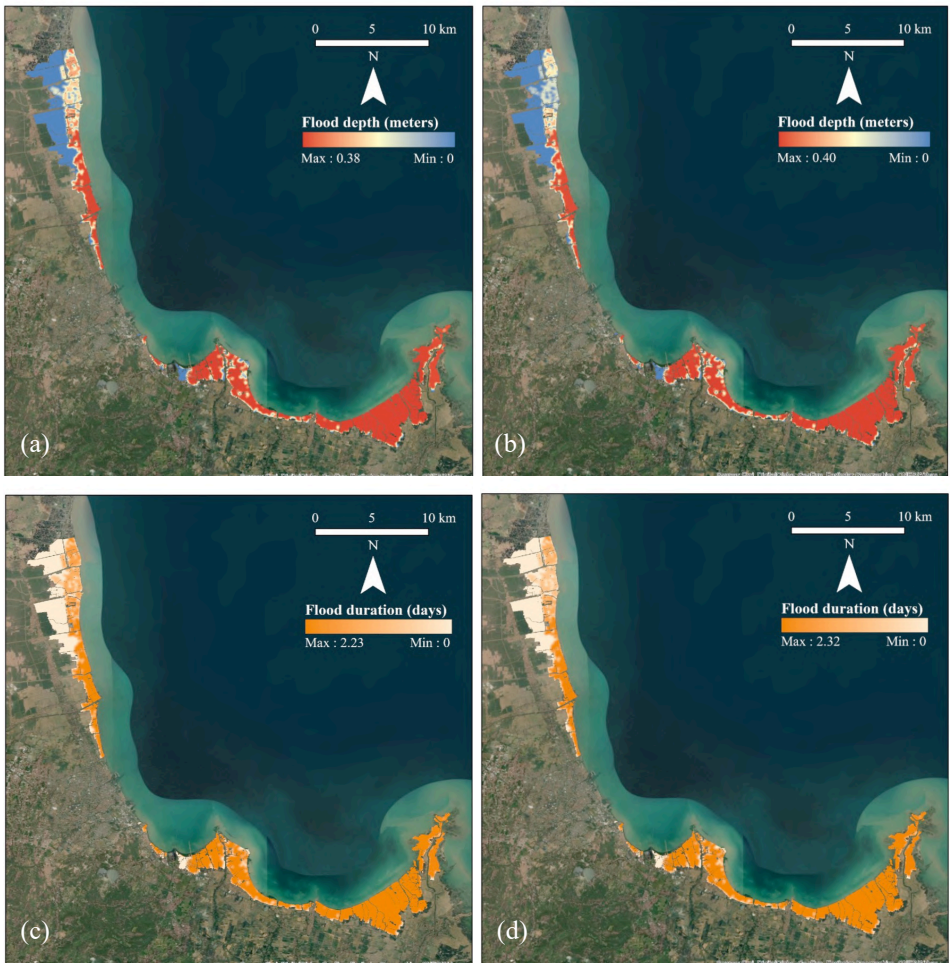

Figure 4.6. Comparison of the magnitude of tidal flooding which are (a) flood depth on Event A (maximum depth of 0.38 m); (b) Event B (maximum depth of 0.40 m); meanwhile tidal flood duration at maximum; (c) 2.23 days for Event A and; (d) 2.32 days for Event B

4.5.2. PV in salt harvesting landscape for the different production stage

In this research, PV is generated through the DDFs, which are used to calculate damage ratios for these multiple events. As mentioned in the previous section, the DDF starts at 0.15 m flood depth and one day or less of submerging. Both parameters are mapped and multiplied to generate a PV map. The GIS

analysis using combined raster datasets shows that the two events express relatively low vulnerability values in both parameters. Event A performs slightly higher in terms of the vulnerability values as related to the timing of flooding. Here, the vulnerability on depth ranges from 0 to 0.28, while vulnerability on duration scored around 0 to 0.44 (see *Figure 4.7 a-c*). The top of the combined vulnerability score for this event was 0.12 (while the lowest value was 0). However, a lower score of combined vulnerability was determined for Event B with a score of 0.11, from the construction stage. At that point, the vulnerability on depth was 0.30, and the duration was 0.39 (see *Figure 4.8a-c*).

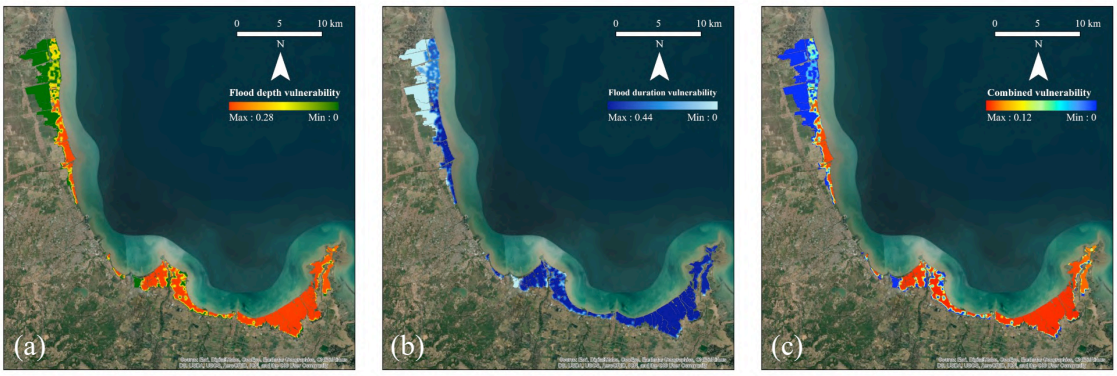

Figure 4.7. Vulnerability level of flood depth for Event A based on; (a) depth function within 0.28 maximum score; (b) duration function within 0.44 as the top score and; (c) combined vulnerability level of 0.12 as the ultimate score

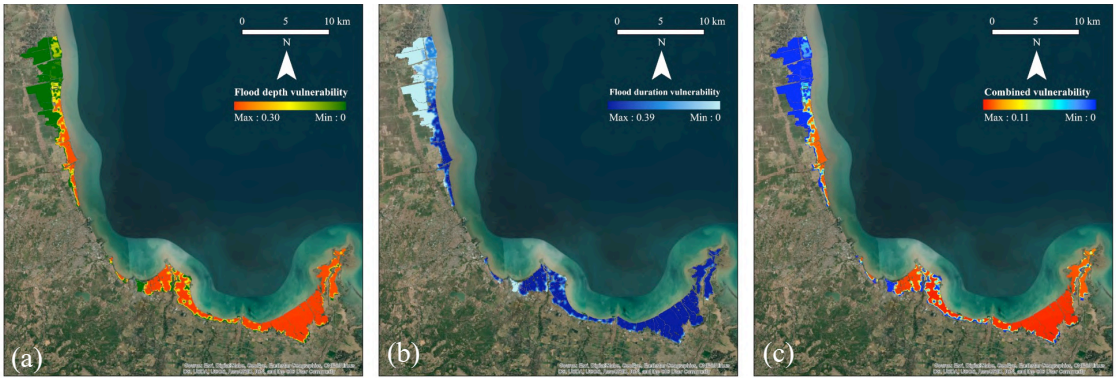

Figure 4.8. Distribution of vulnerability degree of flood depth for Event B based on; a) depth function within 0.30 maximum score; (b) duration function within 0.39 as the top score and; (c) combined vulnerability level of 0.11 as the ultimate value

4.5.3. Estimations of expected tidal flood damage on salt harvesting

Direct loss of salt harvesting due to tidal flooding in both events was examined through a raster dataset analysis combined with a damage function, visualized in *Figure 4.5.* Previous local standard costs and revenue (C/R) were collected based on Munadi *et al.* (2016) and are listed in *Table 4.2* and *Table 4.4.* The loss estimation was estimated by multiplying each cell in a PV map with C/R for the specific year. At that time, the expected costs (*C*) were about IDR 441.64 x 10^9 for 2016 and IDR 170.3 x 10^9 for 2018, and the benefit (*R*) was IDR 938.32 x 10^9 (2016). The model displays loss distribution for both events. As can be seen in

Figure 4.9, the western part had a relatively smaller loss, i.e., the district Kapetakan (section 1), due to the current direction and tidal character in that period, as previously simulated in Nirwansyah and Braun (Nirwansyah and Braun, 2019) using the HDM. Conversely, most of the ponds in Mundu, and Pangenan (section 2), and also Losari (section 3) in the eastern part were more affected by the tidal event. However, there were also minimum impact cases of inundation in a particular part of Astanajapura and Pangenan, which were related to the local elevation.

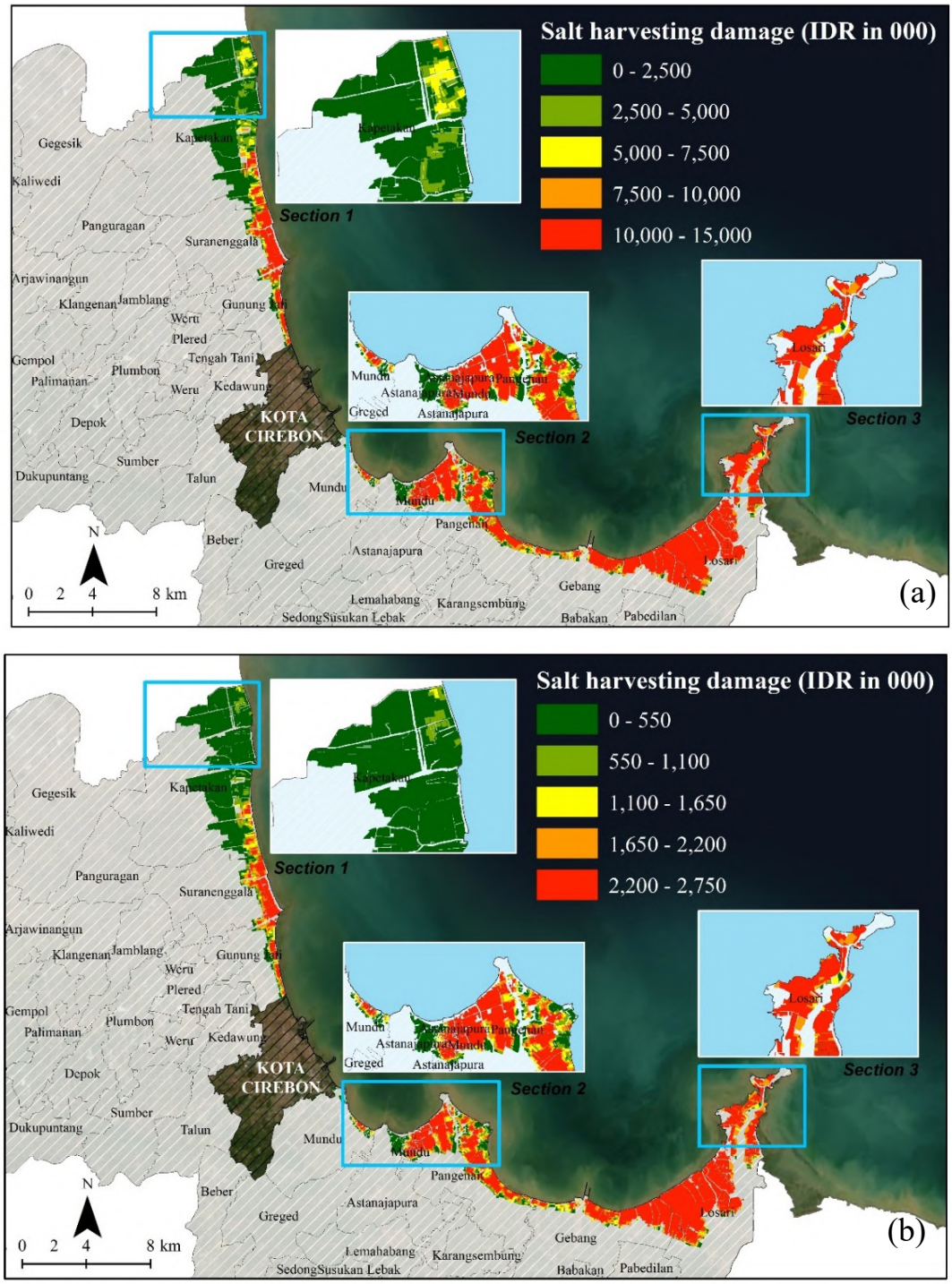

Figure 4.9. Estimated tidal flood damage in the salt harvesting landscape in Cirebon during; (a) Event A (June 2016); and (b) Event B (May 2018)

A stable total salt area of 7,819.32 hectares was counted from the polygon data, the expected damage (D_{tot}) for Event A was IDR 74.11 x 10^9 for Event B was IDR 13.79 x 10^9. Furthermore, the model estimates that the expected loss of Event A reached 5.37 % of its total value (V) or around IDR 1.38 x 10^{12} based on costs (C) and revenues (R) in the particular year. Meanwhile, the estimated loss in 2018 (Event B) has a more significant impact. Here, the loss was calculated as approximately 8.09 % of the total value (V) for 2018. Nonetheless, the damage loss in Event B has a lower value IDR 170.3 x 10^9. As no salt had started to be produced in May and no profits were taken from the transaction, the total loss in this particular event was smaller. In this study, each DDF value shows the difference in total loss based on the timing of the event. Here, the DDFs express distinctive responses that are related to different monetary losses and include C/R. The following *Table 4.6* describes the estimated damage on salt harvesting for the two tidal flood occurrences.

Table 4.6 Estimated cost, revenue (total value) and expected loss on salt harvesting for both events, which represent a different period of production (in thousand IDR)

	Event A	**Event B**
Cost (C)	441,635,194	170,304,790
Revenue (R)	938,318,400	-
Total value (V=C+R)	1,379,953,594	170,304,790
The expected loss for each parcel (D)		
- Min	0.00	0.00
- Max	13,322.72	2,528.27
- Mean	6,912.17	1,286.23
Overall damage (D_{tot})	**74,105,354**	**13,789,773**

4.6. Discussion

According to our knowledge, this is the first study proposing to quantify damage loss on salt harvesting due to tidal flood in coastal regions. The introduced combination of DDF and GIS analysis produces valuable results that enable scenarios to be created for economic loss in salt harvesting. This model contributes to overcoming the absence of C/R aspects by presenting a more detailed estimation of tidal flood damage as a local disruption (Hino *et al.*, 2019). The study applies a synthetic approach previously implemented in an agriculture context involving farmers and their indigenous knowledge (Bhakta Shrestha *et al.*, 2019; Vozinaki *et al.*, 2015). In this case, PV inputs that function as a control for the expected loss can be extrapolated through a numerical model such as HDM. Here, this study employs the datasets from Nirwansyah and Braun (2019) that had already been exported from MIKE 21 into a raster format. Some scenarios of depth and duration can be used to estimate the possibility of loss in the future, including the expected sea-level rise. This model also develops the utilization of geospatial technology, including GIS and elevation data (DEM), with a

combination of C/R and PV for each salt parcel. This efficient technique is an improvement in comparison to previous studies that have been conducted in major agricultural landscapes (Chau *et al.*, 2015; Dutta and Herath, 2003; Okazumi *et al.*, 2014).

The establishment and application of this method in the case of Cirebon was developed through a basic understanding of GIS modelling and identified tidal inundation from the hydrodynamic variables (i.e., depth and duration). Moreover, the model requires the elemental conception of salt harvesting settings and mechanisms that can provide useful information for the damage estimation. This advanced method provides a single value for the damage in each pond rather than using a grid that represents the score on every single pixel. The model was used to examine the expected loss for about 10,721 salt parcels individually, of which about 70% were affected. Although there were lengthy procedures in processing flood duration maps from MIKE to raster data in ArcGIS, the 3-hours separation is relatively consistent with the tidal water level as the previous simulation used a 1-hour timespan. As the PV resulted from multiplying depth and duration, the cell size will define the precision. For this work, we used a 25x25 m raster cell size, compatible with the size of each salt parcel. However, the possible use of smaller cell sizes, i.e., 10x10, or 5x5, is also suggested for more precise results. The authors also recommend customizing the cell size, especially for smaller ponds.

This study demonstrates some limitations that must be considered in future research. First, the method requires relatively up-to-date polygon data on the salt parcels, which probably limits its application in data-scarce regions, especially in the countries of the Global South. Otherwise, it might be possible to delineate the salt pond objects into polygon data for GIS functionalities using object-based image analysis (Blaschke, 2010). Second, the identification of price and alternative costs are highly dependent on local conditions and practiced processing techniques. In this research, the equipment used (see Section 0) and the price of salt will significantly depend on the market conditions (see Section 4.4.3). The actual price of salt from the local market can be taken from a questionnaire or interview with the local farmers. Furthermore, the relevant sampling and its size have to be taken into account and will be influenced by the local settings, including the salt harvester categories based on land ownership. Alternatively, the use of regulated salt prices at the national or regional level could be used. Lastly, the completeness of this model is limited by the lack of attention to other salt harvesting components that may be affected, such as warehouses, accessible roads, and existing stocks (Brémond and Grelot, 2013; Molinari *et al.*, 2019). Those components may increase the expected loss from the hazard events.

4.7. Conclusions

This paper has established a first-time approach to estimating the direct loss in salt harvesting landscapes based on two recorded past events. The model was implemented in Cirebon, West Java, where the calculations were obtained. By using inputs from previous datasets on the hydrodynamic model, GIS application can extend information about typical characteristics of tidal flooding, especially on its depth and duration of inundation. At the same time, the beneficial

function of GIS in this study enhances the salt harvesters' capability to assess PV aspects in salt harvesting landscapes through depth and duration based on their memories of tidal inundation in past events. This model establishes progress in tidal flood modelling, specifically in a minor but important type of agriculture in the coastal region, and encourages further application in other minor economic activities and geographical settings.

Despite the identified restrictions, this paper presents the applicability of the model when estimating the expected loss using limited data, potentially from a marginal area, and could possibly be adapted to different regions in the tropics. Ultimately, however, this model presents the initial approach for damage loss estimation on tidal flooding for salt harvesting landscapes in the tropical region, especially in Cirebon, West Java.

This research also encourages further studies on possible implementations of calibration and validation through various techniques and models including a proposal for validation using multi-parametric approach such as the Analytical Hierarchical Process (AHP). Furthermore, we also propose to include global phenomenon such as sea level rise for future research.

Declaration of Competing Interest

The authors declare no conflict of interest.

Acknowledgment

This project has been conducted as part of doctoral research at the Institute of Geography, University of Cologne, Germany, sponsored by Indonesia Endowment Fund for Education (LPDP), Ministry of Finance of Indonesia addressed to the first author. The authors are thankful for the commitment and effort of the salt farmer representatives and local authorities in Cirebon, who made this project possible. The authors also express their gratitude to Prof. Georg Bareth for constructive inputs, Frauke Haensch for proofreading, and the anonymous reviewers for their valuable suggestions.

Abbreviation

IDR – Indonesian Rupiah
ELCIRC – Eulerian-Lagrangian circulation
GIS – Geographic Information System
PV – Physical Vulnerability
DEM – Digital Elevation Model
GDP – Gross Domestic Product
HDPE – high-density polyethylene
HDM – hydrodynamic model
DDF – depth-duration damage function
C/R – Cost and Revenue
DKP – *Department Kelautan dan Perikanan* (Department of Marine and Fisheries)
PVC - polyvinyl chloride
BIG – Badan Informasi Geospasial (National Geospatial Information Agency of Indonesia)
DEMNAS – Indonesian national seamless digital elevation model
UTM – Universal Transverse Mercator

WGS – World Geodetic System
ASCII - American Standard Code for Information Interchange
DISHIDROS – *Dinas Hidro-Oseanografi* (Indonesian Hydro-Oceanographic Office)

4.8. References

Achmadi, D. (2013), Kajian Pengembangan Sentra Tambak Garam Rakyat Di Kawasan Pesisir Selatan Kabupaten Sampang Provinsi Jawa Timur, IPB.

Antczak, K.A. (2017), "Cultivating Salt: Socio-Natural Assemblages on the Saltpans of the Venezuelan Islands, Seventeenth to Nineteenth Century", Environmental Archaeology, Taylor & Francis, Vol. 0 No. 0, pp. 1–13.

Apriani, M., Hadi, W. and Masduqi, A. (2018), "Physicochemical properties of sea water and bittern in Indonesia: Quality improvement and potential resources utilization for marine environmental sustainability", Journal of Ecological Engineering, Vol. 19 No. 3, pp. 1–10.

Bhakta Shrestha, B., Sawano, H., Ohara, M., Yamazaki, Y. and Tokunaga, Y. (2019), "Methodology for Agricultural Flood Damage Assessment", Recent Advances in Flood Risk Management, Vol. i, IntechOpen, p. 13.

Blaschke, T. (2010), "Object based image analysis for remote sensing", ISPRS Journal of Photogrammetry and Remote Sensing, Elsevier B.V., Vol. 65 No. 1, pp. 2–16.

BPS Cirebon. (2018), Produk Domestik Regional Bruto Kabupaten Cirebon Menurut Lapangan Usaha 2015-2019, edited by Margiono, O., BPS - Statistics of Cirebon Regency, Cirebon, available at: https://doi.org/10.15713/ins.mmj.3.

BPS Provinsi Jawa Barat. (2020), Indikator Strategis Kabupaten/Kota Provinsi Jawa Barat 2019, edited by Bidang Integrasi Pengolahan dan Diseminasi Statistik, Badan Pusat Statistik Provinsi Jawa Barat, Bandung, available at: https://jabar.bps.go.id/publication/download.html?nrbvfeve=ZjBhMDEzZmE3NzRiMzg1MDRkZWY1NjVh&xzmn=aHR0cHM6Ly9qYWJhci5icHMuZ28uaWQvcHVibGljYXRpb24vMjAyMC8wNS8yOS9mMGEwMTNmYTc3NGIzODUwNGRlZjU2NWEvaW5kaWthdG9yLXN0cmF0ZWdpcy1rYWJ1cGF0ZW4ta290YS1wcm92aW5zaS1qYX

Brémond, P. and Grelot, F. (2010), "Comparison of a systemic modelling of farm vulnerability and classical methods to appraise flood damage on agricultural activities", Advancing Sustainability in a Time of Crisis. 11th Biennal Conference of the International Society for Ecological Economics, No. August 2010, pp. 22–25.

Brémond, P. and Grelot, F. (2013), "Review Article: Economic evaluation of flood damage to agriculture - Review and analysis of existing methods", Natural Hazards and Earth System Sciences, Vol. 13 No. 10, pp. 2493–2512.

Chau, V.N., Cassells, S. and Holland, J. (2015), "Economic impact upon agricultural production from extreme flood events in Quang Nam, central Vietnam", Natural Hazards, Vol. 75 No. 2, pp. 1747–1765.

Chen, A.S., Hammond, M.J., Djordjević, S., Butler, D., Khan, D.M. and Veerbeek, W. (2016), "From hazard to impact: flood damage assessment tools

for mega cities", Natural Hazards, Vol. 82 No. 2, pp. 857–890.
Chung, S., Takeuchi, J., Fujihara, M. and Oeurng, C. (2019), "Flood damage assessment on rice crop in the Stung Sen River Basin of Cambodia", Paddy and Water Environment, Springer Singapore, Vol. 17 No. 2, pp. 255–263.
Davis, J. (2000), "Structure, function, and management of the biological system for seasonal solar saltworks", Global Nest, Vol. 2 No. 3, pp. 217–226.
Dharmayanti, S., Suharno and Rifin, A. (2013), "Analysis of Salt Availability Towards Sustainable National Salt Self- Sufficiency Achievement (A Dynamic Model Approach)", Jurnal Sosial Ekonomi Kelautan Dan Perikanan., Vol. 8 No. 1, pp. 103–115.
DHI Water and Environment. (2017), Mike 21 Flow Model FM, Hydrodynamic Module User Guide, DHI Water and Environment, Denmark, available at: https://www.mikepoweredbydhi.com/.
Dutta, D. and Herath, S. (2003), "GIS Based Flood Loss Estimation Modeling in Japan", Journal of Hydrology, Vol. 277 No. 1–2, pp. 24–49.
Dutta, D., Herath, S. and Musiake, K. (2003), "A mathematical model for flood loss estimation", Journal of Hydrology, Vol. 277 No. 1–2, pp. 24–49.
Eleutério, J., Martinez, D. and Rozan, A. (2010), "Developing a GIS tool to assess potential damage of future floods", WIT Transactions on Information and Communication Technologies, Vol. 43 PART I, pp. 381–392.
Forster, S., Kuhlmann, B., Lindenschmidt, K.E. and Bronstert, A. (2008), "Assessing flood risk for a rural detention area", Natural Hazards and Earth System Science, Vol. 8 No. 2, pp. 311–322.
Fuchs, S., Birkmann, J. and Glade, T. (2012), "Vulnerability assessment in natural hazard and risk analysis: current approaches and future challenges", Natural Hazards, Vol. 64 No. 3, pp. 1969–1975.
Gerl, T., Bochow, M. and Kreibich, H. (2014), "Flood Damage Modeling on the Basis of Urban Structure Mapping Using High-Resolution Remote Sensing Data", Water, Vol. 6 No. 8, pp. 2367–2393.
Gozan, M., Ningsih, Y., Efendy, M. and Basri, F.H. (2018), Hikayat Si Induk Bumbu (in Indonesia), edited by Rusi, N., Saripudin, J. and Isaiyas, I., First Edit., Kepustakaan Populer Gramedia, Jakarta.
Guntur, G., Jaziri, A.A., Prihanto, A.A., Arisandi, D.M. and Kurniawan, A. (2018), "Development of salt production technology using prism greenhouse method", IOP Conference Series: Earth and Environmental Science, Vol. 106 No. 1, available at: https://doi.org/10.1088/1755-1315/106/1/012082.
Hino, M., Belanger, S.T., Field, C.B., Davies, A.R. and Mach, K.J. (2019), "High-tide flooding disrupts local economic activity", Science Advances, Vol. 5 No. 2, p. eaau2736.
Hinton, A. (2000), "Tidal changes and coastal hazards: Past, present and future", Natural Hazards, Vol. 21, pp. 173–184.
Huda, F.A. (2015), Economic Assessment of Farm Level Climate Change Adaptation Options: Analytical Approach and Empirical Study for the Coastal Area of Bangladesh, Humboldt-Universität zu Berlin.
ICCSR. (2010), Scientific Basis: Analysis and Projection of Sea Level Rise and Extreme Weather Event, Jakarta.
Jaya, N.T.S.P., Hartati, R. and Widianingsih, W. (2016), "Produksi Garam Dan

Bittern Di Tambak Garam", Jurnal Kelautan Tropis, Vol. 19 No. 1, pp. 43–47.

Karagiorgos, K., Thaler, T., Maris, F. and Fuchs, S. (2016), "Assessing flash flood vulnerability using a multi-vulnerability approach", E3S Web of Conferences, Vol. 7, pp. 3–9.

KKP. (2015), Salt Production of Indonesia (in Bahasa), Jakarta, available at: http://statistik.kkp.go.id/sidatik-dev/Berita/Analisis Produksi Garam Indonesia.pdf.

Kotera, A., Nagano, T., Hanittinan, P. and Koontanakulvong, S. (2016), "Assessing the degree of flood damage to rice crops in the Chao Phraya delta, Thailand, using MODIS satellite imaging", Paddy and Water Environment, Springer Japan, Vol. 14 No. 1, pp. 271–280.

Lai, F. (2013), "Nature and the city: the salt-works park in the urban area of Cagliari (Sardinia, Italy)", Journal of Political Ecology, Vol. 20 No. 1, p. 329.

Lia, E. (2016), "Puluhan Ribu Ton Garam di Cirebon Tersapu Banjir Rob page-2 : Okezone News", Okezone.Com, available at: https://news.okezone.com/read/2016/06/17/525/1418255/puluhan-ribu-ton-garam-di-cirebon-tersapu-banjir-rob?page=2 (accessed 10 June 2019).

Marfai, M.A., King, L., Sartohadi, J., Sudrajat, S., Budiani, S.R. and Yulianto, F. (2008), "The impact of tidal flooding on a coastal community in Semarang, Indonesia", Environmentalist, Vol. 28 No. 3, pp. 237–248.

Mason, J.L. and Kipp Jr., K.L. (1997), Investigation of Salt Loss from the Bonneville Salt Flats, Northwestern Utah, Salt Lake City, Utah, available at: https://pubs.usgs.gov/fs/1997/fs135-97/PDF/FS97-135.pdf.

Merz, B., Kreibich, H., Schwarze, R. and Thieken, A. (2010), "Review article 'Assessment of economic flood damage'", Natural Hazards and Earth System Science, Vol. 10 No. 8, pp. 1697–1724.

Messner, F., Penning-rowsell, E., Green, C., Tunstall, S., Veen, A. Van Der, Tapsell, S., Wilson, T., et al. (2007), "Evaluating flood damages : guidance and recommendations on principles and methods principles and methods", Flood Risk Management: Hazards, Vulnerability and Mitigation Measures, p. 189.

Metrotv. (2016), "700 Hectares of Salt Pond in Cirebon Submerged Coastal Flood (in Bahasa)", Metrotvnews.Com, available at: http://m.metrotvnews.com/jabar/peristiwa/JKR4MYQb-700-hektare-tambak-garam-di-cirebon-terendam-banjir-rob (accessed 29 September 2017).

de Moel, H., van Alphen, J. and Aerts, J.C.J.H. (2009), "Flood maps in Europe - methods, availability and use", Natural Hazards and Earth System Sciences, Vol. 9 No. 2, pp. 289–301.

Molinari, D., Menoni, S., Aronica, G.T., Ballio, F., Berni, N., Pandolfo, C., Stelluti, M., et al. (2014), "Ex post damage assessment: An Italian experience", Natural Hazards and Earth System Sciences, Vol. 14 No. 4, pp. 901–916.

Molinari, D., Scorzini, A.R., Gallazzi, A. and Ballio, F. (2019), "AGRIDE-c, a conceptual model for the estimation of flood damage to crops: development and implementation", Natural Hazards and Earth System Sciences Discussions, pp. 1–24.

Munadi, E., Ardiyanti, S.T., Ingot, S.R., Lestari, T.K., Subekti, N.A., Salam, A.R., Alhayat, A.P., et al. (2016), Info Komoditi Garam, edited by Salim, Z. and

Munadi, E., Badan Pengkajian dan Pengembangan Perdagangan, Jakarta, available at: http://bppp.kemendag.go.id/media_content/2017/08/Isi_BRIK_Garam.pdf.

Nafari, R.H. (2018), Flood Damage Assessment in Urban Areas, The University of Melbourne.

Nagara, G.A., Sasongko, N.A. and Olakunle, O.J. (2010), Introduction to Java Sea, Stavanger, available at: https://doi.org/10.1007/978-1-84882-972-5_26.

Nguyen, N.Y., Ichikawa, Y. and Ishidaira, H. (2017), "Establishing flood damage functions for agricultural crops using estimated inundation depth and flood disaster statistics in data-scarce regions", Hydrological Research Letters, Vol. 11 No. 1, pp. 12–18.

Nirwansyah and Braun. (2019), "Mapping Impact of Tidal Flooding on Solar Salt Farming in Northern Java using a Hydrodynamic Model", ISPRS International Journal of Geo-Information, Vol. 8 No. 10, p. 451.

Okazumi, T., Tanaka, S., Kwak, Y., Shrestha, B.B. and Sugiura, A. (2014), "Flood vulnerability assessment in the light of rice cultivation characteristics in Mekong River flood plain in Cambodia", Paddy and Water Environment, Vol. 12 No. 2, pp. 275–286.

Papathoma-Köhle, M., Cristofari, G., Wenk, M. and Fuchs, S. (2019), "The importance of indicator weights for vulnerability indices and implications for decision making in disaster management", International Journal of Disaster Risk Reduction, Elsevier Ltd, Vol. 36 No. July 2018, p. 101103.

Penning-Rowsell, E.C., Yanyan, W., Watkinson, A.R., Jiang, J. and Thorne, C. (2013), "Socioeconomic scenarios and flood damage assessment methodologies for the Taihu Basin, China", Journal of Flood Risk Management, Vol. 6 No. 1, pp. 23–32.

Picado, A., Dias, J.M. and Fortunato, A.B. (2009), "Effect of flooding the salt pans in the Ria de Aveiro", Journal of Coastal Research, Vol. 2009 No. 2, 56, pp. 1395–1399.

Pratama, M.B. (2019), "Tidal Flood in Pekalongan: Utilizing and Operating Open Resources for Modelling", IOP Conference Series: Materials Science and Engineering, Vol. 676 No. 1, p. 012029.

PSSDAL. (2010), Peta Lahan Garam Indonesia, edited by Saputro, G.B., Edrus, I.N., Hartini, S. and Poniman, A., PSSDAL BAKOSURTANAL, Cibinong, available at: https://perpustakaan.big.go.id/opacbig/index.php?p=show_detail&id=10283.

PT Cirebon Energi Prasarana. (2016), ANDAL: Deskripsi Rinci Rona Lingkungan Hidup Awal, Cirebon.

Rositasari, R., Setiawan, W.B., Supriadi, I.H. and Prayuda, B. (2011), "Coastal Vulnerability Prediction To Climate Change: Study Case in Cirebon Coastal Area", Jurnal Ilmu Dan Teknologi Kelautan Tropis, Vol. 3 No. 1, pp. 52–64.

Sakamoto, T., Van Nguyen, N., Kotera, A., Ohno, H., Ishitsuka, N. and Yokozawa, M. (2007), "Detecting temporal changes in the extent of annual flooding within the Cambodia and the Vietnamese Mekong Delta from MODIS time-series imagery", Remote Sensing of Environment, Vol. 109 No. 3, pp. 295–313.

Schibuola, S. and Byer, P.H. (1993), "Use of Knowledge-Based Systems for the Review of Environmental Impact Assessments", in Kim, T.J. (Ed.), Expert Systems in Environmental Planning, Springer Berlin Heidelberg, Berlin, Heidelberg, pp. 189–204.

Sedivy, V.M. (2009), "Environmental Balance of Salt Production speaks in favour of Solar Saltworks", Global NEST Journal, Vol. 11 No. 1, pp. 41–48.

Sumiati, S. (2015), "Innovation In Improving The Quality Of Salt Production at Coastal Areas: A Literature Study", Integrated Solution to Overcome the Climate Change Impact on Coastal Area, UNISSULA, Semarang, pp. 2–5.

Susanto, H., Rokhati, N. and Santosa, G.W. (2015), "Development of Traditional Salt Production Process for Improving Product Quantity and Quality in Jepara District, Central Java, Indonesia", International Conference on Tropical and Coastal Region Eco-Development 2014 (ICTCRED 2014), Vol. 23, Elsevier B.V., pp. 175–178.

Susetyo, C. (2008), Urban Flood Management In Surabaya City: Anticipating Changes in the Brantas River System, Institute for Geo-information Science and Earth Observation.

Suwarno, Y. (2014), "Quickbird imagery for support to mapping of salt land suitability in Kupang bay, East Nusa Tenggara Province - Indonesia", 35th Asian Conference on Remote Sensing 2014, ACRS 2014: Sensing for Reintegration of Societies, available at: https://www.scopus.com/inward/record.uri?eid=2-s2.0-84925435276&partnerID=40&md5=0d04025f777b49575aea05e87aba5c93.

Takagi, H., Esteban, M., Mikami, T. and Fujii, D. (2016), "Projection of coastal floods in 2050 Jakarta", Urban Climate, Vol. 17, pp. 135–145.

Thieken, A.H., Olschewski, A., Kreibich, H., Kobsch, S. and Merz, B. (2008), "Development and evaluation of FLEMOps - A new Flood Loss Estimation MOdel for the private sector", WIT Transactions on Ecology and the Environment, Vol. 118, pp. 315–324.

Thouret, J.C., Ettinger, S., Guitton, M., Santoni, O., Magill, C., Martelli, K., Zuccaro, G., et al. (2014), "Assessing physical vulnerability in large cities exposed to flash floods and debris flows: The case of Arequipa (Peru)", Natural Hazards, Vol. 73 No. 3, pp. 1771–1815.

Thys, a. (2003), "Sustainability and Impact Aspects of Exploitation of Marine Salt, Magnesium and Bromine", Journal of Coastal Research, Vol. 19 No. 4, pp. 912–918.

tirto.id. (2018), "Banjir Cirebon Rendam Ribuan Rumah, Ketinggian Air 50-60 Cm - Tirto.ID", available at: https://tirto.id/banjir-cirebon-rendam-ribuan-rumah-ketinggian-air-50-60-cm-cF4Y (accessed 30 November 2018).

Trikobery, J., Achmad, R., Kurniawati, N. and Anna, Z. (2017), "Analisis Usaha Tambak Garam di Desa Pengarengan Kecamatan Pangenan Kabupaten Cirebon", Jurnal Perikanan Dan Kelautan, Vol. VIII No. 2, pp. 168–175.

USGS. (2020), Mineral Commodity Summaries, Virginia, available at: https://doi.org/10.3133/mcs2020.

Vieira, N. and Bio, A. (2011), "Spatial and temporal variability of water quality and zooplankton in an artisanal salina", Journal of Sea Research, Elsevier B.V., Vol. 65 No. 2, pp. 293–303.

Vozinaki, A.E.K., Karatzas, G.P., Sibetheros, I.A. and Varouchakis, E.A. (2015),

"An agricultural flash flood loss estimation methodology: the case study of the Koiliaris basin (Greece), February 2003 flood", Natural Hazards, Springer Netherlands, Vol. 79 No. 2, pp. 899–920.

Wang, H., Xu, X. and Zhu, G. (2015), "Landscape changes and a salt production sustainable approach in the state of salt pan area decreasing on the coast of Tianjin, China", Sustainability (Switzerland), Vol. 7 No. 8, pp. 10078–10097.

Warta Ekonomi. (2016), "Kiara Ingin Mendag Audit Garam di Kementerian-nya", 10 August, available at: https://www.wartaekonomi.co.id/read/2016/08/10/109455/news_post.php (accessed 19 July 2020).

Wijayanti, P., Zhu, X., Hellegers, P., Budiyono, Y. and van Ierland, E.C. (2017), "Estimation of river flood damages in Jakarta, Indonesia", Natural Hazards, Springer Netherlands, Vol. 86 No. 3, pp. 1059–1079.

Win, S., Zin, W.W., Kawasaki, A. and San, Z.M.L.T. (2018), "Establishment of flood damage function models: A case study in the Bago River Basin, Myanmar", International Journal of Disaster Risk Reduction, Elsevier Ltd, Vol. 28 No. November 2017, pp. 688–700.

Yang, X., Grönlund, A. and Tanzilli, S. (2002), "Predicting Flood Inundation and Risk Using Geographic Information System and Hydrodynamic Model", Geographic Information Sciences, Vol. 8 No. 1, pp. 48–57.

Zhai, G., Fukuzono, T. and Ikeda, S. (2005), "Modeling Flood Damage: Case of Tokai Flood 2000", Journal of the American Water Resources Association, Vol. 41 No. 1, pp. 77–92.

Chapter 5

Tidal Flood Risk on Salt Farming: Evaluation of Post Events in the Northern Part of Java Using a Parametric Approach

Published as:

Nirwansyah, A.W. and Braun, B. (2021), "Tidal flood risk on salt farming: evaluation of post events in the northern part of Java using a parametric approach". *Geosciences*, Vol. 11 (10)

With kind permission by MDPI.
Original publication available online at:
https://doi.org/10.3390/geosciences11100420

CHAPTER 5 - Tidal flood risk on salt farming: evaluation of post events in the northern part of Java using a parametric approach

Abstract
Tidal flood risk threatens coastal urban areas and their agriculture and aquaculture including salt farming. There is, therefore, an urgency to map and portray risk to reduce casualties and loss. In the floodplain of Cirebon, West Java, where salt farming dominates the landscape, this type of flooding has frequently occurred and disrupted the local economy. Based on two recorded events in 2016 and 2018 as benchmark, this paper formulates an innovative approach to analyse tidal flood risk in salt farming areas. Our study considers the fundamental concepts of hazard and vulnerability, then uses selective parameters to be evaluated in an Analytical Hierarchical Process (AHP) based Geographic Information System. The analytical process includes weighting criteria judged by experts and uses the resulting values to define the spatial characteristics of each salt parcel. Our high-resolution simulations show that the two flood events in 2016 and 2018 affected almost all salt production areas, particularly in the eastern, middle, and western parts of the Cirebon floodplain, although to very different degrees. The study also uses a physically-based approach to validate these results. The damage estimates show a strong positive correlation for economic loss (r=0.81, r=0.84). Finally, the study suggests that our multi-methods approach to assessing tidal flood risk should be considered in disaster mitigation planning and integrated coastal zone management in salt farming areas.

Keywords: tidal flood risk; salt farming; parametric approach; analytical hierarchical process (AHP); GIS

5.1. Introduction

Nowadays, millions of inhabitants have been threatened by floods in coastal regions, with the most destructing impacts in rural coastal communities in developing countries (Munji *et al.*, 2013). People from lower income brackets tend to settle in floodplains in remote rural areas due to lower land prices and possible cultivating activities (Dasgupta, 2007). The physical and social settings have also turned this region into a high-risk region through geohazards such as tsunamis, storm surges, and flooding. These circumstances are worsening, especially in the Global South, due to limited mitigation capacity (Domeneghetti *et al.*, 2015; Pacetti *et al.*, 2017). At the same time, most of the population in this low land area is being supported by fisheries (Gunawan, 2012; Potts *et al.*, 2015) and agriculture products (Howlader and Akanda, 2016) including salt (De Medeiros Rocha *et al.*, 2012; Oren, 2009).

On the north coast of Java, Indonesia, salt farming has been practiced for hundreds of years. Along the shore, traditional salt farmers have produced the salt brine with inputs mainly from the Java Sea, which has a relatively shallow

depth and mostly calm waves. Seawater bitterns are encountered in the sea-salt production and desalination process in which large portions of bittern and brine are processed as by-products and waste products (Apriani *et al.*, 2018). Besides being used as raw material and for food, the local salt product is also used in the chemical industry. Salt farming in this region is of the local culture. However, the area is also vulnerable to coastal hazards (Dede *et al.*, 2019; Willemsen *et al.*, 2019). Flooding occurs due to intense rainfalls and sea-level dynamics. Extreme sea levels resulting from combined events of high tides and storm surges are considered a significant threat for coastal communities and their infrastructure (Lyddon *et al.*, 2018; Quinn *et al.*, 2014).

Tidal flooding has threatened traditional salt farming in Cirebon, West Java, again and again, especially during the production period from April to October. Local and national media have described at least two recent tidal flooding events, in 2016 and 2018 (Lia, 2016; Metrotv, 2016; radarcirebon.com, 2018). Our previous paper modelled those events through a physical-based approach using a numerical model (Nirwansyah and Braun, 2019). In the last few years, risk assessment for this type of flood in the north part of Java has been probed in several studies focusing on urban areas using various methods (Budiyono, 2018; Budiyono *et al.*, 2015; Suroso and Firman, 2018). One example of a coupled method has been practiced in the Eilenburg municipality, Germany. A risk analysis comparison was performed for different scenarios of hydraulic model and flood loss model combinations (Apel *et al.*, 2009). The method also involves the Flood Loss Estimation Model for the private sector (FLEMOps) approach and a benchmark from a previous monetary loss estimation by the Saxonian Relief Bank (SAB). In another case study by (Ward, De Moel, *et al.*, 2011), the damage-scanner model was used to estimate the flood risk through the expected annual damage (EAD) algorithm. That study also addressed the general estimation of different categories based on land use types, including residential, agriculture, commercial, industrial, and recreational. With different flood scenarios in that model, the paper also states that flood with relatively low economic damage per event should also be considered in the flood risk assessment due to frequency (Merz and Thieken, 2009; Ward, De Moel, *et al.*, 2011). Another study in Bangladesh by Adnan *et al.* (2020), has addressed pluvial flood risk with considered the landuse/landcover change (LULC). In that study, a mixed of logistic regression (LR), cellular automata (CA), and Markov Chain were implemented to forecast the LULC based on historical datasets. Several of those studies also optimized the use of geospatial technology such as remote sensing and geographic information system (RS-GIS).

Currently, the established flood risk models are focused on structure, while agriculture have been hardly discussed (Ganji *et al.*, 2012), with a few studies trying to address the economic impact on a farming land using different approaches (Bhakta Shrestha *et al.*, 2019; Chau *et al.*, 2015; Huda, 2015). However, there are still limited studies concerning the flood risk for agricultural areas including the coastal parts of Central (Hartini, 2015) and West Java (Sianturi *et al.*, 2018). Therefore, this article mainly endorses methodological innovation to evaluate tidal flood risk on salt farming land by applying geospatial data and geographic information system technology.

5.2. Conceptual considerations

5.2.1. Concept and definition of hazard, vulnerability, and risk

The concepts of hazard, vulnerability, and risk are widely discussed in numerous studies on natural hazards and disaster risk management. The following sub-sections describe some relevant theoretical considerations and empirical results from previous studies.

5.2.1.1. Hazard (H)

A hazard can be described as the possibility of events of potentially damaging natural phenomena in a particular period and a certain area (Ghosh and Kar, 2018). The hazard also can be simply defined as a threatening natural event, including its magnitude and probability of occurrence (Kron, 2005; Tsakiris *et al.*, 2009). Hazards can contain latent conditions that may characterize future threats and can have multiple causes, including natural (geological, hydrometeorological, biological) and anthropogenic processes (environmental degradation, technological hazards) (ADPC, 2005). Each hazard is characterized by its specific geography, intensity, regularity, and probability (UNISDR, 2009).

Hazard assessment has been conducted in many different areas including coastal regions, with a pronounced focus on hydrometeorology hazards such as cyclones, storm surges, and flooding. Flood hazard measurement aims to identify the flood pattern utilizing relevant parameters such as inundation depth (Dutta *et al.*, 2003; Hadipour *et al.*, 2020; Vozinaki *et al.*, 2015), flood duration (Cai *et al.*, 2019; Dutta *et al.*, 2003; Luu *et al.*, 2018), and even timing of flooding (Black, 1995; Cardona *et al.*, 2012; Glaz and Lingle, 2012). This information can be extracted through hydraulic models with different scenarios (Ronco *et al.*, 2014) or based on past recorded events (Nasiri *et al.*, 2016; Torres *et al.*, 2014).

5.2.1.2. Vulnerability (V)

Researchers define vulnerability in diverse spatial contexts, for different purposes, and with different rationales (Balica et al., 2013). It is widely accepted, however, that vulnerability is a condition influenced by physical, social, economic, and environmental factors that raise the susceptibility of people to a hazard impact (UNDP, 2004). In an engineering conceptualization, vulnerability defines the scale of the region, population, physical structures, or properties exposed to the hazard (Dandapat and Panda, 2017). Thouret *et al.* (2014) extend the description of vulnerability as a degree of damage to a certain object at flood risk with a specified amount and expressed on a scale from 0 to 1 (no damage to full damage).

Vulnerability should be able to portray the specific problem in the context of a locality (Post *et al.*, 2007). At some points, it is also understood that the vulnerability is relative conviction that relies on the society's interpretation as a risk and how community construct their normality at daily basis (Voss, 2008). Previous studies obtained vulnerability measures through selecting relevant parameters, i.e. they focused on the watersheds involving hydrologic and physical components such as elevation, slope, geomorphological condition, soil, and land use (Mohamed and El-Raey, 2020; Radwan *et al.*, 2019). In coastal areas, the

specific characteristics of other parameters such as elevation, coastal slope, distance to the next channel, and distance to sea are used (Hoque *et al.*, 2019; Rimba *et al.*, 2017; Satta, 2014; Silva *et al.*, 2017).

5.2.1.3. Risk (R)

The concept of risk is broadly discussed in various contexts and purposes. Risk is commonly associated with hazard (H) and vulnerability (V), especially in the field of flood risk management. In many cases, the simple equation (eq. 2) is illustrated as follows (ADPC, 2005; Chakraborty and Mukhopadhyay, 2019; UNISDR, 2015b):

$$R = H * V \qquad \text{Eq. 2}$$

UNISDR (2015b) defines risk as a combination of the probability of a hazardous event and its consequences, which result from the interaction between natural or man-made hazards, vulnerability, exposure, and capacity. In this context, the concept of flood risk is closely interrelated to the probability that a high flow event of a given extent happens, which results in specific environmental, financial, and social deficiencies (Balica *et al.*, 2013). As an addition, risk is also dynamic due to the different ability of the society and environment to manage and adapt to the changes (Cardona *et al.*, 2012).

The selection of instruments and approaches for risk analyses mainly relies on the objective and existing information about the hazard and the vulnerability (Khazai *et al.*, 2011). As risk is the combination of hazard and vulnerability, the expected damage can be evaluated by a value combination of the elements-at-risk and the estimated damage function (Baky *et al.*, 2020). The current practice of risk assessment including flood hazards and cost-benefit analyses focuses on damages that can be easily assessed in monetary terms (Meyer *et al.,* 2007). Currently, the coupled flood loss estimation and risk assessment have been practiced in a residential area (Afifi *et al.*, 2019).

5.2.2. Flood risk assessment using a physical-based and multicriteria approach

Different methods in addressing flood risk have been advanced (Sadeghi-Pouya *et al.*, 2017; Xia *et al.*, 2011). According to Balica *et al.*, (2013), there are at least two distinct techniques in flood risk assessment. First, the deterministic approach, which applies physical-based numerical modelling to calculate flood hazard probability, coupled with a damage estimation model that describes the economic loss. This information can be used for flood risk assessments for particular regions. Studies that integrate a physical-based flood simulation and a damage estimation model have been conducted in different regions, usually with a focus on agriculture (Bhakta Shrestha *et al.*, 2019; Dutta *et al.*, 2003; Komolafe *et al.*, 2019; Vozinaki *et al.*, 2015). The second technique is the parametric approach, which uses available datasets to describe the relevant hazard and vulnerability features in a study area (Balica *et al.*, 2013). This approach involves the experts in hazard and vulnerability assessment generating a straightforward risk map based on available data (Ouma and Tateishi, 2014). This method has been applied mainly in data-scarce regions or developing countries.

Recently, the combination of different geospatial data series with a multicriteria approach (MCA) has contributed to flood vulnerability and risk assessment (Kourgialas and Karatzas, 2016). MCA is a suitable method for all relevant types of impacts without any measurement on a single monetary rank (Meyer *et al.*, 2009). The integration of MCA and Geographic Information Systems (GIS) enhances the utilization of the three components of risk (hazard, vulnerability, exposure), including social, economic, and/or environmental vulnerabilities (Rincón *et al.*, 2018). GIS are eminently suited to processing the geospatial data required for flood risk assessment. This technology is also acknowledged for its great flexibility in MCAs, including in the very reliable analytical hierarchical process (AHP) (Cabrera and Lee, 2019; Chakraborty and Mukhopadhyay, 2019; Danumah *et al.*, 2016; Ghosh and Kar, 2018). This semi-quantitative approach has its strength in supporting priority selection and decision-making (Luu *et al.*, 2018). The method has also been widely recognized in the academic literature and has been recently applied in studies on flood risk assessment (de Brito and Evers, 2016; Siddayao *et al.*, 2014). In the present study, AHP was performed and utilized to evaluate the tidal flood risk in salt farming areas through thematic data layers processed on a GIS platform.

5.3. Description of the Case Study Area

The coastal area of Cirebon, West Java, Indonesia has been acknowledged as one of the major centers for traditional salt production in Indonesia. The region covers 990.36 km^2 between 6°30′ and 7°00′ S and 108°40′-108°48′ E. Cirebon borders of the province of Central Java are on the east, the Java Sea to the north, and Indramayu to the west. Cirebon has 40 districts, eight located along the coastline. According to the Development Planning Board (Development Planning Board, 2014), the coastal water area covers 399.6 km^2. The region is geomorphologically diverse, with mountainous areas and also coastal plains (*Figure 5.1*). As mentioned by Hadian *et al.* (Hadian *et al.*, 2017), the region consists of four geological units: alluvium deposits, coastal deposits, results of the young Ciremai Volcano, and the Gintung Formation. The coastal area is structured by mud sediments, silt, and grey clay containing shells deposited several meters thick. Mount Ciremai (3,078 m) is an active stratovolcano and one of the highest active volcanoes in Indonesia. Slope conditions in Cirebon predominantly consist of flat zones (less than 5°), but there are also moderate (5° - 30°) and steep areas (more than 30°) (Suhendra *et al.*, 2018).

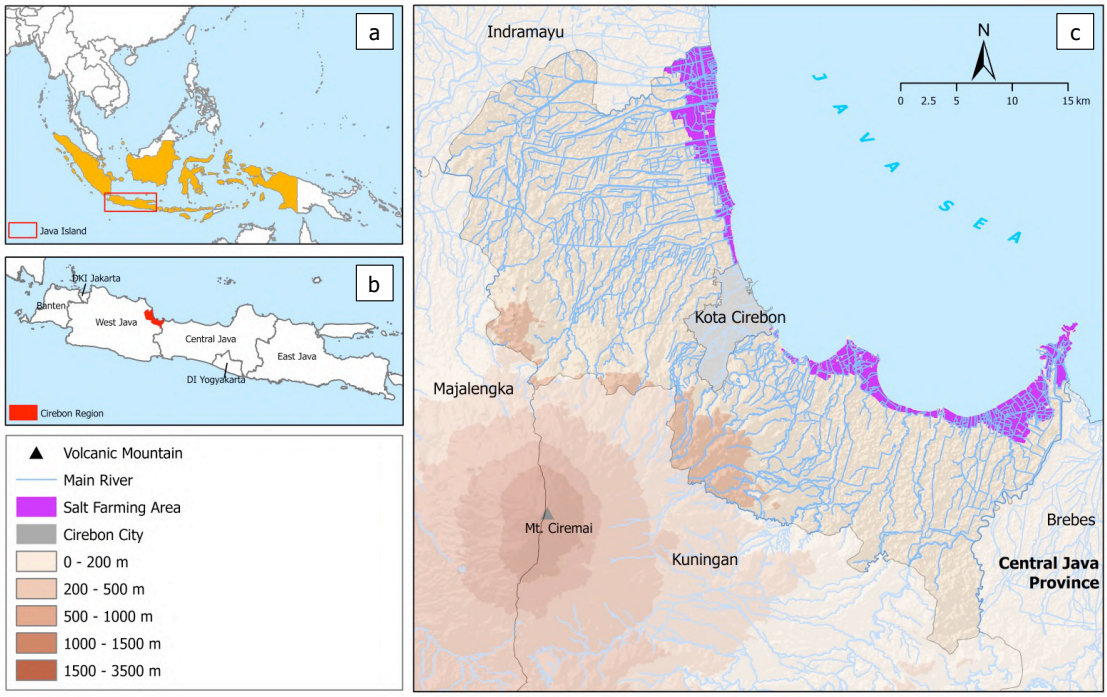

Figure 5.1. Map showing the case study area and its topographical situation. Figure 1 (a) and (b) indicate the case study area in the Southeast Asia region and on Java island, respectively. The red-line box in *Figure 5.1* (a) shows Java as a part of the Indonesian archipelago (orange). In *Figure 5.1* (b), the red box describes the location of the Cirebon region in the West Java province. *Figure 5.1* (c) portrays the topographical condition of the study area, river systems, and salt farming parcels (magenta) located along the coastline.

Salt harvesting predominantly takes place in low-lying areas dominated by alluvial deposits together with mangrove ecosystems along the Cirebon shoreline. The local farmers benefit from tidal cycles that supply the salt ponds with sea water. Solar energy is used to evaporate the sea water into salt brine, especially during the dry season. In this region, the dry season usually lasts from March to September, while the rainy season begins in October and ends in February, with 1,300-1,500 mm/year of rainfall and a mean temperature of 24.2°C (BPS Cirebon, 2020). Most farmers start to store seawater at the beginning of the dry season. In that period, the mean temperature is 32.8°C with a maximum average temperature of 38.6°C in October (BPS Cirebon, 2020). As the dry period begins, the brines are formed in the crystallization pond. Local farmers start to collect brine and produce 0.5-1.0 tons per hectare and day (Munadi *et al.*, 2016; Nirwansyah and Braun, 2019). During the production season in 2019, Cirebon produced at least 135.9 thousand tons of salt (BPS Cirebon, 2020).

5.4. Research Materials and Methodology

5.4.1. Model framework

This study evaluates the tidal flood risk using a parametric approach: the analytical hierarchical process (AHP). In addition, we compare the AHP results with the results of a physical-based model. For this purpose, several indicators from geospatial data and relevant research were carefully chosen to identify risk

components. A total of 9 indicators were selected and arranged into two clusters of risk components. The first cluster consisted of hazard (H) indicators (N=3) (explained in Section 5.4.2), and the second compiled vulnerability (V) indicators (N=6) (described in Section 5.4.3). The selected indicators were used in the AHP analysis to acquire the weighted score (illustrated in Section 5.4.4). All selected indicators in each thematic layer were processed using ArcGIS 10.6. All maps were set on raster format with a 25-m cell size, Universal Transverse Mercator (Zone 48S) projection, and reclassified to optimize the calculation. Ultimately, the risk map gained from the weighted score calculation was validated using a physical-based approach from a former study (elaborated in Section 5.4.6). This data allows an analysis of each pond in the risk analysis with the chosen parameters. Additionally, the cell size has been customized into 25-m for synchronization purpose with the former study. *Figure 5.2* depicts the study's structure.

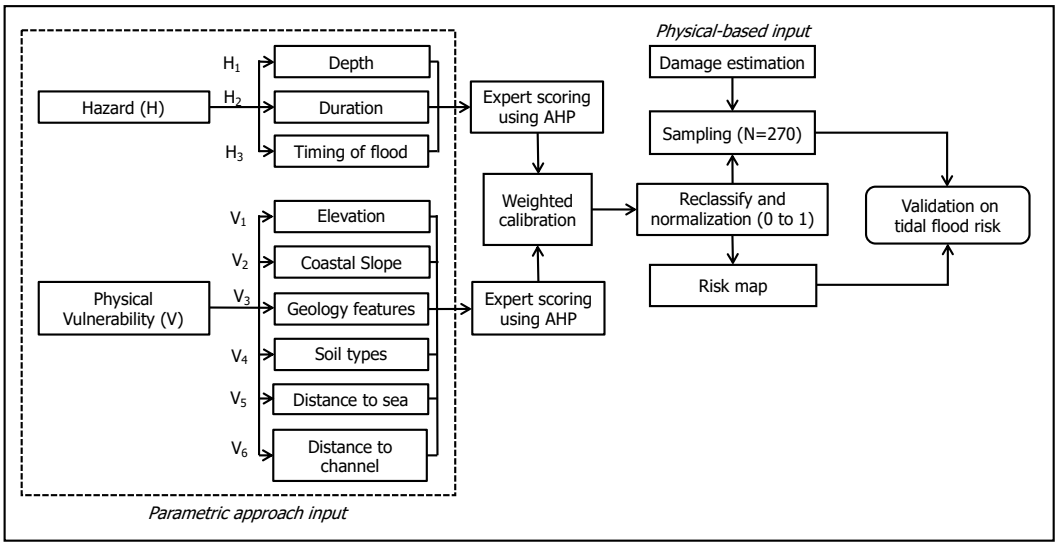

Figure 5.2. Framework on tidal induced flooding risk assessment and comparison between parametric and physical-based approaches.

5.4.2. Tidal flood hazard components

Tidal induced hazards have disrupted most of the coastal communities including salt farmers in this region. This current study uses two recorded events in 2016 and 2018 with 0.38 m and 0.40 m depth (Nirwansyah and Braun, 2019). Those depths were extracted through a hydrodynamic model in DHI MIKE. However, the events occurred at different stages of salt production. The hazard (H) indicators or criteria (shown in *Figure 5.3*) include primary factors—(i) *Depth* (H_1) is mainly extracted from the magnitude of the tide. The flood hazard increases proportionally to the depth of inundation (Luu *et al.*, 2020). The previously mentioned simulation was reclassified into 5 classes (<15 cm; 15–50 cm; 50–100 cm; 100–150 cm; >150 cm) to be judged by selected experts. (ii) *Duration* (H_2) of the tidal flood was 2.23 days for 2016 and 2.32 days for 2018,-events taken from (Nirwansyah and Braun, 2021). In that model, the duration was extracted from individual raster data from hourly hydrodynamic simulation that exported in ArcGIS. Here, we classify the duration of inundation into 3 categories (<2 days; 2-5 days; and >5 days). The duration of flooding is associated with the possible damage level (Molinari, Ballio, *et al.*, 2014; Serinaldi *et al.*, 2018). In salt farming,

the duration of flooding increases the risk that the formed salt brine melts (Nirwansyah and Braun, 2021). (iii) *Time of flood* (H_3) is significant for flood damage in farming activities (Glaz and Lingle, 2012). As mentioned in the previous section, the time dimension has a strong impact depending on the particular event and the response from the environment or community (Ward, De Moel, *et al.*, 2011). For this study, the selected indicators are divided into 3 groups (pre-production, harvesting period, and post-production). The event in 2016 occurred during the harvesting period, whereas the 2018 flood happened in the pre-production period.

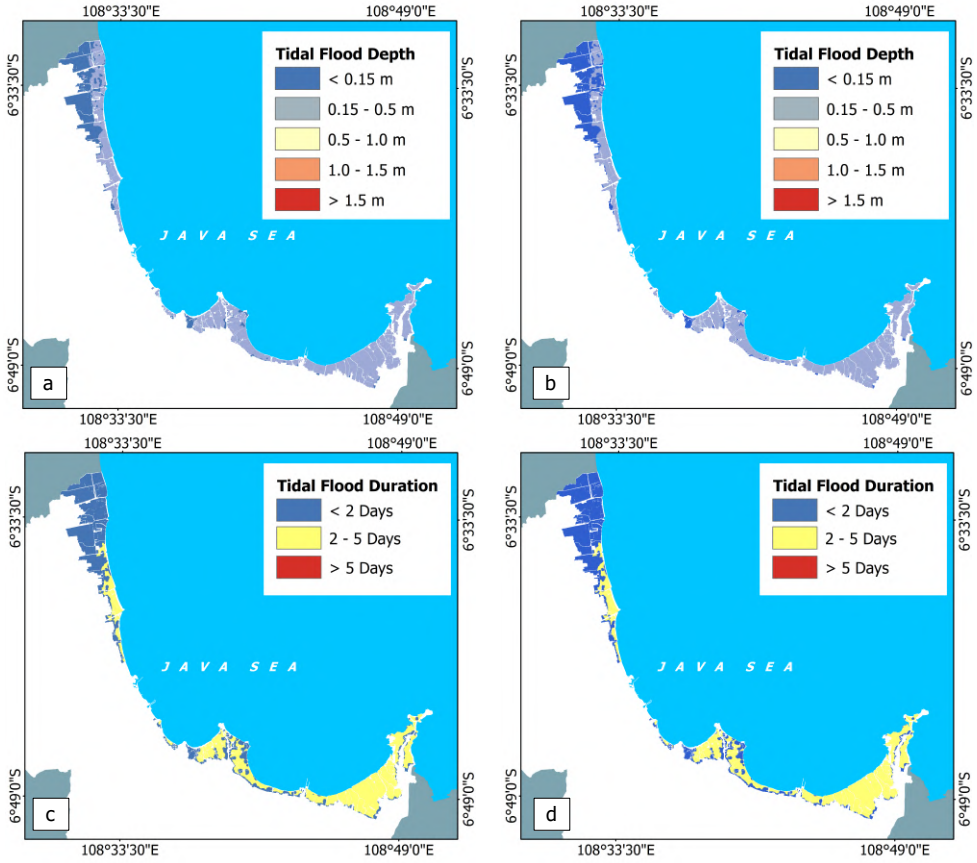

Figure 5.3. Hazard variables of the current study, including (a) flood depth (H_1) in 2016 and (b) flood duration (H_2) in 2016; while (c) and (d) portray depth (H_1) and duration (H_2) of the 2018 tidal flood event.

5.4.3. Vulnerability components

To investigate the vulnerability in coastal zones, a range of parameters and indexes including physical vulnerability can be applied (Baig *et al.*, 2021; Hoque *et al.*, 2019). Several parameters were used to address the vulnerability components (V). These are shown in the thematic maps (*Figure 5.4*). Firstly—(V_1) *elevation* data extracted from topographical data of DEMNAS (0.27 arc-second) resolution from Geospatial Information Agency (here referred to as BIG: *Badan Informasi Geospasial*). The elevation is categorized into 5 groups (0.5 m; 0.5–1 m; 1–1.5 m; 1.5–2 m, and >2 m). This information generally depicts the coastal altitude condition (Luu *et al.*, 2018; Rincón *et al.*, 2018). Generally, this component plays a significant role in identifying areas at risk of flooding during an event (Souissi *et al.*, 2020). Salt farming is mostly located in the coastal plain within 1–

2 m elevation. *Coastal slope* (V_2) indicates the degree of elevation variability in bordering grids (Wang *et al.*, 2011). The possibility of flooding rises as the slope declines, making it a relevant indicator for vulnerability (Rahman *et al.*, 2019). Salt ponds require a relatively slight slope to facilitate the sea water flow and to reduce construction expenses (Gozan *et al.*, 2018). In line with Silva *et al.* (2017) the slope in the case study area has been classified into classes of <0.025%, 0.025–0.04%, 0.04–0.07% 0.07–0.2%, and >0.2%. Another considered indicator, *geological features* (V_3), significantly influences the drainage pattern formation associated with the floodplain formation (Bui *et al.*, 2019). In this study, specific classes were included: flood plain deposits, sand with silts and clays, mountain formations, and younger volcanic formations. This classification was taken from the Directorate of Geology and Environmental Planning (DGTL) vector data. *Soil type* (V_4) is a relevant factor affecting infiltration and runoff during the flood (Cabrera and Lee, 2019). In traditional salt farming, soil type has major implications for productivity, water quality, and pond construction (Mahasin *et al.*, 2020). The DGTL soil map, scale 1:100,000, reveals that the soil of the Cirebon region is divided into four major types, Alluvial, Gleysol, Cambisol, and Latosol, although the salt pond area is dominated by Alluvial. This dominant soil type is the result of sedimentation from streams and rivers or of marine sediments along ocean shorelines (Hillel, 1980). To identify the soil characteristics, Subardja *et al.*, (2014) and Sulaeman *et al.* (2019) have been used as sources for this study. Finally, both *distance to channel* (V_5) and *distance to shore* (V_6) influence the breaching of water during floods and overtopping water from the channel. Here, the study categorizes distance to channel into <200 m, 200–400 m, 400–600 m, 600–1000 m, >1000 m (Lyu *et al.*, 2018) and distance to shore into <250 m, 250–500 m, 500–750 m, 750–1000 m, >1000 m. All mentioned classification references were defined in the level of vulnerability to tidal flood events.

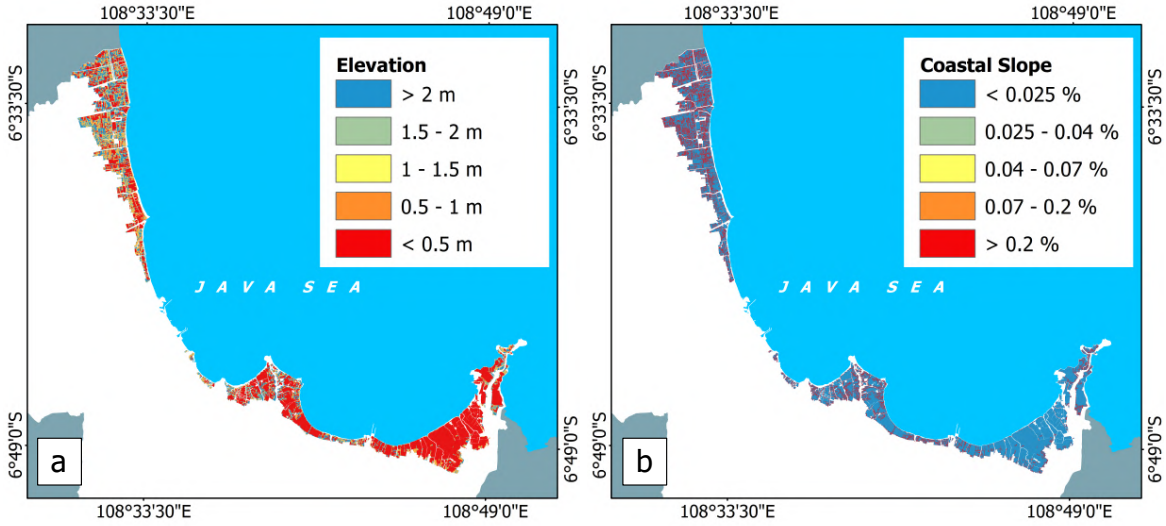

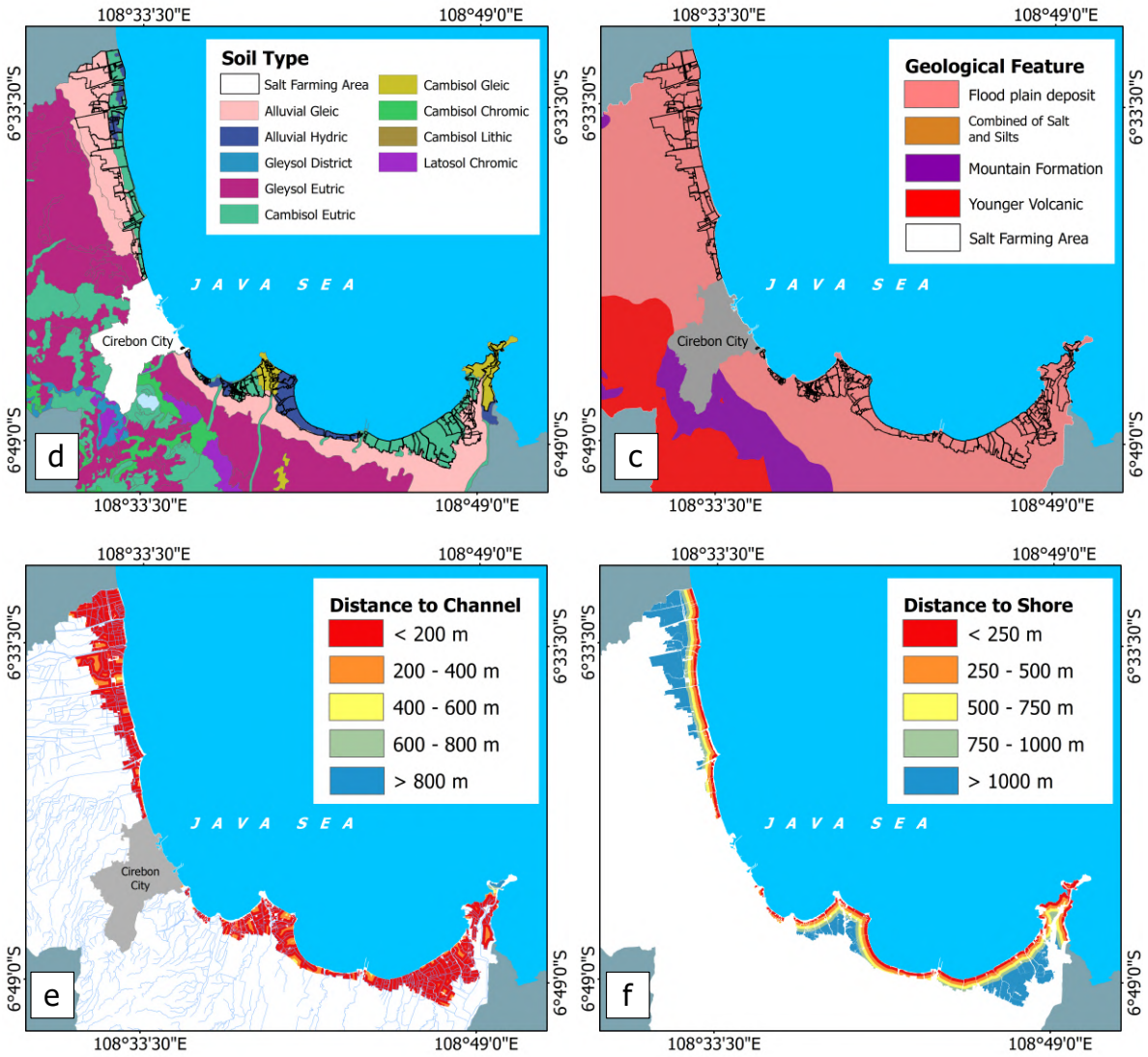

Figure 5.4. Map showing the spatial distribution of vulnerability variables selected for this research including (a) elevation (V_1), (b) coastal slope (V_2), (c) geological features (V_3), (d) type of soil (V_4), (e) distance to channel (V_5), and (f) distance to shore (V_6).

5.4.4. AHP and variable weighting procedure

In various flood risk studies, the analytical hierarchical process (AHP), introduced by Saaty (1977) has been effectively used to conduct flood risk measurements (Chakraborty and Mukhopadhyay, 2019; Danumah *et al.*, 2016; Tehrany *et al.*, 2015). This method selects criteria by ranking the parameters and creating a combination of qualitative and quantitative factors (Luu *et al.*, 2018; Rimba *et al.*, 2017; Rincón *et al.*, 2018). Generally, this approach is a structured technique to deal with complex decisions and to help decision-makers find the most suitable options (Yadollahi and Rosli, 2011). Here, the decision-makers use factual data of the elements and can use their professional judgments to identify the level of importance by using a basic scale of absolute numbers (listed in *Table 5.1*).

Table 5.1 Scale of preference for the AHP model

Intensity importance	Definition	Description
1	- Equal importance	- Two indicators equally influence the parent decision
3	- Weak importance	- One factor is relatively influential over another
5	- Essential or strong importance	- One factor is strongly favored over another
7	- Very strong or demonstrated importance	- One decision factor has significant influence over another
9	- Extreme importance	- Evidence favoring one decision factor over the other is highest order of affirmation
2, 4, 6, 8	- Intermediate values	- When compromise is required, values between two adjacent justification are used
Reciprocals	- Inverse comparison	- A reasonable assumption

Sources: Ramanathan (2001); Saaty (2002)

The AHP was employed to obtain the weight scores of selected criteria and sub-criteria based on an evaluation by the interviewed stakeholders and experts associated with the policy-making process (Luu *et al.*, 2018). Following Cabrera and Lee (2019), four experts from local authorities, including the Ocean and Fisheries Department (DKP) of Cirebon, the Indonesian National Geospatial Agency (BIG), the Spatial Planning Official (BAPPEDA) of the West Java province, and an academic from the geomatic department, Brawijaya University, were involved due to their experiences and their duties regarding salt farming. These experts carefully judged all parameters and the H, V, and R indicators. Due to the COVID-19 pandemic, data collection was conducted via online correspondence by using Zoom from January to March 2021. The collected data was inserted into a template, accessed at https://bpmsg.com/ containing the AHP justification variables. This Excel workbook consists of 20 input worksheets for pair-wise comparison (Goepel, 2013).

In the present research, AHP was employed to allocate weights for H, V, and R factors. The following steps were included in the AHP. A pairwise comparison was performed for all H, V, and R indicators and a matrix was established through scores based on relative importance. A pairwise comparison matrix was utilized to compare and rank the selected H and V domains based on the experts' judgments. The assessment was based on the relationship between the indicators and the risk components. The indicators were reclassified and ranked. Here, different ranks were applied from 1 to 3, 1 to 4, and 1 to 5. Finally, the normalized rank was counted by dividing the column value by the sum of the ranking's score. After doing so, the total score for each indicator was 1. Table 2 represents the rankings and the normalized scores of all selected indicators used in the present work.

Table 5.2 Hazard and vulnerability components for the current study

Risk components	Indicators	Functional relation	Classes	Unit	Rank	Normalized score
Hazard (H)	Depth (H_1)	Direct	> 150	cm	1	0.33
			100 – 150		2	0.27
			50 – 100		3	0.20
			15 – 50		4	0.13
			< 15		5	0.07
	Duration (H_2)	Direct	> 5	day	1	0.50
			2 – 5		2	0.33
			< 2		3	0.17
	Timing (H_3)	Conditional	Harvesting period		1	0.50
			Post-production period		2	0.33
			Construction period		3	0.17
Vulnerability (V)	Elevation (V_1)	Inverse	< 0.5	meter	1	0.33
			0.5 – 1		2	0.27
			1 – 1.5		3	0.20
			1.5 – 2		4	0.13
			> 2		5	0.07
	Coastal slope (V_2)	Inverse	< 0.025	%	1	0.33
			0.025 – 0.04		2	0.27
			0.04 – 0.07		3	0.20
			0.07 – 0.2		4	0.13
			> 0.2		5	0.07
	Geology feature (V_3)	Direct	Flood plain deposits		1	0.40
			Sand with silts and clay		2	0.30
			Mountain formation		3	0.20
			Younger volcanic		4	0.10
	Soil type (V_4)	Inverse	Alluvial Gleic		1	0.40
			Gleysol		2	0.30
			Cambisol		3	0.20
			Latosol		4	0.10
	Distance to channel (V_5)	Inverse	< 200	meter	1	0.33
			200 – 400		2	0.27
			400 – 600		3	0.20
			600 – 800		4	0.13
			>800		5	0.07
	Distance to shore (V_6)	Inverse	< 250	meter	1	0.33
			250 – 500		2	0.27
			500 – 750		3	0.20
			750 – 1000		4	0.13
			>1000		5	0.07

In the AHP model, the Eigenvalue of the matrix expresses the priority value of variables (Ghosh and Kar, 2018; Rimba *et al.*, 2017). The estimations were completed by dividing each column by the value of their sum (Rincón *et al.*, 2018). Ultimately, the mean values of each row were carefully estimated and used as weights in the objective hierarchy in the H and V domains. In addition, to establish consistency of the comparison matrix, a standardized Consistency Ratio (CR) test was generated. The ratio confirms the justification or preference to be consistent if the CR < 0.10, and reliable results can be supposed in the model (Komi *et al.*, 2016). Meanwhile, the greater CR value does not necessarily mean a greater accuracy (Luu *et al.*, 2018). The consistency ratio test is formulated in eq 3:

$$CR = CI / RI \quad \text{Eq. 3}$$

where CI is described as the consistency index and RI refers to a random index whose value is stated by the number of criteria (n) (Chakraborty and Mukhopadhyay, 2019). The consistency index is expressed in the following eq 4.

$$CI = (\lambda max - N) / (N - 1) \quad \text{Eq. 4}$$

Here, λmax represents the maximum Eigenvalue of the comparison matrix while n describes the number of criteria for each variable of H (N = 3), V (N = 6), and R (N = 2). In the present study, the CR and CI for H were calculated as 0.012 and 0.03 while RI was 0.58. For the V variable, the CR was estimated as 0.019, CI was measured as 0.07, and RI as 1.24. The value of RI standardized in the AHP was taken from *Table 5.3.*

Table 5.3 Random index (RI) matrix of the same dimension

Number of criteria	2	3	4	5	6	7	8	9	10	11
RI	0.00	0.58	0.90	1.12	1.24	1.32	1.41	1.45	1.49	1.51

Source: Saaty *et al.*, (2003)

5.4.5. Estimating H, V and R tidal flood indices

A composite risk map (R) in the raster data format was expected to be the result of this model in 25-m cell size. The weight input from the previous process in the AHP was used to construct the mathematical formulation with H and V criteria (see eq 5 and 6). The weight score from previous expert inputs and the calculations were combined by using weighted overlay in ESRI ArcGIS 10.6, which generated hazard maps (H) for the 2016 and 2018 cases and a vulnerability map (V), with map algebra tools in the software. The risk assessment result was incorporated into a GIS platform to provide a flood risk map (Luu *et al.*, 2020). The following expressions describe the risk as the ultimate result of the MCA approach for H and V with incorporated expert judgment.

$$H = 0.109 \times H_1 + 0.567 \times H_2 + 0.324 \times H_3 \quad \text{Eq. 5}$$

$$V = 0.161 \times V_1 + 0.137 \times V_2 + 0.086 \times V_3 + 0.11 \times V_4 + 0.265 \times V_5 + 0.241 \times V_6 \quad \text{Eq. 6}$$

In line with eq 6, the R is measured by combining both H and V inputs. Here, both weighted components were calculated using a similar procedure in ArcGIS 10.6. In the final map, the scores of risk are normalized into a 0 to 1 range (Luu and von Meding, 2018). The results of the weighted overlay analysis were classified using equal intervals, i.e., five levels: very low (0-0.20), low (0.20-0.40), moderate (0.40-0.60), high (0.60-0.80), and very high (0.80-1.00).

$$\text{Composite of R index} = 0.39 \times H * 0.61 \times V \quad \text{Eq. 7}$$

For the calculation, salt parcel shapefile in 1:15,000 scale acquired from National Geospatial Agency was used to extract raster values by using a zonal statistic operation in ArcGIS.

5.4.6. Relationship between the multi-criteria and physical-based approach

Previous comparison analysis has been presented in established damage models e.g. (Jongman *et al.*, 2012; Meyer and Pine, 2004). However, there is still no direct evaluation of the relation between economic loss from a physical-based

approach and risk value from an MCA, especially in salt farming land. Although this combined approach was implemented previously in Afifi *et al.* (2019), no specific correlations were performed. In the study, the simple correlation was obtained in order to evaluate the relation between risk level and monetary damage for both tidal flood events. Since there were no approved reports from the responsible authorities for both recorded tidal flood events, about 270 salt parcels were taken as samples according to the proportional number for each risk class, while the damage calculation was taken from the previous numerical model by Nirwansyah and Braun (2021). These parcels contain information on the monetary damage for both selected periods. For this purpose, we used the 'create random points tool' in ArcGIS and extracted values from parcel data in vector format by using the 'identity' feature. The monetary loss was evaluated by using the depth-duration damage function taken from Nirwansyah and Braun (2021) and was then compared to the scores of both risks. Following Molinari *et al.* (2020), a simple Pearson correlation coefficient (r) was applied to identify both approaches' relation to each other in a statistical context.

5.5. Results and Discussion

5.5.1. Tidal hazard on salt ponds

In this study, the indicators from the selected variables (H_1-H_3) were processed following the conditions of tidal flooding records in 2016 and 2018. Two hazard maps can be drawn from the model that portrays the tidal occurrence during those two events. The interviewed experts believe that duration (H_2) has the most significant impact on the tidal flood hazard (0.567 weight score). Depth (H_1) and the timing of flooding (H_3) have the least effects on salt farming, according to our experts. The indicators have, respectively, 0.109 and 0.324 weight scores in Eq 5. The hazard map features five classification areas from very low to very high, as shown in *Figure 5.5a-b*. For the 2016 hazard, the very low (VL) class extends over 43.63% of all salt ponds while in 2018 about 42.43% fall into this class. Moreover, about 3.33% of the production area has been grouped in the low (L) class for 2016, and 3.20% for the 2018 event. These areas experience relatively low depth and short inundation during the floods in both tide events. Some districts such as Kapetakan and Suranenggala (west part) have been allocated to this class. Small areas in the districts of Mundu and Pangenan (middle part) have also been allocated to this class. The moderate class (M) covers 3.12% (2016) and 3.74% (2018). The class for very high (VH) hazards comprises 45.59% (2016) and 47.24% (2018) of the total salt farming in Cirebon, West Java. These two areas essentially displayed higher depths and relatively longer durations in 2016 and 2018. Both flood events have mostly affected the eastern part of the region, including Losari, Gebang, and the middle part, including Mundu and Astanajapura.

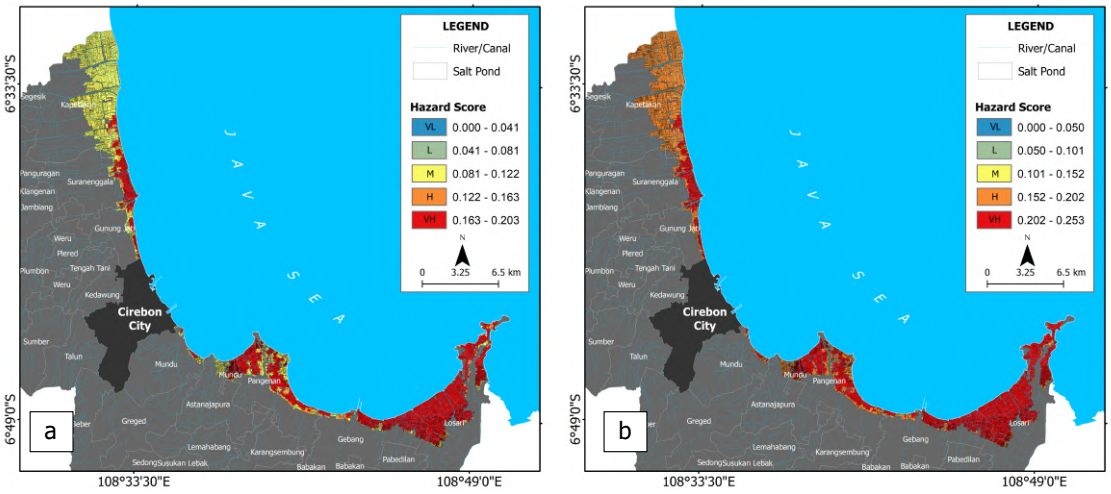

Figure 5.5. Hazard scores due to tidal flooding during the 2016 (a) and the 2018 (b) events.

5.5.2. Tidal flood vulnerability of salt ponds

The five combined vulnerability indicators (V_1-V_5) are shown combined in a single vulnerability map (*Figure 5.6)*. The experts agreed that each indicator shows a quantifiably different response to tidal flood hazards. Eq 6 clearly shows that the distance to the next channel has been considered as the most influential factor for tidal-induced flooding (26.5%). On the other hand, experts suggest that geological features have the least contribution to the vulnerability level of salt farming due to tidal flood (8.6%). The area with a very low (VL) vulnerability represents only 0.46% of the total salt pond area. This category is essentially dominated by areas with relatively higher elevation, steeper slopes formed by flood plain deposits, mixed types of soils (Alluvial, Gleysol, and Cambisol), and located far from a channel and the shore. No area is labelled as low (L) vulnerability and only 2.07% are assigned to the moderate (M) class. The H and VH classes represent 57.03% and 40.44% of the areas, respectively. These classes dominate in almost all salt production areas, including the western, eastern, and middle parts. The analysis shows that all of these areas are characterized by low elevation, flat flood plain deposits, and Cambisol and Alluvial soils. They are also located close to channels and the sea. Not surprisingly, these categories apply to highly productive areas where farmers can easily extract saline water directly from the ocean and transfer it to their ponds.

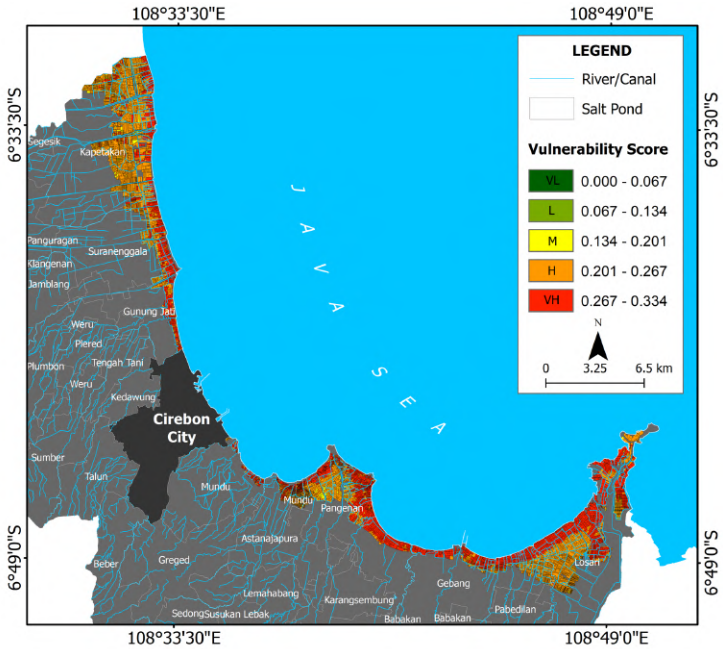

Figure 5.6. Vulnerability score represented in a map that is based on multi-criteria input.

5.5.3. Tidal flood risk of salt ponds

The tidal flood risk (R) map combining H and V layers outlines five levels of risk, varying from very low to very high (VL to VH). In addition, the V element plays a bigger role than H for the tidal flood risk in salt farming, as described in Eq 7. Here, the interviewed experts have suggested a proportion for both components, where H and V, respectively, contribute 39% and 61% to the resulting risk. The two studied events also present different stages of farming. Our calculations reveal that VL represents 4.06% and 12.72% of the study sites for the 2016 and 2018 floods, while L extends to 15.13% and 33.36% of the total salt farming area. Areas in these two categories had minimum flood depths and durations. Moreover, these areas are mostly located on higher elevations, have relatively steep slopes, and are far off channels and the shoreline. They are characterized by mixed soil types and were formed by flood plain deposits. They can be found especially in the western part of the region, for instance in Kapetakan (see top box in *Figure 5.7a-b*). The moderate (M) category of risk covers 18.02% (2016) and 30.52% (2018) of the total area of salt farming in Cirebon while the H class accounts for about 38.54% (2016) and 21.9% (2018). The VH class covered 24.26% of the area in 2016 and only 1.5% in 2018. H and VH areas had maximum flood depths and durations. This aspect is also physically illustrated by low elevation flat slopes and proximity to the shore and channels. Furthermore, these areas have mixed soil types and geological features dominated by flood plain deposits. Usually, traditional salt farmers tend to choose this type of location due to impervious soil that is suitable for the salt pan surface layer. In Cirebon, these two classes dominate the eastern and middle part, including Losari, Gebang, Pangenan, Mundu, and Astanajapura. *Figure 5.7* shows the levels of risk in the salt farming area of Cirebon based on tidal flood occurrences in the past.

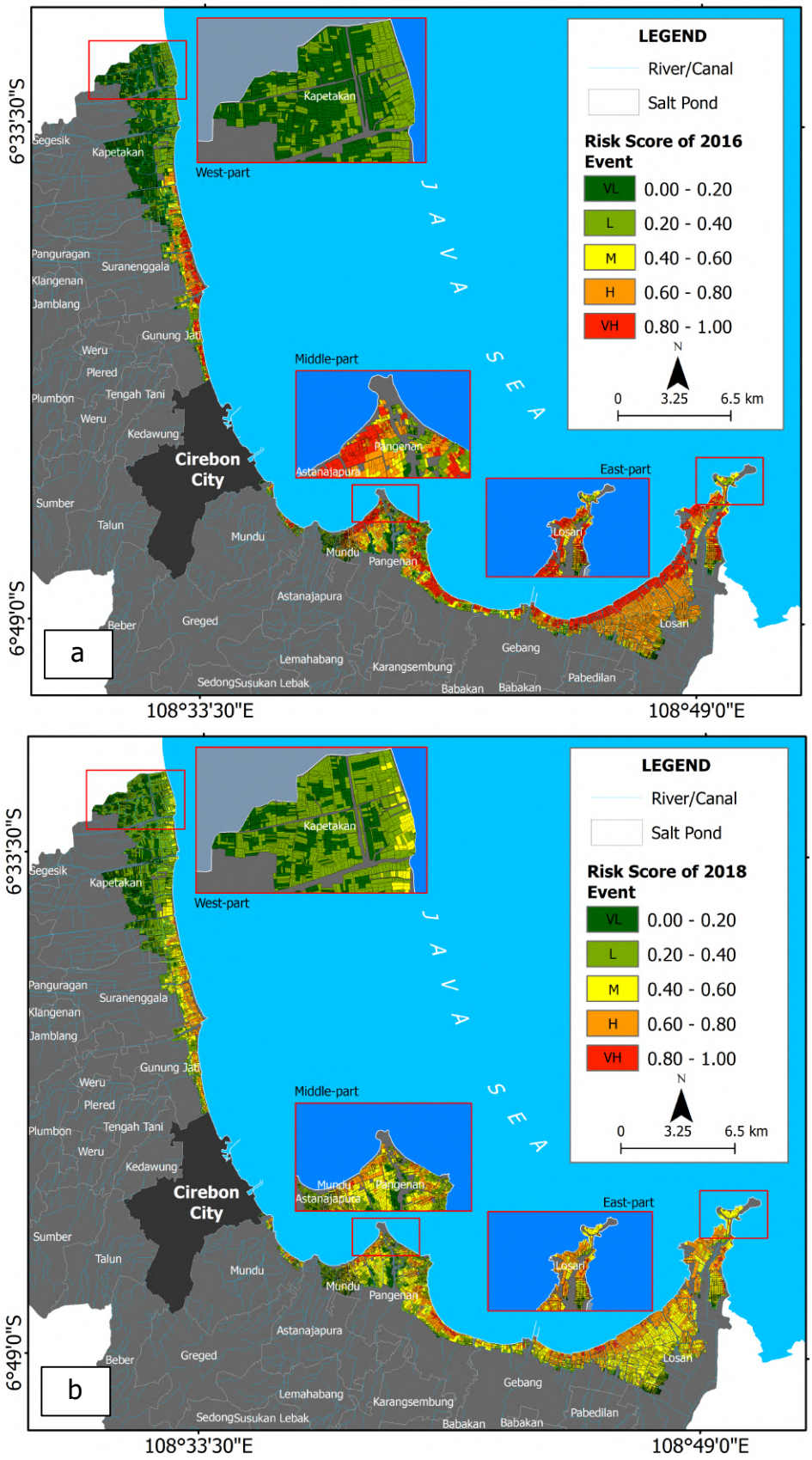

Figure 5.7. Tidal flood risk on salt farming area in Cirebon, West Java based on the evaluation of the 2016 (a) and 2018 (b) events.

5.5.4. Validation

Although there are no official reports on the two flood events in 2016 and 2018, previous numerical simulations can be taken as an alternative to validate the model (Nirwansyah and Braun, 2021). According to that paper, in the pre-production period, where the salt has not yet been produced, the total damage value was 170.3 billion rupiahs while total value during the harvesting period was estimated at 1.38 trillion rupiahs (Nirwansyah and Braun, 2021). This value includes all costs and revenues (C/R) of the production for the whole area. In this phase, the Pearson value shows a correlation for these periods: in 2016 the value comprises 0.81 and in 2018 the value increases to 0.84. These strongly positive correlations are associated with monetary loss that has been estimated based on the numerical model and the risk score of the current approach. Nevertheless, the impact on monetary aspects has proven to be similar to that in the previous model by (Nirwansyah and Braun, 2021).

The maximum loss on each parcel is estimated to be 13,322.46 thousand rupiahs (2016 event) and 2,492.14 thousand rupiahs (2018 event). Both calculations are close to the physical-based model, where a monetary loss of 13,322.72 thousand rupiahs for the 2016 event was calculated and the 2018 event showed a 2,528.87 thousand rupiahs loss on each parcel. *Table 5.4* compares the evaluation of the current multicriteria approach with that of the physical-based method.

Table 5.4 Parametric approach comparison using Pearson correlation test with input from simulated damage by the previous physical-based model* (loss is presented in thousand rupiahs)

	2016 event		2018 event	
	Parametric	**Physical-based**	**Parametric**	**Physical-based**
Minimum loss (each parcel)	0.00	0.00	0.00	0.00
Maximum loss (each parcel)	13,287.28	13,322.72	2.491.73	2,528.72
Mean	6,500.68	6,912.17	1,240.87	1,286.23
Estimated total damage	77,290,054	74,105,354	13,596,499	13,789,773
Sample (N=270 parcels)				
Pearson coefficient (r)	0,81		0,84	
Type of correlation	Strongly positive		Strongly positive	

**The values were extracted from previous study by Nirwansyah and Braun (2021)*

5.5.5. Discussion

5.5.5.1. Implementation of AHP for tidal flood mapping in salt farming

This study presents the assessment of risk for salt farming in Cirebon through a combination of hazard and vulnerability parameters. The selected events in 2016 and 2018 showed a relatively low level of risk caused by the hazard magnitude (H), which ranges between 0.203 and 0.253 while the maximum vulnerability (V) score reaches a level of 0.334. However, both components have highlighted the higher risk areas, especially the ones close to the coast and/or to channels, where the salt ponds are impacted the most (see *Figure 5.8).* In extreme cases, the risk can increase drastically due to maximum tides coupled with storm surges, river floods, and sea-level rise (Karegar *et al.*, 2017; Moftakhari *et al.*, 2017). Such a scenario will potentially trigger massive

disruptions in almost all salt production areas that have minimum structural protection. We expect that our model can be applied to different periods and geographical contexts. Moreover, to assess flood risk in salt farming, several other scenarios of depth and duration are also possible, especially when the absence of historical data records needs to be overcome.

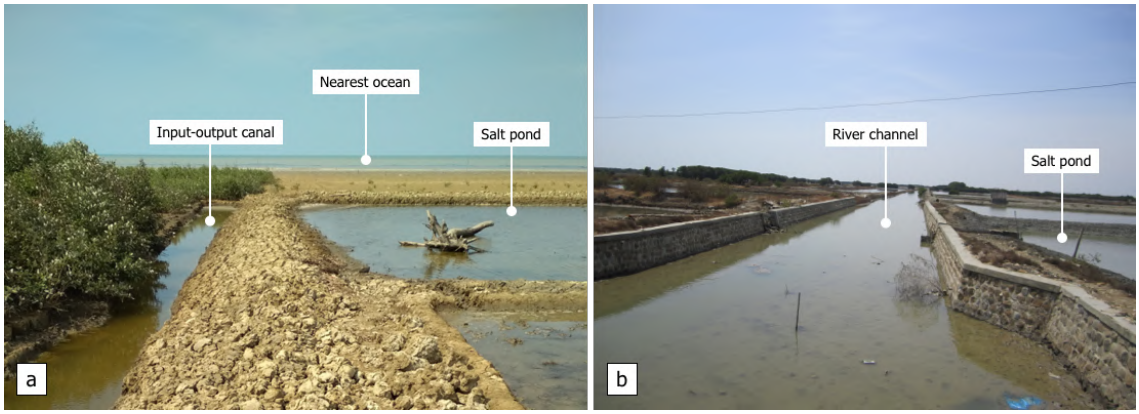

Figure 5.8. The example sequence of a salt production pond in very high risk based on its physical condition and location (a) close to the shoreline and (b) close to channels (picture taken by Nirwansyah in the Pangenan district).

In this study, a combined AHP-GIS approach has been implemented to address tidal flood risk for salt farming. The AHP approach has been efficiently and successfully implemented in other flood risk assessments (Cabrera and Lee, 2019; Chakraborty and Mukhopadhyay, 2019; Danumah *et al.*, 2016; Ghosh and Kar, 2018; Rincón *et al.*, 2018). The study involves depth and duration as common aspects in flood hazard assessment. We introduced the timing of flooding as an additional indicator as it allows for different responses on each salt production stage. The present study also underlines that vulnerability has a higher impact on flood risk in salt farming compared to the hazard. This is especially true for factors such as distance to channels or distance to the coast. Other physical conditions such as geological features, soil types, topography, and coastal slopes have less implications for salt farming vulnerability. Although several studies suggest that elevation and slope elements have a substantial impact on coastal vulnerability assessment (CVA) (Díez-Herrero and Garrote, 2020; Mani Murali *et al.*, 2013; Rey *et al.*, 2020), we argue for considering other parameters in further research, such as the shoreline change range (Kantamaneni *et al.*, 2019; Satta *et al.*, 2016) and rates of sea-level rise, the latter being a global phenomenon that will increasingly impact agricultural activities in coastal areas throughout the world (Anh, 2014; Ruane *et al.*, 2013).

5.5.5.2. Combined parametric and physical-based approaches

The physical-based model, with the advantage of being able to simulate flood occurrences, was used in validating this study. The physical-based approach could compensate for a lack of official damage reports for coastal agricultural land in Cirebon, West Java, and is, additionally, a solution to handling the complicated and coupled set of the equation especially in hydrodynamic processes such as flooding (Balica *et al.*, 2013). This approach considers the

hydrodynamic condition of the tide that influences the magnitude, the momentum, the tidal character, and the velocity and timing of the stream (Parker, 2007). However, our model requires various historical data that might be unavailable in many less developed areas. The parametric approach has been designed for these situations to address hazards and vulnerability through selected, commonly available indicators. Our study also applies a weighting technique, as it proposes considering inter-dependency among variables in the final expression (Lein and Abel, 2010; Nasiri *et al.*, 2016). Finally, the study explored the accuracy of both approaches by applying a simple statistical correlation analysis.

5.5.5.3. Possible uncertainties

Many studies appreciate how the AHP can give a better understanding of the topic, especially with a weight given to each indicator (Cabrera and Lee, 2019). However, there are possibilities for several uncertainties for the current study. First, the elevation data has been noticed as causing uncertainty in the risk model due to errors and extreme smoothing (Yunus *et al.*, 2016). Although this study used DEMNAS elevation data with a relatively fine resolution, there is possible space for uncertainty in comparison to real salt farming conditions. Second, the subjectivity inherent in the AHP weighting, as it depends on expert opinion in scoring variables (Cabrera and Lee, 2019; Cai *et al.*, 2019), also applies to this study. The lack on documented expertise in salt farming meant that the selection for experts for the study was limited to local experts and authorities with experience in research and management for coastal of West Java. However, during AHP, there was consistency measuring, which can be acknowledged as indirect control of the uncertainty in the criteria weighting stage (de Brito and Evers, 2016). Third, an uncertainty aspect may also relate to selection, comparison and ranking of the multiple criteria (Bathrellos *et al.*, 2013). At same time, this study is also concerned with the multi-facets of hazard, vulnerability and risk, which are represented by the indicator selection. Here, the indicator selection for each parameter has considered a tidal flooding event with the aspects of depth, duration and timing, and also the characteristic of salt farming itself in low-lying areas, with its operation based on seasonality.

5.6. Conclusion

This research aimed at evaluating the risk of tidal flooding for salt farmers in northern Java. The model is based on two recorded events in 2016 and 2018 and developed criteria for each component of hazard and vulnerability. The combination of AHP and GIS proved to be useful for tidal risk assessments in situations where data and official damage reports are scarce. However, physical-based approaches can support the validity of our AHP model. Notwithstanding these methodological advancements, sea-level rise, land subsidence, and stronger storm surges will increase the risks for many economic activities in less developed coastal areas of Indonesia and many other tropical countries in the years and decades to come. For this reason, flood risk assessments should be systematically integrated into decision-making processes in disaster mitigation planning and coastal zone management.

Supplementary Materials: There will be supplementary data of correlation analysis for all two risks in Excel format.

Author Contributions: Conceptualization, A.W.N. and B.B.; methodology, software, validation, formal analysis and writing / original draft preparation, A.W.N.; writing-review & editing, A.W.N. and B.B.; supervision, B.B.

Funding: The authors would like to acknowledge the financial support provided by Indonesia Endowment Fund for Education (LPDP) provided to the first author (code of LPDP: PRJ-115 /LPDP.3/2017).

Data Availability Statement: Not applicable.

Acknowledgments: This project has been part of the doctoral research of the first author at the Institute of Geography, University of Cologne, Germany. The authors are thankful for the contribution of all experts interviewed for this study. The authors also express their gratitude to the co-supervisors of the PhD thesis for constructive inputs, Frauke Haensch for proofreading, and the anonymous reviewers for their valuable critics and suggestions.

Conflicts of Interest: The authors declare no conflict of interest. The funders had no role in the design of the study; in the collection, analyses, or interpretation of data; in the writing of the manuscript, or in the decision to publish the results.

5.7. References

Adnan, M.S.G., Abdullah, A.Y.M., Dewan, A. and Hall, J.W. (2020), "The effects of changing land use and flood hazard on poverty in coastal Bangladesh", Land Use Policy, Elsevier, Vol. 99 No. March, p. 104868.

ADPC. (2005), A Primer: Disaster Risk Management in Asia, edited by Apikul, C., Noson, L., Karumaratne, G. and Choong, W., ADPC, Bangkok, available at: http://www.adpc.net/udrm/primer/pdf/primer_volume1.pdf.

Afifi, Z., Chu, H.J., Kuo, Y.L., Hsu, Y.C., Wong, H.K. and Ali, M.Z. (2019), "Residential flood loss assessment and risk mapping from high-resolution simulation", Water (Switzerland), Vol. 11 No. 4, pp. 1–15.

Anh, N.L. (2014), Climate Proofing Aquaculture: A Case Study on Pangasius Farming in the Mekong Delta, Vietnam, Wageningen.

Apel, H., Aronica, G.T., Kreibich, H. and Thieken, A.H. (2009), "Flood risk analyses - How detailed do we need to be?", Natural Hazards, Vol. 49 No. 1, pp. 79–98.

Apriani, M., Hadi, W. and Masduqi, A. (2018), "Physicochemical properties of sea water and bittern in Indonesia: Quality improvement and potential resources utilization for marine environmental sustainability", Journal of Ecological Engineering, Vol. 19 No. 3, pp. 1–10.

Baig, M.R.I., Shahfahad, Ahmad, I.A., Tayyab, M., Asgher, M.S. and Rahman, A. (2021), "Coastal Vulnerability Mapping by Integrating Geospatial Techniques and Analytical Hierarchy Process (AHP) along the Vishakhapatnam Coastal Tract, Andhra Pradesh, India", Journal of the Indian Society of Remote Sensing, Springer India, Vol. 49 No. 2, pp. 215–231.

Baky, M.A. Al, Islam, M. and Paul, S. (2020), "Flood Hazard, Vulnerability and Risk Assessment for Different Land Use Classes Using a Flow Model", Earth Systems and Environment, Springer International Publishing, Vol. 4

No. 1, pp. 225–244.
Balica, S.F.F., Popescu, I., Beevers, L. and Wright, N.G.G. (2013), "Parametric and physically based modelling techniques for flood risk and vulnerability assessment: A comparison", Environmental Modelling and Software, Elsevier Ltd, Vol. 41, pp. 84–92.
Bathrellos, G.D., Gaki-Papanastassiou, K., Skilodimou, H.D., Skianis, G.A. and Chousianitis, K.G. (2013), "Assessment of rural community and agricultural development using geomorphological–geological factors and GIS in the Trikala prefecture (Central Greece)", Stochastic Environmental Research and Risk Assessment, Vol. 27 No. 2, pp. 573–588.
Bhakta Shrestha, B., Sawano, H., Ohara, M., Yamazaki, Y. and Tokunaga, Y. (2019), "Methodology for Agricultural Flood Damage Assessment", Recent Advances in Flood Risk Management, Vol. i, IntechOpen, p. 13.
Black, A.R. (1995), "Flood seasonality and physical controls in flood risk estimation", Scottish Geographical Magazine, Vol. 111 No. 3, pp. 187–190.
BPS Cirebon. (2020), Cirebon Regency in Figure, edited by BPS-Statistics of Cirebon Regency, BPS-Statistics of Cirebon Regency, Cirebon.
de Brito, M.M. and Evers, M. (2016), "Multi-criteria decision-making for flood risk management: a survey of the current state of the art", Natural Hazards and Earth System Sciences, Vol. 16 No. 4, pp. 1019–1033.
Budiyono, Y. (2018), Flood Risk Modeling in Jakarta Development: Development and Usefulness in a Time of Climate Change, Vrije Universiteit Amsterdam, Amsterdam.
Budiyono, Y., Aerts, J., Brinkman, J.J., Marfai, M.A. and Ward, P. (2015), "Flood risk assessment for delta mega-cities: a case study of Jakarta", Natural Hazards, Vol. 75 No. 1, pp. 389–413.
Bui, D.T., Ngo, P.T.T., Pham, T.D., Jaafari, A., Minh, N.Q., Hoa, P.V. and Samui, P. (2019), "A novel hybrid approach based on a swarm intelligence optimized extreme learning machine for flash flood susceptibility mapping", Catena, Elsevier, Vol. 179 No. March, pp. 184–196.
Cabrera and Lee. (2019), "Flood-Prone Area Assessment Using GIS-Based Multi-Criteria Analysis: A Case Study in Davao Oriental, Philippines", Water, Vol. 11 No. 11, p. 2203.
Cai, T., Li, X., Ding, X., Wang, J. and Zhan, J. (2019), "Flood risk assessment based on hydrodynamic model and fuzzy comprehensive evaluation with GIS technique", International Journal of Disaster Risk Reduction, Elsevier Ltd, Vol. 35 No. February, p. 101077.
Cardona, O.-D., van Aalst, M.K., Birkmann, J., Forndham, M., McGregor, G., Perez, R., Pulwarty, R.S., et al. (2012), Determinants of Risk : Exposure and Vulnerability, Managing the Risks of Extreme Events and Disasters to Advance Climate Change Adaptation - A Special Report of Working Groups I and II of the Intergovernmental Panel on Climate Change (IPCC), Cambridge, available at: https://www.ipcc.ch/site/assets/uploads/2018/03/SREX-Chap2_FINAL-1.pdf.
Chakraborty, S. and Mukhopadhyay, S. (2019), "Assessing flood risk using analytical hierarchy process (AHP) and geographical information system (GIS): application in Coochbehar district of West Bengal, India", Natural Hazards, Springer Netherlands, Vol. 99 No. 1, pp. 247–274.

Chau, V.N., Cassells, S. and Holland, J. (2015), "Economic impact upon agricultural production from extreme flood events in Quang Nam, central Vietnam", Natural Hazards, Vol. 75 No. 2, pp. 1747–1765.
Dandapat, K. and Panda, G.K. (2017), "Flood vulnerability analysis and risk assessment using analytical hierarchy process", Modeling Earth Systems and Environment, Springer International Publishing, Vol. 3 No. 4, pp. 1627–1646.
Danumah, J.H., Odai, S.N., Saley, B.M., Szarzynski, J., Thiel, M., Kwaku, A., Kouame, F.K., et al. (2016), "Flood risk assessment and mapping in Abidjan district using multi-criteria analysis (AHP) model and geoinformation techniques, (cote d'ivoire)", Geoenvironmental Disasters, Geoenvironmental Disasters, Vol. 3 No. 1, available at: https://doi.org/10.1186/s40677-016-0044-y.
Dasgupta, A. (2007), "Floods and poverty traps: Evidence from Bangladesh", Economic and Political Weekly, Vol. 42 No. 30, pp. 3166–3171.
Dede, M., Widiawaty, M.A., Pramulatsih, G.P., Ismail, A., Ati, A. and Murtianto, H. (2019), "Integration of participatory mapping, crowdsourcing and geographic information system in flood disaster management (case study Ciledug Lor, Cirebon)", Journal of Information Technology and Its Utilization, Vol. 2 No. 2, p. 44.
Development Planning Board. (2014), Middle Term of Development Plan, Cirebon, available at: http://bappeda.cirebonkab.go.id/wp-content/uploads/2015/11/Dokumen-Final-RPJMD-2014-2019.pdf.
Díez-Herrero, A. and Garrote, J. (2020), "Flood Risk Analysis and Assessment, Applications and Uncertainties: A Bibliometric Review", Water, Vol. 12 No. 7, p. 2050.
Domeneghetti, A., Gandolfi, S., Castellarin, A., Brandimarte, L., Di Baldassarre, G., Barbarella, M. and Brath, A. (2015), "Flood risk mitigation in developing countries: Deriving accurate topographic data for remote areas under severe time and economic constraints", Journal of Flood Risk Management, Vol. 8 No. 4, pp. 301–314.
Dutta, D., Herath, S. and Musiake, K. (2003), "A mathematical model for flood loss estimation", Journal of Hydrology, Vol. 277 No. 1–2, pp. 24–49.
Ganji, Z., Shokoohi, A. and Samani, J.M. V. (2012), "Developing an agricultural flood loss estimation function (case study: Rice)", Natural Hazards, Vol. 64 No. 1, pp. 405–419.
Ghosh, A. and Kar, S.K. (2018), "Application of analytical hierarchy process (AHP) for flood risk assessment: a case study in Malda district of West Bengal, India", Natural Hazards, Springer Netherlands, Vol. 94 No. 1, pp. 349–368.
Glaz, B. and Lingle, S.E. (2012), "Flood Duration and Time of Flood Onset Effects on Recently Planted Sugarcane", Agronomy Journal, Vol. 104 No. 3, pp. 575–583.
Goepel, K.D. (2013), "Implementing the Analytic Hierarchy Process as a Standard Method for Multi-Criteria Decision Making in Corporate Enterprises – a New AHP Excel Template with Multiple Inputs", Proceedings of the International Symposium on the Analytic Hierarchy Process, Vol. 2, pp. 1–10.
Gozan, M., Ningsih, Y., Efendy, M. and Basri, F.H. (2018), Hikayat Si Induk

Bumbu (in Indonesia), edited by Rusi, N., Saripudin, J. and Isaiyas, I., First Edit., Kepustakaan Populer Gramedia, Jakarta.
Gunawan, B.I. (2012), Shrimp Fisheries and Aquaculture: Making a Living in the Coastal Frontier of Berau, Indonesia.
Hadian, M.S.D., Riyan Rahmat Hardadi, Barkah, M.N., Suganda, B.R., Putra, D.B.E. and Sulaksana, N. (2017), "Groundwater Characteristic and Quality of Unconfined Aquifer in Cirebon City", Proceedings of the 2nd Joint Conference of Utsunomiya University and Universitas Padjadjaran, pp. 48–54.
Hadipour, V., Vafaie, F. and Deilami, K. (2020), "Coastal flooding risk assessment using a GIS-based spatial multi-criteria decision analysis approach", Water (Switzerland), Vol. 12 No. 9, available at: https://doi.org/10.3390/W12092379.
Hartini, S. (2015), Modeling of Flood Risk of Agriculture Land Area in Part of North Coast of Central Java, Universitas Gadjah Mada.
Hillel, D. (1980), Fundamentals of Soil Physics, Fundamentals of Soil Physics, Elsevier, available at: https://doi.org/10.1016/C2009-0-03109-2.
Hoque, M.A.A., Tasfia, S., Ahmed, N. and Pradhan, B. (2019), "Assessing spatial flood vulnerability at kalapara upazila in Bangladesh using an analytic hierarchy process", Sensors (Switzerland), Vol. 19 No. 6, pp. 1–19.
Howlader, M.S. and Akanda, M.G.R. (2016), "Problems in Adaptation to Climate Change Effects on Coastal Agriculture by the Farmers of Patuakhali District of Bangladesh", American Journal of Rural Development, Vol. 4 No. 1, pp. 10–14.
Huda, F.A. (2015), Economic Assessment of Farm Level Climate Change Adaptation Options: Analytical Approach and Empirical Study for the Coastal Area of Bangladesh, Humboldt-Universität zu Berlin.
Jongman, B., Kreibich, H., Apel, H., Barredo, J.I., Bates, P.D., Feyen, L., Gericke, A., et al. (2012), "Comparative flood damage model assessment: Towards a European approach", Natural Hazards and Earth System Science, Vol. 12 No. 12, pp. 3733–3752.
Kantamaneni, K., Sudha Rani, N.N.V., Rice, L., Sur, K., Thayaparan, M., Kulatunga, U., Rege, R., et al. (2019), "A Systematic Review of Coastal Vulnerability Assessment Studies along Andhra Pradesh, India: A Critical Evaluation of Data Gathering, Risk Levels and Mitigation Strategies", Water, Vol. 11 No. 2, p. 393.
Karegar, M.A., Dixon, T.H., Malservisi, R., Kusche, J. and Engelhart, S.E. (2017), "Nuisance Flooding and Relative Sea-Level Rise: the Importance of Present-Day Land Motion", Scientific Reports, Vol. 7 No. 1, p. 11197.
Khazai, B., Daniell, J. and Apel, H. (Gfdrr). (2011), Risk Analysis Course Manual, Washington DC.
Komi, K., Amisigo, B. and Diekkrüger, B. (2016), "Integrated Flood Risk Assessment of Rural Communities in the Oti River Basin, West Africa", Hydrology, Vol. 3 No. 4, p. 42.
Komolafe, A.A., Herath, S. and Avtar, R. (2019), "Establishment of detailed loss functions for the urban flood risk assessment in Chao Phraya River basin, Thailand", Geomatics, Natural Hazards and Risk, Taylor & Francis, Vol. 10 No. 1, pp. 633–650.
Kourgialas, N.N. and Karatzas, G.P. (2016), "A flood risk decision making

approach for Mediterranean tree crops using GIS; climate change effects and flood-tolerant species", Environmental Science & Policy, Elsevier Ltd, Vol. 63, pp. 132–142.
Kron, W. (2005), "Flood Risk = Hazard • Values • Vulnerability", Water International, Vol. 30 No. 1, pp. 58–68.
Lein, J.K. and Abel, L.E. (2010), "Hazard vulnerability assessment: How well does nature follow our rules?", Environmental Hazards, Vol. 9 No. 2, pp. 147–166.
Lia, E. (2016), "Puluhan Ribu Ton Garam di Cirebon Tersapu Banjir Rob page-2 : Okezone News", Okezone.Com, available at: https://news.okezone.com/read/2016/06/17/525/1418255/puluhan-ribu-ton-garam-di-cirebon-tersapu-banjir-rob?page=2 (accessed 10 June 2019).
Luu, C. and von Meding, J. (2018), "A flood risk assessment of Quang Nam, Vietnam using spatial multicriteria decision analysis", Water (Switzerland), Vol. 10 No. 4, pp. 1–16.
Luu, C., Von Meding, J. and Kanjanabootra, S. (2018), "Assessing flood hazard using flood marks and analytic hierarchy process approach: a case study for the 2013 flood event in Quang Nam, Vietnam", Natural Hazards, Springer Netherlands, Vol. 90 No. 3, pp. 1031–1050.
Luu, C., Tran, H.X., Pham, B.T., Al-Ansari, N., Tran, T.Q., Duong, N.Q., Dao, N.H., et al. (2020), "Framework of spatial flood risk assessment for a case study in quang binh province, Vietnam", Sustainability (Switzerland), Vol. 12 No. 7, pp. 1–17.
Lyddon, C., Brown, J.M., Leonardi, N. and Plater, A.J. (2018), "Flood Hazard Assessment for a Hyper-Tidal Estuary as a Function of Tide-Surge-Morphology Interaction", Estuaries and Coasts, pp. 1565–1586.
Lyu, H.M., Sun, W.J., Shen, S.L. and Arulrajah, A. (2018), "Flood risk assessment in metro systems of mega-cities using a GIS-based modeling approach", Science of the Total Environment, Elsevier B.V., Vol. 626, pp. 1012–1025.
Mahasin, M.Z., Rochwulaningsih, Y. and Sulistiyono, S.T. (2020), "Coastal Ecosystem as Salt Production Centre in Indonesia", E3S Web of Conferences, Vol. 202, available at: https://doi.org/10.1051/e3sconf/202020207042.
Mani Murali, R., Ankita, M., Amrita, S. and Vethamony, P. (2013), "Coastal vulnerability assessment of Puducherry coast, India, using the analytical hierarchical process", Natural Hazards and Earth System Sciences, Vol. 13 No. 12, pp. 3291–3311.
De Medeiros Rocha, R., Costa, D.F., Lucena-Filho, M.A., Bezerra, R.M., Medeiros, D.H., Azevedo-Silva, A.M., Araújo, C.N., et al. (2012), "Brazilian solar saltworks - ancient uses and future possibilities", Aquatic Biosystems, Vol. 8 No. 1, p. 8.
Merz, B. and Thieken, A.H. (2009), "Flood risk curves and uncertainty bounds", Natural Hazards, Vol. 51 No. 3, pp. 437–458.
Metrotv. (2016), "700 Hectares of Salt Pond in Cirebon Submerged Coastal Flood (in Bahasa)", Metrotvnews.Com, available at: http://m.metrotvnews.com/jabar/peristiwa/JKR4MYQb-700-hektare-tambak-garam-di-cirebon-terendam-banjir-rob (accessed 29 September 2017).
Meyer, J.C. and Pine, J. (2004), "Comparative Analysis Between Different Flood

Assessment Technologies In Hazus-MH", Dept. Env. Sci., Vol. Master of, p. 72.
Meyer, V., Haase, D. and Scheuer, S. (2007), GIS-Based Multicriteria Analysis as Decision Support in Flood Risk Management, No. 6/2007, Leipzig, available at: http://hdl.handle.net/10419/45237.
Meyer, V., Scheuer, S. and Haase, D. (2009), "A multicriteria approach for flood risk mapping exemplified at the Mulde river, Germany", Natural Hazards, Vol. 48 No. 1, pp. 17–39.
Moftakhari, H.R., Aghakouchak, A., Sanders, B.F. and Matthew, R.A. (2017), "Earth's Future Special Section: Cumulative hazard: The case of nuisance flooding Earth' s Future", Earth's Future, No. 5, pp. 214–223.
Mohamed, S.A. and El-Raey, M.E. (2020), "Vulnerability assessment for flash floods using GIS spatial modeling and remotely sensed data in El-Arish City, North Sinai, Egypt", Natural Hazards, Springer Netherlands, Vol. 102 No. 2, pp. 707–728.
Molinari, D., Ballio, F., Handmer, J. and Menoni, S. (2014), "On the modeling of significance for flood damage assessment", International Journal of Disaster Risk Reduction, Elsevier, Vol. 10 No. PA, pp. 381–391.
Molinari, D., Scorzini, A.R., Arrighi, C., Carisi, F., Castelli, F., Gallazzi, A., Galliani, M., et al. (2020), "Are flood damage models converging to reality? Lessons learnt from a blind test", No. February, pp. 1–32.
Munadi, E., Ardiyanti, S.T., Ingot, S.R., Lestari, T.K., Subekti, N.A., Salam, A.R., Alhayat, A.P., et al. (2016), Info Komoditi Garam, edited by Salim, Z. and Munadi, E., Badan Pengkajian dan Pengembangan Perdagangan, Jakarta, available at: http://bppp.kemendag.go.id/media_content/2017/08/Isi_BRIK_Garam.pdf.
Munji, C.A., Bele, M.Y., Nkwatoh, A.F., Idinoba, M.E., Somorin, O.A. and Sonwa, D.J. (2013), "Vulnerability to coastal flooding and response strategies: The case of settlements in Cameroon mangrove forests", Environmental Development, Elsevier, Vol. 5 No. 1, pp. 54–72.
Nasiri, H., Mohd Yusof, M.J. and Mohammad Ali, T.A. (2016), "An overview to flood vulnerability assessment methods", Sustainable Water Resources Management, Springer International Publishing, Vol. 2 No. 3, pp. 331–336.
Nirwansyah, A.W. and Braun, B. (2021), "Assessing the degree of tidal flood damage to salt harvesting landscape using synthetic approach and GIS - Case study: Cirebon, West Java", International Journal of Disaster Risk Reduction, Elsevier Ltd, Vol. 55 No. January, p. 102099.
Nirwansyah and Braun. (2019), "Mapping Impact of Tidal Flooding on Solar Salt Farming in Northern Java using a Hydrodynamic Model", ISPRS International Journal of Geo-Information, Vol. 8 No. 10, p. 451.
Oren, A. (2009), "Saltern evaporation ponds as model systems for the study of primary production processes under hypersaline conditions", Aquatic Microbial Ecology, Vol. 56 No. 2–3, pp. 193–204.
Ouma, Y.O. and Tateishi, R. (2014), "Urban flood vulnerability and risk mapping using integrated multi-parametric AHP and GIS: Methodological overview and case study assessment", Water (Switzerland), Vol. 6 No. 6, pp. 1515–1545.
Pacetti, T., Caporali, E. and Rulli, M.C. (2017), "Floods and food security: A

method to estimate the effect of inundation on crops availability", Advances in Water Resources, Elsevier Ltd, Vol. 110, pp. 494–504.
Parker, B.B. (2007), Tidal Analysis and Prediction, No. 2007925298, NOAA Special Publication, Silver Spring, Maryland, available at: https://tidesandcurrents.noaa.gov.
Post, J., Zosseder, K., Strunz, G., Birkmann, J., Gebert, N., Setiadi, N., Anwar, H.Z., et al. (2007), "Risk and vulnerability assessment to tsunami and coastal hazards in Indonesia: Conceptual framework and indicator development", International Symposium on Disaster in Indonesia, Padang, Indonesia (26-28 July 2007), Padang, pp. 26–29.
Potts, W.M., Götz, A. and James, N. (2015), "Review of the projected impacts of climate change on coastal fishes in southern Africa", Reviews in Fish Biology and Fisheries, Springer International Publishing, Vol. 25 No. 4, pp. 603–630.
Quinn, N., Lewis, M., Wadey, M.P. and Haigh, I.D. (2014), "Assessing the temporal variability in extreme storm-tide time series for coastal flood risk assessment", Journal of Geophysical Research: Oceans, Vol. 119 No. 8, pp. 4983–4998.
radarcirebon.com. (2018), "Waspada Rob Susulan, Ini Sebabnya", available at: http://www.radarcirebon.com/waspada-rob-sususlan-ini-sebabnya.html (accessed 26 March 2021).
Radwan, F., Alazba, A.A. and Mossad, A. (2019), "Flood risk assessment and mapping using AHP in arid and semiarid regions", Acta Geophysica, Springer International Publishing, Vol. 67 No. 1, pp. 215–229.
Rahman, M., Ningsheng, C., Islam, M.M., Dewan, A., Iqbal, J., Washakh, R.M.A. and Shufeng, T. (2019), "Flood Susceptibility Assessment in Bangladesh Using Machine Learning and Multi-criteria Decision Analysis", Earth Systems and Environment, Springer International Publishing, Vol. 3 No. 3, pp. 585–601.
Ramanathan, R. (2001), "A note on the use of the analytic hierarchy process for environmental impact assessment", Journal of Environmental Management, Vol. 63 No. 1, pp. 27–35.
Rey, W., Martínez-Amador, M., Salles, P., Mendoza, E.T., Trejo-Rangel, M.A., Franklin, G.L., Ruiz-Salcines, P., et al. (2020), "Assessing different flood risk and damage approaches: A case of study in progreso, Yucatan, Mexico", Journal of Marine Science and Engineering, Vol. 8 No. 2, p. 137.
Rimba, A., Setiawati, M., Sambah, A. and Miura, F. (2017), "Physical Flood Vulnerability Mapping Applying Geospatial Techniques in Okazaki City, Aichi Prefecture, Japan", Urban Science, Vol. 1 No. 1, p. 7.
Rincón, D., Khan, U. and Armenakis, C. (2018), "Flood Risk Mapping Using GIS and Multi-Criteria Analysis: A Greater Toronto Area Case Study", Geosciences, Vol. 8 No. 8, p. 275.
Ronco, P., Gallina, V., Torresan, S., Zabeo, A., Semenzin, E., Critto, A. and Marcomini, A. (2014), "The KULTURisk Regional Risk Assessment methodology for water-related natural hazards – Part 1 : Physical – environmental", pp. 5399–5414.
Ruane, A.C., Major, D.C., Yu, W.H., Alam, M., Hussain, S.G., Khan, A.S., Hassan, A., et al. (2013), "Multi-factor impact analysis of agricultural

production in Bangladesh with climate change", Global Environmental Change, Elsevier Ltd, Vol. 23 No. 1, pp. 338–350.
Saaty, T.L. (1977), "A scaling method for priorities in hierarchical structures", Journal of Mathematical Psychology, Vol. 15 No. 3, pp. 234–281.
Saaty, T.L. (2002), "Decision making with the Analytic Hierarchy Process", Scientia Iranica, Vol. 9 No. 3, pp. 215–229.
Saaty, T.L., Vargas, L.G. and Dellmann, K. (2003), "The allocation of intangible resources: The analytic hierarchy process and linear programming", Socio-Economic Planning Sciences, Vol. 37 No. 3, pp. 169–184.
Sadeghi-Pouya, A., Nouri, J., Mansouri, N. and Kia-Lashaki, A. (2017), "Developing an index model for flood risk assessment in the western coastal region of Mazandaran, Iran", Journal of Hydrology and Hydromechanics, Vol. 65 No. 2, pp. 134–145.
Satta, A. (2014), An Index-Based Method to Assess Vulnerabilities and Risks of Mediterranean Coastal Zones to Multiple Hazards, Ca' Foscari University of Venice.
Satta, A., Snoussi, M., Puddu, M., Flayou, L. and Hout, R. (2016), "An index-based method to assess risks of climate-related hazards in coastal zones: The case of Tetouan", Estuarine, Coastal and Shelf Science, Vol. 175 No. April, pp. 93–105.
Serinaldi, F., Loecker, F., Kilsby, C.G. and Bast, H. (2018), "Flood propagation and duration in large river basins: a data-driven analysis for reinsurance purposes", Natural Hazards, Springer Netherlands, Vol. 94 No. 1, pp. 71–92.
Sianturi, R., Jetten, V., Ettema, J. and Sartohadi, J. (2018), "Distinguishing between Hazardous Flooding and Non-Hazardous Agronomic Inundation in Irrigated Rice Fields: A Case Study from West Java", Remote Sensing, Vol. 10 No. 7, p. 1003.
Siddayao, G.P., Valdez, S.E. and Fernandez, P.L. (2014), "Analytic Hierarchy Process (AHP) in Spatial Modeling for Floodplain Risk Assessment", International Journal of Machine Learning and Computing, Vol. 4 No. 5, pp. 450–457.
Silva, S.F., Martinho, M., Capitão, R., Reis, T., Fortes, C.J. and Ferreira, J.C. (2017), "An index-based method for coastal-flood risk assessment in low-lying areas (Costa de Caparica, Portugal)", Ocean & Coastal Management, Vol. 144, pp. 90–104.
Souissi, D., Zouhri, L., Hammami, S., Msaddek, M.H., Zghibi, A. and Dlala, M. (2020), "GIS-based MCDM–AHP modeling for flood susceptibility mapping of arid areas, southeastern Tunisia", Geocarto International, Taylor & Francis, Vol. 35 No. 9, pp. 991–1017.
Subardja, D.S., Ritung, S., Anda, M., Sukarman, Suryani, E. and Subandiono, R.E. (2014), Petunjuk Teknis Klasifikasi Tanah Nasional, edited by Hikmatullah, H., Suparto, S., Tafakresnanto, C., Suratman, S. and Nugroho, K., I/2014., Balai Besar Penelitian dan Pengembangan Sumberdaya Lahan, Bogor, available at: http://bbsdlp.litbang.pertanian.go.id/ind/index.php/publikasi-3/petunjuk-teknis?download=21:klasifikasi-tanah-nasional.
Suhendra, Amron, A. and Hilmi, E. (2018), "The pattern of coastline change

based on the characteristics of sediment and coastal slope in Pangenan coast of Cirebon, West Java", edited by Prayogo, N.A. and Amron, A.E3S Web of Conferences, Vol. 47, p. 06001.
Sulaeman, Y., Poggio, L., Minasny, B. and Nursyamsi, D. (Eds.). (2019), Tropical Wetlands – Innovation in Mapping and Management, CRC Press, available at: https://doi.org/10.1201/9780429264467.
Suroso, D.S.A. and Firman, T. (2018), "The role of spatial planning in reducing exposure towards impacts of global sea level rise case study: Northern coast of Java, Indonesia", Ocean and Coastal Management, Elsevier, Vol. 153 No. June 2017, pp. 84–97.
Tehrany, M.S., Pradhan, B., Mansor, S. and Ahmad, N. (2015), "Flood susceptibility assessment using GIS-based support vector machine model with different kernel types", Catena, Elsevier B.V., Vol. 125, pp. 91–101.
Thouret, J.C., Ettinger, S., Guitton, M., Santoni, O., Magill, C., Martelli, K., Zuccaro, G., et al. (2014), "Assessing physical vulnerability in large cities exposed to flash floods and debris flows: The case of Arequipa (Peru)", Natural Hazards, Vol. 73 No. 3, pp. 1771–1815.
Torres, M.A., Jaimes, M.A., Reinoso, E. and Ordaz, M. (2014), "Event-based approach for probabilistic flood risk assessment", International Journal of River Basin Management, Vol. 12 No. 4, pp. 377–389.
Tsakiris, G., Nalbantis, I. and Pistrika, A. (2009), "Critical Technical Issues on the EU Flood Directive", European Water, Vol. 2526 No. November 2007, pp. 39–51.
UNDP. (2004), Reducing Disaster Risk: A Challenge for Development-a Global Report, Disaster and Crisis Management, available at: http://www.ifrc.org/en/what-we-do/disaster-management/preparing-for-disaster/risk-reduction/reducing-disaster-risk/.
UNISDR. (2009), 2009 UNISDR Terminology on Disaster Risk Reduction, International Stratergy for Disaster Reduction (ISDR), UNISDR, Geneva, available at: www.unisdr.org/publications.
UNISDR. (2015), "Proposed Updated Terminology on Disaster Risk Reduction: A Technical Review", No. August, pp. 1–31.
Voss, M. (2008), "The vulnerable can't speak. An integrative vulnerability approach to disaster and climate change research", Behemoth, Vol. 1 No. 3, available at: https://doi.org/10.1524/behe.2008.0022.
Vozinaki, A.E.K., Karatzas, G.P., Sibetheros, I.A. and Varouchakis, E.A. (2015), "An agricultural flash flood loss estimation methodology: the case study of the Koiliaris basin (Greece), February 2003 flood", Natural Hazards, Springer Netherlands, Vol. 79 No. 2, pp. 899–920.
Wang, Y., Li, Z., Tang, Z. and Zeng, G. (2011), "A GIS-Based Spatial Multi-Criteria Approach for Flood Risk Assessment in the Dongting Lake Region, Hunan, Central China", Water Resources Management, Vol. 25 No. 13, pp. 3465–3484.
Ward, P.J., De Moel, H. and Aerts, J.C.J.H. (2011), "How are flood risk estimates affected by the choice of return-periods?", Natural Hazards and Earth System Science, Vol. 11 No. 12, pp. 3181–3195.
Willemsen, P., van der Lelij, A.C. and Wesenbeeck, B. Van. (2019), Risk Assessment North Coast Java, available at:

https://www.ecoshape.org/app/uploads/sites/2/2020/02/1220476-002-ZKS-0007_v0.1-Risk-Assessment-North-Coast-Java-final.pdf.

Xia, J., Falconer, R.A., Lin, B. and Tan, G. (2011), "Numerical assessment of flood hazard risk to people and vehicles in flash floods", Environmental Modelling and Software, Elsevier Ltd, Vol. 26 No. 8, pp. 987–998.

Yadollahi, M. and Rosli, M.Z. (2011), "Development of the Analytical Hierarchy Process (AHP) method for rehabilitation project ranking before disasters", WIT Transactions on the Built Environment, Vol. 119, pp. 209–220.

Yunus, A., Avtar, R., Kraines, S., Yamamuro, M., Lindberg, F. and Grimmond, C. (2016), "Uncertainties in Tidally Adjusted Estimates of Sea Level Rise Flooding (Bathtub Model) for the Greater London", Remote Sensing, Vol. 8 No. 5, p. 366.

Chapter 6
Concluding Discussion

CHAPTER 6 - Concluding Discussion

6.1. Brief Overview

This thesis has followed the need to construct a new approach and inventive method, contributing to the addressing of tidal flood risk in a data-scarce environment. The results of this thesis integrate the utilization of spatial data, and GIS in the context of tidal flooding. In what follows, the empirical evidence provided in this dissertation presents an evaluation of flood risk on data-scarce regions that are represented through salt farming areas using a numerical model. The dissertation has also developed an approach to addressing hazards and vulnerability as a fundamental element of risk in salt harvesting within the exercise of expert judgment. Conceptually, this thesis expands the broader view of flood risk in salt farming, especially in rural coastal settings with poor data availability. The outcomes of the study should encourage policy-makers to implement risk evaluations for salt farming by using available geospatial data, including numerical modeling and GIS. Lastly, this thesis proposes new insights and better understanding of the specific setting of salt farming against tidal floods to collaborate on disaster risk reduction, integrated coastal planning, and salt self-sufficiency policies.

6.2. The Empirical Findings

The empirical results of this thesis deliver fundamental insights from the particular case of Cirebon, West Java, as regards the overall understanding of tidal flood implications on rural coastal land with the salt farming setting, based on recorded events as well as the economic damage and risk. The results are elaborated according to the previous research questions (RQ):

6.2.1. Objective 1: Determine the tidal flooding event and its implication on salt farming land

Based on **RQ 1**, the implications of tidal flood events in a data-poor environment on salt farming has been performed through hydrodynamic simulation. For the first time, this method was presented to extract the condition of tidal inundation, as documented in two different years. This method employs inputs from bathymetry data, detailed elevation information, water level from a local station, wind speed and velocity, and salt parcels data from BIG. Furthermore, DHI MIKE had been employed to process the numerical simulation and export it to the GIS platform. The maps displayed in Chapter 3 show that more than 80% of the salt ponds in Cirebon were submerged both in the 2016 and 2018 simulated events with 0.38 m and 0.40 m of depth (**RQ 5**). The GIS analysis also depicts that almost all coastal districts close to the Java Sea were affected by these events. The current study prefers to consider local hydrodynamic conditions that are related to salt farming activities. The hydrodynamic parameters used in the current study support the coastal nature evaluation with limited data availability (Nayak

and Bajaji, 2016). However, using the HDM demands higher resolution data input, which, from many Global South regions, is rarely accessible.

6.2.2. Objective 2: Estimating economic damage on salt farming due to tidal flooding in two different production stage

In many steps of this thesis, GIS has given beneficial support in the data analysis, including combining DDF to raster data from a previous numerical hydrodynamic model that has been presented in the first publication (Chapter 4) that contains flood depth information. This important data has been extracted to expose the flood duration. Both aspects are used to illustrate the physical vulnerability (PV) condition. This approach was practiced for the first time in the salt farming case, although there were previous studies by Mason & Kipp Jr. (1997) and Picado, Dias, & Fortunato (2009) that encouraged further research on the disruption in salt farming, particularly due to flooding (as mentioned in subchapter 4.1). To address this issue, the detailed salt parcel data taken from the Indonesian national geospatial agency (BIG) has given researchers the ability to transfer economic loss investigation to the individual pond level. This method was responded to by several former studies that used coarse estimation and simple assumptions, driven by the limited data availability. By combining both the previous numerical model and GIS, the study generates not only the flood depth (f_d) but also duration (f_t) information that is beneficial in the vulnerability and risk analysis. Ultimately, based on the analysis, the two selected events in 2016 had an 0.38 m high and lasted 2.23 days, while the 2018 flood event had inundated for 2.32 days within 0.40 m depth (as explained in Chapter 4, subchapter 4.2.1).

The results already depicted **RQ 2,** which newly established DDF for salt farming land. In this current dissertation, we enrich the utilization of the synthetic approach for DDF settings derived from (Bhakta Shrestha *et al.*, 2019; Vozinaki *et al.*, 2015) in agriculture and plantation contexts that were modified through an extensive examination of the physical structure of salt farming involving the dike condition, channel connection, and salt's ability to withstand against tidal floods. Here, the study has successfully employed the salt farmer group leaders' experience to address the level of damage on each flood condition at the different stages of production through the 'what-if' questionnaire (see *Table 4.3*). In addition to this key finding, the combined local stakeholder information has revealed the connection between depth and duration aspects of tidal flooding, with the damage level of salt farming individually, as can be seen in *Figure 4.5*. In summary, all local information from farmers can be integrated into the flood loss evaluation; thus, the stage has answered **RQ 3**.

Documenting comprehensive disaster losses and impacts will facilitate governments to measure and quantify the socioeconomic costs of recurrent disasters (ESCAP and UNISDR, 2012). The previous multi-events performed in the tidal flood simulation provide a valuable benchmark to perceive the significant impact of flooding in the past and estimate the economic damage. The extreme tidal events in 2016 and 2018's monetary loss have been quantified by using coupled geospatial datasets and indigenous knowledge of local farmers. This approach, implemented in subchapter 4.2.3, uncovers approximately IDR 74.11 x

10^9 and IDR 13.79 x 10^9 of loss that represents around 5.37% and 8.1% of the total value (**RQ 5**). Both values have been summarized based on 10,721 individual salt parcels affected by tidal submersion. However, there is no official record of loss from the local authority.

6.2.3. Objective 3: Evaluating risk on salt farming towards tidal flooding by using geospatial data

In order to examine the flood risk, the previous physical-based approach has been compared to the GIS parametric method (**RQ 4**). This objective has been initiated to deal with limited data records required in a numerical model. The parametric approach is usually practiced with a coastal vulnerability assessment (CVA) with various types of land use, although this current dissertation has applied the assessment in the single land use with a combination of several available data layers (see subchapter 5.4.1). This approach is also highly recommended for policy-makers regarding its simplicity and operation in flood management and adaptation planning (Balica *et al.*, 2013). The physical-based approach has shown relatively consistent results with the parametric approach. In this regard, two approaches were capable of exposing the risk in salt farming caused by a tidal event at two different stages of production.

Hazard assessment in this thesis establishes initial improvement by involving the timing of flooding (H_3) in the parametric approach. Here, the study interprets salt production as a seasonal activity that occurs in the dry season, while tidal flooding hazards could lead to the disruption of the farming activity. Corresponding to **RQ 5**, the hazard maps shown in *Figure 6.6* portrayed that in 2016, most of the salt pond in the on-site study of Cirebon has faced very high tidal flood hazards, especially in the east part and middle part, while the west part has faced a relatively medium level. Furthermore, the 2016 case also demonstrates that flooding also occurs in the harvesting period where, mainly, salt farmers harvest raw salt and receive revenue in the market transaction. The tidal flood event had directly reduced the income of local farmers, as no salt could be collected during the inundation. In the 2018 case, the hazard level increased, especially in the west part, to a high level towards the escalation of flood depth and duration. Meanwhile, the timing of flooding has a relatively lower score as it happened in the construction period. Both events have shown the tidal hazard dynamic in Cirebon that also can possibly happen in the following years. In addition, this activity confronts extreme weather anomalies, uncertain prices, and obscured policy (Helmi and Sasaoka, 2018).

Subchapter 5.2 has presented both hazard and vulnerability indicators into MCA formulation that includes nine parameters of two components as input to GIS analysis. In addition, AHP-GIS that were exercised in the current research shows that all selected experts underline that the vulnerability (V) aspect has a greater impact on the tidal flood risk upon salt farming land than the hazard (H). In addition, flood duration (H_2) was agreed to be the main contributor to hazard parameters. The justification of all parameters and indicators are reflected in the risk (R) formulation (see subchapter 5.3). Through this formula, it found the distance to the channel (V_5) in the vulnerability aspect (**RQ 6**). Tidal flooding has occurred frequently in the coastal areas, especially along the northern coast of

Java, where seawater also probes the salt pond through a connected channel. The inundation affects the crystallization process and, at a certain level, will melt the formed salt brine. Some other parameters, such as slope, geology features, soil types, and topography condition, have relatively less contribution to the vulnerability aspect for salt farming.

In the vulnerability map, as can be seen in previous *Figure 5.7*, the study reveals that most of the salt ponds in Cirebon are situated in an area of very high vulnerability for tidal flooding. In the current study, it is shown that most of the vulnerable areas are also connected to the nearest channel location and ocean. Furthermore, there is still no adequate structural protection established to defend the traditional salt pond from extreme tide until the present. In many cases, farmers have to face the hazardous condition against the high tide and halt production during flooding, especially in the harvesting period. However, some farmers also try to transfer the packed salt to higher locations, including along the street or even in their houses. The following problem from the inundated water was also the declining quality of the product due to high moisture. Within this situation, the suffering farmers have to arrange additional efforts to restore the collected salt until it is ready to sell on the market. All processes have mostly increased the cost together with the pond cleaning and dike reparation that are still uncovered in the current dissertation.

In the final part, this thesis firstly evaluates tidal flood risks on salt farming on behalf of the two recorded events by propagating both the hazard (H) and vulnerability (V)'s evaluated scores. These combined layers have highlighted at least 20-30% of the salt farming areas that were categorized from high to very high (see subchapter 5.3), based on prior experts' judgment in the AHP process. Secondly, based on the risk score calculation in the parametric approach, the correlation gives valuable feedback to prior damage estimation that contains cost and revenue (C/R). Here, to answer **RQ 7**, these approaches showed that both risk score and economic loss were strongly correlated. However, Chen, Li, & Chen (2021) suggested that the flood risk value is not always parallel with economic loss. Therefore, this thesis assesses both loss and risk that is significant to set priority in flood prevention as well as resource allocation. However, in many cases, the capacity of society in many studies is also considered a significant aspect to reduce the risk in a particular region or community (Cardona *et al.*, 2012; Hillmann *et al.*, 2015; Kantamaneni *et al.*, 2019).

6.3. The Methodological Contribution

6.3.1. Improving tidal flood simulation and mapping by coupling hydrodynamic model and GIS for coastal salt farming

The sole use of the hydrodynamic model (HDM) has been acknowledged as one of the essential tools in flood modeling (Vu and Ranzi, 2017; Yang *et al.*, 2002). GIS has given researchers an opportunity to integrate risk components, including hazard, exposure, and vulnerability, and display the spatial distribution of risk into a map (Rincón *et al.*, 2018). Combining a hydrodynamic model and GIS is a way to examine overall impacts of floods, including their extents, depths, and related damage in different periods (Yang *et al.*, 2002). These inputs can be integrated into flood risk evaluation. The current study also responds to

proposals to expose the impact of flooding in different types of agriculture and rural activities, regarding its oversimplified and relatively low-estimated monetary damage (Brémond and Grelot, 2013; Forster *et al.*, 2008; Merz *et al.*, 2010).

The study has developed a method in Chapter 3 to assess tidal flood hazards based on a physical-based hydrodynamic model in data-scarce regions. Consequently, there was some methodological improvement in mixing both high-resolution datasets, especially with the input on the hydrodynamic model itself, such as elevation data (DEM) from DEMNAS and bathymetry data from BATNAS. These two-acquired data sets, accessed from BIG, have allowed the simulation of the tidal process in the selected study location. Then, the on-site water level data from the local station has been employed with a 1-hour resolution. Moreover, the 1:15,000 salt parcel in vector format taken from BIG has been useful to specifically address salt farming areas in the flood hazard analysis. The simulation employed DHI MIKE and also employed global data as additional input as well as in the calibration stage. These data sets involve wind data from OGIMET, calibration data from TPXO9 for water elevation (ζ), and velocity (both vertical and horizontal) by using TMD. However, the lack of observed and real-world data to restricting and validate is admitted as one of the limitations of the hydrodynamic approach (Bates, 2004). Ultimately, within available data, addressing salt farms in flood hazard analysis has been encouraged as significant added value in the research.

The presented study works on a local scale and domain only, by using an unstructured triangular grid with a varied range between 2,800 m to 120 m in the MIKE FM module. Although the established methodology is applicable to use smaller sizes, the duration of computation and the hardware requirement limit the operational application. On the other side, this challenge will also arise when simulating broader regions (Seenath *et al.*, 2016). On the positive side, this technique results from the elevation during the highest water level (*HWL*) and its specific time occurrence. This data was relatively challenging to be provided in most conventional bathtub models that mostly rely on a scenario. Then, the HDM files in the study were transferred to GIS, mainly to initiate spatial analysis of tidal flood distribution. The study exploits the use of vector salt parcel data as input in the individual analysis, including for further economic loss analysis and tidal flood risk analysis applied in the following parts.

6.3.2. Using local knowledge to establish DDF in economic loss evaluation

Damage function has been developed in Chapter 4. The damage function integrates the hydrodynamic inputs and local information, where 14 group representatives of salt farmers were involved in the damage assessment. In an agricultural setting, the study has implemented a comparable approach by Win, Zin, Kawasaki, & San (2018) in using the depth and duration of flood in the damage function construction. At the same time, physical vulnerability (PV) was considered a major tangible aspect to evaluate the possible economic loss. The damage function establishment was also successfully extended into different curves based on each production stage in salt farming, namely the pre-production and construction period, harvesting period, and post-production period. These curves (as depicted in previous *Figure 4.5*) also individually portray depth and

duration function at stand-alone curves that can be used simultaneously in the damage formulation. Inspired by a previous review on Brémond & Grelot (2013), this dissertation has finally responded to the necessity of a new approach to address instantaneous damage of flooding that can be observed and mapped.

6.3.3. Bridging perspective gaps between the salt farmers and authorities in addressing flood risk

Balica et al. (2013) has initiated two distinct approaches to examine the general applicability in decision-maker practice on flood risk management. The two approaches comparison, as presented in Chapter 5 of this dissertation, firstly proposes an important mission to disseminate the verified information on flood impact and tidal flood risk level at very fine spatial resolution in salt farming. Within the input of local knowledge in appraising economic loss based on previous events, this model evaluates flood impacts based on farmer perspectives. Secondly, part of this chapter also designates knowledge and expert-based judgment in a parametric approach. This type of approach also involves several data layers in GIS that portray the simplified reality. Both hydrodynamic and GIS are commonly applied in coastal flood vulnerability assessments (Seenath *et al.*, 2016).

In this thesis, the experts examined the selected layers in the tidal flood risk on salt farming. This procedure has been commonly imposed in MCA and involved AHP due to its simplicity and flexibility (de Brito and Evers, 2016). In addition, to implement the AHP, the risk indicators and proxy variables were firstly identified (Hadipour *et al.*, 2020). At the same time, the selected data has also considered the availability for this region. Previous studies have shown limitations on verifying results, including on their hazard or vulnerability maps (Danumah *et al.*, 2016; Elkhrachy, 2015; Gigović *et al.*, 2017). However, the current study has initiated the validation of the composed risk map with simulated historical events. As explained in subchapter 5.4, the AHP risk map has been verified by using a physical-based numerical approach and shows a strong correlation at two different production stages.

6.4. Policy Implications

6.4.1. Disaster risk reduction for salt farming community

Disaster risk reduction (DRR) is an approach to reduce disaster risk, involving several stages before, during, and post-disaster and addressing sustainable goals (Dewi, 2018). The stage includes prevention and hazard identification. The Sendai Framework for Disaster Risk Reduction (SFDRR) priority is to understand the risk as a global target in DRR (Pearson and Pelling, 2015). The significance of understanding disaster risk was also referred to as the top priority for disaster-risk management within evidence-based policymaking and implementation (Kwak, 2017). As a result, the 3rd UN World Conference on DRR (WCDRR) in Sendai 2015 highlighted the significance of "geospatial data, remote sensing technologies and related instruments and strengthening in situ climate data observations" to contribute in noticing disaster risk and effective disaster risk communication (UNISDR, 2015c). This guideline also promoted disaster risk

assessment, mapping, and management, including rural development planning in coastal plain areas. Firstly, the current study promotes the issues of flood mapping and disaster risk assessment in the coastal region, especially in a non-urban area with data-scarce conditions.

Secondly, this thesis contributes to a broader understanding of economic implications in certain communities towards tidally induced flooding. The flooding in the coastal area can have considerably different social implications determined by population distribution, infrastructure, and economic activity along the coastline (Moore and Obradovich, 2020). As mentioned earlier, the recognition of the flood implication in the salt farming area is unavailable. The economic characteristics and the mechanisms of salt farming are relatively fragile to a hydro-meteorological condition, as well as coastal dynamics such as tidal magnitudes. Thus, the localized measures of inundation and the effects of it on coastal communities should be evaluated in different flooding events or scenarios (Hino *et al.*, 2019; Merz *et al.*, 2010). In this case, the flood threshold can also be noticeable through the local tidal gauges or from computer simulation. In salt farming, tidal flooding has disrupted the production activity, although at a minor economic level (as can be read in subchapter 4.2.3). Previous numerical simulations and GIS presented in the study were proven to be useful in addressing the data limitation in rural areas. This finding gives awareness for further policy advancement in disaster reduction for non-urban areas, i.e., in salt farming towards tidal flooding.

In addition, sea-level rise as an impact of global warming has been noticed and projected to be more severe in the upcoming decades (Förster *et al.*, 2011; Neumann *et al.*, 2015; Spencer *et al.*, 2016; Ward, Marfai, *et al.*, 2011). With higher sea levels, the local flooding baseline can be reached faster, even during average high tides (Dahl *et al.*, 2017). This high tide commonly occurs during the new and full moon phase. The mixed gravitational force of the moon (M) and sun (S) during these times gives a greater force on Earth's oceans, and high tides become slightly higher than usual, while low tides are slightly lower (Spanger-Siegfried *et al.*, 2014). In some coastal regions, such as the United States, there has been a study mentioning that the trend of high tide flooding will increase due to the combined effect of SLR and tidal amplitude (Jacobs *et al.*, 2018). However, in Tuvalu, the "king tide" has a submerged coastal area, driven by the tide, the warm-water effect, and oceanic factors (Lin *et al.*, 2014). To be considered, the new release of SLR information from the global study community, such as from the IPCC Assessment Report (AR), provides future sea-level conditions that include climate scenarios (Nicholls *et al.*, 2021). In the recent AR 6, that relative SLR will contribute to the increase in magnitude and frequency of severe coastal floods in a flood plain (IPCC, 2021).

Within the condition mentioned in the previous paragraph, extensive monitoring should be implemented to forecast the next extreme events in the future. This monitoring mainly requires homogenous long-series data with an optimum spatial resolution (Marfai, Almohammad, *et al.*, 2008). In Indonesia, the tide gauge monitoring was started several years ago by BIG and stored in cloud storage that can be accessed for research and forecasting purposes. By combining in situ tide data from local stations, geospatial data from satellites such as TOPEX or Sentinel generation, hydrodynamic model, and GIS, the coastal monitoring,

especially for a non-urban area, can be applied to support DRR and create a policy that accommodates local community. Furthermore, the authority can enhance risk knowledge to such groups as salt farmers with training and preparedness, especially those who are also highly vulnerable to coastal hazards.

6.4.2. Integrated coastal zone planning and management policy

There is currently a global transformation towards more adaptive and integrated mechanisms in flood risk management (Ward *et al.*, 2013). Future challenges of climate change and SLR have triggered nations to develop and apply the integrated policy in coastal zone management programs and target sustainable coastal zones' exploration and exploitation (Vellinga and Klein, 1993). In addition, this integrated policy accommodates local community activities and considers the possible impacts. Furthermore, land use policies integrate the potential of land and water and also conduct structured vulnerability assessment as well as improve the strategy of flood mitigation (Handayani *et al.*, 2020). Hurlimann & March (2012) conclude that land use planning is acknowledged as a superior tool to eliminate extreme weather exposure and sensitivity in a different scenario.

The combined increasing costs and excessive losses and damages among marginal groups drive the urgency of integrative prevention, mitigation, and preparedness in the development policy (De Haen and Hemrich, 2007). As a minority, salt farmers have rarely been involved in integrated land-use planning, as well as mitigation strategies. This thesis has been presented the inherent information of hazard, vulnerability, and risk in coastal areas with salt farming domination to be considered in the integrated planning policy. At a certain point, the current study is also acknowledging the local community information through group representatives to address the tidal flood issue and optimize the data into a damage estimation formula. In the Indonesian context, this valuable procedure has supported the zonation planning of the coastal area and small islands (RZWP3K[9]) in preventive and mitigation action, mainly in the salt farming area.

This study finds the possible integration in a physical-based approach with a common parametric method that is mostly applied in land use planning. This approach involves the fundamental identification of land characteristics, which is described into several thematic layers (slope, soil type, geological type, etc.). The expert judgment of each parameter in AHP-GIS can also be implemented based on available data in the region. Otherwise, the damage function can be applied by using mainly input from tidal flood depth and duration information. Therefore, this economic loss data can be standardized and stored as a baseline for natural disaster risk management (Châu, 2014). Ultimately, the study has measured the risk of salt farming towards tidal flooding, especially during the construction period (January-May) and harvesting period (June-October). For this reason, addressing the previous two events should lead the coastal planning within the involvement of structural measures such as breakwater

[9] *Rencana Zonasi Wilayah Pesisir dan Pulau-Pulau Kecil (RZWP3K)* is regulated through Indonesia Law No. 27 -of 2007 about on Management of Coastal Area and Small Islands. Government Regulation Number 64 of 2010 was prepared to regulate disaster mitigation in planning the management of coastal areas and small islands, mitigation of activities that have the potential to cause damage to coastal areas and small islands, as well as the responsibilities of the Government, local governments, and the local community.

structure, groin, and sluice gate (see *Figure 6.1a-c*). Moreover, a soft engineering approach has started to be used, such as mangroves plantation reducing tidal wave destruction during high tide and restoring the coastal ecosystem (as depicted in *Figure 6.1d*). The study also specifically proposes a detailed risk map as one of the effective non-engineering approaches in flood control and disaster mitigation (Zhong *et al.*, 2014).

Figure 6.1. Coastal protection measures in a coastal area of Cirebon, including (a) breakwater (taken from Rawaurip village); (b) groin structure in Gebang district; (c) water sluice gate (photo credit: radarcirebon.com, 2018); and mangrove plant surrounding the pond (captured in Suranenggala district)

6.4.3. Salt self-sufficiency commitment and possible disruption due to tidal flooding

The demand for salt has been rising as the population and industries increase. As mentioned earlier, salt is not only used for food, but it is also used for an additional compound in manufactures; thus, the availability of this substance is crucial for operational sustainability. The possible implication of the scarcity of salt in the market due to uncertain climate and flooding occurrence in the salt center could lead to the following crisis of those industries. Meanwhile, in some industries, salt is categorized as unsubstituted material and needs to be fulfilled (Dharmayanti *et al.*, 2013). In the Indonesia context, the salt commodity is ruled by a national institution to maintain its stock in the market, while at the same side, the farmers are encouraged to increase the quantity and quality of the product (Herman *et al.*, 2014). Furthermore, Regulation No. 9 of 2018 on the Procedures for Fishery and Salt Commodities and Regulation 92/2018 has regulated the issuance of a permit for the importation of the salt commodity that requires the salt database, including available salt stock, future product forecasting, and

possible disruption during the production period. Following the salt self-sufficiency task of the central government, the study proposes initial data and methods to estimate the salt stock and impact on tidal flooding events. The findings of this thesis could lead the authority, especially the Ministry of Marine and Fisheries, as salt farming custodians and its product to engage the tidal flooding issue in the road map of the salt self-sufficiency program together with the technology implementation and human capacity improvement.

Currently, almost 70% of traditional salt farming is mainly located in Java Island (Susanto *et al.*, 2015), as a hotspot of coastal flooding, land subsidence, and SLR. Salt self-sufficiency targets should also address the disaster risk in the coastal area as an epicenter of salt farming activities. Salt farming could also apply a low-risk technology transition (Maflahah and Asfan, 2020). This transformation has reduced land and weather condition dependency, and at the same time, increased productivity. Currently, some technical advancements, including the current geomembrane HDPE plastic and greenhouse prism technology, can be applied with modification to local conditions (as can be seen in the below *Figure 6.2*). These technologies have been established in many places in Indonesia, such as Lamongan (Guntur *et al.*, 2018; Kurniawan *et al.*, 2019), Tuban (Jaziri *et al.*, 2019), and Sumenep (Indrawati and Yuwana, 2019). To increase the income, the local farmers can also invest in *Artemia sp.*, which has been applied to improve the quality of salt effectively (Anh, 2011; Tackaert and Sorgeloos, 1993).

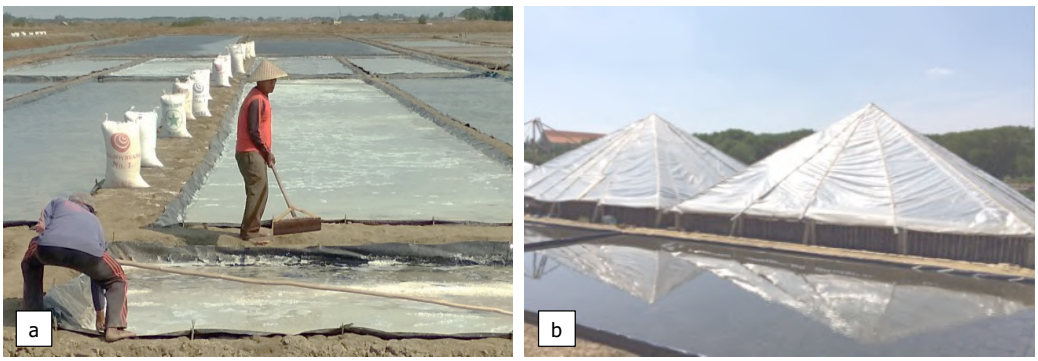

Figure 6.2. Current technology applied in Indonesian salt farming, including (a) geomembrane HDPE plastic (taken from Kapetakan district); and (b) greenhouse prism structure for weather-proved salt production utilized in Lamongan, East Java (photo credit: Kurniawan et al., 2019).

6.5. Limitations and Recommendations for The Future Research

The research findings presented in this dissertation have several limitations discussed in the following section. Here, this thesis also submits some proposals for future scientific research.

First, complex hydrodynamic models require several data sets, including the bottom friction value as defined by Manning's coefficient. In this case, the current study applies a compromised value of 32 m $^{1/3}$/s due to the limitation of data (Elsaesser *et al.*, 2010). At some points, this score will affect the flow path and peak time of flooding in the simulation. Thus, this setting of the score can influence the water run-up simulation. On the other side, this numerical model also requires a high resolution of elevation data provided by DEMNAS. It should be noticed that the purchased topography data cannot truly represent the

condition of salt farming land in Cirebon and its features. In this regard, the possible use of LiDAR screening can improve the visualization of detailed topographical features.

Second, this current study predominantly relies on pixel size as a geometric component. As presented in subchapter 4.1.1, the study employs 25-m spatial resolution to visualize tidal flood mapping on salt farming areas in Cirebon, West Java. Through a higher spatial resolution, future studies may support the tidal flood modeling on salt farming in greater detail and cover several regions that use a smaller pond size. In this thesis, the salt parcel data from BIG was utilized for vector-based flood analysis. On the other hand, it is open to integrating an object-based image analysis (OBIA) to rationalize the salt pond for the latest update condition (Blaschke, 2010). Furthermore, the updating data of salt parcels needs to anticipate the dynamic in the coastal process, including erosion occurrence that may affect the salt farming existences. Nonetheless, in the current study area, the sedimentation process tends to dominate the coastal processes (Khadijah *et al.*, 2020).

Third, this study has examined the background for an in-depth investigation of economic loss determinants in the context of salt farming. Here, the study expects homogenous conditions of salt production practice in the typical traditional "*Maduranese method*" as already described in subchapter 4.1.3. However, some farmers may have been practicing different techniques such as the "*Portuguese method*," including to use the HDPE geomembrane and other advanced technology that may affect C/R variables, as well as the productivity standard applied for this study. Furthermore, the study involved a small sample representative and ignored the category of salt farmers based on their ownership of land in the DDF designation. In the context of pricing, the study also employs local standardized prices that cannot fully be incorporated in the direct market transaction, including interrelation between farmers and intermediaries. Finally, the study mainly focuses on direct instantaneous damage assessment of tidal flooding that affects salt production. As mentioned in subchapter 4.3, other indirect impacts were possible to evaluate after the events, including disruption of other infrastructures such as roads, warehouses, or even collected salt stocks (Brémond and Grelot, 2013; Molinari *et al.*, 2019). Further research could also extend the model with different price and flood scenarios and possibly add the SLR rate and also land subsidence sequence in this particular region.

Fourth, this dissertation involves a parametric approach that consists of selected indicators representing each hazard and vulnerability. These selected indicators were employed according to their structure, representativeness, applicability, and quantifiability (Cai *et al.*, 2019). In addition, the AHP was taken in order to examine the weighting of each component and indicator. Previous studies have involved AHP with all its strengths and benefits; however, there are several potential methods in MCA that might be able to be implemented, including Analytic Network Process (ANP) and the technique for order preference by similarity to the ideal solution (TOPSIS) (de Brito *et al.*, 2019). In addition, those techniques require experts during the assessment process. Related to this, the current study has employed four experts due to their relevant expertise and experience in salt farming. All experts consist of mostly government officers and academics, with no participation from NGOs or private sectors. Furthermore,

future studies should involve more participants from the government, especially from disaster risk management authorities and also stakeholders, such as insurance companies, to comprehend the risk analysis.

References for Chapter 1, 2 and 6

Addo, K.A., Larbi, L., Amisigo, B. and Ofori-Danson, P.K. (2011), "Impacts of coastal inundation due to climate change in a CLUSTER of urban coastal communities in Ghana, West Africa", Remote Sensing, Vol. 3 No. 9, pp. 2029–2050.

Adelekan, I.O. (2010), "Vulnerability of poor urban coastal communities to flooding in Lagos, Nigeria", Environment and Urbanization, Vol. 22 No. 2, pp. 433–450.

Adelekan, I.O. and Asiyanbi, A.P. (2016), "Flood risk perception in flood-affected communities in Lagos, Nigeria", Natural Hazards, Springer Netherlands, Vol. 80 No. 1, pp. 445–469.

Anh, N.T.N. (2011), Optimisation of Artemia Biomass Production in Salt Ponds in Vietnam and Use as Feed Ingredient in Local Aquaculture, University of Gent, Ghent University.

Apel, H., Aronica, G.T., Kreibich, H. and Thieken, A.H. (2009), "Flood risk analyses - How detailed do we need to be?", Natural Hazards, Vol. 49 No. 1, pp. 79–98.

Apel, H., Thieken, A.H., Merz, B. and Blöschl, G. (2006), "A probabilistic modelling system for assessing flood risks", Natural Hazards, Vol. 38 No. 1–2, pp. 79–100.

Apriani, M., Hadi, W. and Masduqi, A. (2018), "Physicochemical properties of sea water and bittern in Indonesia: Quality improvement and potential resources utilization for marine environmental sustainability", Journal of Ecological Engineering, Vol. 19 No. 3, pp. 1–10.

Baky, M.A. Al, Islam, M. and Paul, S. (2020), "Flood Hazard, Vulnerability and Risk Assessment for Different Land Use Classes Using a Flow Model", Earth Systems and Environment, Springer International Publishing, Vol. 4 No. 1, pp. 225–244.

Balica, S.F.F., Popescu, I., Beevers, L. and Wright, N.G.G. (2013), "Parametric and physically based modelling techniques for flood risk and vulnerability assessment: A comparison", Environmental Modelling and Software, Elsevier Ltd, Vol. 41, pp. 84–92.

Bates, P.D. (2004), "Remote sensing and flood inundation modelling", Hydrological Processes, Vol. 18 No. 13, pp. 2593–2597.

Bates, P.D., Neal, J., Sampson, C., Smith, A. and Trigg, M. (2017), Progress Toward Hyperresolution Models of Global Flood Hazard, Risk Modeling for Hazards and Disasters, Elsevier Inc., available at: https://doi.org/10.1016/B978-0-12-804071-3.00009-4.

Bhakta Shrestha, B., Sawano, H., Ohara, M., Yamazaki, Y. and Tokunaga, Y. (2019), "Methodology for Agricultural Flood Damage Assessment", Recent Advances in Flood Risk Management, Vol. i, IntechOpen, p. 13.

Birkmann, J. (2006), "Measuring vulnerability to promote disaster-resilient societies: Conceptual frameworks and definitions", Measuring Vulnerability to Natural Hazards; Towards Disaster Resilient Societies, Vol. 01, pp. 9–54.

Blaschke, T. (2010), "Object based image analysis for remote sensing", ISPRS Journal of Photogrammetry and Remote Sensing, Elsevier B.V., Vol. 65 No.

1, pp. 2–16.
Bott, L.-M. (2020), Living with Sea Level Change and Coastal Flooding -- Collective Responses of Households and Communities in Indonesia, University of Cologne, available at: https://kups.ub.uni-koeln.de/10541/1/Bott_Dissertation_2020.pdf.
Böttle, M. (2016), Coastal Floods in View of Sea Level Rise : Assessing Damage Costs and Adaptation Measures, University of Potsdam, available at: https://publishup.uni-potsdam.de/frontdoor/index/index/docId/9107.
BPS Cirebon. (2020), Cirebon Regency in Figure, edited by BPS-Statistics of Cirebon Regency, BPS-Statistics of Cirebon Regency, Cirebon.
Brémond, P. and Grelot, F. (2010), "Comparison of a systemic modelling of farm vulnerability and classical methods to appraise flood damage on agricultural activities", Advancing Sustainability in a Time of Crisis. 11th Biennal Conference of the International Society for Ecological Economics, No. August 2010, pp. 22–25.
Brémond, P. and Grelot, F. (2013), "Review Article: Economic evaluation of flood damage to agriculture - Review and analysis of existing methods", Natural Hazards and Earth System Sciences, Vol. 13 No. 10, pp. 2493–2512.
Brito, M.M. De. (2018), A Participatory Multi-Criteria Approach for Flood Vulnerability Assessment, University of Bonn.
de Brito, M.M., Almoradie, A. and Evers, M. (2019), "Spatially-explicit sensitivity and uncertainty analysis in a MCDA-based flood vulnerability model", International Journal of Geographical Information Science, Vol. 8816, available at:https://doi.org/10.1080/13658816.2019.1599125.
de Brito, M.M. and Evers, M. (2016), "Multi-criteria decision-making for flood risk management: a survey of the current state of the art", Natural Hazards and Earth System Sciences, Vol. 16 No. 4, pp. 1019–1033.
De Brito, M.M., Evers, M. and Delos Santos Almoradie, A. (2018), "Participatory flood vulnerability assessment: A multi-criteria approach", Hydrology and Earth System Sciences, Vol. 22 No. 1, pp. 373–390.
Budiyono, Y. (2018), Flood Risk Modeling in Jakarta Development: Development and Usefulness in a Time of Climate Change, Vrije Universiteit Amsterdam, Amsterdam.
Bui, D.T., Ngo, P.T.T., Pham, T.D., Jaafari, A., Minh, N.Q., Hoa, P.V. and Samui, P. (2019), "A novel hybrid approach based on a swarm intelligence optimized extreme learning machine for flash flood susceptibility mapping", Catena, Elsevier, Vol. 179 No. March, pp. 184–196.
Cabrera and Lee. (2019), "Flood-Prone Area Assessment Using GIS-Based Multi-Criteria Analysis: A Case Study in Davao Oriental, Philippines", Water, Vol. 11 No. 11, p. 2203.
Cai, T., Li, X., Ding, X., Wang, J. and Zhan, J. (2019), "Flood risk assessment based on hydrodynamic model and fuzzy comprehensive evaluation with GIS technique", International Journal of Disaster Risk Reduction, Elsevier Ltd, Vol. 35 No. February, p. 101077.
Cardona, O.-D., van Aalst, M.K., Birkmann, J., Forndham, M., McGregor, G., Perez, R., Pulwarty, R.S., et al. (2012), Determinants of Risk: Exposure and Vulnerability, Managing the Risks of Extreme Events and Disasters to Advance Climate Change Adaptation - A Special Report of Working Groups I

and II of the Intergovernmental Panel on Climate Change (IPCC), Cambridge, available at: https://www.ipcc.ch/site/assets/uploads/2018/03/SREX-Chap2_FINAL-1.pdf.
Castree, N. (2005), "The epistemology of particulars: Human geography, case studies and 'context'", Geoforum, Vol. 36 No. 5, pp. 541–544.
Chakraborty, S. and Mukhopadhyay, S. (2019), "Assessing flood risk using analytical hierarchy process (AHP) and geographical information system (GIS): application in Coochbehar district of West Bengal, India", Natural Hazards, Springer Netherlands, Vol. 99 No. 1, pp. 247–274.
Châu, V.N. (2014), Assessing the Impacts of Extreme Floods on Agriculture in Vietnam: Quang Nam Case Study, Massey University, New Zealand, available at: https://mro.massey.ac.nz/handle/10179/6250.
Chau, V.N., Cassells, S. and Holland, J. (2015), "Economic impact upon agricultural production from extreme flood events in Quang Nam, central Vietnam", Natural Hazards, Vol. 75 No. 2, pp. 1747–1765.
Chen, Y., Li, J. and Chen, A. (2021), "Does high risk mean high loss: Evidence from flood disaster in southern China", Science of The Total Environment, Elsevier B.V., Vol. 785 No. 15, p. 147127.
CRED, EM-DAT and UNDRR. (2021), 2020 The Non-COVID Year in Disasters: Global Trends and Perspectives, Brussels, available at: https://emdat.be/sites/default/files/adsr_2020.pdf.
CRED and UNDRR. (2020), Human Cost of Disasters: An Overview of the Last 20 Years 2009-2019, Brussels, available at: https://cred.be/sites/default/files/CRED-Disaster-Report-Human-Cost2000-2019.pdf.
Cutter, S.L., Boruff, B.J. and Shirley, W.L. (2003), "Social vulnerability to environmental hazards", Social Science Quarterly, Vol. 84 No. 2, pp. 242–261.
Dahl, K.A., Fitzpatrick, M.F. and Spanger-Siegfried, E. (2017), "Sea level rise drives increased tidal flooding frequency at tide gauges along the U.S. East and Gulf Coasts: Projections for 2030 and 2045", edited by Schumann, G.J.-P. PLOS ONE, Vol. 12 No. 2, p. e0170949.
Dano, U., Balogun, A.-L., Matori, A.-N., Wan Yusouf, K., Abubakar, I., Said Mohamed, M., Aina, Y., et al. (2019), "Flood Susceptibility Mapping Using GIS-Based Analytic Network Process: A Case Study of Perlis, Malaysia", Water, Vol. 11 No. 3, p. 615.
Danumah, J.H., Odai, S.N., Saley, B.M., Szarzynski, J., Thiel, M., Kwaku, A., Kouame, F.K., et al. (2016), "Flood risk assessment and mapping in Abidjan district using multi-criteria analysis (AHP) model and geoinformation techniques, (cote d'ivoire)", Geoenvironmental Disasters, Geoenvironmental Disasters, Vol. 3 No. 1, available at: https://doi.org/10.1186/s40677-016-0044-y.
Dassanayake, D.R., Burzel, A. and Oumeraci, H. (2015), "Methods for the Evaluation of Intangible Flood Losses and Their Integration in Flood Risk Analysis", Coastal Engineering Journal, Vol. 57 No. 1, pp. 1540007-1-1540007–35.
Davis, J. (2000), "Structure, function, and management of the biological system for seasonal solar saltworks", Global Nest, Vol. 2 No. 3, pp. 217–226.
Development Planning Board. (2014), Middle Term of Development Plan, Cirebon, available at: http://bappeda.cirebonkab.go.id/wp-

content/uploads/2015/11/Dokumen-Final-RPJMD-2014-2019.pdf.
Dewan, A. (2013), Floods in a Megacity, Springer Netherlands, Dordrecht, available at: https://doi.org/10.1007/978-94-007-5875-9.
Dewi, R.S. (2018), Multitemporal Image Analysis for Monitoring Fuzzy Shorelines, University of Twente, Enschede, The Netherlands, 4 January, available at: https://doi.org/10.3990/1.9789036546331.
Dharmayanti, S., Suharno and Rifin, A. (2013), "Analysis of Salt Availability Towards Sustainable National Salt Self- Sufficiency Achievement (A Dynamic Model Approach)", Jurnal Sosial Ekonomi Kelautan Dan Perikanan., Vol. 8 No. 1, pp. 103–115.
DHI Water and Environment. (2017), Mike 21 Flow Model FM, Hydrodynamic Module User Guide, DHI Water and Environment, Denmark, available at: https://www.mikepoweredbydhi.com/.
Didier, D., Baudry, J., Bernatchez, P., Dumont, D., Sadegh, M., Bismuth, E., Bandet, M., et al. (2018), "Multihazard simulation for coastal flood mapping: Bathtub versus numerical modelling in an open estuary, Eastern Canada", Journal of Flood Risk Management, Vol. 12 No. March 2019, pp. 1–19.
Durand, J.R. and Petit, D. (1995), "The Java Sea Environment", in Nurhakim, S. (Ed.), Biodynex: Biology, Dynamics and Exploitation of the Small Pelagig Fishes in the Java Sea, Agency for Agricultural Research and Development, Jakarta, pp. 15–38.
Dutta, D., Herath, S. and Musiake, K. (2003), "A mathematical model for flood loss estimation", Journal of Hydrology, Vol. 277 No. 1–2, pp. 24–49.
Elkhrachy, I. (2015), "Flash Flood Hazard Mapping Using Satellite Images and GIS Tools: A case study of Najran City, Kingdom of Saudi Arabia (KSA)", The Egyptian Journal of Remote Sensing and Space Science, Authority for Remote Sensing and Space Sciences, Vol. 18 No. 2, pp. 261–278.
Elsaesser, B., Bell, A.K., Shannon, N. and Robinson, C. (2010), "Storm surge hind-and forecasting using Mike21FM-Simulation of surges around the Irish Coast", Proceedings of the International MIKE by DHI Conference--Modelling in a World of Change, Copenhagen, Denmark. See Http://Www. Dhisoftware. Com/GlobalEvents/PastMajorEvents/MIKEByDHI2010/PresentationsAndPapers. Aspx (Accessed 17/01/2013), No. January 2017.
ESCAP and UNISDR. (2012), The Asia-Pacific Disaster Report 2012: Reducing Vulnerability and Exposure to Disasters, Bangkok, available at: http://www.unescap.org/publications/detail.asp?id=1512.
Fernandez, P., Mourato, S. and Moreira, M. (2016), "Social vulnerability assessment of flood risk using GIS-based multicriteria decision analysis. A case study of Vila Nova de Gaia (Portugal)", Geomatics, Natural Hazards and Risk, Taylor & Francis, Vol. 7 No. 4, pp. 1367–1389.
Förster, H., Sterzel, T., Pape, C.A., Moneo-Lain, M., Niemeyer, I., Boer, R. and Kropp, J.P. (2011), "Sea-level rise in Indonesia: On adaptation priorities in the agricultural sector", Regional Environmental Change, Vol. 11 No. 4, pp. 893–904.
Forster, S., Kuhlmann, B., Lindenschmidt, K.E. and Bronstert, A. (2008), "Assessing flood risk for a rural detention area", Natural Hazards and Earth System Science, Vol. 8 No. 2, pp. 311–322.

GFDRR. (2010), Disaster Damage, Loss and Needs Assessment: Training Guidelines, No. 53002, Dhaka, available at: http://documents.worldbank.org/curated/en/816981467998808920/pdf/530020WP0P110410Box345586B01PUBLIC1.pdf.

Ghosh, A. and Kar, S.K. (2018), "Application of analytical hierarchy process (AHP) for flood risk assessment: a case study in Malda district of West Bengal, India", Natural Hazards, Springer Netherlands, Vol. 94 No. 1, pp. 349–368.

Gigović, L., Pamučar, D., Bajić, Z. and Drobnjak, S. (2017), "Application of GIS-Interval Rough AHP Methodology for Flood Hazard Mapping in Urban Areas", Water, Vol. 9 No. 6, p. 360.

Gilard, O. (2016), "Hazards, Vulnerability and Risk", Climate Change and Agriculture Worldwide, Springer Netherlands, Dordrecht, pp. 19–29.

Glaz, B. and Lingle, S.E. (2012), "Flood Duration and Time of Flood Onset Effects on Recently Planted Sugarcane", Agronomy Journal, Vol. 104 No. 3, pp. 575–583.

Godfrey, A., Ciurean, R.L., van Westen, C.J., Kingma, N.C. and Glade, T. (2015), "Assessing vulnerability of buildings to hydro-meteorological hazards using an expert-based approach - An application in Nehoiu Valley, Romania", International Journal of Disaster Risk Reduction, Elsevier, Vol. 13, pp. 229–241.

Goepel, K.D. (2013), "Implementing the Analytic Hierarchy Process as a Standard Method for Multi-Criteria Decision Making in Corporate Enterprises – a New AHP Excel Template with Multiple Inputs", Proceedings of the International Symposium on the Analytic Hierarchy Process, Vol. 2, pp. 1–10.

Green, J.A.M., Bowers, D.G. and Byrne, H.A.M. (2018), "A mechanistic classification of double tides", Ocean Science Discussions, Vol. 1 No. June, pp. 1–15.

Guntur, G., Jaziri, A.A., Prihanto, A.A., Arisandi, D.M. and Kurniawan, A. (2018), "Development of salt production technology using prism greenhouse method", IOP Conference Series: Earth and Environmental Science, Vol. 106 No. 1, available at: https://doi.org/10.1088/1755-1315/106/1/012082.

Hadipour, V., Vafaie, F. and Deilami, K. (2020), "Coastal flooding risk assessment using a GIS-based spatial multi-criteria decision analysis approach", Water (Switzerland), Vol. 12 No. 9, available at: https://doi.org/10.3390/W12092379.

De Haen, H. and Hemrich, G. (2007), "The economics of natural disasters: Implications and challenges for food security", Agricultural Economics, Vol. 37 No. S1, pp. 31–45.

Haigh, I.D. (2017), "Tides and Water Levels", Encyclopedia of Maritime and Offshore Engineering, pp. 1–13.

Handayani, W., Chigbu, U.E., Rudiarto, I. and Surya Putri, I.H. (2020), "Urbanization and increasing flood risk in the Northern Coast of Central Java-Indonesia: An assessment towards better land use policy and flood management", Land, Vol. 9 No. 10, available at: https://doi.org/10.3390/LAND9100343.

Helmi, A. and Sasaoka, M. (2018), "Dealing with socioeconomic and climate-related uncertainty in small-scale salt producers in rural Sampang, Indonesia", Journal of Rural Studies, Vol. 59 No. February, pp. 88–97.

Herman, S., Noor, E. and Mulyadi, D. (2014), "Prediction of The Trend of Crisis Key Factors to Support Policy Formulation of Consumption Salt Trade System in Indonesia", Journal of Information Engineering and Applications, Vol. 4 No. 6, pp. 34–42.

Hillmann, F., Pahl, M., Rafflenbeul, B. and Sterly, H. (2015), Environmental Change, Adaptation and Migration, edited by Hillmann, F., Pahl, M., Rafflenbeul, B. and Sterly, H.Climate Change 2013 - The Physical Science Basis, Vol. 1, Palgrave Macmillan UK, London, available at:https://doi.org/10.1057/9781137538918.

Hino, M., Belanger, S.T., Field, C.B., Davies, A.R. and Mach, K.J. (2019), "High-tide flooding disrupts local economic activity", Science Advances, Vol. 5 No. 2, p. eaau2736.

Hsu, T.-W., Shih, D.-S., Li, C.-Y., Lan, Y.-J. and Lin, Y.-C. (2017), "A Study on Coastal Flooding and Risk Assessment under Climate Change in the Mid-Western Coast of Taiwan", Water, Vol. 9 No. 6, p. 390.

Hurlimann, A.C. and March, A.P. (2012), "The role of spatial planning in adapting to climate change", Wiley Interdisciplinary Reviews: Climate Change, Vol. 3 No. 5, pp. 477–488.

ICCSR. (2010), Scientific Basis: Analysis and Projection of Sea Level Rise and Extreme Weather Event, Jakarta.

Indrawati, S. and Yuwana, L. (2019), "The Development of Modified Prism Green House (PGH) to Form Quality Pure Salt in Rural Nambakor Sumenep, Indonesia", Indian Journal of Science and Technology, Vol. 12 No. 15, pp. 1–6.

IPCC. (2021), Summary for Policymakers. Climate Change 2021: The Physical Science Basis. Contribution of Working Group I to the Sixth Assessment Report of the Intergovernmental Panel on Climate Change, available at: https://www.ipcc.ch/report/ar6/wg1/downloads/report/IPCC_AR6_WGI_SPM.pdf.

Islam, M.N., Malak, M.A. and Islam, M.N. (2013), "Community-based disaster risk and vulnerability models of a coastal municipality in Bangladesh", Natural Hazards, Vol. 69 No. 3, pp. 2083–2103.

Jacobs, J.M., Cattaneo, L.R., Sweet, W. and Mansfield, T. (2018), "Recent and Future Outlooks for Nuisance Flooding Impacts on Roadways on the U.S. East Coast", Transportation Research Record: Journal of the Transportation Research Board, Vol. 2672 No. 2, pp. 1–10.

Jaziri, A.A., Amin, A.A., I, S.M., Setiawan, W., Prihantono, A.A. and Kurniawan, A. (2019), "Preliminary Analysis of A Low-Cost Greenhouse For Salt Production in Tuban, East Java, Indonesia", Nusantara Science and Technology Proceedings, Vol. 2018, Galaxy Science, pp. 309–315.

Jonkman, S.N., Steenbergen, R.D.J.M., Morales-Nápoles, O., Vrouwenvelder, A.C.W.M. and Vrijling, J.K. (2016), "Probabilistic Design: Risk and Reliability Analysis in Civil Enigneering", Delft University of Technology, Delft, available at: https://repository.tudelft.nl/islandora/object/uuid:e53b8dca-a0db-4433-b9f9-

e190a507f99f/datastream/OBJ/download.
Kabenge, M., Elaru, J., Wang, H. and Li, F. (2017), "Characterizing flood hazard risk in data-scarce areas, using a remote sensing and GIS-based flood hazard index", Natural Hazards, Springer Netherlands, Vol. 89 No. 3, pp. 1369–1387.
Kalligeris, N., Winters, M., Gallien, T., Tang, B.-X., Lucey, J. and Delisle, M.-P. (2018), "Coastal Flood Modeling Challenges in Defended Urban Backshores", Geosciences, Vol. 8 No. 12, p. 450.
Kantamaneni, K., Sudha Rani, N.N.V., Rice, L., Sur, K., Thayaparan, M., Kulatunga, U., Rege, R., et al. (2019), "A Systematic Review of Coastal Vulnerability Assessment Studies along Andhra Pradesh, India: A Critical Evaluation of Data Gathering, Risk Levels and Mitigation Strategies", Water, Vol. 11 No. 2, p. 393.
Kappes, M.S., Papathoma-Köhle, M. and Keiler, M. (2012), "Assessing physical vulnerability for multi-hazards using an indicator-based methodology", Applied Geography, Elsevier Ltd, Vol. 32 No. 2, pp. 577–590.
Khadijah, Saraswati, R. and Wibowo, A. (2020), "Coastline Changes On The Coast of Cirebon Using Landsat", edited by Warsito, B., Sudarno and Triadi Putranto, T.E3S Web of Conferences, Vol. 202, p. 15016.
KKP. (2015), Salt Production of Indonesia (in Bahasa), Jakarta, available at: http://statistik.kkp.go.id/sidatik-dev/Berita/Analisis Produksi Garam Indonesia.pdf.
Koropitan, A.F. and Ikeda, M. (2008), "Three-dimensional modeling of tidal circulation and mixing over the Java Sea", Journal of Oceanography, Vol. 64 No. 1, pp. 61–80.
Kreibich, H., Piroth, K., Seifert, I., Maiwald, H., Kunert, U., Schwarz, J., Merz, B., et al. (2009), "Is flow velocity a significant parameter in flood damage modelling?", Natural Hazards and Earth System Science, Vol. 9 No. 5, pp. 1679–1692.
Kron, W. (2005), "Flood Risk = Hazard • Values • Vulnerability", Water International, Vol. 30 No. 1, pp. 58–68.
Kubal, C., Haase, D., Meyer, V. and Scheuer, S. (2009), "Integrated urban flood risk assessment – adapting a multicriteria approach to a city", Natural Hazards and Earth System Science, Vol. 9 No. 6, pp. 1881–1895.
Kurniawan, A., Jaziri, A.A., Prihanto, A.A. and Guntur, G. (2019), "ANALYSIS OF SEA SALT QUALITY FROM THE GREEN HOUSE PRISM METHOD IN SEDAYU LAWAS VILLAGE, LAMONGAN REGENCY, EAST JAVA", Jurnal Kelautan Nasional, Vol. 14 No. 2, pp. 95–102.
Kwak, Y. (2017), "Nationwide Flood Monitoring for Disaster Risk Reduction Using Multiple Satellite Data", ISPRS International Journal of Geo-Information, Vol. 6 No. 7, p. 203.
Larson, M., Hung, N.M., Hanson, H., Sundström, A. and Södervall, E. (2014), "Impacts of Typhoons on the Vietnamese Coastline: A Case Study of Hai Hau Beach and Ly Hoa Beach.", Coastal Disasters and Climate Change in Vietnam: Engineering and Planning Perspectives, pp. 17–42.
Leitold, R. (2020), Private Sector Engagement in Flood Risk Reduction and Climate Change Adaptation –, University of Cologne.
Leksono, A., Atmodjo, W. and Maslukah, L. (2013), "Studi Arus Laut Pada

Musim Barat di Perairan Pantai Kota Cirebon", Jurnal Oseanografi, Vol. 2 No. 2008, pp. 206–213.
Lia, E. (2016), "Puluhan Ribu Ton Garam di Cirebon Tersapu Banjir Rob page-2 : Okezone News", Okezone.Com, available at: https://news.okezone.com/read/2016/06/17/525/1418255/puluhan-ribu-ton-garam-di-cirebon-tersapu-banjir-rob?page=2 (accessed 10 June 2019).
Lin, C.-C., Ho, C.-R. and Cheng, Y.-H. (2014), "Interpreting and analyzing King Tide in Tuvalu", Natural Hazards and Earth System Sciences, Vol. 14 No. 2, pp. 209–217.
Lotsch, A., Dick, W. and Manuamorn, O.P. (2010), Assessment of Innovative Approaches for Flood Risk Management and Financing in Agriculture, No. 71620, Washington DC, available at:https://doi.org/10.1596/27577.
Luu, C. and von Meding, J. (2018), "A flood risk assessment of Quang Nam, Vietnam using spatial multicriteria decision analysis", Water (Switzerland), Vol. 10 No. 4, pp. 1–16.
Luu, C., Von Meding, J. and Kanjanabootra, S. (2018), "Assessing flood hazard using flood marks and analytic hierarchy process approach: a case study for the 2013 flood event in Quang Nam, Vietnam", Natural Hazards, Springer Netherlands, Vol. 90 No. 3, pp. 1031–1050.
Luu, C., Tran, H.X., Pham, B.T., Al-Ansari, N., Tran, T.Q., Duong, N.Q., Dao, N.H., et al. (2020), "Framework of spatial flood risk assessment for a case study in quang binh province, Vietnam", Sustainability (Switzerland), Vol. 12 No. 7, pp. 1–17.
Lyu, H.M., Sun, W.J., Shen, S.L. and Arulrajah, A. (2018), "Flood risk assessment in metro systems of mega-cities using a GIS-based modeling approach", Science of the Total Environment, Elsevier B.V., Vol. 626, pp. 1012–1025.
Maflahah, I. and Asfan. (2020), "Benefit-cost for selecting technology in salt production", IOP Conference Series: Earth and Environmental Science, Vol. 475 No. 1, available at:https://doi.org/10.1088/1755-1315/475/1/012091.
Malczewski, J. (1999), GIS and Multicriteria Decision Analysis, John Wiley & Sons, Inc., Toronto.
Malgwi, M.B., Fuchs, S. and Keiler, M. (2020), "A generic physical vulnerability model for floods: Review and concept for data-scarce regions", Natural Hazards and Earth System Sciences, Vol. 20 No. 7, pp. 2067–2090.
Marfai, M. (2011), "Impact of coastal inundation on ecology and agricultural land use case study in central Java, Indonesia", Quaestiones Geographicae, Vol. 30 No. 3, pp. 19–32.
Marfai, M.A., Almohammad, H., Dey, S., Susanto, B. and King, L. (2008), "Coastal dynamic and shoreline mapping: Multi-sources spatial data analysis in Semarang Indonesia", Environmental Monitoring and Assessment, Vol. 142 No. 1–3, pp. 297–308.
Marfai, M.A. and King, L. (2008), "Tidal inundation mapping under enhanced land subsidence in Semarang, Central Java Indonesia", Natural Hazards, Vol. 44 No. 1, pp. 93–109.
Marfai, M.A., King, L., Sartohadi, J., Sudrajat, S., Budiani, S.R. and Yulianto, F. (2008), "The impact of tidal flooding on a coastal community in Semarang, Indonesia", Environmentalist, Vol. 28 No. 3, pp. 237–248.

Martínez-Graña, A.M., Boski, T., Goy, J.L., Zazo, C. and Dabrio, C.J. (2016), "Coastal-flood risk management in central Algarve: Vulnerability and flood risk indices (South Portugal)", Ecological Indicators, Vol. 71, pp. 302–316.
Mason, J.L. and Kipp Jr., K.L. (1997), Investigation of Salt Loss from the Bonneville Salt Flats , Northwestern Utah, Salt Lake City, Utah, available at: https://pubs.usgs.gov/fs/1997/fs135-97/PDF/FS97-135.pdf.
Merz, B., Kreibich, H., Schwarze, R. and Thieken, A. (2010), "Review article 'Assessment of economic flood damage'", Natural Hazards and Earth System Science, Vol. 10 No. 8, pp. 1697–1724.
Merz, B. and Thieken, A.H. (2009), "Flood risk curves and uncertainty bounds", Natural Hazards, Vol. 51 No. 3, pp. 437–458.
Metrotv. (2016), "700 Hectares of Salt Pond in Cirebon Submerged Coastal Flood (in Bahasa)", Metrotvnews.Com, available at: http://m.metrotvnews.com/jabar/peristiwa/JKR4MYQb-700-hektare-tambak-garam-di-cirebon-terendam-banjir-rob (accessed 29 September 2017).
de Moel, H., van Alphen, J. and Aerts, J.C.J.H. (2009), "Flood maps in Europe - methods, availability and use", Natural Hazards and Earth System Sciences, Vol. 9 No. 2, pp. 289–301.
Moftakhari, H.R., AghaKouchak, A., Sanders, B.F., Allaire, M. and Matthew, R.A. (2018), "What Is Nuisance Flooding? Defining and Monitoring an Emerging Challenge", Water Resources Research, Vol. 54 No. 7, pp. 4218–4227.
Moftakhari, H.R., Aghakouchak, A., Sanders, B.F. and Matthew, R.A. (2017), "Earth's Future Special Section: Cumulative hazard: The case of nuisance flooding Earth' s Future", Earth's Future, No. 5, pp. 214–223.
Molinari, D., Ballio, F., Handmer, J. and Menoni, S. (2014), "On the modeling of significance for flood damage assessment", International Journal of Disaster Risk Reduction, Elsevier, Vol. 10 No. PA, pp. 381–391.
Molinari, D., Scorzini, A.R., Gallazzi, A. and Ballio, F. (2019), "AGRIDE-c, a conceptual model for the estimation of flood damage to crops: development and implementation", Natural Hazards and Earth System Sciences Discussions, pp. 1–24.
Moore, F.C. and Obradovich, N. (2020), "Using remarkability to define coastal flooding thresholds", Nature Communications, Springer US, Vol. 11 No. 1, pp. 1–8.
Mun'im, A. (2015), "Salt Farmers Business Analysis and Its Role in The Economy, 2012 (Case Study: PUGAR Salt Farmers)", Jurnal Sosial Ekonomi Kelautan Dan Perikanan., Vol. 10 No. 2, pp. 217–228.
Munadi, E., Ardiyanti, S.T., Ingot, S.R., Lestari, T.K., Subekti, N.A., Salam, A.R., Alhayat, A.P., et al. (2016), Info Komoditi Garam, edited by Salim, Z. and Munadi, E., Badan Pengkajian dan Pengembangan Perdagangan, Jakarta, available at: http://bppp.kemendag.go.id/media_content/2017/08/Isi_BRIK_Garam.pdf.
Nagara, G.A., Sasongko, N.A. and Olakunle, O.J. (2010), Introduction to Java Sea, Stavanger, available at: https://doi.org/10.1007/978-1-84882-972-5_26.
Nayak, D. and Bajaji, R. (2016), "Numerical modeling of tides , currents and

waves off Maharashtra coast", Indian Journal of Geo-Marine Sciences, Vol. 45 No. October, pp. 1255–1263.
Neubert, M., Naumann, T., Hennersdorf, J. and Nikolowski, J. (2016), "The Geographic Information System-based flood damage simulation model HOWAD", Journal of Flood Risk Management, Vol. 9 No. 1, pp. 36–49.
Neumann, B., Vafeidis, A.T., Zimmermann, J. and Nicholls, R.J. (2015), "Future Coastal Population Growth and Exposure to Sea-Level Rise and Coastal Flooding - A Global Assessment", PLoS ONE, Vol. 10 No. 3, pp. 1–34.
Nguyen, N.Y., Ichikawa, Y. and Ishidaira, H. (2017), "Establishing flood damage functions for agricultural crops using estimated inundation depth and flood disaster statistics in data-scarce regions", Hydrological Research Letters, Vol. 11 No. 1, pp. 12–18.
Nicholls, R.J. and Cazenave, A. (2010), "Sea-level rise and its impact on coastal zones", Science, Vol. 328 No. 5985, pp. 1517–1520.
Nicholls, R.J., Hanson, S.E., Lowe, J.A., Slangen, A.B.A., Wahl, T., Hinkel, J. and Long, A.J. (2021), "Integrating new sea-level scenarios into coastal risk and adaptation assessments: An ongoing process", WIREs Climate Change, Vol. 12 No. 3, pp. 1–27.
Okazumi, T., Tanaka, S., Kwak, Y., Shrestha, B.B. and Sugiura, A. (2014), "Flood vulnerability assessment in the light of rice cultivation characteristics in Mekong River flood plain in Cambodia", Paddy and Water Environment, Vol. 12 No. 2, pp. 275–286.
Olbert, A.I., Comer, J., Nash, S. and Hartnett, M. (2017), "High-resolution multi-scale modelling of coastal flooding due to tides, storm surges and rivers inflows. A Cork City example", Coastal Engineering, Elsevier, Vol. 121 No. December 2016, pp. 278–296.
Papathoma-Köhle, M., Gems, B., Sturm, M. and Fuchs, S. (2017), "Matrices, curves and indicators: A review of approaches to assess physical vulnerability to debris flows", Earth-Science Reviews, Elsevier B.V, Vol. 171 No. 2016, pp. 272–288.
Parodi, M.U. (2019), Investigating Uncertainty in Coastal Flood Risk Assessment in Small Island Developing States A Case Study in São Tomé and Príncipe, TU Delft, available at: repository.tudelft.nl.
Parrott, A., Brooks, W., Harmar, O. and Pygott, K. (2009), "Role of rural land use management in flood and coastal risk management", Journal of Flood Risk Management, Vol. 2 No. 4, pp. 272–284.
Paul, J.D., Buytaert, W., Allen, S., Ballesteros-Cánovas, J.A., Bhusal, J., Cieslik, K., Clark, J., et al. (2018), "Citizen science for hydrological risk reduction and resilience building", WIREs Water, Vol. 5 No. 1, pp. 1–15.
Pearson, L. and Pelling, M. (2015), "The UN Sendai Framework for Disaster Risk Reduction 2015–2030: Negotiation Process and Prospects for Science and Practice", Journal of Extreme Events, Vol. 02 No. 01, p. 1571001.
Picado, A., Dias, J.M. and Fortunato, A.B. (2009), "Effect of flooding the salt pans in the Ria de Aveiro", Journal of Coastal Research, Vol. 2009 No. 2, 56, pp. 1395–1399.
PSSDAL. (2010), Peta Lahan Garam Indonesia, edited by Saputro, G.B., Edrus, I.N., Hartini, S. and Poniman, A., PSSDAL BAKOSURTANAL, Cibinong, available at:

https://perpustakaan.big.go.id/opacbig/index.php?p=show_detail&id=10283.
PT Cirebon Energi Prasarana. (2016), ANDAL: Deskripsi Rinci Rona Lingkungan Hidup Awal, Cirebon.
radarcirebon.com. (2018), "Waspada Rob Susulan, Ini Sebabnya", available at: http://www.radarcirebon.com/waspada-rob-sususlan-ini-sebabnya.html (accessed 26 March 2021).
Raji, O., Del Rio, L., Gracia, F.J. and Benavente, J. (2011), "The use of LIDAR data for mapping coastal flooding hazard related to storms in Cadiz Bay (SW Spain)", Journal of Coastal Research, No. 64, pp. 1881–1885.
Ray, R.D. and Foster, G. (2016), "Future nuisance flooding at Boston caused by astronomical tides alone", Earth's Future, Vol. 4 No. 12, pp. 578–587.
Rentschler, J. and Salhab, M. (2020), People in Harm's Way Flood: Exposure and Poverty in 189 Countries, No. 9447, Washing, available at: https://openknowledge.worldbank.org/handle/10986/34655.
Rey, W., Martínez-Amador, M., Salles, P., Mendoza, E.T., Trejo-Rangel, M.A., Franklin, G.L., Ruiz-Salcines, P., et al. (2020), "Assessing different flood risk and damage approaches: A case of study in progreso, Yucatan, Mexico", Journal of Marine Science and Engineering, Vol. 8 No. 2, p. 137.
Rey, W., Salles, P., Mendoza, E.T., Torres-Freyermuth, A. and Appendini, C.M. (2018), "Assessment of coastal flooding and associated hydrodynamic processes on the south-eastern coast of Mexico, during Central American cold surge events", Natural Hazards and Earth System Sciences, Vol. 18 No. 6, pp. 1681–1701.
Rimba, A., Setiawati, M., Sambah, A. and Miura, F. (2017), "Physical Flood Vulnerability Mapping Applying Geospatial Techniques in Okazaki City, Aichi Prefecture, Japan", Urban Science, Vol. 1 No. 1, p. 7.
Rincón, D., Khan, U. and Armenakis, C. (2018), "Flood Risk Mapping Using GIS and Multi-Criteria Analysis: A Greater Toronto Area Case Study", Geosciences, Vol. 8 No. 8, p. 275.
Rositasari, R., Setiawan, W.B., Supriadi, I.H. and Prayuda, B. (2011), "Coastal Vulnerability Prediction To Climate Change: Study Case in Cirebon Coastal Area", Jurnal Ilmu Dan Teknologi Kelautan Tropis, Vol. 3 No. 1, pp. 52–64.
Roy, D.C. and Blaschke, T. (2015), "Spatial vulnerability assessment of floods in the coastal regions of Bangladesh", Geomatics, Natural Hazards and Risk, Taylor & Francis, Vol. 6 No. 1, pp. 21–44.
Le Roy, S., Pedreros, R., André, C., Paris, F., Lecacheux, S., Marche, F. and Vinchon, C. (2015), "Coastal flooding of urban areas by overtopping: Dynamic modelling application to the Johanna storm (2008) in Gâvres (France)", Natural Hazards and Earth System Sciences, Vol. 15 No. 11, pp. 2497–2510.
Saaty, T.L. (1977), "A scaling method for priorities in hierarchical structures", Journal of Mathematical Psychology, Vol. 15 No. 3, pp. 234–281.
Sadek, M. and Li, X. (2019), "Low-Cost Solution for Assessment of Urban Flash Flood Impacts Using Sentinel-2 Satellite Images and Fuzzy Analytic Hierarchy Process: A Case Study of Ras Ghareb City, Egypt", Advances in Civil Engineering, Vol. 2019 No. May, available at: https://doi.org/10.1155/2019/2561215.

Seenath, A., Wilson, M. and Miller, K. (2016), "Hydrodynamic versus GIS modelling for coastal flood vulnerability assessment: Which is better for guiding coastal management?", Ocean and Coastal Management, Elsevier Ltd, Vol. 120, pp. 99–109.

Seifi, F., Deng, X. and Baltazar Andersen, O. (2019), "Assessment of the Accuracy of Recent Empirical and Assimilated Tidal Models for the Great Barrier Reef, Australia, Using Satellite and Coastal Data", Remote Sensing, Vol. 11 No. 10, p. 1211.

Serinaldi, F., Loecker, F., Kilsby, C.G. and Bast, H. (2018), "Flood propagation and duration in large river basins: a data-driven analysis for reinsurance purposes", Natural Hazards, Springer Netherlands, Vol. 94 No. 1, pp. 71–92.

Setiadi, H.A. (2013), "Identification of Building Damage and Infrastructure Function due to Citarum Flood in Bandung Regency", pp. 51–64.

Shokoohi, A., Ganji, Z., Samani, J.M.V. and Singh, V.P. (2018), "Analysis of spatial and temporal risk of agricultural loss due to flooding in paddy farms", Paddy and Water Environment, Springer Japan, Vol. 16 No. 4, pp. 737–748.

Siddayao, G.P., Valdez, S.E. and Fernandez, P.L. (2014), "Analytic Hierarchy Process (AHP) in Spatial Modeling for Floodplain Risk Assessment", International Journal of Machine Learning and Computing, Vol. 4 No. 5, pp. 450–457.

Simpson, A.L., Balog, S., Moller, D.K., Strauss, B.H. and Saito, K. (2015), "An urgent case for higher resolution digital elevation models in the world's poorest and most vulnerable countries", Frontiers in Earth Science, Vol. 3 No. March 2016, available at: https://doi.org/10.3389/feart.2015.00050.

Souissi, D., Zouhri, L., Hammami, S., Msaddek, M.H., Zghibi, A. and Dlala, M. (2020), "GIS-based MCDM–AHP modeling for flood susceptibility mapping of arid areas, southeastern Tunisia", Geocarto International, Taylor & Francis, Vol. 35 No. 9, pp. 991–1017.

Spanger-Siegfried, E., Fitzpatrick, M. and Dahl, K. (2014), Encroaching Tides: How Sea Level Rise and Tidal Flooding Threaten U.S. East and Gulf Coast Communities over the Next 30 Years, Union of Concerned Scientists, Cambridge.

Spencer, T., Schuerch, M., Nicholls, R.J., Hinkel, J., Lincke, D., Vafeidis, A.T., Reef, R., et al. (2016), "Global coastal wetland change under sea-level rise and related stresses: The DIVA Wetland Change Model", Global and Planetary Change, Elsevier B.V., Vol. 139, pp. 15–30.

Suhendra, Amron, A. and Hilmi, E. (2018), "The pattern of coastline change based on the characteristics of sediment and coastal slope in Pangenan coast of Cirebon, West Java", edited by Prayogo, N.A. and Amron, A.E3S Web of Conferences, Vol. 47, p. 06001.

Susanto, H., Rokhati, N. and Santosa, G.W. (2015), "Development of Traditional Salt Production Process for Improving Product Quantity and Quality in Jepara District, Central Java, Indonesia", International Conference on Tropical and Coastal Region Eco-Development 2014 (ICTCRED 2014), Vol. 23, Elsevier B.V., pp. 175–178.

Suwarno, Y. (2014), "Quickbird imagery for support to mapping of salt land suitability in Kupang bay, East Nusa Tenggara Province - Indonesia", 35th

Asian Conference on Remote Sensing 2014, ACRS 2014: Sensing for Reintegration of Societies, available at: https://www.scopus.com/inward/record.uri?eid=2-s2.0-84925435276&partnerID=40&md5=0d04025f777b49575aea05e87aba5c93.
Tackaert, W. and Sorgeloos, P. (1993), "The use of brine shrimp Artemia in biological management of solar saltworks", Seventh Symposium on Salt, Vol. 1, Elsevier Science Publisher B.V., Amsterdam, pp. 617–622.
Takagi, H., Esteban, M., Mikami, T. and Fujii, D. (2016), "Projection of coastal floods in 2050 Jakarta", Urban Climate, Vol. 17, pp. 135–145.
Takara, K. (2013), "Consideration of Disaster Risk and Floods", Journal of Flood Risk Management, Vol. 6 No. 4, pp. 289–289.
Tehrany, M.S., Pradhan, B., Mansor, S. and Ahmad, N. (2015), "Flood susceptibility assessment using GIS-based support vector machine model with different kernel types", Catena, Elsevier B.V., Vol. 125, pp. 91–101.
Thouret, J.C., Ettinger, S., Guitton, M., Santoni, O., Magill, C., Martelli, K., Zuccaro, G., et al. (2014), "Assessing physical vulnerability in large cities exposed to flash floods and debris flows: The case of Arequipa (Peru)", Natural Hazards, Vol. 73 No. 3, pp. 1771–1815.
Toan, T.Q. (2014), Climate Change and Sea Level Rise in the Mekong Delta: Flood, Tidal Inundation, Salinity Intrusion, and Irrigation Adaptation Methods, Coastal Disasters and Climate Change in Vietnam: Engineering and Planning Perspectives, Elsevier Inc., available at: https://doi.org/10.1016/B978-0-12-800007-6.00009-5.
UNISDR. (2009), 2009 UNISDR Terminology on Disaster Risk Reduction, International Stratergy for Disaster Reduction (ISDR), UNISDR, Geneva, available at: www.unisdr.org/publications.
UNISDR. (2015a), The Human Cost of Weather-Related Disasters 1995-2015, Brussels, available at: https://www.unisdr.org/2015/docs/climatechange/COP21_WeatherDisastersReport_2015_FINAL.pdf.
UNISDR. (2015b), "Proposed Updated Terminology on Disaster Risk Reduction: A Technical Review", No. August, pp. 1–31.
UNISDR. (2015c), Sendai Framework for Disaster Risk Reduction 2015-2030, Geneva, available at: https://www.preventionweb.net/files/43291_sendaiframeworkfordrren.pdf.
Vandenberg-Rodes, A., Moftakhari, H.R., Agha Kouchak, A., Shahbaba, B., Sanders, B.F. and Matthew, R.A. (2016), "Projecting nuisance flooding in a warming climate using generalized linear models and Gaussian processes", Journal of Geophysical Research: Oceans, Vol. 121 No. 11, pp. 8008–8020.
Vanderkimpen, P. and Peeters, P. (2008), "Flood modeling for risk evaluation: a MIKE FLOOD sensitivity analysis", Proceedings of the International Conference on Fluvial Hydraulics, Cesme, Izmir, Turkey, September 3-5, 2008: River Flow 2008, pp. 2335–2344.
Vatsa, K.S. (2004), "Risk, vulnerability, and asset-based approach to disaster risk management", International Journal of Sociology and Social Policy, Vol. 24 No. 10/11, pp. 1–48.
Vellinga, P. and Klein, R.J.T. (1993), "Climate change, sea level rise and integrated coastal zone management: An IPCC approach", Ocean & Coastal

Management, Vol. 21 No. 1, pp. 245–268.
Villagrán de León, J.C. (2006), "Vulnerability: A Conceptual and methodological review", UNU-EHS, Bornheim.
Vozinaki, A.E.K., Karatzas, G.P., Sibetheros, I.A. and Varouchakis, E.A. (2015), "An agricultural flash flood loss estimation methodology: the case study of the Koiliaris basin (Greece), February 2003 flood", Natural Hazards, Springer Netherlands, Vol. 79 No. 2, pp. 899–920.
Vu, T.T. and Ranzi, R. (2017), "Flood risk assessment and coping capacity of floods in central Vietnam", Journal of Hydro-Environment Research, International Association for Hydro-environment Engineering and Research, Asia Pacific Division, Vol. 14, pp. 44–60.
Wang, H., Xu, X. and Zhu, G. (2015), "Landscape changes and a salt production sustainable approach in the state of salt pan area decreasing on the coast of Tianjin, China", Sustainability (Switzerland), Vol. 7 No. 8, pp. 10078–10097.
Wang, Y., Li, Z., Tang, Z. and Zeng, G. (2011), "A GIS-Based Spatial Multi-Criteria Approach for Flood Risk Assessment in the Dongting Lake Region, Hunan, Central China", Water Resources Management, Vol. 25 No. 13, pp. 3465–3484.
Ward, P.J., Marfai, M.A., Yulianto, F., Hizbaron, D.R. and Aerts, J.C.J.H. (2011), "Coastal inundation and damage exposure estimation: a case study for Jakarta", Natural Hazards, Vol. 56 No. 3, pp. 899–916.
Ward, P.J., De Moel, H. and Aerts, J.C.J.H. (2011), "How are flood risk estimates affected by the choice of return-periods?", Natural Hazards and Earth System Science, Vol. 11 No. 12, pp. 3181–3195.
Ward, P.J., Pauw, W.P., van Buuren, M.W. and Marfai, M. a. (2013), "Governance of flood risk management in a time of climate change: the cases of Jakarta and Rotterdam", Environmental Politics, Vol. 22 No. 3, pp. 518–536.
Webster, T.L. (2010), "Flood risk mapping using LiDAR for annapolis Royal, Nova Scotia, Canada", Remote Sensing, Vol. 2 No. 9, pp. 2060–2082.
WHO. (2009), "WHO guidelines for indoor air quality: dampness and mould", WHO Regional Office for Europe, Copenhagen.
Win, S., Zin, W.W., Kawasaki, A. and San, Z.M.L.T. (2018), "Establishment of flood damage function models: A case study in the Bago River Basin, Myanmar", International Journal of Disaster Risk Reduction, Elsevier Ltd, Vol. 28 No. November 2017, pp. 688–700.
Winsemius, H.C., Aerts, J.C.J.H., Van Beek, L.P.H., Bierkens, M.F.P., Bouwman, A., Jongman, B., Kwadijk, J.C.J., et al. (2016), "Global drivers of future river flood risk", Nature Climate Change, Vol. 6 No. 4, pp. 381–385.
Wolf, J. (2009), "Coastal flooding: impacts of coupled wave–surge–tide models", Natural Hazards, Vol. 49 No. 2, pp. 241–260.
Yang, X., Grönlund, A. and Tanzilli, S. (2002), "Predicting Flood Inundation and Risk Using Geographic Information System and Hydrodynamic Model", Geographic Information Sciences, Vol. 8 No. 1, pp. 48–57.
Zalite, K. (2016), Radar Remote Sensing for Monitoring Forest Floods and Agricultural Grasslands, University of Tartu Press, available at: www.tyk.ee.
Zhong, G., Liu, S., Han, C. and Huang, W. (2014), "Urban Flood Maping for Jiaxing City Based on Hydrodynamic Modeling and GIS Analysis", Journal of Coastal Research, Vol. 68 No. 2013, pp. 168–175.

Appendices

Appendix A. Tidal observation for June 2016

TIDAL OBSERVATION ANALYSIS USING LEAST SQUARE

Location
Lokasi : Cirebon
Instrument
Alat : radar gauge, pressure gauge dan float gauge (operated by Badan Informasi Geospasial BIG)
Unit
Satuan : meter
District
Kabupaten : Cirebon
Time Zone from GMT
Zona Waktu. : + 7:00
Period
Periode : June 2016

Day	Date	hour																						
		0:00	1:00	2:00	3:00	4:00	5:00	6:00	7:00	8:00	9:00	10:00	11:00	12:00	13:00	14:00	15:00	16:00	17:00	18:00	19:00	20:00	21:00	22:00	23:00
1	1-sJun-16	0.970	0.970	0.990	1.022	0.835	0.656	0.852	1.063	1.179	1.230	1.284	1.320	1.318	1.252	1.090	0.897	0.738	0.666	0.651	0.673	0.731	0.828	0.942	1.034
2	2-Jun-16	1.071	1.041	0.973	0.902	0.851	0.831	0.852	0.917	1.026	1.162	1.283	1.352	1.350	1.287	1.181	1.040	0.885	0.744	0.655	0.632	0.675	0.759	0.859	0.955
3	3-Jun-16	1.027	1.052	1.026	0.963	0.892	0.841	0.830	0.866	0.945	1.057	1.182	1.286	1.342	1.330	1.262	1.149	1.007	0.861	0.740	0.670	0.658	0.700	0.780	0.879
4	4-Jun-16	0.971	1.032	1.046	1.018	0.963	0.900	0.850	0.838	0.879	0.970	1.084	1.189	1.263	1.294	1.284	1.229	1.124	0.984	0.847	0.747	0.699	0.697	0.733	0.805
5	5-Jun-16	0.899	0.988	1.042	1.049	1.014	0.960	0.908	0.874	0.866	0.889	0.952	1.048	1.148	1.226	1.258	1.237	1.174	1.081	0.971	0.862	0.776	0.726	0.721	0.763
6	6-Jun-16	0.841	0.929	1.005	1.051	1.060	1.032	0.982	0.929	0.887	0.867	0.883	0.936	1.008	1.090	1.164	1.201	1.186	1.130	1.053	0.963	0.875	0.801	0.755	0.750
7	7-Jun-16	0.793	0.870	0.956	1.028	1.076	1.091	1.074	1.036	0.984	0.926	0.884	0.881	0.921	0.983	1.041	1.078	1.094	1.091	1.082	1.046	0.967	0.864	0.781	0.764
8	8-Jun-16	0.798	0.847	0.897	0.965	1.048	1.113	1.130	1.100	1.049	0.999	0.950	0.901	0.860	0.858	0.903	0.975	1.039	1.075	1.081	1.061	1.024	0.967	0.893	0.824
9	9-Jun-16	0.787	0.797	0.848	0.928	1.016	1.098	1.156	1.178	1.159	1.106	1.031	0.947	0.874	0.830	0.825	0.856	0.913	0.978	1.029	1.053	1.048	1.015	0.957	0.887
10	10-Jun-16	0.827	0.799	0.815	0.875	0.967	1.076	1.182	1.252	1.262	1.214	1.130	1.035	0.942	0.856	0.797	0.779	0.808	0.873	0.947	1.004	1.034	1.034	1.004	0.948
11	11-Jun-16	0.881	0.824	0.802	0.829	0.899	0.997	1.102	1.193	1.248	1.258	1.222	1.144	1.036	0.918	0.816	0.759	0.752	0.788	0.855	0.928	0.989	1.026	1.030	0.994
12	12-Jun-16	0.931	0.864	0.819	0.813	0.853	0.931	1.030	1.134	1.223	1.280	1.285	1.229	1.124	0.997	0.877	0.787	0.743	0.737	0.777	0.850	0.931	0.995	1.026	1.019
13	13-Jun-16	0.975	0.913	0.856	0.822	0.830	0.887	0.988	1.100	1.192	1.249	1.270	1.256	1.200	1.096	0.962	0.834	0.750	0.724	0.745	0.798	0.867	0.940	1.000	1.030
14	14-Jun-16	1.012	0.959	0.896	0.847	0.830	0.858	0.925	1.012	1.108	1.198	1.261	1.277	1.235	1.144	1.025	0.903	0.801	0.742	0.726	0.756	0.819	0.895	0.966	1.014
15	15-Jun-16	1.024	0.995	0.945	0.894	0.862	0.862	0.901	0.969	1.055	1.146	1.220	1.256	1.240	1.177	1.077	0.960	0.850	0.772	0.734	0.740	0.783	0.851	0.925	0.987
16	16-Jun-16	1.022	1.017	0.983	0.936	0.898	0.882	0.898	0.945	1.018	1.108	1.187	1.229	1.225	1.178	1.104	1.007	0.902	0.809	0.749	0.735	0.763	0.819	0.887	0.953

17	17-Jun-16	1.003	1.021	1.009	0.974	0.936	0.916	0.931	0.972	1.015	1.059	1.116	1.182	1.221	1.201	1.125	1.022	0.925	0.847	0.790	0.753	0.745	0.778	0.849	0.927
18	18-Jun-16	0.984	1.009	1.009	0.993	0.970	0.946	0.934	0.945	0.982	1.041	1.107	1.161	1.187	1.178	1.133	1.061	0.972	0.882	0.808	0.762	0.749	0.770	0.821	0.886
19	19-Jun-16	0.948	0.992	1.013	1.012	0.992	0.968	0.953	0.956	0.979	1.023	1.078	1.131	1.166	1.171	1.142	1.083	1.005	0.921	0.845	0.789	0.759	0.761	0.796	0.854
20	20-Jun-16	0.917	0.968	1.002	1.015	1.008	0.988	0.971	0.965	0.976	1.005	1.049	1.097	1.136	1.154	1.143	1.103	1.040	0.964	0.889	0.826	0.783	0.767	0.783	0.827
21	21-Jun-16	0.885	0.942	0.987	1.015	1.023	1.011	0.994	0.982	0.982	0.997	1.025	1.059	1.091	1.116	1.126	1.113	1.071	1.007	0.937	0.873	0.823	0.792	0.785	0.808
22	22-Jun-16	0.856	0.915	0.969	1.008	1.030	1.031	1.018	1.001	0.987	0.978	0.982	1.001	1.032	1.065	1.089	1.094	1.076	1.039	0.988	0.931	0.876	0.830	0.805	0.807
23	23-Jun-16	0.838	0.888	0.946	1.000	1.042	1.061	1.056	1.035	1.009	0.984	0.963	0.955	0.966	0.992	1.022	1.045	1.055	1.046	1.021	0.981	0.934	0.885	0.844	0.822
24	24-Jun-16	0.829	0.864	0.919	0.980	1.037	1.080	1.100	1.094	1.065	1.022	0.973	0.932	0.910	0.914	0.936	0.966	0.997	1.021	1.029	1.017	0.986	0.941	0.893	0.855
25	25-Jun-16	0.838	0.850	0.889	0.951	1.021	1.088	1.132	1.144	1.123	1.081	1.023	0.955	0.893	0.852	0.845	0.867	0.911	0.959	0.998	1.017	1.016	0.993	0.951	0.900
26	26-Jun-16	0.859	0.844	0.865	0.919	0.994	1.074	1.143	1.186	1.194	1.167	1.106	1.018	0.919	0.833	0.783	0.775	0.804	0.862	0.928	0.983	1.016	1.023	0.999	0.951
27	27-Jun-16	0.896	0.856	0.847	0.878	0.944	1.032	1.124	1.202	1.249	1.250	1.204	1.117	1.004	0.877	0.764	0.709	0.716	0.766	0.837	0.908	0.973	1.021	1.036	1.006
28	28-Jun-16	0.943	0.879	0.841	0.847	0.895	0.975	1.072	1.176	1.263	1.309	1.296	1.224	1.107	0.968	0.831	0.724	0.670	0.673	0.728	0.815	0.909	0.988	1.037	1.037
29	29-Jun-16	0.994	0.928	0.866	0.831	0.844	0.904	1.000	1.116	1.233	1.322	1.354	1.318	1.222	1.086	0.933	0.789	0.684	0.635	0.652	0.721	0.821	0.923	1.007	1.050
30	30-Jun-16	0.881	0.824	0.802	0.829	0.899	0.997	1.102	1.193	1.248	1.258	1.222	1.144	1.036	0.918	0.816	0.759	0.752	0.788	0.855	0.928	0.989	1.026	1.030	0.994

Tidal Characteristic

No	Constituents	Symbol	Description	Period (hour)	ω (rad/hour)	A	B	g° phase	H=Amplitude (m)
0.	Average water level	Z_0		-	-				0.939
1.	Main lunar constituent	M_2	semi diurnal	12.4206	0.50587	0.1402	-0.0285	348.5030°	0.143
2.	Main solar constituent	S_2		12.0000	0.52360	0.0325	-0.0530	301.5434°	0.062
3.	Lunar constituent, due to Earth-Moon distance	N_2		12.6582	0.49637	0.0298	0.0320	47.1122°	0.044
4.	Soli-lunar constituent, due to the change of declination	K_2		11.9673	0.52503	0.0290	0.0423	55.6088°	0.051
5.	Soli-lunar constituent	K_1	diurnal	23.9346	0.26251	-0.0924	-0.0541	210.3582°	0.107
6.	Main lunar constituent	O_1		25.8194	0.24335	-0.0240	-0.0317	232.8392°	0.040
7.	Main solar constituent	P_1		24.0658	0.26108	-0.0327	0.0264	141.0540°	0.042
8.	Main lunar constituent	M_4	quarterly	6.2103	1.01174	0.0002	-0.0008	281.9952°	0.001
9.	Soli-lunar constituent	MS_4		6.1033	1.02947	0.0007	-0.0023	286.1082°	0.002

	Symbol	Calculation			Elev.	HHWL	MHWL	MSL	MLWL	CDL	LLWL	LAT
Higher High-Water Level	HHWL	$Z_0+(M_2+S_2+K_2+K_1+O_1+P_1)$	1.3847	≈	1.4	0.0	0.2	0.5	0.8	0.8	0.9	1.0
Mean High Water Level	MHWL	$Z_0+(M_2+K_1+O_1)$	1.2292	≈	1.2	-0.2	0.0	0.3	0.6	0.6	0.7	0.8
Mean Sea Level	MSL	Z_0	0.9393	≈	0.9	-0.5	-0.3	0.0	0.3	0.3	0.4	0.5
Mean Low Water Level	MLWL	$Z_0-(M_2+K_1+O_1)$	0.6493	≈	0.6	-0.8	-0.6	-0.3	0.0	0.0	0.1	0.2
Chart Datum Level	CDL	$Z_0-(M_2+S_2+K_1+O_1)$	0.5871	≈	0.6	-0.8	-0.6	-0.3	0.0	0.0	0.1	0.2
Lower Low Water Level	LLWL	$Z_0-(M_2+S_2+K_2+K_1+O_1+P_1)$	0.4938	≈	0.5	-0.9	-0.7	-0.4	-0.1	-0.1	0.0	0.1
Lowest Astronomical Tide	LAT	Z_0-(all constituents)	0.4468	≈	0.4	-1.0	-0.8	-0.5	-0.2	-0.2	-0.1	0.0

Appendix B. Tidal observation for May 2018

TIDAL OBSERVATION ANALYSIS USING LEAST SQUARE

Location
Lokasi : Cirebon
Instrument
Alat : radar gauge, pressure gauge dan float gauge (operated by Badan Informasi Geospasial BIG)
Unit
Satuan : meter
District
Kabupaten : Cirebon
Time Zone from GMT
Zona Waktu. : + 7:00
Period
Periode : May 2018

Day	Date	hour																							
		0:00	1:00	2:00	3:00	4:00	5:00	6:00	7:00	8:00	9:00	10:00	11:00	12:00	13:00	14:00	15:00	16:00	17:00	18:00	19:00	20:00	21:00	22:00	23:00
1	1-May-18	0.930	0.929	0.839	0.537	0.928	1.229	1.018	0.792	0.724	0.934	1.001	0.988	0.953	0.948	1.047	1.159	1.183	1.083	0.982	0.942	0.925	0.881	0.804	0.736
2	2-May-18	0.727	0.784	0.856	0.895	0.910	0.933	0.965	0.983	0.971	0.937	0.908	0.907	0.935	0.969	0.995	1.019	1.048	1.069	1.065	1.029	0.970	0.904	0.848	0.805
3	3-May-18	0.773	0.759	0.776	0.824	0.890	0.949	0.986	1.001	1.002	0.997	0.979	0.946	0.916	0.902	0.916	0.951	0.989	1.018	1.034	1.034	1.013	0.971	0.912	0.848
4	4-May-18	0.791	0.755	0.751	0.784	0.845	0.919	0.985	1.031	1.052	1.052	1.032	0.992	0.942	0.897	0.875	0.884	0.916	0.957	0.995	1.021	1.025	1.004	0.960	0.898
5	5-May-18	0.829	0.772	0.745	0.758	0.806	0.878	0.957	1.027	1.080	1.107	1.101	1.058	0.985	0.909	0.861	0.852	0.869	0.901	0.942	0.987	1.019	1.023	0.994	0.937
6	6-May-18	0.866	0.799	0.760	0.764	0.808	0.876	0.959	1.038	1.096	1.127	1.125	1.091	1.029	0.951	0.879	0.834	0.828	0.854	0.903	0.957	1.001	1.021	1.011	0.972
7	7-May-18	0.908	0.834	0.775	0.754	0.772	0.820	0.896	0.987	1.075	1.136	1.154	1.124	1.064	0.982	0.898	0.833	0.808	0.822	0.863	0.921	0.978	1.016	1.023	0.997
8	8-May-18	0.942	0.870	0.799	0.752	0.744	0.780	0.854	0.945	1.036	1.124	1.172	1.160	1.084	0.982	0.895	0.839	0.812	0.800	0.815	0.870	0.947	1.010	1.034	1.015
9	9-May-18	0.965	0.902	0.838	0.785	0.760	0.779	0.843	0.935	1.029	1.102	1.141	1.140	1.102	1.032	0.937	0.842	0.776	0.760	0.785	0.842	0.911	0.974	1.016	1.026
10	10-May-18	1.001	0.942	0.870	0.808	0.778	0.792	0.845	0.928	1.022	1.110	1.165	1.171	1.130	1.053	0.957	0.858	0.777	0.734	0.738	0.784	0.860	0.936	0.993	1.019
11	11-May-18	1.012	0.970	0.907	0.843	0.803	0.807	0.857	0.936	1.023	1.103	1.159	1.177	1.154	1.096	1.003	0.890	0.784	0.716	0.702	0.734	0.799	0.876	0.945	0.994
12	12-May-18	1.012	0.990	0.937	0.877	0.831	0.815	0.840	0.900	0.989	1.096	1.181	1.210	1.150	1.087	1.045	0.975	0.855	0.721	0.654	0.673	0.748	0.829	0.885	0.929
13	13-May-18	0.972	0.996	0.973	0.912	0.850	0.821	0.840	0.896	0.968	1.044	1.126	1.193	1.222	1.195	1.117	1.006	0.887	0.782	0.711	0.678	0.688	0.735	0.808	0.882
14	14-May-18	0.940	0.968	0.961	0.931	0.893	0.862	0.852	0.875	0.929	1.006	1.093	1.170	1.216	1.218	1.172	1.089	0.980	0.866	0.766	0.703	0.679	0.696	0.742	0.807
15	15-May-18	0.872	0.923	0.946	0.941	0.916	0.884	0.861	0.863	0.897	0.965	1.048	1.122	1.169	1.195	1.198	1.162	1.080	0.964	0.852	0.767	0.719	0.701	0.706	0.739

16	16-May-18	0.799	0.867	0.918	0.938	0.934	0.917	0.901	0.896	0.904	0.930	0.974	1.032	1.097	1.153	1.186	1.181	1.135	1.057	0.965	0.874	0.795	0.738	0.707	0.709
17	17-May-18	0.745	0.804	0.865	0.912	0.940	0.946	0.935	0.917	0.905	0.907	0.924	0.958	1.008	1.065	1.112	1.142	1.148	1.123	1.064	0.981	0.893	0.815	0.757	0.722
18	18-May-18	0.717	0.746	0.805	0.876	0.938	0.977	0.988	0.978	0.959	0.939	0.914	0.890	0.888	0.933	1.006	1.074	1.114	1.121	1.104	1.066	1.005	0.922	0.834	0.762
19	19-May-18	0.723	0.725	0.763	0.827	0.902	0.972	1.018	1.028	1.008	0.974	0.932	0.886	0.847	0.836	0.868	0.935	1.012	1.073	1.106	1.106	1.075	1.016	0.934	0.843
20	20-May-18	0.766	0.725	0.731	0.782	0.865	0.957	1.034	1.081	1.087	1.057	1.002	0.928	0.846	0.782	0.766	0.802	0.872	0.957	1.036	1.090	1.106	1.081	1.019	0.929
21	21-May-18	0.833	0.759	0.729	0.750	0.817	0.917	1.023	1.107	1.151	1.151	1.110	1.032	0.922	0.801	0.711	0.691	0.741	0.828	0.923	1.010	1.072	1.097	1.076	1.008
22	22-May-18	0.908	0.810	0.754	0.766	0.828	0.913	1.015	1.138	1.274	1.391	1.388	1.227	0.987	0.780	0.696	0.721	0.726	0.692	0.713	0.849	1.014	1.106	1.102	1.026
23	23-May-18	0.935	0.862	0.810	0.785	0.803	0.867	0.969	1.087	1.192	1.259	1.273	1.228	1.132	0.994	0.839	0.699	0.619	0.611	0.671	0.773	0.888	0.986	1.049	1.063
24	24-May-18	1.022	0.939	0.843	0.766	0.738	0.776	0.863	0.983	1.115	1.228	1.295	1.298	1.235	1.114	0.957	0.798	0.668	0.602	0.605	0.671	0.776	0.886	0.978	1.032
25	25-May-18	1.034	0.982	0.898	0.814	0.759	0.760	0.818	0.910	1.027	1.159	1.269	1.324	1.300	1.210	1.074	0.919	0.772	0.659	0.605	0.617	0.689	0.793	0.893	0.971
26	26-May-18	1.012	1.000	0.946	0.869	0.800	0.765	0.785	0.853	0.952	1.069	1.184	1.275	1.310	1.272	1.170	1.029	0.882	0.751	0.663	0.627	0.650	0.719	0.812	0.901
27	27-May-18	0.966	0.992	0.972	0.922	0.861	0.811	0.792	0.818	0.884	0.980	1.091	1.194	1.260	1.267	1.212	1.112	0.986	0.856	0.744	0.673	0.653	0.685	0.751	0.831
28	28-May-18	0.905	0.958	0.977	0.959	0.917	0.867	0.831	0.826	0.857	0.922	1.008	1.100	1.175	1.215	1.205	1.149	1.058	0.950	0.844	0.760	0.710	0.698	0.723	0.778
29	29-May-18	0.849	0.915	0.958	0.971	0.957	0.926	0.893	0.871	0.866	0.888	0.942	1.015	1.083	1.131	1.151	1.137	1.090	1.016	0.932	0.847	0.777	0.735	0.725	0.749
30	30-May-18	0.872	0.923	0.946	0.941	0.916	0.884	0.861	0.863	0.897	0.965	1.048	1.122	1.169	1.195	1.198	1.162	1.080	0.964	0.852	0.767	0.719	0.701	0.706	0.739

Tidal Characteristic

No	Constituents	Symbol	Description	Period (hour)	ω (rad/hour)	A	B	g^o phase	H=Amplitude (m)
0.	Average water level	Z_0		-	-				0.902
1.	Main lunar constituent	M_2	semi diurnal	12.4206	0.50587	-0.0975	-0.1045	226.9882°	0.143
2.	Main solar constituent	S_2		12.0000	0.52360	0.0584	0.0076	7.4532°	0.059
3.	Lunar constituent, due to Earth-Moon distance	N_2		12.6582	0.49637	-0.0394	0.0273	145.2381°	0.048
4.	Soli-lunar constituent, due to the change of declination	K_2		11.9673	0.52503	0.0041	-0.0005	353.4864°	0.004
5.	Soli-lunar constituent	K_1	diurnal	23.9346	0.26251	-0.0820	0.0333	157.9236°	0.088
6.	Main lunar constituent	O_1		25.8194	0.24335	-0.0354	0.0345	135.7192°	0.049
7.	Main solar constituent	P_1		24.0658	0.26108	-0.0047	-0.0132	250.4634°	0.014
8.	Main lunar constituent	M_4	quarterly	6.2103	1.01174	0.0040	-0.0007	350.3952°	0.004
9.	Soli-lunar constituent	MS_4		6.1033	1.02947	0.0006	0.0000	0.4570°	0.001

	Symbol	Calculation			Elev.	HHWL	MHWL	MSL	MLWL	CDL	LLWL	LAT
Higher High Water Level	HHWL	$Z_0+(M_2+S_2+K_2+K_1+O_1+P_1)$	1.2597	≈	1.3	0.0	0.1	0.4	0.7	0.7	0.8	0.8
Mean High Water Level	MHWL	$Z_0+(M_2+K_1+O_1)$	1.1827	≈	1.2	-0.1	0.0	0.3	0.6	0.6	0.7	0.7
Mean Sea Level	MSL	Z_0	0.9019	≈	0.9	-0.4	-0.3	0.0	0.3	0.3	0.4	0.4
Mean Low Water Level	MLWL	$Z_0-(M_2+K_1+O_1)$	0.6211	≈	0.6	-0.7	-0.6	-0.3	0.0	0.0	0.1	0.1
Chart Datum Level	CDL	$Z_0-(M_2+S_2+K_1+O_1)$	0.5621	≈	0.6	-0.7	-0.6	-0.3	0.0	0.0	0.1	0.1
Lower Low Water Level	LLWL	$Z_0-(M_2+S_2+K_2+K_1+O_1+P_1)$	0.5440	≈	0.5	-0.8	-0.7	-0.4	-0.1	-0.1	0.0	0.0
Lowest Astronomical Tide	LAT	Z_0-(all constituents)	0.4914	≈	0.5	-0.8	-0.7	-0.4	-0.1	-0.1	0.0	0.0

Appendix C. Damage function based on depth

Construction and Production	0.2 m	0.25 m	0.5 m	0.75 m	1 m	1.25 m	1.5 m
R- 1	0	10	40	75	100	100	100
R- 2	0	15	45	75	100	100	100
R- 3	0	20	65	85	100	100	100
R- 4	0	20	60	80	98	100	100
R- 5	0	25	40	85	100	100	100
R- 6	0	20	50	85	95	100	100
R- 7	0	20	55	75	100	100	100
R- 8	0	15	45	70	95	100	100
R- 9	0	20	50	75	100	100	100
R- 10	0	25	50	85	95	100	100
R- 11	0	25	60	80	100	100	100
R- 12	0	20	55	85	99	100	100
R- 13	0	20	45	80	100	100	100
R- 14	0	25	40	85	95	100	100
Mean	0	20	50	80	98	100	100

Harvesting	0.2 m	0.25 m	0.5 m	0.75 m	1 m	1.25 m	1.5 m
R- 1	0	30	80	90	100	100	100
R- 2	0	35	77	95	100	100	100
R- 3	0	25	70	80	100	100	100
R- 4	0	20	85	95	100	100	100
R- 5	0	20	70	90	100	100	100
R- 6	0	25	75	90	100	100	100
R- 7	0	30	77	85	100	100	100
R- 8	0	30	70	90	100	100	100
R- 9	0	20	75	95	100	100	100
R- 10	0	25	65	95	100	100	100
R- 11	0	25	80	90	100	100	100
R- 12	0	20	75	85	100	100	100
R- 13	0	25	76	80	100	100	100
R- 14	0	20	75	100	100	100	100
Mean	0	25	75	90	100.0	100	100

Off-Production	0.2 m	0.25 m	0.5 m	0.75 m	1 m	1.25 m	1.5 m
R- 1	0	10	35	50	95	100	100
R- 2	0	5	20	35	100	100	100
R- 3	0	5	25	50	100	100	100
R- 4	0	10	35	60	100	100	100
R- 5	0	5	30	60	100	100	100
R- 6	0	5	25	55	95	100	100
R- 7	0	0	25	50	100	100	100
R- 8	0	0	5	20	100	100	100
R- 9	0	5	10	40	100	100	100
R- 10	0	0	20	40	100	100	100
R- 11	0	5	20	50	95	100	100
R- 12	0	10	30	60	100	100	100
R- 13	0	5	35	65	100	100	100
R- 14	0	5	35	65	100	100	100
Mean	0	5	25	50	99	100	100

Appendix D. Damage function based on duration

Pre-Production	≤ 1 days	2 days	3 days	4 days	5 days	6 days	≥ 7 days
R- 1	0	35	55	75	88	100	100
R- 2	0	20	45	70	85	100	100
R- 3	0	25	55	85	93	100	100
R- 4	0	30	55	80	90	100	100
R- 5	0	25	55	85	93	100	100
R- 6	0	20	50	80	90	100	100
R- 7	0	15	45	75	88	100	100
R- 8	0	25	48	70	85	100	100
R- 9	0	35	53	70	85	100	100
R- 10	0	30	53	75	88	100	100
R- 11	0	15	43	70	85	100	100
R- 12	0	30	48	65	83	100	100
R- 13	0	20	48	75	88	100	100
R- 14	0	25	50	75	88	100	100
Mean	0	25	50	75	88	100	100
Harvesting	≤ 1 days	2 days	3 days	4 days	5 days	6 days	≥ 7 days
R- 1	30	35	55	75	88	100	100
R- 2	35	45	63	80	90	100	100
R- 3	25	65	70	75	88	100	100
R- 4	20	55	75	95	98	100	100
R- 5	20	40	65	90	95	100	100
R- 6	25	50	70	90	95	100	100
R- 7	30	45	65	85	93	100	100
R- 8	30	70	73	75	88	100	100
R- 9	20	75	70	65	83	100	100
R- 10	25	30	45	60	80	100	100
R- 11	25	60	65	70	85	100	100
R- 12	20	50	63	75	88	100	100
R- 13	25	50	58	65	83	100	100
R- 14	20	30	40	50	75	100	100
Mean	25	50	63	75	88	100.0	100
Off-Production	≤ 1 days	2 days	3 days	4 days	5 days	6 days	≥ 7 days
R- 1	10	35	43	50	73	95	100
R- 2	5	20	28	35	68	100	100
R- 3	5	25	38	50	75	100	100
R- 4	10	35	48	60	80	100	100
R- 5	5	30	45	60	80	100	100
R- 6	5	25	40	55	75	95	100
R- 7	0	25	38	50	75	100	100
R- 8	0	5	13	20	60	100	100
R- 9	5	10	25	40	70	100	100
R- 10	0	20	30	40	70	100	100
R- 11	5	20	35	50	73	95	100
R- 12	10	30	45	60	80	100	100
R- 13	5	35	50	65	83	100	100
R- 14	5	35	50	65	83	100	100
Mean	5	25	38	50	74	98.9	100

R = Farmer representative

Appendix E. List of informant and experts

List of informants for damage function establishment

No	Farmer	District	Status	Date
1	R-1	Losari	Worker	18/11/2019
2	R-2	Losari	Owner	19/11/2019
3	R-3	Gebang	Owner	23/11/2019
4	R-4	Gebang	Worker	24/11/2019
5	R-5	Mundu	Owner	28/11/2019
6	R-6	Pangenan	Owner	04/12/2019
7	R-7	Pangenan	Worker	04/12/2019
8	R-8	Mundu	Worker	07/12/2019
9	R-9	Suranenggala	Owner	09/12/2019
10	R-10	Pangenan	Worker	10/12/2019
11	R-11	Gunungjati	Owner	12/12/2019
12	R-12	Gunungjati	Owner	13/12/2019
13	R-13	Suranenggala	Worker	15/12/2019
14	R-14	Suranenggala	Worker	15/12/2019

R = Farmer representative

List of expert interviews

No	Type of Organization	Institution	Location	Date
1	Local governmental authority	Department of Ocean and Fisheries of Cirebon	Cirebon (via Zoom)	29/1-02/02/2021
2	Central government authority	National of Geospatial Agency	Cibinong (via Zoom)	08/11/2019
3	Research institute	Universitas Brawijaya	Malang (via Zoom)	22/02/2021
4	Provincial government authority	BAPPEDA	Bandung (via Zoom)	30/04/2021

Appendix F. Own Contribution

Article 1 (Chapter 3), Article 2 (Chapter 4) and Article 3 (Chapter 5) was co-authored by Boris Braun (Institute of Geography, University of Cologne, Germany). All articles are research papers presented based on empirical data collected during two field work in Cirebon, West Java between August 2018 and November 2019. This research for this dissertation has been sponsored by Indonesia Endowment Fund for Education (LPDP) under the Education Scholarship for Indonesia *Beasiswa Pendidikan Indonesia* with contract code: PRJ-115 /LPDP.3/2017.

My contributions for the three articles were the following:

1. Literature review;
2. Developing research question and model;
3. Organizing data collection and field survey;
4. Coordinating with local stakeholders (farmers, and local government institution);
5. Developing and choose suitable numerical model;
6. Assisting research assistance from (UNDIP) on implementing hydrodynamic model of DHI MIKE including inputs and boundaries;
7. Developing the synthetic questionnaires for depth and duration;
8. Data cleaning and analyzing in ArcGIS;
9. Zoom interview on expert for Analytical Hierarchical Process (AHP);
10. Individually implementing statistical and correlation analysis using Excel;
11. Independent writing of all manuscript;
12. Revision of all manuscripts under the supervision of Boris Braun (all articles), student assistant for proof-reading.

Appendix G. Eigenständigkeitserklärung Appendix

Ich versichere, dass ich die von mir vorgelegte Dissertation mit dem Titel: „Evaluating Tidal Flood Risk on Salt Farming Land– Empirical and Methodological Insights from a Case Study in Northern Java".

selbständig angefertigt, die benutzten Quellen und Hilfsmittel vollständig angegeben und die Stellen der Arbeit − einschließlich Tabellen, Karten und Abbildungen −, die anderen Werken im Wortlaut oder dem Sinn nach entnommen sind, in jedem Einzelfall als Entlehnung kenntlich gemacht habe; dass diese Dissertation noch keiner anderen Fakultät oder Universität zur Prüfung vorgelegen hat; dass sie − abgesehen von unten angegebenen Teilpublikationen − noch nicht veröffentlicht worden ist, sowie, dass ich eine solche Veröffentlichung vor Abschluss des Promotionsverfahrens nicht vorneh- men werde. Die Bestimmungen der Promotionsordnung sind mir bekannt. Die von mir vorgelegte Dissertation ist von Prof. Dr. Boris Braun betreut worden. Teilpublikationen:

- Nirwansyah and Braun. (2019), "Mapping Impact of Tidal Flooding on Solar Salt Farming in Northern Java using a Hydrodynamic Model", *ISPRS International Journal of Geo-Information*, Vol. 8 No. 10, p. 451.DOI: 10.3390/ijgi8100451
- Nirwansyah, A.W. and Braun, B. (2021), "Assessing the degree of tidal flood damage to salt harvesting landscape using synthetic approach and GIS - Case study: Cirebon, West Java", International Journal of Disaster Risk Reduction, Elsevier Ltd, Vol. 55 No. January, p. 102099. DOI: 10.1016/j.ijdrr.2021.102099
- Nirwansyah, A.W. and Braun, B. (2021), "Tidal Flood Risk on Salt Farming: Evaluation of Post Events in the Northern Part of Java Using a Parametric Approach", Geosciences, Vol. 11 No. 10, p. 420. DOI: 10.3390/geosciences11100420

04.10.2021, Bergheim

Datum, ort	Anang Widhi Nirwansyah

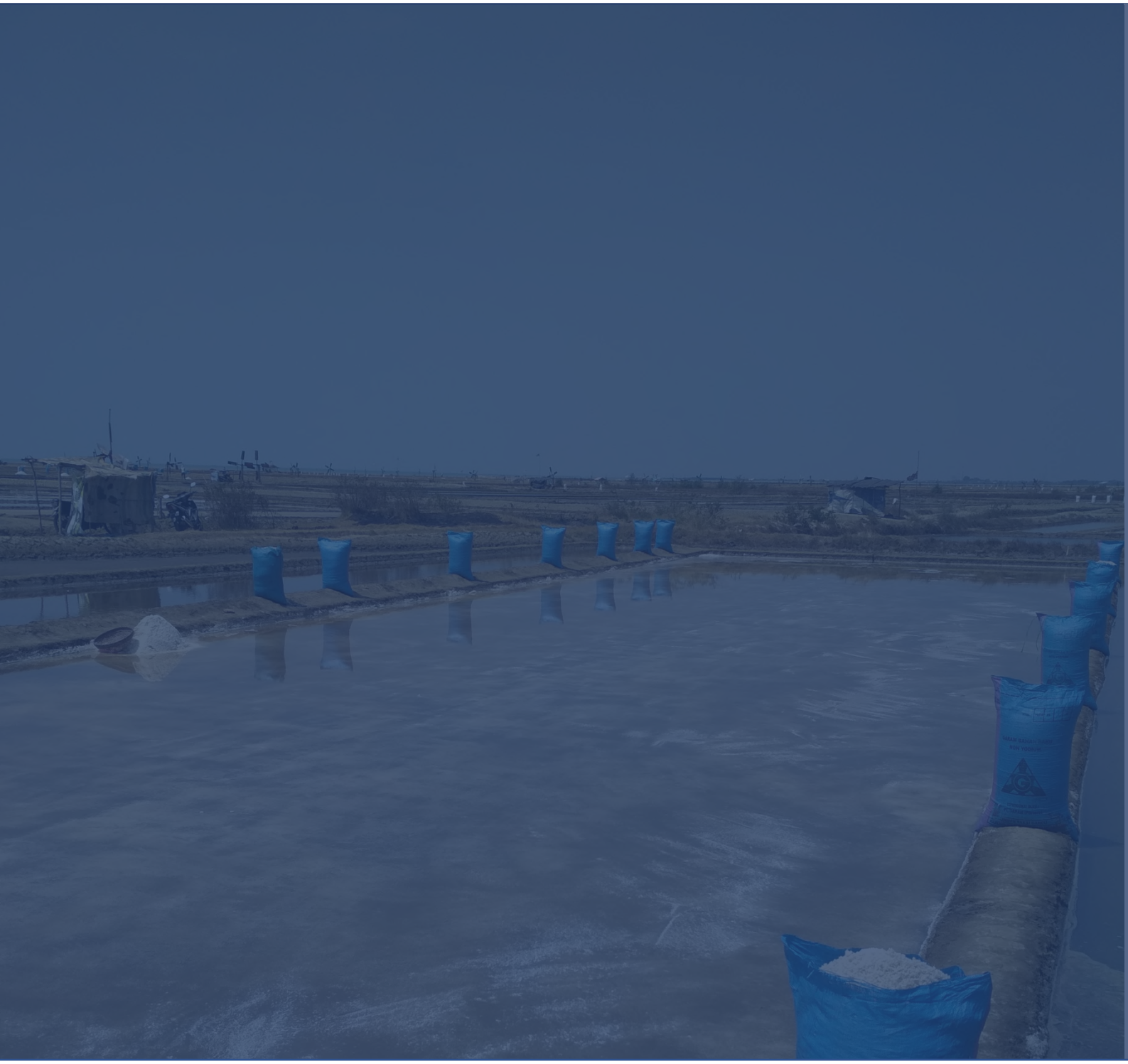

Universität zu Köln